TYPE I CHAPERONINS: MECHANISM AND BEYOND

EDITED BY: Adina Breiman and Abdussalam Azem
PUBLISHED IN: Frontiers in Molecular Biosciences

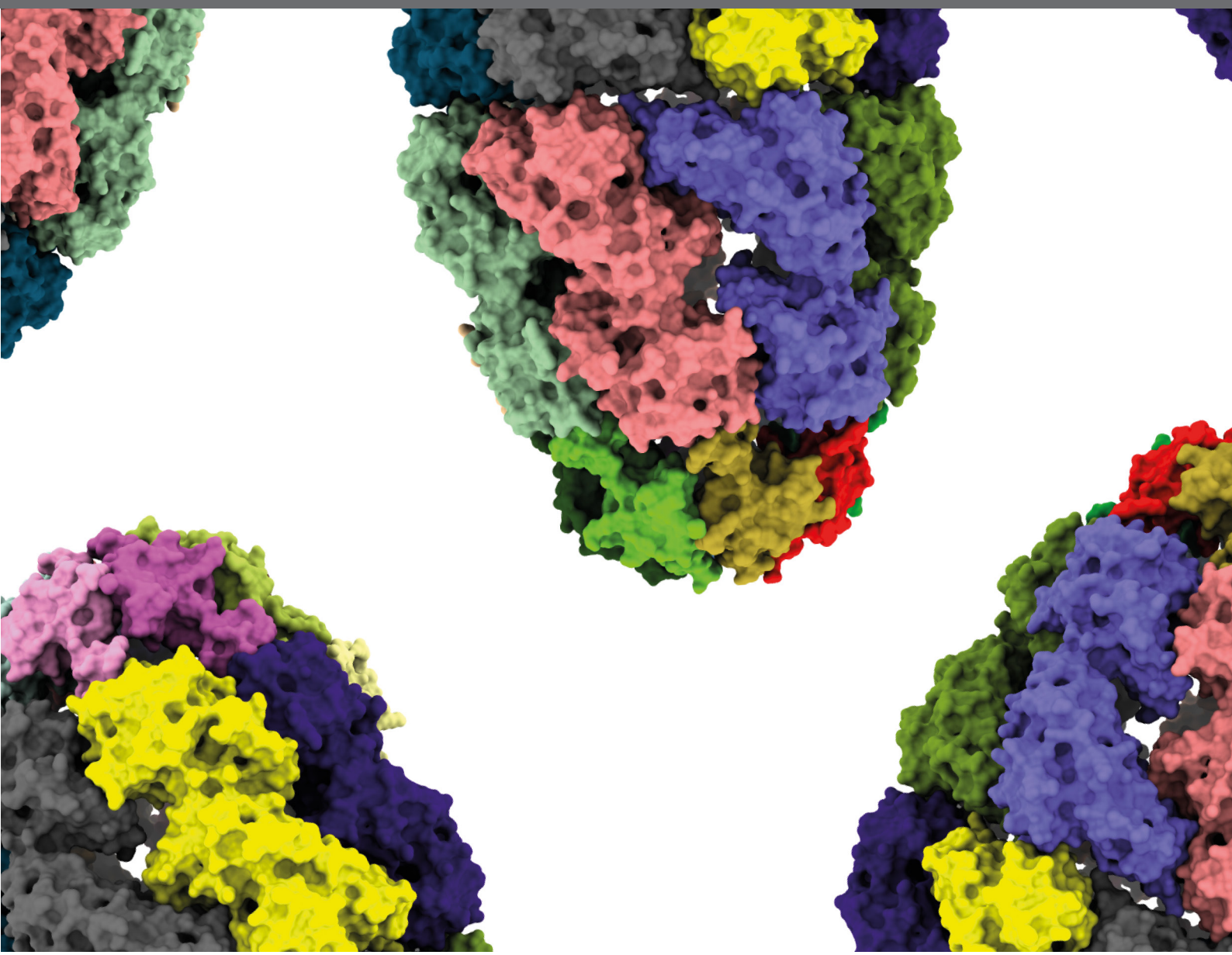

frontiers Research Topics

frontiers

ISSN 1664-8714
ISBN 978-2-88945-575-1
DOI 10.3389/978-2-88945-575-1

About Frontiers

Frontiers is more than just an open-access publisher of scholarly articles: it is a pioneering approach to the world of academia, radically improving the way scholarly research is managed. The grand vision of Frontiers is a world where all people have an equal opportunity to seek, share and generate knowledge. Frontiers provides immediate and permanent online open access to all its publications, but this alone is not enough to realize our grand goals.

Frontiers Journal Series

The Frontiers Journal Series is a multi-tier and interdisciplinary set of open-access, online journals, promising a paradigm shift from the current review, selection and dissemination processes in academic publishing. All Frontiers journals are driven by researchers for researchers; therefore, they constitute a service to the scholarly community. At the same time, the Frontiers Journal Series operates on a revolutionary invention, the tiered publishing system, initially addressing specific communities of scholars, and gradually climbing up to broader public understanding, thus serving the interests of the lay society, too.

Dedication to Quality

Each Frontiers article is a landmark of the highest quality, thanks to genuinely collaborative interactions between authors and review editors, who include some of the world's best academicians. Research must be certified by peers before entering a stream of knowledge that may eventually reach the public - and shape society; therefore, Frontiers only applies the most rigorous and unbiased reviews.
Frontiers revolutionizes research publishing by freely delivering the most outstanding research, evaluated with no bias from both the academic and social point of view. By applying the most advanced information technologies, Frontiers is catapulting scholarly publishing into a new generation.

What are Frontiers Research Topics?

Frontiers Research Topics are very popular trademarks of the Frontiers Journals Series: they are collections of at least ten articles, all centered on a particular subject. With their unique mix of varied contributions from Original Research to Review Articles, Frontiers Research Topics unify the most influential researchers, the latest key findings and historical advances in a hot research area! Find out more on how to host your own Frontiers Research Topic or contribute to one as an author by contacting the Frontiers Editorial Office: researchtopics@frontiersin.org

TYPE I CHAPERONINS: MECHANISM AND BEYOND

Topic Editors:
Adina Breiman, Tel Aviv University, Israel
Abdussalam Azem, Tel Aviv University, Israel

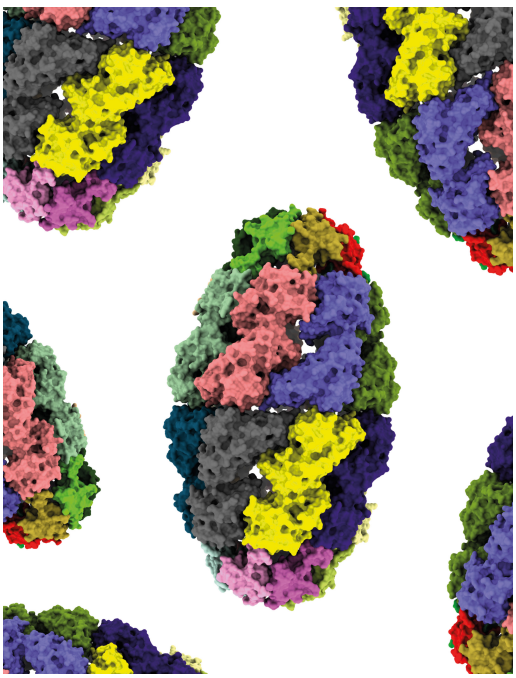

Cartoon of chaperonin football complex.
Image: Fady Jebara, Malay Patra and Joel Hirsch.

Type I chaperonins are key players in maintaining the proteome of bacteria and organelles of bacterial origin. They are well known for their crucial role in mediating protein folding. For almost three decades, the molecular mechanism of chaperonin function has been the subject of intensive research. Still, surprising new mechanistic discoveries are constantly reported. It seems that we are far from having a full understanding of the chaperonin mode of action. Chaperonins are not simply protein folding machines. They also perform diverse extramitochondrial tasks, mainly related to inflammatory and signal transduction processes. This eBook constitutes ten articles highlighting the latest developments related to the divers functions of Type I chaperonins. As its title, mechanism and beyond, the collection starts with mechanistic view, continues with extracellular functions and ends with biotechnological applications of Type I chaperonins.

Citation: Breiman, A., Azem, A., eds (2018). Type I Chaperonins: Mechanism and Beyond. Lausanne: Frontiers Media. doi: 10.3389/978-2-88945-575-1

Table of Contents

frontiers in Molecular Biosciences

EDITORIAL
published: 31 July 2018
doi: 10.3389/fmolb.2018.00072

Editorial: Type I Chaperonins: Mechanism and Beyond

Adina Breiman[1]* *and Abdussalam Azem*[2]*

[1] School of Plant Sciences and Food Security, Tel Aviv, Israel, [2] School of Neurobiology, Biochemistry and Biophysics, George S. Wise Faculty of Life Sciences, Tel Aviv University, Tel Aviv, Israel

Keywords: chaperonin 60, chaperonins, GroEL, HSP10, GroES

Editorial on the Research Topic

Type I Chaperonins: Mechanism and Beyond

Chaperone proteins control almost all aspects of proteostasis, such as protein synthesis, translocation, folding, and degradation. As such, chaperones accompany every protein from its birth until its death. Chaperonins constitute a highly conserved subgroup of molecular chaperones that is divided into two groups, Type I and Type II. For Type I chaperonins, the protein folding function is mediated by the Hsp60 (also known as Cpn60) chaperonin, which serves as a folding chamber for denatured protein, assisted by its 10 kDa co-chaperonin, Hsp10 (or Cpn10). For Type II chaperonins, the protein folding function is handleed by a single Hsp60 protein, CCT/TRiC (Horwich et al., 2006, p. 5464; Dekker et al., 2011; Skjaerven et al., 2015). Several important milestones are worth mentioning that led to our current understanding of the molecular of function of Type I chaperonins. The latter were discovered in the 1970s as bacterial host proteins that are essential for the assembly of phage particles (Georgopoulos et al., 1973). During the same period, the heat shock response of some chaperones was discovered (Ritossa, 1962). Conditions known to compromise protein folding. Additional *in vivo* studies showed that chaperonins are key players in the assembly process of RuBisCO in plants and that they are important for the folding of newly translocated proteins into the mitochondrial matrix as well (Hemmingsen et al., 1988; Roy et al., 1988; Cheng et al., 1989; Goloubinoff et al., 1989).

These discoveries led to general recognition of Type I chaperonins as important protein nano machines that play a key role in cellular protein folding and assembly. *In vitro* reconstitution of their protein folding activity using denatured dimeric RuBisCO as a model system opened the door to a new field of research, which focused on *in vitro* mechanistic aspects of chaperonin function (Goloubinoff et al., 1989). The friendly nature of the Escherichia coli chaperonins, in particular the profound stability of the protein oligomers, enabled their extensive investigation, which established them as the prototype chaperonin model system. Notably, the preponderance of research in the field focused on mechanistic aspects of this bacterial chaperone system.

With time, investigation of chaperonins from chloroplasts, mitochondria, and numerous additional bacterial strains, revealed a wide range of divergence from the *E. coli* paradigm. The vast diversity among chaperonins and atypical systems such as those as discovered in bacteriophages, is reviewed in two manuscripts (Ansari and Mande; Bhatt et al.).

In the case of chloroplast chaperonins, the most striking observation was that these chaperonins assemble into hetero-oligomeric tetradecamers that are composed of several homologous subunits, in contrast to the homo oligomeric nature of bacterial chaperonins. The chloroplast chaperonins are the subject of three manuscripts in this research topic (Zhao and Liu; Vitlin Gruber and Feiz; Vitlin Gruber et al.). Two of them highlight the sophisticated RuBisCO assembly pathway, with new assembly factors identified in recent years, and the complexity of the chloroplast chaperonin system. Recent discoveries in the field represent an important step toward possibly engineering more efficient RuBisCO thereby potentially increasing crop yield.

OPEN ACCESS

Edited by:
Anat Ben-Zvi,
Ben-Gurion University of the Negev, Israel

Reviewed by:
Paolo De Los Rios,
École Polytechnique Fédérale de Lausanne, Switzerland
Hays S. Rye,
Texas A&M University, United States

***Correspondence:**
Adina Breiman
adinab@tauex.tau.ac.il
Abdussalam Azem
azema@tauex.tau.ac.il

Specialty section:
This article was submitted to Protein Folding, Misfolding and Degradation, a section of the journal Frontiers in Molecular Biosciences

Received: *08 June 2018*
Accepted: *09 July 2018*
Published: *31 July 2018*

Citation:
Breiman A and Azem A (2018) Editorial: Type I Chaperonins: Mechanism and Beyond. Front. Mol. Biosci. 5:72. doi: 10.3389/fmolb.2018.00072

With regard to mitochondrial chaperonins, these were also found to exhibit unique structural properties and retain unexpected extra-organelle moonlighting functions. As such, they were found to function in a variety of processes, including signal transduction events that may regulate immunity and inflammation (Athanasas-Platsis et al., 2004; Grundtman et al., 2011; Jia et al., 2011; Juwono and Martinus, 2016). Mitochondrial Hsp60 was suggested to adopt variations in its oligomeric state, in a nucleotide and concentration-dependent manner that may affect its function. Vilasi et al. review the oligomeric variability of mitochondrial Hsp60 and its link to functions that are not related to protein folding (cytosolic and extracellular) (Vilasi et al.). Due to their extra mitochondrial functions, in particular in tumors, Hsp60 has been considered to be a potential target for anticancer drugs. Meng et al. provide an updated review of available compounds that inhibit or affect the function of Hsp60 chaperonins (Meng et al.), with an eye toward using them as anticancer drugs.

In the biotechnology arena, O'Neil et al. developed a highly sophisticated system that utilizes immobilized GroEL on sensors for the detection of aggregated proteins among the various species in solution (O'Neil et al.).

For almost three decades, research on the bacterial GroEL/GroES chaperonin molecular mechanism of function has been central in the field of chaperone proteins (Thirumalai and Lorimer, 2001; Horwich et al., 2006; Gruber and Horovitz, 2016; Hayer-Hartl et al., 2016). The identity of active forms during the reaction cycle, whether the symmetrical $(GroEL)_{14}$ $((GroES)_7)_2$ (also named footballs) or the asymmetrical $(GroEL)_{14}(GroES)_7$ complexes (bullets), the role of chaperonins in the cycle (e.g., passive or active) and the role of ATP (Goloubinoff et al., 2018) all are discussed in several of the contributions, particularly in Weiss et al. The molecular function of the mitochondrial Hsp60/Hsp10 chaperonin system receives special attention in this context. Initially, it was suggested that Hsp60 operates as a single ring (Nielsen and Cowan, 1998; Nielsen et al., 1999), rather than a double ring as suggested for GroEL. In Weiss et al, based on results obtained in several studies, an alternative model was endorsed for the Hsp60 reaction cycle (Weiss et al.). This model proposes that mitochondrial Hsp60 alternates between single ring and double ring structures. This "equatorial split" is probably essential for the proper function of the mitochondrial system. Notably, such equatorial split mechanism was originally suggested for Thermus Thermophilus (Ishii et al., 1995), proposed also for GroEL (Taguchi, 2015) and recently received additional experimental support (Yan et al., 2018). Notably, preventing the equatorial split of the rings, by either formation of S-S bonds (Yan et al., 2018) or covalent fusion, still allows for significant protein folding activity by GroEL (Farr et al., 2003). Thus, the functional significance of the ring split for GroEL still requires further investigation.

AUTHOR CONTRIBUTIONS

All authors listed have made a substantial, direct and intellectual contribution to the work, and approved it for publication.

FUNDING

AA is supported by United States—Israel Binational Science Foundation (no. 2015214) and the Israel Science Foundation (No. 1507/13).

ACKNOWLEDGMENTS

We thank Dr. Celeste Weiss for critically reading this manuscript.

REFERENCES

Athanasas-Platsis, S., Somodevilla-Torres, M. J., Morton, H., and Cavanagh, A. C. (2004). Investigation of the immunocompetent cells that bind early pregnancy factor and preliminary studies of the early pregnancy factor target molecule. *Immunol. Cell Biol.* 82, 361–369. doi: 10.1111/j.0818-9641.2004.01260.x

Cheng, M. Y., Hartl, F. U., Martin, J., Pollock, R. A., Kalousek, F., Neupert, W., et al. (1989). Mitochondrial heat-shock protein hsp60 is essential for assembly of proteins imported into yeast mitochondria. *Nature* 337, 620–625. doi: 10.1038/337620a0

Dekker, C., Willison, K. R., and Taylor, W. R. (2011). On the evolutionary origin of the chaperonins. *Proteins* 79, 1172–1192. doi: 10.1002/prot.22952

Farr, G. W., Fenton, W. A., Chaudhuri, T. K., Clare, D. K., Saibil, H. R., and Horwich, A. L. (2003). Folding with and without encapsulation by cis- and trans-only GroEL-GroES complexes. *EMBO J.* 22, 3220–3230. doi: 10.1093/emboj/cdg313

Georgopoulos, C. P., Hendrix, R. W., Casjens, S. R., and Kaiser, A. D. (1973). Host participation in bacteriophage lambda head assembly. *J. Mol. Biol.* 76, 45–60. doi: 10.1016/0022-2836(73)90080-6

Goloubinoff, P., Christeller, J. T., Gatenby, A. A., and Lorimer, G. H. (1989). Reconstitution of active dimeric ribulose bisphosphate carboxylase from an unfoleded state depends on two chaperonin proteins and Mg-ATP. *Nature* 342, 884–889. doi: 10.1038/342884a0

Goloubinoff, P., Sassi, A. S., Fauvet, B., Barducci, A., and De Los Rios, P. (2018). Chaperones convert the energy from ATP into the nonequilibrium stabilization of native proteins. *Nat. Chem. Biol.* 14, 388–395. doi: 10.1038/s41589-018-0013-8

Gruber, R., and Horovitz, A. (2016). Allosteric mechanisms in chaperonin machines. *Chem. Rev.* 116, 6588–6606. doi: 10.1021/acs.chemrev.5b00556

Grundtman, C., Kreutmayer, S. B., Almanzar, G., Wick, M. C., and Wick, G. (2011). Heat shock protein 60 and immune inflammatory responses in atherosclerosis. *Arterioscler. Thromb. Vasc. Biol.* 31, 960–968. doi: 10.1161/ATVBAHA.110.217877

Hayer-Hartl, M., Bracher, A., and Hartl, F. U. (2016). The GroEL-GroES chaperonin machine: a nano-cage for protein folding. *Trends Biochem. Sci.* 41, 62–76. doi: 10.1016/j.tibs.2015.07.009

Hemmingsen, S. M., Woolford, C., van der Vies, S. M., Tilly, K., Dennis, D. T., Georgopoulos, C. P., et al. (1988). Homologous plant and bacterial proteins chaperone oligomeric protein assembly. *Nature* 333, 330–334. doi: 10.1038/333330a0

Horwich, A. L., Farr, G. W., and Fenton, W. A. (2006). GroEL-GroES-mediated protein folding. *Chem. Rev.* 106, 1917–1930. doi: 10.1021/cr040435v

Ishii, N., Taguchi, H., Sasabe, H., and Yoshida, M. (1995). Equatorial split of holo-chaperonin from *Thermus thermophilus* by ATP and K+. *FEBS Lett.* 362, 121–125. doi: 10.1016/0014-5793(95)00222-U

Jia, H., Halilou, A. I., Hu, L., Cai, W., Liu, J., and Huang, B. (2011). Heat shock protein 10 (Hsp10) in immune-related diseases: one coin, two sides. *Int. J. Biochem. Mol. Biol.* 2, 47–57.

Juwono, J., and Martinus, R. D. (2016). Does Hsp60 Provide a Link between mitochondrial stress and inflammation in diabetes mellitus? *J. Diabetes Res.* 2016:8017571. doi: 10.1155/2016/8017571

Nielsen, K. L., and Cowan, N. J. (1998). A single ring is sufficient for productive chaperonin-mediated folding *in vivo*. *Mol. Cell* 2, 93–99. doi: 10.1016/S1097-2765(00)80117-3

Nielsen, K. L., McLennan, N., Masters, M., and Cowan, N. J. (1999). A single-ring mitochondrial chaperonin (Hsp60-Hsp10) can substitute for GroEL-GroES *in vivo*. *J. Bacteriol.* 181, 5871–5875.

Ritossa, F. A. (1962). A new puffing pattern induced by temperature shock and DNP in Drosophila. *Experientia* 188, 571–573. doi: 10.1007/BF02172188

Roy, H., Cannon, S., and Gilson, M. (1988). Assembly of Rubisco from native subunits. *Biochim. Biophys. Acta* 957, 323–334. doi: 10.1016/0167-4838(88)90221-X

Skjaerven, L., Cuellar, J., Martinez, A., and Valpuesta, J. M. (2015). Dynamics, flexibility, and allostery in molecular chaperonins. *FEBS Lett.* 589, 2522–2532. doi: 10.1016/j.febslet.2015.06.019

Taguchi, H. (2015). Reaction cycle of chaperonin GroEL and via symmetric "Football" intermediate. *J. Mol. Biol.* 427, 2912–2918. doi: 10.1016/j.jmb.2015.04.007

Thirumalai, D., and Lorimer, G. H. (2001). Chaperonin-mediated protein folding. *Annu. Rev. Biophys. Biomol. Struct.* 30, 245–269. doi: 10.1146/annurev.biophys.30.1.245

Yan, X., Shi, Q., Bracher, A., Milicic, G., Singh, A. K., Hartl, F. U., et al. (2018). GroEL ring separation and exchange in the chaperonin reaction. *Cell* 172, 605.e11–617.e11. doi: 10.1016/j.cell.2017.12.010

Conflict of Interest Statement: The authors declare that the research was conducted in the absence of any commercial or financial relationships that could be construed as a potential conflict of interest.

frontiers in Molecular Biosciences

REVIEW
published: 08 December 2016
doi: 10.3389/fmolb.2016.00080

Dynamic Complexes in the Chaperonin-Mediated Protein Folding Cycle

*Celeste Weiss *, Fady Jebara, Shahar Nisemblat and Abdussalam Azem **

George S. Weiss Faculty of Life Sciences, Department of Biochemistry and Molecular Biology, Tel Aviv University, Tel Aviv, Israel

The GroEL–GroES chaperonin system is probably one of the most studied chaperone systems at the level of the molecular mechanism. Since the first reports of a bacterial gene involved in phage morphogenesis in 1972, these proteins have stimulated intensive research for over 40 years. During this time, detailed structural and functional studies have yielded constantly evolving concepts of the chaperonin mechanism of action. Despite of almost three decades of research on this oligomeric protein, certain aspects of its function remain controversial. In this review, we highlight one central aspect of its function, namely, the active intermediates of its reaction cycle, and present how research to this day continues to change our understanding of chaperonin-mediated protein folding.

Keywords: chaperonin, GroEL, GroES, protein folding, football, symmetric, chaperone

OPEN ACCESS

Edited by:
Anat Ben-Zvi,
Ben-Gurion University of the Negev, Israel

Reviewed by:
Matthias Peter Mayer,
Heidelberg University, Germany
Walid A. Houry,
University of Toronto, Canada

****Correspondence:***
Celeste Weiss
celeste@tauex.tau.ac.il
Abdussalam Azem
azema@tauex.tau.ac.il

Specialty section:
This article was submitted to Protein Folding, Misfolding and Degradation, a section of the journal Frontiers in Molecular Biosciences

Received: *10 October 2016*
Accepted: *23 November 2016*
Published: *08 December 2016*

Citation:
Weiss C, Jebara F, Nisemblat S and Azem A (2016) Dynamic Complexes in the Chaperonin-Mediated Protein Folding Cycle. Front. Mol. Biosci. 3:80. doi: 10.3389/fmolb.2016.00080

INTRODUCTION

Extensive studies carried over the years to uncover the mechanism behind functioning of the bacterial GroEL/GroES chaperonins led to a generally accepted description of their pathway of operation. The individual components that assemble to form the active complexes have been crystallized and, the interactions that mediate formation of the complexes have been clearly described. Yet, due to the highly dynamic nature of the system, many aspects of their operation remain obscure, and conflicting models describing their function are endorsed. Major controversy in the field is related to nature of the active species in the chaperonin-mediated protein folding cycle: Is it really a case of mutually exclusive models, as many think i.e., is the active form either a symmetrical complex (American football-like complex) or an asymmetric complex (bullet-shaped complex)? Are there additional factors that affect the active species? Are there additional species that participate in the cycle? The discovery of divergent chaperonins in chloroplast and mitochondria has added an additional dimension to this discussion. Do all type I chaperonins operate utilizing the same functional mechanism? In this review, we present the evolution of our understanding of the chaperonin cycle and attempt to convey the fine differences between the two major views of the GroEL–GroES reaction mechanism. We also show how the study of organellar chaperonins can contribute to our understanding of the mechanism by which type I chaperonins carry out their protein folding function.

THE KEY PLAYERS

The name chaperonins was coined almost three decades ago to describe the 60 kDa heat shock protein family, a group of ubiquitous proteins that share primary sequence homology, in some cases as low as 20–30% (Hemmingsen et al., 1988; Hill and Hemmingsen, 2001). They are divided into two groups: type I chaperonins and type II chaperonins. The latter is found in the eukaryotic cytosol (CCT and TCP-1) and Archaea, while type I is located in bacteria, mitochondria, and chloroplasts (Hill and Hemmingsen, 2001). The primary role of chaperonins is to prevent aggregation of nascent and misfolded polypeptides and ultimately facilitate their correct (re) folding (Goloubinoff et al., 1989a,b; Horwich et al., 2007; Saibil et al., 2013; Hayer-Hartl et al., 2016). How this occurs is still not completely understood and is the topic of much debate (Jewett and Shea, 2010), however, accumulating evidence suggests that in the case of misfolded proteins, the chaperonin exerts an unfoldase action on the protein, overcoming the free energy barrier (Todd et al., 1996; Walter et al., 1996; Finka et al., 2016). In addition, to the major protein-folding activities, moonlighting functions were also reported for plant and various bacterial systems harboring multiple chaperonin homologs (Lund, 2009; Henderson et al., 2013; Vitlin Gruber et al., 2013; Fares, 2014). The most widely studied prototype at the mechanistic level is the GroEL chaperonin of *Escherichia coli*. Its ∼60 kDa subunits assemble into barrel-shaped structures built of two heptameric rings (Hendrix, 1979; Höhn and Wuttke, 1979; Braig et al., 1994; Xu et al., 1997) composed of identical subunits. Each subunit contains three functional domains: the equatorial domain, site of the ATP binding pocket; the apical domain, which binds substrate and GroES; the intermediate domain, which connects the previous two and allows for dynamic structural changes within the molecule (**Figure 1**). The tetradecameric cylinders harbor the binding sites for unfolded/misfolded substrate proteins, which reside inside the barrel lumen (the Anfinsen cage; Buckle et al., 1997; Chaudhuri and Gupta, 2005; Chen et al., 2013). Due to its double ring assembly, each GroEL molecule can bind two substrate molecules with high affinity (Viitanen et al., 1992; Llorca et al., 1997; Taguchi et al., 2004). In the absence of necessary co-factors, some substrate proteins can bind tightly to the GroEL molecule for extended periods of time in an unfolded conformation (Goloubinoff et al., 1989a; Viitanen et al., 1992; Hartman et al., 1993; Hartmann and Eisenstein, 2000). The folding reaction proceeds through multiple steps, during which the chaperone undergoes major ordered and concerted conformational changes (Hartman et al., 1993; Weissman et al., 1994). The driving force for these conformational changes, as well as their timing, is provided by ATP hydrolysis and the binding of the co-chaperonin GroES (Todd et al., 1994). The latter is itself an oligomeric protein, which assembles into a single heptameric ring arranged in a dome-like structure (Hunt et al., 1996; Mande et al., 1996).

THE MAJOR COMPLEXES

Early after the discovery of chaperonins, it became clear that modulation of GroEL activity is governed by complex formation with GroES, which occurs only following nucleotide-induced conformational changes in the GroEL oligomer (Goloubinoff et al., 1989a,b; Roseman et al., 2001). This discovery was followed by extensive research aimed at identifying the active form of the GroEL–GroES complex. In their pioneering study, Langer and coworkers used EM to identify two forms of the chaperonin *in vitro*: the apo form, consisting of the GroEL tetradecamer alone, without GroES, and a complex containing one tetradecamer of GroEL bound to one GroES heptamer, formed in the presence of ADP (Langer et al., 1992). This form was suggested to be the active form of the system and became known as the asymmetric, bullet-shaped complex (Langer et al., 1992). Subsequently, a third chaperonin complex was observed in the presence of ATP, by several groups (Azem et al., 1994b; Harris et al., 1994; Llorca et al., 1994; Schmidt et al., 1994). The third form is composed of one GroEL barrel sandwiched in between two GroES heptamers, in a symmetric complex, known as the "football" (American)—like complex. High-resolution crystal structures were obtained for all three forms over the years (**Figure 1**) (Braig et al., 1994, 1995; Boisvert et al., 1996; Xu et al., 1997; Chen and Sigler, 1999; Bartolucci et al., 2005; Fei et al., 2013, 2014; Koike-Takeshita et al., 2014). In these studies, contacts between the subunits within rings and between GroEL/GroES oligomers have been delineated. More importantly, structural changes that occur during the reaction cycle have also been elucidated, through the analysis of various nucleotide-bound forms (Roseman et al., 1996, 2001; Ranson et al., 2001, 2006; Clare et al., 2009, 2012). It has become clear from the vast number of studies that the system is very dynamic in the presence of ATP, and what we are able to capture at any one point, in the test tube, may not necessarily reflect the only active form of the reaction (Todd et al., 1994; Yang et al., 2013; Taguchi, 2015; Yamamoto and Ando, 2016). Indeed, the concentration and type of nucleotide, the presence of mono- and divalent cations and other parameters may determine the form of the complex that is detected and efficiency of protein folding activity (Todd et al., 1993; Azem et al., 1994a, 1995; Diamant et al., 1995; Engel et al., 1995). In a single cycle of ATP hydrolysis, GroEL will bind one or two substrate protein monomers, bind one or two GroES heptamers, bind and hydrolyze 14 ATP, fold the substrate protein, and eject the bound components, all in a matter of seconds (**Figure 2**). What we observe in the standard biophysical examination is the steady state levels of the complexes with a strong bias for the rate-limiting complex of the cycle under the tested conditions (Todd et al., 1994; Fei et al., 2013; Yang et al., 2013; Taguchi, 2015; Yamamoto and Ando, 2016).

THE REACTION CYCLE

If the forms that we observe in the test tube do not necessarily reflect the only present or active ones, how can we accurately map out the reaction cycle of the system? The answer to this question comes from numerous kinetic and mechanistic studies (for a review see Skjærven et al., 2015; Taguchi, 2015) that enable us to peek into what is really happening in order to identify shorter-lived complexes. To simplify the arguments, we will focus on events that occur in the presence of unfolded substrate protein. Assuming that we have initiated the cycle with the simplest component, the apo GroEL, then the next step will be binding

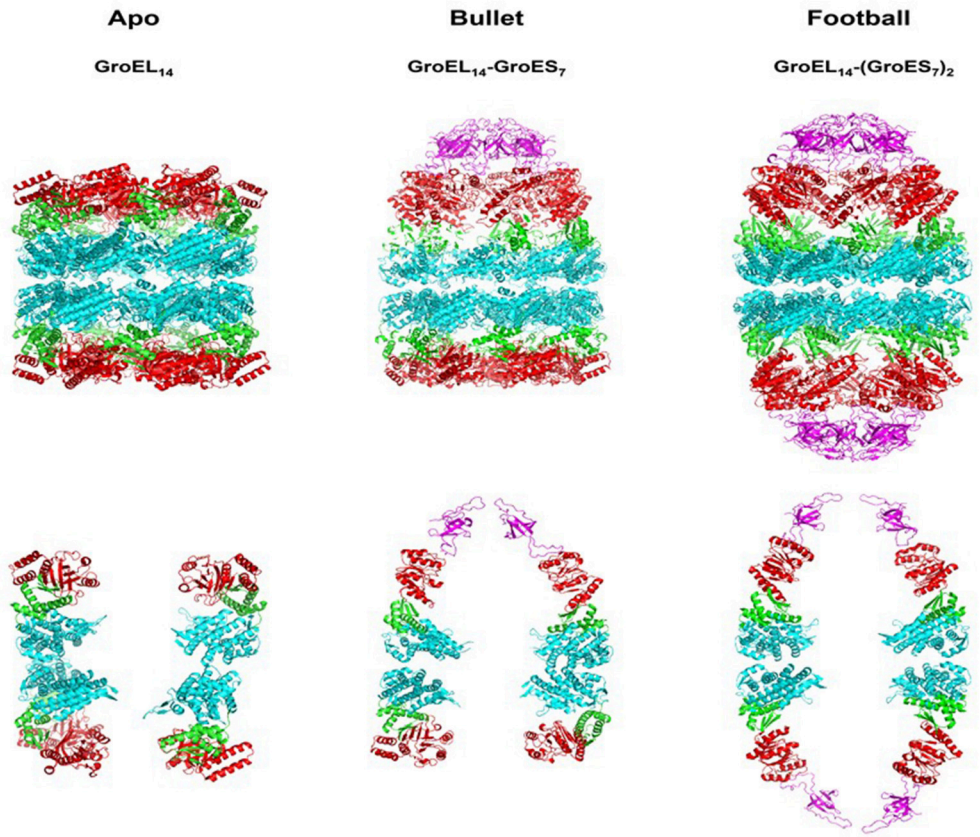

FIGURE 1 | Crystallographic models showing the architecture of the major chaperonin complexes. Left figure, unliganded, apo $GroEL_{14}$, PDB code 4WGL; Center figure, $GroEL_{14}$ with one bound $GroES_7$ co-chaperonin ("bullet"), PDB code 1AON; right figure, $GroEL_{14}$ with two bound GroES co-chaperonin heptamers ("football"), PDB code 4PKO. The GroES co-chaperonin is colored purple. The three domains of each GroEL subunit are color coded as follows: Apical domain, red; Equatorial domain, cyan; Intermediate domain, green. The top row of figures shows the full structure of each oligomer. The bottom row presents two subunits of each ring, in order to better visualize the spatial orientation of each subunit and its domains. The figure was generated using the PyMOL program (The PyMOL Molecular Graphics System, version 1.5.0.4; Schrödinger, LLC; available at www.pymol.org).

of ATP and/or substrate protein followed by GroES binding, which leads to formation of the folding-competent form. What follows this step constitutes the crux of the controversy. The canonical view suggested that the complex moves through the asymmetric "bullet" cycle (**Figure 2A**) (Horwich et al., 2006; Hayer-Hartl et al., 2016) while an alternative understanding suggested that the reaction proceeds via the symmetric "football" cycle (**Figure 2B**) (for reviews see Grallert and Buchner, 2001; Taguchi, 2015).

In the first model, the GroEL tetradecamer alternates between the bullet complex and the apo form, complexed with nucleotide. An important feature of this mechanism is the sequential nature, by which binding of ATP and substrate protein to the *trans* ring stimulates release of GroES, ADP and sequestered substrate from the *cis* ring (Rye et al., 1999). According to this model, the strong negative cooperativity in nucleotide binding between the two GroEL rings (Gruber and Horovitz, 2016) ensures that nucleotide binding to one ring will suppress nucleotide binding and hydrolysis in the opposing ring (Horwich et al., 2007). Thus, a complex with nucleotide and GroES bound on both sides will not form. For many years, this model was almost universally accepted as that which accurately describes the GroEL reaction cycle.

In an alternative model, known as the symmetrical "football" model, the complex alternates between the symmetric complex and the asymmetric form. Despite the negative cooperativity in nucleotide binding that exists between the two rings, conformations with ATP occupying both rings have been described (Clare et al., 2012), along with numerous reports of football structures, which have GroES bound to both sides (Azem et al., 1994b; Harris et al., 1994; Llorca et al., 1994; Schmidt et al., 1994). The involvement of these species in refolding was inferred from many early kinetic studies on GroE-mediated refolding to their native state of foldable substrates such as Rubisco, mMDH, and a maltose binding protein variant, all of which demonstrated a clear correlation between the efficiency of refolding and the occurrence of symmetric GroEL14/GroES14 complexes (Azem et al., 1995; Sparrer et al., 1997; Ben-Zvi et al., 1998; Beissinger et al., 1999).

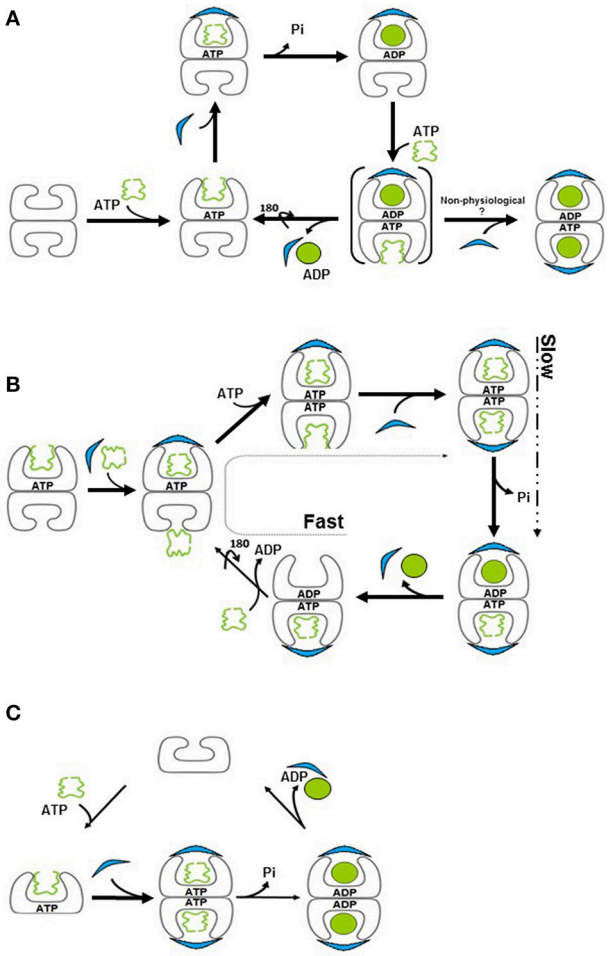

FIGURE 2 | Models for the chaperonin reaction cycle. (A) Unfolded protein binds to the apo ("brick") form of GroEL and is capped by GroES in the presence of ATP, forming the "*cis*" ring. Binding of ATP to the opposite, "*trans*" ring induces release of GroES, ADP and folded protein from the "cis" ring, such that protein folding cycles between one side and the other. Brackets signify a transient species. **(B)** In the presence of substrate protein, ADP to ATP exchange is extremely rapid, resulting in formation of, a symmetric "football" intermediate, in which protein folding takes place simultaneously in both rings. ATP hydrolysis is now the slower, rate-limiting step, resulting in the accumulation of the football form. This form reverts briefly to a bullet conformation upon ATP hydrolysis. **(C)** The mitochondrial chaperonin exists in equilibrium between single- and double-ringed forms. Upon binding of ATP and GroES, the equilibrium is shifted to the double-ringed form. Protein folding takes place in both chambers and release of the cochaperonin transpires upon ATP hydrolysis.

Were the symmetric complexes to represent a side-abortive reaction or dead end, then one would not expect to see such a correlation, rather, the opposite of what was observed. This correlation was substantiated by sophisticated mechanistic studies demonstrating the importance of the symmetric intermediate in the protein folding cycle (Koike-Takeshita et al., 2008; Sameshima et al., 2010a; Takei et al., 2012; Yang et al., 2013; Ye and Lorimer, 2013; Fei et al., 2014; Yamamoto and Ando, 2016).

RECENT DEVELOPMENTS AND OUTSTANDING QUESTIONS

Earlier studies showed that in the presence of substrate, the chaperonin complex behaves differently than in its absence (Motojima and Yoshida, 2003; Motojima et al., 2004). Further investigation demonstrated that substrate protein facilitates the formation of symmetric, football complexes (Sameshima et al., 2010a). Recent studies using FRET-based analyses concluded that the substrate protein accelerates ADP exchange, in the complex (Ye and Lorimer, 2013; Fei et al., 2014). Thus, the football model posits that if we follow the kinetics of formation and dissociation of cycle intermediates, we will find that both exist in solution (symmetrical and asymmetrical complexes). However, when we use steady state analyses to detect complexes, the form that precedes the rate-limiting step is that which will primarily be observed. Since ADP exchange in the presence of substrate protein occurs very fast relative to ATP hydrolysis, the major species observed in the presence of substrate protein is the football (Takei et al., 2012; Ye and Lorimer, 2013; Iizuka and Funatsu, 2016; **Figure 2B**). In the absence of substrate protein, the rate-limiting step is the release of ADP, leading to population of the species preceding this step, the asymmetric form.

Is function of the two rings coordinated or do they function as independent folding chambers? Consistent with conclusions of early kinetic studies, single-molecule analyses demonstrate that the first GroES to interact with GroEL is not necessarily the first one to dissociate from the symmetric complex. Rather, the dissociation may occur randomly (Corrales and Fersht, 1996; Sameshima et al., 2010b). A new study using state of the art AFM to dissect molecular events related to GroES binding revealed that that inherently different types of football species can exist, and they will alternate or not, in release of GroES, depending upon the nature of the specific football species (Yamamoto and Ando, 2016). The authors postulate that complete exchange of seven ADPs with seven ATPs ensures that the system goes through an alternating pathway, while incomplete exchange of nucleotide at the *trans*-ring may cause the cycle to go through a non-alternating pathway in which the newly bound GroES dissociates first.

Although the above studies suggest that GroEL may function as two independent folding chambers, a number of facts indicate that the picture is not entirely clear. Firstly, why would such an elaborate system of cooperativity be conserved in *E. coli* if it is not essential? In the classic model, negative cooperativity is taken to its extreme, so that nucleotide binding on one ring completely precludes binding in the opposing ring (Horwich, 2011). But perhaps the effect is not so drastic. In fact, when initial rates of ATP hydrolysis were measured in GroEL as a function of ATP concentration, two transitions were observed, with respective midpoints of 16 and 160 μM (Yifrach and Horovitz, 1995). This data suggests that, despite negative cooperativity, both sides are expected to be saturated with nucleotide under most experimental or cellular conditions. Even in the presence of 0.5 mM ADP (which is inhibitory for refolding and prevents football formation) and 1.5 mM ATP, a majority of football species was observed, which would require that nucleotide be

bound to both rings (Azem et al., 1995). However, it is still possible that negative cooperativity retained in this structure, may contribute to alternating release of GroES, resulting in a more efficient machine. This would be consistent with the fact that the majority of GroES release was shown to occur via polarity change (69%) by way of a football complex (Yamamoto and Ando, 2016). Another reason for retaining such a cooperative system could be the fact that GroEL is able to fold large proteins that cannot be accommodated inside the cavity underneath the GroES (Chaudhuri et al., 2009; Dahiya and Chaudhuri, 2014; Pastor et al., 2016). In this instance, it is possible that release of the *cis*-bound substrate must be induced by *trans* binding of substrate, ATP and GroES in a fully alternating mechanism, although in this case, the folding protein would not have the benefit of encapsulation.

THE PHYSIOLOGICAL RELEVANCE

It is evident, as discussed above, that at least *in vitro*, both types of complexes, symmetrical and asymmetrical, co-exist. Thus, the debate has changed its focus to the physiological relevance of the various forms observed. It has been well established that the velocity of the GroEL–GroES reaction cycle and the partitioning between various complexes depends on many important factors such as concentration and ratio of nucleotide, as well as concentrations of magnesium and potassium (reviewed in Grallert and Buchner, 2001; Sameshima et al., 2008, substrate protein Sameshima et al., 2010a; Yang et al., 2013; Ye and Lorimer, 2013; Fei et al., 2014, GroEL and GroES Azem et al., 1994b). The latter two are often expressed as ratios, but this could be misleading. In an *E. coli* cell under normal conditions, the concentration of GroEL is estimated to be $\sim$35 μM protomer (Lorimer, 1996). This concentration can be even much higher under conditions of heat stress. To the best of our knowledge, most *in vitro* assays of GroEL are carried out at concentrations much $<$10 μM for the chaperonin. In most biophysical studies, the concentrations used are on the order of 1 μM and even much less. At these concentrations, we know that the chloroplast and mitochondrial chaperonins dissociate to monomers in the presence of ATP (Bloom et al., 1983; Lissin, 1995; Viitanen et al., 1998; Bonshtien et al., 2009). Since some oligomers or complexes may dissociate upon dilution, we cannot assume that we are working under the exact physiological conditions or that the species that we observe necessarily reflect those relevant to the cell. Moreover, the local concentrations of the above and other small effectors are difficult to determine *in vivo* in a precise manner, making it even more complicated to define the active species. Another factor that may affect the oligomeric state includes temperature (Goloubinoff et al., 1997; Llorca et al., 1998). One way of investigating the physiological relevance of folding intermediates would be to follow the reaction cycle *in vivo*, not an easy task at all. The only laboratory with a monopoly on physiological conditions is the cell itself. Until then, the significance of the *in vitro* experiments for the actual situation *in vivo* will remain an open question.

DIVERGENT MECHANISMS? INSIGHT FROM STRUCTURAL STUDIES OF THE MITOCHONDRIAL CHAPERONIN

The human mitochondria harbor a type I chaperonin system (Hsp60), which is related, at least at the primary sequence level, to the bacterial machinery. Surprisingly, the mitochondrial chaperonin was isolated as single ring and it was traditionally regarded as active in this form (Nielsen and Cowan, 1998). However, subsequent studies using analytical ultracentrifugation and electron microscopy showed that the protein exists in dynamic equilibrium between single and double rings (Levy-Rimler et al., 2001; Vilasi et al., 2014). While Hsp60 is detected predominantly as a single ring, upon addition of ATP and mitochondrial co-chaperonin, the equilibrium is shifted toward formation of double-ringed, football shaped structures (Levy-Rimler et al., 2001). This observation again reinforces the relevance of working as close as possible to physiological conditions. However, at concentrations that are used routinely in the field, the mitochondrial chaperonin dissociates not only to single rings but also to 60 kDa monomers (Viitanen et al., 1998). The fact that most of the apo-protein is single ringed, even in the presence of bound substrate, while in the presence of ATP and co-chaperonin the protein oligomerizes to primarily the football form, presents an additional challenge to the prevailing theory of chaperonin function, since the complex does not even seem to pass through the asymmetric, bullet-shaped complex. Instead, a small amount of "half footballs" are observed- one ring of Hsp60 bound to one ring of Hsp10 (Viitanen et al., 1998). Similar structures were observed for the *Thermus thermophilus* chaperonin as well (Ishii et al., 1995). This suggests that the mitochondrial homolog may function using its own unique reaction mechanism, in which the tetradecamer exists as a football in its protein-folding state, but dissociates into two single rings at some point during the cycle (**Figure 2C**). Dissociation to single rings was observed previously both for mHsp60 (Levy-Rimler et al., 2002) and for Cpn60 from *T. thermophilus* (Todd et al., 1995; Taguchi, 2015). For mHsp60, hydrolysis of ATP to ADP was proposed to cause a drastic decrease in co-chaperonin binding, allowing rapid dissociation of the mitochondrial Hsp10 and release of the encapsulated protein (Nielsen and Cowan, 1998).

Additional evidence for a unique mechanism can be gleaned from the recent crystal structure of a mitochondrial Hsp60 variant in complex with Hsp10, which crystallized as a football complex that displays one subunit in a different conformation than the other six in the ring (Nisemblat et al., 2015). This is in stark contrast to GroEL, for which one hallmark of its mechanism is the high level of cooperativity between subunits in each ring, which results in their concerted movement (Saibil et al., 2013). Moreover, the crystallized mHsp60–mHsp10 structure shows ADP in all the 14 sites, a conformation which cannot exist for GroEL–GroES due to the strong inter-ring negative cooperativity of nucleotide binding. Finally, in this football structure, the surface contact area between the two rings is much more extensive than for the GroEL football or bullet (Nisemblat

et al., 2015). Such an extensive interface is not consistent with the weak inter-ring interaction observed upon binding of ATP to the second ring of GroEL (Clare et al., 2012). Thus, a large body of evidence suggests that the mitochondrial chaperonin may have evolved a unique mechanism related to its specific functions. This mechanism seems to involve primarily football structures during the folding cycle that alternate with half footballs and single rings.

More recently, a novel phage-encoded Cpn60 was described which was also proposed to function via single ringed intermediates. In this case, the apo form of the chaperonin is tetradecameric. However, upon nucleotide binding, the oligomer dissociates into two heptameric rings with a largely expanded cavity, able to accommodate larger substrate proteins than other known chaperonins (Molugu et al., 2016). Thus, similar to what was proposed for the mitochondrial and *T. thermophilus* chaperonins, phi-EL seems to incorporate a single-ringed intermediate in its reaction cycle.

CONCLUDING REMARKS

Although a large body of data has accumulated concerning the chaperonin system and its mechanism of action, there are still a number of open questions concerning its reaction cycle(s) and the nature of the active species. The existence of different species in the functional cycle is now almost universally accepted and has paved the way for research into the role of each species in the molecular mechanism. Cutting-edge technologies applied to this system are allowing dissection of the protein folding events at the molecular level, describing how both symmetric and asymmetric species cooperate to facilitate protein folding. Investigation of GroEL homologs from different systems has also contributed interesting twists to the discussion of chaperonin mechanism. However, despite the wealth of research on the chaperonin system, most studies to date have been carried out *in vitro* on the *E. coli* GroEL and GroES. It will be intriguing to examine in depth the mechanistic divergence of organellar chaperonins from the *E. coli* paradigm at the molecular level and try to understand what advantages they provide to their respective systems. Analysis of the mitochondrial Hsp60 has already highlighted involvement of the symmetric football structure in the reaction cycle, as well as possible half-footballs. It will also be interesting to analyze intermediates in the highly complex chloroplast chaperonin system, for which multiple homologous products are expressed for both the GroEL- and GroES-like genes, forming a variety of labile hetero-oligomeric complexes *in vitro*.

AUTHOR CONTRIBUTIONS

CW, AA, SN, and FJ wrote the paper. FJ and SN designed the figures.

FUNDING

This work was funded by the Israel Science Foundation (ISF-1507/13) and the United States - Israel Binational Science Foundation (BSF-2015214).

REFERENCES

Azem, A., Diamant, S., and Goloubinoff, P. (1994a). Effect of divalent cations on the molecular structure of the GroEL oligomer. *Biochemistry* 33, 6671–6675.

Azem, A., Diamant, S., Kessel, M., Weiss, C., and Goloubinoff, P. (1995). The protein-folding activity of chaperonins correlates with the symmetric GroEL14(GroES7)2 heterooligomer. *Proc. Natl. Acad. Sci. U.S.A.* 92, 12021–12025. doi: 10.1073/pnas.92.26.12021

Azem, A., Kessel, M., and Goloubinoff, P. (1994b). Characterization of a functional GroEL14(GroES7)2 chaperonin hetero-oligomer. *Science* 265, 653–656.

Bartolucci, C., Lamba, D., Grazulis, S., Manakova, E., and Heumann, H. (2005). Crystal structure of wild-type chaperonin GroEL. *J. Mol. Biol.* 354, 940–951. doi: 10.1016/j.jmb.2005.09.096

Beissinger, M., Rutkat, K., and Buchner, J. (1999). Catalysis, commitment and encapsulation during GroE-mediated folding. *J. Mol. Biol.* 289, 1075–1092. doi: 10.1006/jmbi.1999.2780

Ben-Zvi, A. P., Chatellier, J., Fersht, A. R., and Goloubinoff, P. (1998). Minimal and optimal mechanisms for GroE-mediated protein folding. *Proc. Natl. Acad. Sci. U.S.A.* 95, 15275–15280. doi: 10.1073/pnas.95.26.15275

Bloom, M. V., Milos, P., and Roy, H. (1983). Light-dependent assembly of ribulose-1,5-bisphosphate carboxylase. *Proc. Natl. Acad. Sci. U.S.A.* 80, 1013–1017. doi: 10.1073/pnas.80.4.1013

Boisvert, D. C., Wang, J., Otwinowski, Z., Horwich, A. L., and Sigler, P. B. (1996). The 2.4 A crystal structure of the bacterial chaperonin GroEL complexed with ATP gamma S. *Nat. Struct. Biol.* 3, 170–177.

Bonshtien, A. L., Parnas, A., Sharkia, R., Niv, A., Mizrahi, I., Azem, A., et al. (2009). Differential effects of co-chaperonin homologs on cpn60 oligomers. *Cell Stress Chaperones* 14, 509–519. doi: 10.1007/s12192-009-0104-2

Braig, K., Adams, P. D., and Brünger, A. T. (1995). Conformational variability in the refined structure of the chaperonin GroEL at 2.8 A resolution. *Nat. Struct. Biol.* 2, 1083–1094. doi: 10.1038/nsb1295-1083

Braig, K., Otwinowski, Z., Hegde, R., Boisvert, D. C., Joachimiak, A., Horwich, A. L., et al. (1994). The crystal structure of the bacterial chaperonin GroEL at 2.8 A. *Nature* 371, 578–586.

Buckle, A. M., Zahn, R., and Fersht, A. R. (1997). A structural model for GroEL-polypeptide recognition. *Proc. Natl. Acad. Sci. U.S.A.* 94, 3571–3575. doi: 10.1073/pnas.94.8.3571

Chaudhuri, T. K., and Gupta, P. (2005). Factors governing the substrate recognition by GroEL chaperone: a sequence correlation approach. *Cell Stress Chaperones* 10, 24–36. doi: 10.1379/CSC-64R1.1

Chaudhuri, T. K., Verma, V. K., and Maheshwari, A. (2009). GroEL assisted folding of large polypeptide substrates in *Escherichia coli*: present scenario and assignments for the future. *Prog. Biophys. Mol. Biol.* 99, 42–50. doi: 10.1016/j.pbiomolbio.2008.10.007

Chen, D. H., Madan, D., Weaver, J., Lin, Z., Schröder, G. F., Chiu, W., et al. (2013). Visualizing GroEL/ES in the act of encapsulating a folding protein. *Cell* 153, 1354–1365. doi: 10.1016/j.cell.2013.04.052

Chen, L., and Sigler, P. B. (1999). The crystal structure of a GroEL/peptide complex: plasticity as a basis for substrate diversity. *Cell* 99, 757–768. doi: 10.1016/S0092-8674(00)81673-6

Clare, D. K., Bakkes, P. J., van Heerikhuizen, H., van der Vies, S. M., and Saibil, H. R. (2009). Chaperonin complex with a newly folded protein encapsulated in the folding chamber. *Nature* 457, 107–110. doi: 10.1038/nature07479

Clare, D. K., Vasishtan, D., Stagg, S., Quispe, J., Farr, G. W., Topf, M., et al. (2012). ATP-triggered conformational changes delineate substrate-binding and -folding mechanics of the GroEL chaperonin. *Cell* 149, 113–123. doi: 10.1016/j.cell.2012.02.047

Corrales, F. J., and Fersht, A. R. (1996). Kinetic significance of GroEL14.(GroES7)2 complexes in molecular chaperone activity. *Fold. Des.* 1, 265–273.

Dahiya, V., and Chaudhuri, T. K. (2014). Chaperones GroEL/GroES accelerate the refolding of a multidomain protein through modulating on-pathway intermediates. *J. Biol. Chem.* 289, 286–298. doi: 10.1074/jbc.M113.518373

Diamant, S., Azem, A., Weiss, C., and Goloubinoff, P. (1995). Increased efficiency of GroE-assisted protein folding by manganese ions. *J. Biol. Chem.* 270, 28387–28391. doi: 10.1074/jbc.270.47.28387

Engel, A., Hayer-Hartl, M. K., Goldie, K. N., Pfeifer, G., Hegerl, R., Müller, S., et al. (1995). Functional significance of symmetrical versus asymmetrical GroEL-GroES chaperonin complexes. *Science* 269, 832–836.

Fares, M. A. (2014). The evolution of protein moonlighting: adaptive traps and promiscuity in the chaperonins. *Biochem. Soc. Trans.* 42, 1709–1714. doi: 10.1042/BST20140225

Fei, X., Yang, D., LaRonde-LeBlanc, N., and Lorimer, G. H. (2013). Crystal structure of a GroEL-ADP complex in the relaxed allosteric state at 2.7 A resolution. *Proc. Natl. Acad. Sci. U.S.A.* 110, E2958–E2966. doi: 10.1073/pnas.1311996110

Fei, X., Ye, X., LaRonde, N. A., and Lorimer, G. H. (2014). Formation and structures of GroEL:GroES2 chaperonin footballs, the protein-folding functional form. *Proc. Natl. Acad. Sci. U.S.A.* 111, 12775–12780. doi: 10.1073/pnas.1412922111

Finka, A., Mattoo, R. U., and Goloubinoff, P. (2016). Experimental milestones in the discovery of molecular chaperones as polypeptide unfolding enzymes. *Annu. Rev. Biochem.* 85, 715–742. doi: 10.1146/annurev-biochem-060815-014124

Goloubinoff, P., Christeller, J. T., Gatenby, A. A., and Lorimer, G. H. (1989a). Reconstitution of active dimeric ribulose bisphosphate carboxylase from an unfoleded state depends on two chaperonin proteins and Mg-ATP. *Nature* 342, 884–889.

Goloubinoff, P., Diamant, S., Weiss, C., and Azem, A. (1997). GroES binding regulates GroEL chaperonin activity under heat shock. *FEBS Lett.* 407, 215–219. doi: 10.1016/S0014-5793(97)00348-7

Goloubinoff, P., Gatenby, A. A., and Lorimer, G. H. (1989b). GroE heat-shock proteins promote assembly of foreign prokaryotic ribulose bisphosphate carboxylase oligomers in *Escherichia coli*. *Nature* 337, 44–47.

Grallert, H., and Buchner, J. (2001). Review: a structural view of the GroE chaperone cycle. *J. Struct. Biol.* 135, 95–103. doi: 10.1006/jsbi.2001.4387

Gruber, R., and Horovitz, A. (2016). Allosteric mechanisms in chaperonin machines. *Chem. Rev.* 116, 6588–6606. doi: 10.1021/acs.chemrev.5b00556

Harris, J. R., Plückthun, A., and Zahn, R. (1994). Transmission electron microscopy of GroEL, GroES, and the symmetrical GroEL/ES complex. *J. Struct. Biol.* 112, 216–230. doi: 10.1006/jsbi.1994.1022

Hartman, D. J., Surin, B. P., Dixon, N. E., Hoogenraad, N. J., and Høj, P. B. (1993). Substoichiometric amounts of the molecular chaperones GroEL and GroES prevent thermal denaturation and aggregation of mammalian mitochondrial malate dehydrogenase *in vitro*. *Proc. Natl. Acad. Sci. U.S.A.* 90, 2276–2280. doi: 10.1073/pnas.90.6.2276

Hartmann, W. K., and Eisenstein, E. (2000). Interaction of non-native polypeptide substrates with the *Escherichia coli* chaperonin GroEL. *Methods Mol. Biol.* 140, 97–109. doi: 10.1385/1-59259-061-6:97

Hayer-Hartl, M., Bracher, A., and Hartl, F. U. (2016). The GroEL-GroES chaperonin machine: a nano-cage for protein folding. *Trends Biochem. Sci.* 41, 62–76. doi: 10.1016/j.tibs.2015.07.009

Hemmingsen, S. M., Woolford, C., van der Vies, S. M., Tilly, K., Dennis, D. T., Georgopoulos, C. P., et al. (1988). Homologous plant and bacterial proteins chaperone oligomeric protein assembly. *Nature* 333, 330–334.

Henderson, B., Fares, M. A., and Lund, P. A. (2013). Chaperonin 60: a paradoxical, evolutionarily conserved protein family with multiple moonlighting functions. *Biol. Rev. Camb. Philos. Soc.* 88, 955–987. doi: 10.1111/brv.12037

Hendrix, R. W. (1979). Purification and properties of groE, a host protein involved in bacteriophage assembly. *J. Mol. Biol.* 129, 375–392. doi: 10.1016/0022-2836(79)90502-3

Hill, J. E., and Hemmingsen, S. M. (2001). Arabidopsis thaliana type I and II chaperonins. *Cell Stress Chaperones* 6, 190–200. doi: 10.1379/1466-1268(2001)006<0190:ATTIAI>2.0.CO;2

Höhn, K. G., and Wuttke, W. (1979). Ontogeny of catecholamine turnover rates in limbic and hypothalamic structures in relation to serum prolactin and gonadotropin levels. *Brain Res.* 179, 281–293. doi: 10.1016/0006-8993(79)90444-X

Horwich, A. L. (2011). Protein folding in the cell: an inside story. *Nat. Med.* 17, 1211–1216. doi: 10.1038/nm.2468

Horwich, A. L., Farr, G. W., and Fenton, W. A. (2006). GroEL-GroES-mediated protein folding. *Chem. Rev.* 106, 1917–1930. doi: 10.1021/cr040435v

Horwich, A. L., Fenton, W. A., Chapman, E., and Farr, G. W. (2007). Two families of chaperonin: physiology and mechanism. *Annu. Rev. Cell Dev. Biol.* 23, 115–145. doi: 10.1146/annurev.cellbio.23.090506.123555

Hunt, J. F., Weaver, A. J., Landry, S. J., Gierasch, L., and Deisenhofer, J. (1996). The crystal structure of the GroES co-chaperonin at 2.8 A resolution. *Nature* 379, 37–45.

Iizuka, R., and Funatsu, T. (2016). Chaperonin GroEL uses asymmetric and symmetric reaction cycles in response to the concentration of non-native substrate proteins. *Biophys. Physicobiol.* 13, 63–69. doi: 10.2142/biophysico.13.0_63

Ishii, N., Taguchi, H., Sasabe, H., and Yoshida, M. (1995). Equatorial split of holo-chaperonin from *Thermus thermophilus* by ATP and K+. *FEBS Lett.* 362, 121–125. doi: 10.1016/0014-5793(95)00222-U

Jewett, A. I., and Shea, J. E. (2010). Reconciling theories of chaperonin accelerated folding with experimental evidence. *Cell. Mol. Life Sci.* 67, 255–276. doi: 10.1007/s00018-009-0164-6

Koike-Takeshita, A., Arakawa, T., Taguchi, H., and Shimamura, T. (2014). Crystal structure of a symmetric football-shaped GroEL:GroES2-ATP14 complex determined at 3.8A reveals rearrangement between two GroEL rings. *J. Mol. Biol.* 426, 3634–3641. doi: 10.1016/j.jmb.2014.08.017

Koike-Takeshita, A., Yoshida, M., and Taguchi, H. (2008). Revisiting the GroEL-GroES reaction cycle via the symmetric intermediate implied by novel aspects of the GroEL(D398A) mutant. *J. Biol. Chem.* 283, 23774–23781. doi: 10.1074/jbc.M802542200

Langer, T., Pfeifer, G., Martin, J., Baumeister, W., and Hartl, F. U. (1992). Chaperonin-mediated protein folding: GroES binds to one end of the GroEL cylinder, which accommodates the protein substrate within its central cavity. *EMBO J.* 11, 4757–4765.

Levy-Rimler, G., Bell, R. E., Ben-Tal, N., and Azem, A. (2002). Type I chaperonins: not all are created equal. *FEBS Lett.* 529, 1–5. doi: 10.1016/S0014-5793(02)03178-2

Levy-Rimler, G., Viitanen, P., Weiss, C., Sharkia, R., Greenberg, A., Niv, A., et al. (2001). The effect of nucleotides and mitochondrial chaperonin 10 on the structure and chaperone activity of mitochondrial chaperonin 60. *Eur. J. Biochem.* 268, 3465–3472. doi: 10.1046/j.1432-1327.2001.02243.x

Lissin, N. M. (1995). *In vitro* dissociation of self-assembly of three chaperonin 60s: the role of ATP. *FEBS Lett.* 361, 55–60. doi: 10.1016/0014-5793(95)00151-X

Llorca, O., Galán, A., Carrascosa, J. L., Muga, A., and Valpuesta, J. M. (1998). GroEL under heat-shock. Switching from a folding to a storing function. *J. Biol. Chem.* 273, 32587–32594.

Llorca, O., Marco, S., Carrascosa, J. L., and Valpuesta, J. M. (1994). The formation of symmetrical GroEL-GroES complexes in the presence of ATP. *FEBS Lett.* 345, 181–186. doi: 10.1016/0014-5793(94)00432-3

Llorca, O., Marco, S., Carrascosa, J. L., and Valpuesta, J. M. (1997). Symmetric GroEL-GroES complexes can contain substrate simultaneously in both GroEL rings. *FEBS Lett.* 405, 195–199. doi: 10.1016/S0014-5793(97)00186-5

Lorimer, G. H. (1996). A quantitative assessment of the role of the chaperonin proteins in protein folding *in vivo*. *FASEB J.* 10, 5–9.

Lund, P. A. (2009). Multiple chaperonins in bacteria–why so many? *FEMS Microbiol. Rev.* 33, 785–800. doi: 10.1111/j.1574-6976.2009.00178.x

Mande, S. C., Mehra, V., Bloom, B. R., and Hol, W. G. (1996). Structure of the heat shock protein chaperonin-10 of *Mycobacterium leprae*. *Science* 271, 203–207.

Molugu, S. K., Hildenbrand, Z. L., Morgan, D. G., Sherman, M. B., He, L., Georgopoulos, C., et al. (2016). Ring separation highlights the protein-folding mechanism used by the phage EL-encoded chaperonin. *Structure* 24, 537–546. doi: 10.1016/j.str.2016.02.006

Motojima, F., Chaudhry, C., Fenton, W. A., Farr, G. W., and Horwich, A. L. (2004). Substrate polypeptide presents a load on the apical domains of the chaperonin GroEL. *Proc. Natl. Acad. Sci. U.S.A.* 101, 15005–15012. doi: 10.1073/pnas.0406132101

Motojima, F., and Yoshida, M. (2003). Discrimination of ATP, ADP, and AMPPNP by chaperonin GroEL: hexokinase treatment revealed the exclusive role of ATP. *J. Biol. Chem.* 278, 26648–26654. doi: 10.1074/jbc.M300806200

Nielsen, K. L., and Cowan, N. J. (1998). A single ring is sufficient for productive chaperonin-mediated folding *in vivo*. *Mol. Cell* 2, 93–99. doi: 10.1016/S1097-2765(00)80117-3

Nisemblat, S., Yaniv, O., Parnas, A., Frolow, F., and Azem, A. (2015). Crystal structure of the human mitochondrial chaperonin symmetrical football complex. *Proc. Natl. Acad. Sci. U.S.A.* 112, 6044–6049. doi: 10.1073/pnas.1411718112

Pastor, A., Singh, A. K., Fisher, M. T., and Chaudhuri, T. K. (2016). Protein folding on biosensor tips: folding of maltodextrin glucosidase monitored by its interactions with GroEL. *FEBS J.* 283, 3103–3114. doi: 10.1111/febs.13796

Ranson, N. A., Clare, D. K., Farr, G. W., Houldershaw, D., Horwich, A. L., and Saibil, H. R. (2006). Allosteric signaling of ATP hydrolysis in GroEL-GroES complexes. *Nat. Struct. Mol. Biol.* 13, 147–152. doi: 10.1038/nsmb1046

Ranson, N. A., Farr, G. W., Roseman, A. M., Gowen, B., Fenton, W. A., Horwich, A. L., et al. (2001). ATP-bound states of GroEL captured by cryo-electron microscopy. *Cell* 107, 869–879. doi: 10.1016/S0092-8674(01)00617-1

Roseman, A. M., Chen, S., White, H., Braig, K., and Saibil, H. R. (1996). The chaperonin ATPase cycle: mechanism of allosteric switching and movements of substrate-binding domains in GroEL. *Cell* 87, 241–251. doi: 10.1016/S0092-8674(00)81342-2

Roseman, A. M., Ranson, N. A., Gowen, B., Fuller, S. D., and Saibil, H. R. (2001). Structures of unliganded and ATP-bound states of the *Escherichia coli* chaperonin GroEL by cryoelectron microscopy. *J. Struct. Biol.* 135, 115–125. doi: 10.1006/jsbi.2001.4374

Rye, H. S., Roseman, A. M., Chen, S., Furtak, K., Fenton, W. A., Saibil, H. R., et al. (1999). GroEL-GroES cycling: ATP and non-native polypeptide direct alternation of folding-active rings. *Cell* 97, 325–338. doi: 10.1016/S0092-8674(00)80742-4

Saibil, H. R., Fenton, W. A., Clare, D. K., and Horwich, A. L. (2013). Structure and allostery of the chaperonin GroEL. *J. Mol. Biol.* 425, 1476–1487. doi: 10.1016/j.jmb.2012.11.028

Sameshima, T., Iizuka, R., Ueno, T., and Funatsu, T. (2010a). Denatured proteins facilitate the formation of the football-shaped GroEL-$(GroES)_2$ complex. *Biochem. J.* 427, 247–254. doi: 10.1042/BJ20091845

Sameshima, T., Iizuka, R., Ueno, T., Wada, J., Aoki, M., Shimamoto, N., et al. (2010b). Single-molecule study on the decay process of the football-shaped GroEL-GroES complex using zero-mode waveguides. *J. Biol. Chem.* 285, 23159–23164. doi: 10.1074/jbc.M110.122101

Sameshima, T., Ueno, T., Iizuka, R., Ishii, N., Terada, N., Okabe, K., et al. (2008). Football- and bullet-shaped GroEL-GroES complexes coexist during the reaction cycle. *J. Biol. Chem.* 283, 23765–23773. doi: 10.1074/jbc.M802541200

Schmidt, M., Rutkat, K., Rachel, R., Pfeifer, G., Jaenicke, R., Viitanen, P., et al. (1994). Symmetric complexes of GroE chaperonins as part of the functional cycle. *Science* 265, 656–659.

Skjærven, L., Cuellar, J., Martinez, A., and Valpuesta, J. M. (2015). Dynamics, flexibility, and allostery in molecular chaperonins. *FEBS Lett.* 589(19 Pt A), 2522–2532. doi: 10.1016/j.febslet.2015.06.019

Sparrer, H., Rutkat, K., and Buchner, J. (1997). Catalysis of protein folding by symmetric chaperone complexes. *Proc. Natl. Acad. Sci. U.S.A.* 94, 1096–1100. doi: 10.1073/pnas.94.4.1096

Taguchi, H. (2015). Reaction cycle of chaperonin GroEL via symmetric "football" intermediate. *J. Mol. Biol.* 427, 2912–2918. doi: 10.1016/j.jmb.2015.04.007

Taguchi, H., Tsukuda, K., Motojima, F., Koike-Takeshita, A., and Yoshida, M. (2004). BeF(x) stops the chaperonin cycle of GroEL-GroES and generates a complex with double folding chambers. *J. Biol. Chem.* 279, 45737–45743. doi: 10.1074/jbc.M406795200

Takei, Y., Iizuka, R., Ueno, T., and Funatsu, T. (2012). Single-molecule observation of protein folding in symmetric GroEL-(GroES)2 complexes. *J. Biol. Chem.* 287, 41118–41125. doi: 10.1074/jbc.M112.398628

Todd, M. J., Lorimer, G. H., and Thirumalai, D. (1996). Chaperonin-facilitated protein folding: optimization of rate and yield by an iterative annealing mechanism. *Proc. Natl. Acad. Sci. U.S.A.* 93, 4030–4035. doi: 10.1073/pnas.93.9.4030

Todd, M. J., Viitanen, P. V., and Lorimer, G. H. (1993). Hydrolysis of adenosine 5′-triphosphate by *Escherichia coli* GroEL: effects of GroES and potassium ion. *Biochemistry* 32, 8560–8567. doi: 10.1021/bi00084a024

Todd, M. J., Viitanen, P. V., and Lorimer, G. H. (1994). Dynamics of the chaperonin ATPase cycle: implications for facilitated protein folding. *Science* 265, 659–666.

Todd, M. J., Walke, S., Lorimer, G., Truscott, K., and Scopes, R. K. (1995). The single-ring *Thermoanaerobacter brockii* chaperonin 60 (Tbr-EL7) dimerizes to Tbr-EL14.Tbr-ES7 under protein folding conditions. *Biochemistry* 34, 14932–14941.

Viitanen, P. V., Gatenby, A. A., and Lorimer, G. H. (1992). Purified chaperonin 60 (groEL) interacts with the non-native states of a multitude of *Escherichia coli* proteins. *Protein Sci.* 1, 363–369. doi: 10.1002/pro.5560010308

Viitanen, P. V., Lorimer, G., Bergmeier, W., Weiss, C., Kessel, M., and Goloubinoff, P. (1998). Purification of mammalian mitochondrial chaperonin 60 through *in vitro* reconstitution of active oligomers. *Meth. Enzymol.* 290, 203–217. doi: 10.1016/S0076-6879(98)90020-9

Vilasi, S., Carrotta, R., Mangione, M. R., Campanella, C., Librizzi, F., Randazzo, L., et al. (2014). Human Hsp60 with its mitochondrial import signal occurs in solution as heptamers and tetradecamers remarkably stable over a wide range of concentrations. *PLoS ONE* 9:e97657. doi: 10.1371/journal.pone.0097657

Vitlin Gruber, A., Nisemblat, S., Zizelski, G., Parnas, A., Dzikowski, R., Azem, A., et al. (2013). P. falciparum cpn20 is a bona fide co-chaperonin that can replace GroES in *E. coli*. *PLoS ONE* 8:e53909. doi: 10.1371/journal.pone.0053909

Walter, S., Lorimer, G. H., and Schmid, F. X. (1996). A thermodynamic coupling mechanism for GroEL-mediated unfolding. *Proc. Natl. Acad. Sci. U.S.A.* 93, 9425–9430. doi: 10.1073/pnas.93.18.9425

Weissman, J. S., Kashi, Y., Fenton, W. A., and Horwich, A. L. (1994). GroEL-mediated protein folding proceeds by multiple rounds of binding and release of non-native forms. *Cell* 78, 693–702. doi: 10.1016/0092-8674(94)90533-9

Xu, Z., Horwich, A. L., and Sigler, P. B. (1997). The crystal structure of the asymmetric GroEL-GroES-(ADP)7 chaperonin complex. *Nature* 388, 741–750.

Yamamoto, D., and Ando, T. (2016). Chaperonin GroEL-GroES functions as both alternating and non-alternating engines. *J. Mol. Biol.* 428, 3090–3101. doi: 10.1016/j.jmb.2016.06.017

Yang, D., Ye, X., and Lorimer, G. H. (2013). Symmetric GroEL:GroES2 complexes are the protein-folding functional form of the chaperonin nanomachine. *Proc. Natl. Acad. Sci. U.S.A.* 110, E4298–E4305. doi: 10.1073/pnas.1318862110

Ye, X., and Lorimer, G. H. (2013). Substrate protein switches GroE chaperonins from asymmetric to symmetric cycling by catalyzing nucleotide exchange. *Proc. Natl. Acad. Sci. U.S.A.* 110, E4289–E4297. doi: 10.1073/pnas.1317702110

Yifrach, O., and Horovitz, A. (1995). Nested cooperativity in the ATPase activity of the oligomeric chaperonin GroEL. *Biochemistry* 34, 5303–5308. doi: 10.1021/bi00016a001

Conflict of Interest Statement: The authors declare that the research was conducted in the absence of any commercial or financial relationships that could be construed as a potential conflict of interest.

frontiers in Molecular Biosciences

REVIEW
published: 25 January 2018
doi: 10.3389/fmolb.2017.00099

Chaperonin of Group I: Oligomeric Spectrum and Biochemical and Biological Implications

*Silvia Vilasi[1], Donatella Bulone[1], Celeste Caruso Bavisotto[2,3], Claudia Campanella[2,3], Antonella Marino Gammazza[2,3], Pier L. San Biagio[1], Francesco Cappello[2,3], Everly Conway de Macario[4] and Alberto J. L. Macario[3,4]**

[1] Institute of Biophysics, National Research Council, Palermo, Italy, [2] Section of Human Anatomy, Department of Experimental Biomedicine and Clinical Neuroscience (BIONEC), University of Palermo, Palermo, Italy, [3] Euro-Mediterranean Institute of Science and Technology (IEMEST), Palermo, Italy, [4] Department of Microbiology and Immunology, School of Medicine, University of Maryland at Baltimore, and Institute of Marine and Environmental Technology (IMET), Columbus Center, Baltimore, MD, United States

Chaperonins play various physiological roles and can also be pathogenic. Elucidation of their structure, e.g., oligomeric status and post-translational modifications (PTM), is necessary to understand their functions and mechanisms of action in health and disease. Group I chaperonins form tetradecamers with two stacked heptameric rings. The tetradecamer is considered the typical functional complex for folding of client polypeptides. However, other forms such as the monomer and oligomers with smaller number of subunits than the classical tetradecamer, also occur in cells. The properties and functions of the monomer and oligomers, and their roles in chaperonin-associated diseases are still incompletely understood. Chaperonin I in eukaryotes occurs in various locations, not just the mitochondrion, which is its canonical place of residence and function. Eukaryotic Chaperonin I, namely Hsp60 (designated HSP60 or HSPD1 in humans) has, indeed, been found in the cytosol; the plasma-cell membrane; on the outer surface of cells; in the intercellular space; in biological liquids such as lymph, blood, and cerebrospinal fluid; and in secretions, for instance saliva and urine. Hsp60 has also been found in cell-derived vesicles such as exosomes. The functions of Hsp60 in all these non-canonical locales are still poorly characterized and one of the questions not yet answered is in what form, i.e., monomer or oligomer, is the chaperonin present in these non-canonical locations. In view of the steady increase in interest on chaperonopathies over the last several years, we have studied human HSP60 to determine its role in various diseases, its locations in cells and tissues and migrations in the body, and its post-translational modifications that might have an impact on its location and function. We also carried out experiments to characterize the oligomeric status of extramitochondrial of HSP60 in solution. Here, we provide an overview of our results, focusing on the oligomeric equilibrium and stability of the various forms of HSP60 in comparison with GroEL. We also discuss post-translational modifications associated with anti-cancer drugs to indicate the potential of Hsp60 in Medicine, as a biomarker and etiopathogenic factor.

Keywords: Hsp60, GroEL, monomer, heptamer, tetradecamer, post-translation modification, chaperonopathies, non-canonical locales

OPEN ACCESS

Edited by:
Abdussalam Azem,
Tel Aviv University, Israel

Reviewed by:
Peter Bross,
Aarhus University, Denmark
Ophry Pines,
Hebrew University of Jerusalem, Israel

***Correspondence:**
Alberto J. L. Macario
ajlmacario@som.umaryland.edu

Specialty section:
This article was submitted to Protein Folding, Misfolding and Degradation, a section of the journal Frontiers in Molecular Biosciences

Received: *04 November 2017*
Accepted: *28 December 2017*
Published: *25 January 2018*

Citation:
Vilasi S, Bulone D, Caruso Bavisotto C, Campanella C, Marino Gammazza A, San Biagio PL, Cappello F, Conway de Macario E and Macario AJL (2018) Chaperonin of Group I: Oligomeric Spectrum and Biochemical and Biological Implications. Front. Mol. Biosci. 4:99. doi: 10.3389/fmolb.2017.00099

Research on molecular chaperones is steadily increasing not only because they are key elements in cellular and organismal normal physiology but also because, if abnormal, they can become etiopathogenic and contribute to the development of diseases, the chaperonopathies. These are pathologic conditions in which chaperones abnormal in composition-structure (e.g., mutations or post-translational modifications), quantitative levels, location in the cell or outside it, or function (loss or excess of it, gain of new function) play an etiopathogenic role, either primary or auxiliary. Chaperonins of Group I and II have indeed been identified as pathogenic factors in a number of conditions. For example, chaperonins of Group I, the object of this review, can cause serious diseases (a subgroup of chaperonopathies that may be called chaperoninopathies) if mutated at critical sites (Bross et al., 2008; Bross and Fernandez-Guerra, 2016), or can contribute to the initiation and/or progression of certain types of cancer, and chronic and autoimmune disorders (Macario et al., 2013; Cappello et al., 2014; Wick et al., 2014; Wick, 2016; Rahman et al., 2017; van Eden et al., 2017; Calderwood, 2018; Pockley and Henderson, 2018).

While the clinical and pathological manifestations of many chaperonopathies are reasonably well-characterized, the pathogenic mechanisms underpinning the lesions observed in tissues and organs of patients are still poorly understood. For example, little is known on the impact of point-mutations on the chaperone molecule's intrinsic properties (e.g., stability in the face of stressors, ability to interact with the required partners to exercise chaperoning functions, flexibility, and oligomeric organization in solution) and chaperoning and non-chaperoning (moonlighting) functions, inside, or outside the cell. It is, therefore, imperative to elucidate the properties of the chaperone molecules under physiologic conditions and in situations resembling those occurring in patients as a required preliminary step to improving diagnosis, treatment, and prevention of chaperonopathies. Here, we briefly discuss some results pertaining to the Group I chaperonins Hsp60 and GroEL, obtained in a variety of laboratories, including ours.

The best characterized chaperonin of Group I, GroEL, forms tetradecamers with two stacked heptameric rings (Horwich et al., 2007). The tetradecamer is the typical functional complex that carries out the folding of client polypeptides. However, in mammalian cells, other forms of the Group I chaperonin, such as the monomer and oligomers with smaller number of subunits than the classical tetradecamer, are known to occur. A single ring seems to be sufficient for productive protein folding *in vivo* (Nielsen and Cowan, 1998), and the requirement of double rings football-shaped intermediates is still under debate (Viitanen et al., 1992). The properties and functions of the monomer and oligomers are also incompletely understood. Likewise, the impact of oligomeric organization on Hsp60 loss of function of some pathological situations has not yet been elucidated, despite the fact that this is a particularly interesting issue since destabilization of the mitochondrial HSP60 oligomer characterizes the MitCHAP-60 disease, a severe neurodegenerative condition associated to the Asp3Gly mutation in HSP60 (Parnas et al., 2009).

Chaperonin I in eukaryotes occurs in various locations, not just the mitochondrion, which is its canonical place of residence and function. Eukaryotic Chaperonin I, namely Hsp60 (designated HSP60 or HSPD1 in humans) has, indeed, been found in the cytosol; the plasma-cell membrane; on the outer surface of cells; in the intercellular space; in biological liquids such as lymph, blood, and cerebrospinal fluid; and in secretions, for instance saliva and urine (Cechetto et al., 2000; Cappello et al., 2008; Macario et al., 2013; Calderwood, 2018; Pockley and Henderson, 2018; more references can be found at http://hsp60.com/localization/). Extra-mitochondrial functions of HSP60 have also been observed in yeast (Kalderon et al., 2015). Hsp60 has also been found in cell-derived vesicles such as exosomes (Merendino et al., 2010; Campanella et al., 2012). The functions of Hsp60 in all these non-canonical locales are still poorly characterized and one of the questions not yet answered is in what form, i.e., monomer or oligomer, is the chaperonin present in these non-canonical locales.

Over the last several years we have studied human HSP60 in several systems to determine its location in cells and tissues, its migrations in the body, and its post-translational modifications that might have an impact on its location and function. We have also carried out experiments to elucidate the oligomeric status of human extramitochondrial HSP60 in solution and we have investigated its role in various diseases. Our observations are discussed in this brief review along with pertinent data from other laboratories.

The nomenclature of heat shock proteins and molecular chaperones is rather confusing and to facilitate the reading of this review we will use the following terms: chaperoning system is the complete set of chaperones, co-chaperones, and chaperone co-factors, and other closely interacting receptors and molecules of an organism. A chaperoning team is the functional complex formed by two or more identical or closely related subunits, e.g., the tetradecamer characteristic of GroEL and HSPD1. Teams participate in networks which consist of two or more interacting teams, e.g., Hsp70-prefoldin-Hsp90. We will use the terms HSP60 or HSPD1 for the human chaperonin of Group I, but in referring to this chaperonin in general, without specifying the species we will use Hsp60.

THE HUMAN HSP60 AND ASSOCIATED DISEASES

The realization that abnormal chaperones can cause disease opened new avenues to study chaperones and provided incentive to re-evaluate these molecules by medical researchers and practitioners (Macario and Conway de Macario, 2005). A case in point is human HSP60 because it was discovered that mutations in it caused specific diseases (Bross and Fernandez-Guerra, 2016). Noteworthy is that the ability of the mutant chaperonin to form oligomers was affected (Parnas et al., 2009). In addition, a missense mutation, Leu73Phe, of HSP10, the co-chaperone of HSP60, was recently reported to be associated to a severe

neurological and developmental disorder (Bie et al., 2016). The detailed molecular mechanism involving the mutant HSP10 that causes the lesions observed has not yet been fully elucidated. However, studies with the purified mutant protein *in vitro* demonstrated that it has poor thermal stability, and its refolding ability and resistance to proteolysis are very much impaired. The availability of this mutant offers a unique opportunity to study the impact of the mutation on the interactions between HSP10 and HSP60 and, thereby, learn about the intrinsic mechanism of formation of the complete HSP60/HSP10 complex.

Hsp60 is classically considered a mitochondrial protein with its coding gene residing in the cell nucleus. This implies that after being synthesized in the cytosol, the Hsp60 protein must migrate into mitochondria. Therefore, one may predict that there are at least two intracellular populations of Hsp60, one present in the cytosol and the other inside the organelle. In some pathological conditions, this equilibrium can be altered, with abnormal accumulation of Hsp60 in the cytosol. In addition, as mentioned above, Hsp60 has been found in other locations beyond the mitochondrion. It is generally believed that the intramitochondrial chaperoning function of Hsp60 requires the formation of tetradecamers but little is known about the structure of the chaperonin in other locations. In this brief review we examine some of the properties of the spectrum of Hsp60 forms that have been identified, monomers, heptamers, and tetradecamers. We discuss the possibility that the human HSP60 chaperonin may also function as a single ring and may form symmetrical football-shaped intermediates, similarly to GroEL.

THE HUMAN HSP60 GENE (*HSPD1*)

The human mitochondrial chaperonin HSP60 is encoded in the gene *HSPD1* (also written *hspd1*) which is localized in chromosome 2 head to head with the gene that codes for the HSP10 co-chaperonin, designated *HSP10* (also written *cpn60* or *HSPE1*), and the two genes are separated by a bidirectional promoter (Hansen et al., 2003).

Only one *HSPD1* gene and 22 *HSPD1* pseudogenes were found in the human genome (Mukherjee et al., 2010). **Figure 1** shows a Maximum Likelihood (ML) tree of mammalian Hsp60 (Cpn60) proteins, including genes and pseudogenes from human, mouse, and rat. Interestingly, ML trees built with translations of only the most conserved pseudogenes showed consistent association of the human pseudogenes with Hsp60 from primates, whereas pseudogenes from mouse and rat all associated with murid Hsp60 sequences, indicating their relatively recent origin, **Figure 2**. The human HSP60 pseudogenes are distributed over several chromosomes (1, 3, 4, 5, 6, 8, 10, 11, 12, 13, 20, and 21) but none is present on chromosome 2, in which the *HSPD1* gene is located.

While there is considerable information on the genomics of *HSPD1* available from studies directly on the human genome, knowledge of the structure and properties of the human protein has recently advanced based on the crystallization of the human mitochondrial HSP60 (Nisemblat et al., 2014, 2015), and is still mostly grounded to a considerable extent on studies of prokaryotic, especially bacterial GroEL.

GroEL

The study of Group I chaperonins was stimulated by seminal reports that appeared in the late 1970's and the 1980's. For example, a gene was identified in which certain mutations directly correlated to impairment of bacteriophage λ growth, and the gene product was found to be a 60 kDa protein, which was later named GroEL (Georgopoulos and Hohn, 1978). A similar protein was identified in chloroplasts, associated with Rubisco with an amino-acid sequence over 40% similar to GroEL (Ellis and van der Vies, 1988). This protein was characterized by "assisting" functions, which inspired the name "molecular chaperone" (Ellis et al., 1989).

In another work, it was established that a mitochondrial protein had the ability to assist protein folding and that increased in response to heat shock (McMullin and Hallberg, 1988). This protein formed two stacked heptameric rings (Ostermann et al., 1989) and was found to have the ability of self-assembling (Cheng et al., 1990). It was also proposed that these 60 kDa proteins present in chloroplasts, mitochondria, and bacteria such as *Escherichia coli*, and whose genes were heat-inducible should be named chaperonins (Hemmingsen et al., 1988). Subsequent work in many laboratories (Saibil et al., 2013; Nisemblat et al., 2015; Okamoto et al., 2015; Weiss et al., 2016; Chen et al., 2017; Illingworth et al., 2017; Ishii, 2017; Liu et al., 2017; Roh et al., 2017) unveiled the structure and chaperoning cycle of the Hsp60 chaperonins and revealed various features that are shared by these proteins, for instance the formation of rings and more complex structures made of two stacked rings with a central cavity or cage, which was found to be essential in client polypeptide folding.

The typical GroEL complex is constituted of two identical rings with seven identical subunits each, so the complete team is a homo-tetradecamer with a central cavity or cage (Hohn et al., 1979). The GroEL subunit has three domains, apical, intermediate, and equatorial. While GroEL is typically present in bacteria, similar and evolutionarily-related structures also occur in some archaea (e.g., *Methanosarcina mazei*; Conway de Macario et al., 2003), in the mitochondria of eukaryotes, for instance *Neurospora crassa* (Hutchinson et al., 1989) and humans (Hansen et al., 2003; Mukherjee et al., 2010), and in the chloroplast of plants (Dickson et al., 2000).

The chaperoning function of GroEL tetradecamers requires allosteric changes and communication between the team members, i.e., subunits and rings (Goloubinoff et al., 1989). The chaperoning mechanism, according to this model, proceeds through a series of coordinated steps and is initiated by the binding of the client polypeptide (substrate) to the apical domain via hydrophobic residues (Horwich, 2011). Then, upon binding of ATP to the equatorial domain the apical and intermediate domains rearrange allowing transition of the complex from *trans* to *cis* conformation, thus the central cavity encapsulates the substrate (**Figure 3**). The other member of the chaperoning

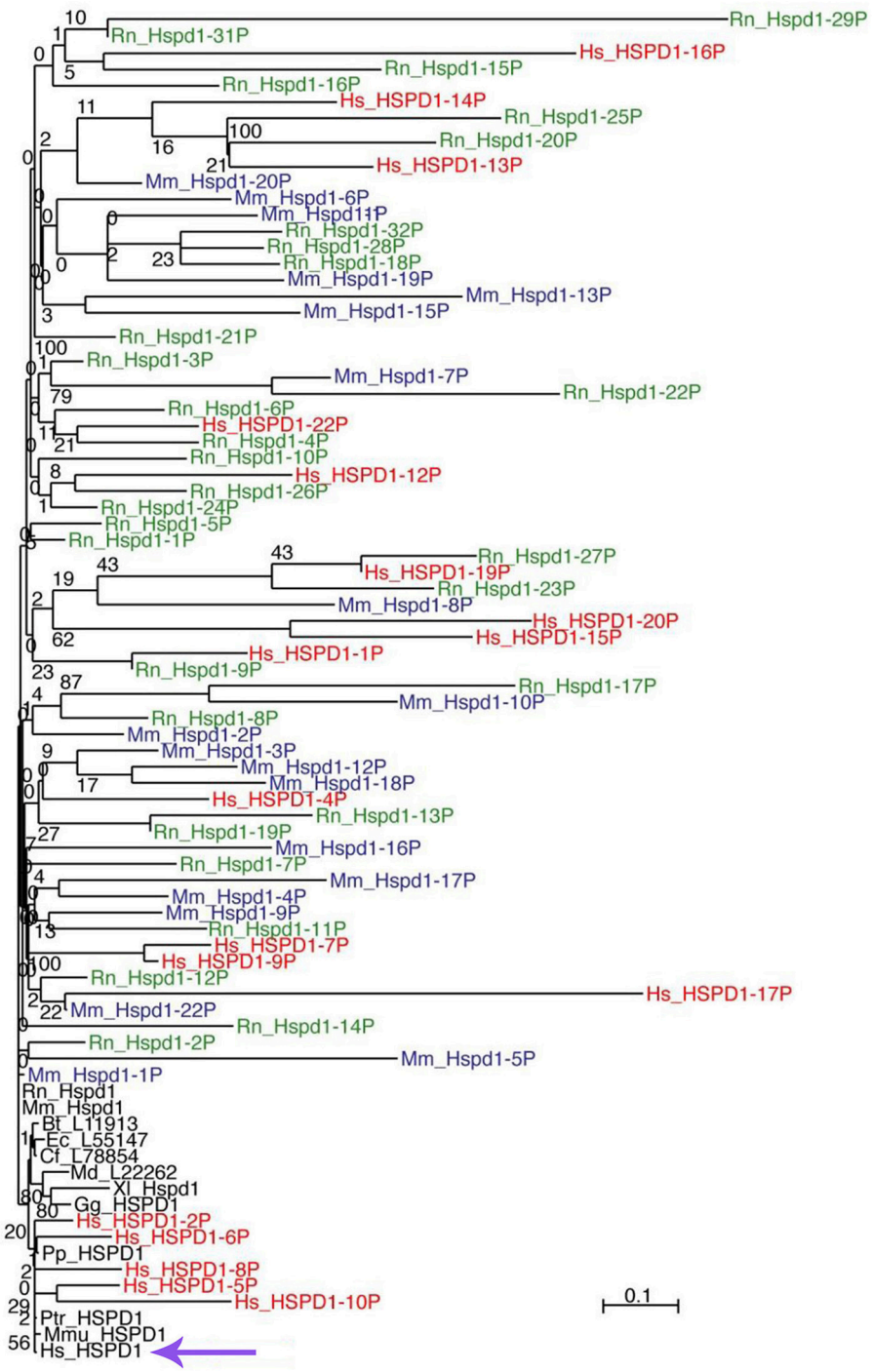

FIGURE 1 | ML tree of mammalian Hsp60 (Cpn60) sequences, including genes (black font) and pseudogenes from human (red font), mouse (blue font), and rat (green font). The scale bar represents the indicated number of substitutions per position for a unit branch length. The species tested are not all included in this representation of the tree to avoid overcrowding. In the following list of abbreviations of the names of the species tested, those shown in the figure are in bold face: **Bt**, ***Bos taurus*** (cow); **Cf,** ***Canis lupus familiaris*** (dog); Dn, *Dasypus novemcinctus* (nine-banded armadillo); Dr, *Danio rerio* (zebrafish); **Ec,** ***Equus caballus*** (horse); Ga, *Gasterosteus aculeatus* (stickleback, fish); **Gg,** ***Gallus gallus domesticus*** (chicken); **Hs,** ***Homo sapiens*** (human); La, *Loxodonta africana* (african bush elephant); **Md,** ***Monodelphis domestica*** (south american gray short-tailed opossum, marsupial); **Mm,** ***Mus musculus*** (mouse); **Mmu,** ***Macaca mulatta*** (rhesus monkey); Mmur, *Microcebus murinus* (gray mouse lemur); Oa, *Ornithorhynchus anatinus* (platypus); Ol, *Oryzias latipes* (the medaka or japanese killifish); **Pp,** ***Pongo pygmaeus*** (northwest bornean orangutan); **Ptr,** ***Pan troglodytes*** (chimpanzee); **Rn,** ***Rattus norvegicus*** (rat); Tn, *Tetraodon nigroviridis* (spotted green pufferfish); Tr, *Takifugu rubripes* (japanese pufferfish); **Xl,** ***Xenopus laevis*** (african clawed frog, amphibian); Xt, *Xenopus tropicalis* (western clawed frog, amphibian). The violet arrow at the bottom indicates the human HSPD1.

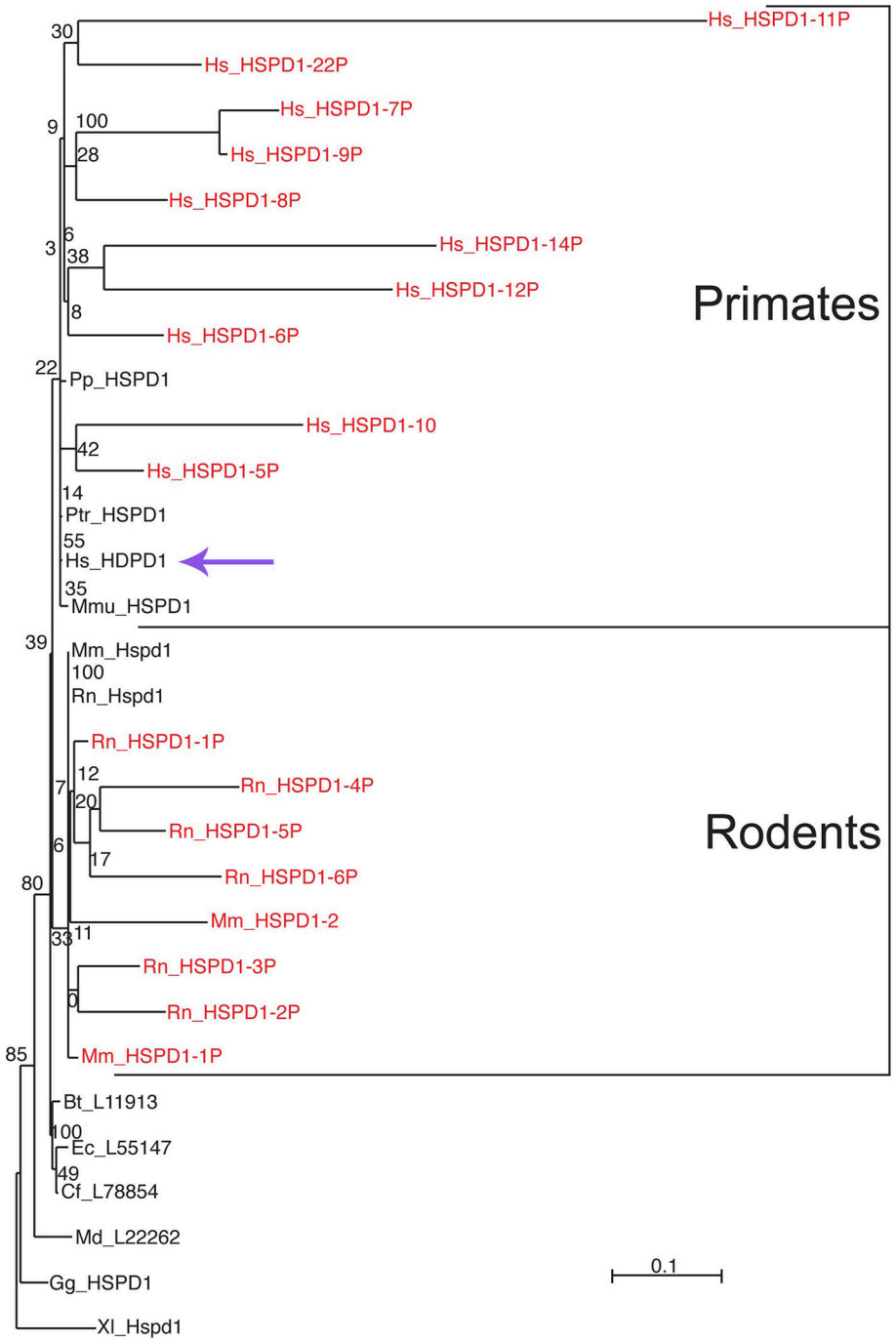

FIGURE 2 | Differential clustering of human, mouse, and rat Hsp60-related pseudogenes. Pseudogenes are in red font. Human pseudogenes are clustered with primate Hsp60 (Cpn60) sequences whereas mouse and rat pseudogenes are clustered with rodent counterparts, indicating independent evolution of these pseudogenes in these species. For species abbreviations see legend for **Figure 1**. The scale bar represents the indicated number of substitutions per position for a unit branch length. The violet arrow indicates the human HSPD1. Source: Mukherjee et al. (2010) (Original publisher BioMed Central: BMC Evol Biol.).

complex, the homo-heptameric GroES, binds the same apical hydrophobic residues, which leads to the release of the substrate into the cage for folding, using energy provided by ATP hydrolysis (**Figure 3**). ATP hydrolysis in the *cis* ring is followed by binding of ATP to the *trans* ring, which causes dissociation of the *cis* complex, thereby releasing the folded substrate, ADP, and GroES. In this model, the GroES heptamer can bind a ring only after its release from the other, so that the entire

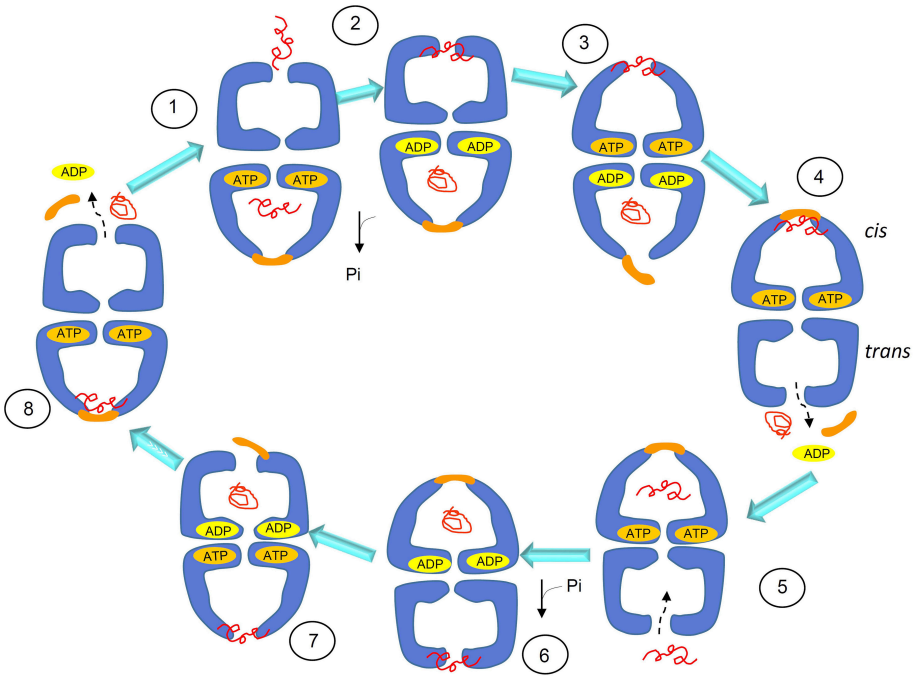

FIGURE 3 | Schematics of the substrate-folding cycle of GroEL. This model of the cycle involves asymmetric, bullet-shaped intermediates and proceeds as follows: when the substrate (the client peptide in need of assistance for folding) binds to the apical domain of one of the two rings, the bound ring rearranges to form a cis complex with GroES, allowing substrate encapsulation inside the cage and folding with energy from ATP hydrolysis. GroES binding to the *cis* ring can occur only when ADP and the folded protein are released to the outside from the cage of the *trans* ring. Therefore, the cycle intermediate is an asymetric bullet-shaped oligomeric chaperoning complex. Adapted with permission from Macmillan Publishers Ltd. Horwich (2011).

chaperoning complex has an asymmetric bullet-shaped structure (**Figure 3**). Therefore, this model of GroEL function involves two GroEL heptamers and one GroES heptamer, assembled in an asymmetric, bullet-shaped GroEL-GroES complex. This model, widely accepted for many years, is currently challenged by recent single-molecule studies that revealed the presence, during the GroEL cycle, of symmetric, football-shaped intermediates of the GroEL tetradecamer with a GroES heptamer on each end (Taguchi, 2015). These football-shaped structures were stabilized under specific experimental conditions and then crystallized and solved (Fei et al., 2014; Koike-Takeshita et al., 2014). It was found that, due to the structural features of the interface, the negative cooperativity between rings in the football-shaped complex mainly involving two D helices, is reduced as compared with the cooperativity between the rings of the bullet-shaped complex. A GroES heptamer binding in one ring is not dependent on a GroES heptamer being released from the other, and substrate folding can occur at both GroEL rings simultaneously, thus causing the formation of symmetric complexes. The presence of the symmetric complexes is not incompatible with bullet-shaped structures as they can coexist, but, as revealed by Fluorescence Resonance Energy Transfer (FRET), the presence of substrate is crucial for shifting the equilibrium toward symmetric intermediates (Sameshima et al., 2010). This role of the substrate influencing the GroEL oligomeric structural organization and function is in line with results obtained by multi-scale simulations (Coluzza et al., 2008).

Similarly to what happens for the chaperonin from the bacterium *Thermus thermophilus* (Ishii et al., 1995), in the presence of K^+ and Mg-ATP, the symmetric football-shaped complex undergoes a dynamic transition consisting of equatorial split, which leads to the formation of single rings (Koike-Takeshita et al., 2014). Although the functional role of the split is not yet fully understood, this observation could be relevant to interpret some results obtained with mammalian, e.g., human mitochondrial HSP60, as discussed later in this review.

FROM BACTERIA TO MITOCHONDRIA

In contrast to the abundance of studies on the bacterial Hsp60, research on the human counterpart had a slow start and took off when the amino-acid sequence of the human protein was found similar to those of bacterial and plant chaperonins. By means of immunofluorescence and biochemical fractionation techniques, it was shown that mammalian Hsp60 is primarily present in the mitochondrial matrix (Gupta and Austin, 1987). Despite the high degree of sequence similarity to GroEL, human HSP60 has some peculiar features in oligomer organization. By Gel Filtration and Sucrose Density Gradient Centrifugation, it was found to occur as a homo-oligomer of seven subunits of ∼440,000 Mr (Jindal et al., 1989). Single active rings were also found in other mammalian Hsp60, like that from Chinese hamster ovary (CHO) that shares a high sequence similarity with the human counterpart (Picketts et al., 1989).

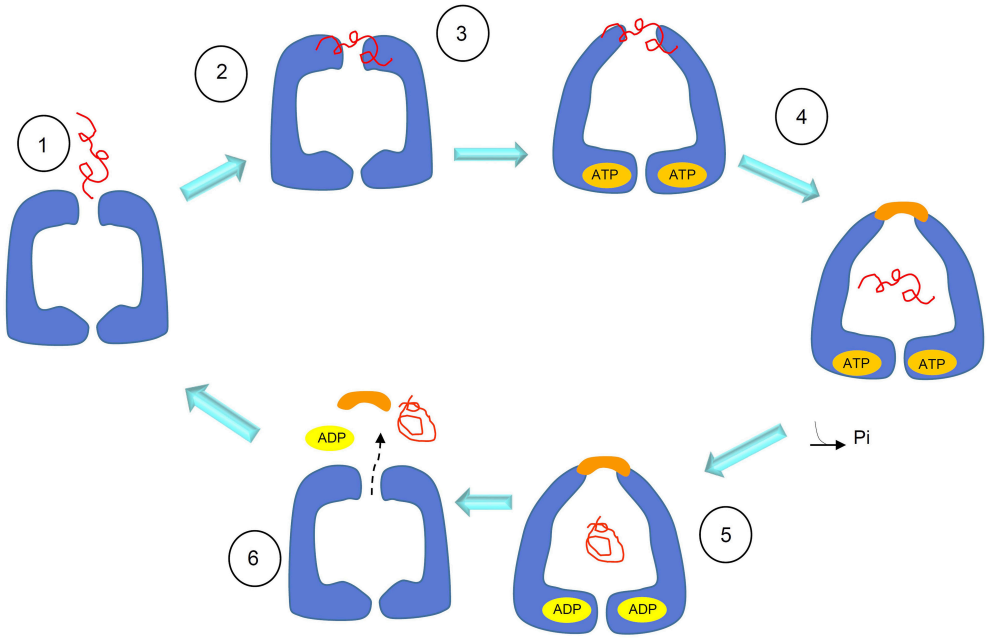

FIGURE 4 | Schematics of the substrate-folding cycle of GroEL single rings. According to this proposed mechanism, when the substrate binds to the apical domain of the single ring, the latter rearranges to form a complex with the Hsp10 heptamer. This allows substrate encapsulation and folding with energy from ATP hydrolysis. In contrast to what happens with the full, bullet-shaped complex described in **Figure 3**, the interaction between the single Hsp60 ring with the Hsp10 heptamer in the presence of ADP becomes so weak that the ring opens and both, the Hsp10 heptamer and the client-protein are released. Adapted with permission from Macmillan Publishers Ltd. Horwich (2011).

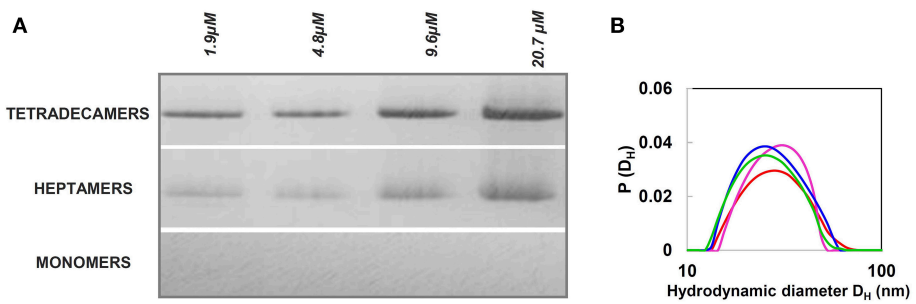

FIGURE 5 | Naïve HSP60 forms oligomers over a wide range of concentrations. **(A)** Blue Native Gel Electrophoresis (4–16%) image of naïve HSP60 in the concentration range 1.9–4.8 μM. The pattern reveals that the protein exists in two oligomeric forms independently of the concentration. **(B)** Size distribution from Dynamic Light Scattering of the naïve HSP60 at various concentrations (1.9 μM: red, 4.8 μM: green, 9.6 μM: blue, 20.7 μM: pink). Adapted from Vilasi et al. (2014). PLOS ONE, according to Creative Commons Attribution (CC BY) policy.

When a protocol to purify recombinant Hsp60 without a His-tag became available (Viitanen et al., 1992), extensive studies were performed to understand the structure and oligomeric organization of the mammalian mitochondrial chaperonin. Moreover, it became possible to cleave the N-terminal mitochondrial targeting signal (MTS) present in the eukaryotic Hsp60 and obtain the mature Hsp60 as it occurs inside mitochondria, designated mtHsp60. The protein was mainly obtained as monomers and heptamers. This seems to be a general result: in the absence of ATP and mtHsp10 (mitochondrial Hsp10, or Cpn10), mtHsp60 occurs primarily as a single ring with a mass of 440 kDa (Levy-Rimler et al., 2001). Tetradecamers would form only upon dissociation of the initial oligomers in the presence of ATP at low temperature, followed by incubation at 30°C with mtHsp10 and ATP (Viitanen et al., 1992). Surprisingly, the mammalian mtHsp60 as single toroidal ring was found to be able, in the presence of Mg-ATP and mtHsp10, of facilitating folding of non-native ribulase-P2 carboxylase, forming with it a stable complex. However, in these experiments, a two-ring complex seemed to be an obligatory participant in productive substrate folding (Viitanen et al., 1992). The formation of single rings was also detected, in the absence of substrate, in studies on human mtHSP60 (Nielsen and Cowan, 1998). By electron microscopy (EM), single rings appeared not only from

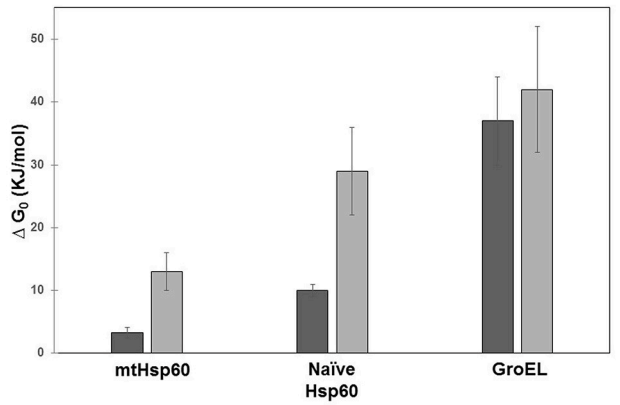

FIGURE 6 | Free energy of unfolding of mitochondrial HSP60, naïve HSP60, and GroEL. The free energy was calculated from the denaturation profile induced by guanidine hydrochloride evaluated by Circular Dichroism (CD) (dark gray) and Small X-Ray Angle Scattering (SAXS) (light gray). Details on data analysis are reported in Ricci et al. (2016, 2017). GroEL appears more stable than human chaperonins and mitochondrial mature HSP60 less stable than naïve HSP60. In contrast to GroEL, significant is the difference between results from the two techniques for the two HSP60 forms. This is due to: a) the different protein concentrations required by the two methods used (orders of magnitude $\approx 1\,\mu$M for CD and $\approx 20\,\mu$M for SAXS), which have a more marked effect on human chaperonins; and b) the data-analysis model applied, which in the case of CD considers the two-state unfolding model that has been shown to work well with GroEL.

wild type HSP60, but also as chimeric complexes composed of equatorial HSP60 and apical GroEL. Instead, wild type GroEL and chimeric complexes formed by HSP60 apical domain and GroEL equatorial domain appeared as tetradecamers (Nielsen and Cowan, 1998). These observations showed that the ability to form single or double rings is confined to the equatorial part of the protein and in particular, as observed for the mutant $GroEL_{SR1}$, crucial are the residues R452, E464, S463, and V464, that, when mutated into alanine, cause GroEL to form single rings, too. However, contrary to wild type Hsp60, $GroEL_{SR1}$ is unable to release client proteins, with the exception of rhodanese. Instead, $Hsp60_{SR1}$, a mutant with mutations at the same positions of mutated residues of $GroEL_{SR1}$, and considered to be unable of forming tetradecamers, refolds and releases client proteins. It can, therefore, be inferred that the formation of tetradecamer intermediates, as discussed earlier (Viitanen et al., 1992), is not obligatory for productive folding of substrates, and that an alternative pathway may exist (**Figure 4**) (Nielsen and Cowan, 1998; Weiss et al., 2016).

More recently, a mutant (E321K) of the human mtHSP60 was crystallized and its structure solved (Weiss et al., 2016). The mutation confers high stability to the open conformation of mtHSP60 so to generate a very stable complex between mtHSP60 and mtHSP10, and with a molecular symmetry that facilitated its crystallization. Thus, the structure of this complex was revealed by X-ray Diffraction Analysis, showing the existence of a football-shaped double-ring oligomer that, although similar to that found for GroEL differs from it in various features (Nisemblat et al., 2014). Similarly to GroEL, the N-terminal and C-terminal regions of HSP60 are located in the equatorial domain of the protein that is involved in the inter-ring interface of the oligomeric chaperonin. The rings can both simultaneously bind ATP and one of the seven monomers in each ring is somewhat different from the others so to create an internal asymmetry. In the football-shape model, the rings independently bind substrate, ATP, and mtHsp10 and, only after that, they join together before encapsulating and refolding the substrate. The mutant mtHsp60E321K, even if not able to release the folded substrate, can encapsulate and refold client proteins such as the Enhanced Green Fluorescent Protein (EGFP). Therefore, it cannot be excluded that the symmetric, football-shaped intermediate is present also in the chaperoning cycle of the wild type mtHsp60.

In conclusion, it can be hypothesized that different functional mechanisms, involving various types of oligomers, may occur with Hsp60 single rings (Nielsen and Cowan, 1998; Weiss et al., 2016). It is likely that the chaperonin may follow a given pathway depending on substrate type and on micro-environmental conditions such as those occurring under physiological and stress situations.

HSP60 OUTSIDE MITOCHONDRIA

In eukaryotic cells Hsp60 is typically located inside mitochondria, which presumably evolved from prokaryotes via endosymbiosis (Gupta, 1995). mtHsp60 is encoded in a nuclear gene and is synthesized in the cytosol with an MTS. This N-terminal sequence forms a positively charged amphiphilic α-helix, which is essential for mitochondrial import. The post-translational import of Hsp60 into mitochondria is, like for other cytosolic proteins that translocate into the organelle, a very intricate process that involves protein translocation complexes such as TOM in the outer membrane and TIM in the inner membrane. The import mechanism is regulated by the membrane potential $\Delta\Psi$ that, when dissipated by potassium ionophores, inhibits the maturation of Hsp60 (Gupta and Austin, 1987).

The sequence of MTS in the human HSP60 was deduced from the cDNA entire gene sequence compared with that of the matured protein, in which the N-terminal MTS was missing. The MTS consists of 26 amino acids: 5′-Met-Leu-Arg-Leu-Pro-Thr-Val-Phe-Arg-Gln-Met-Arg-Pro-Val-Ser-Arg-Val-Leu-Ala-Pro-His-Leu-Thr-Arg-Ala-Tyr-3′. Based on studies on GroEL structure (Clare et al., 2012), it can be expected that the MTS fits inside the central cavity of HSP60 oligomers. Structural details on naïve HSP60 based on SAXS and Molecular Dynamics studies can be found in a relatively recent report (Spinello et al., 2015).

When the Hsp60 N-terminus is analyzed by PONDR VLXT, a neural networks disorder predictor, it appears that in the absence of MTS, residues adjacent to it undergo an order-disorder transition, probably related to the functional role that the chaperonin plays in mitochondria (Ricci et al., 2017).

In our studies, we focused on stability and structure of the HSP60 with MTS, which we designate naïve HSP60, as it occurs after being synthesized in the cytosol and before entering the mitochondria (Vilasi et al., 2014). These studies were stimulated by the increased awareness of the potential roles of Hsp60 in

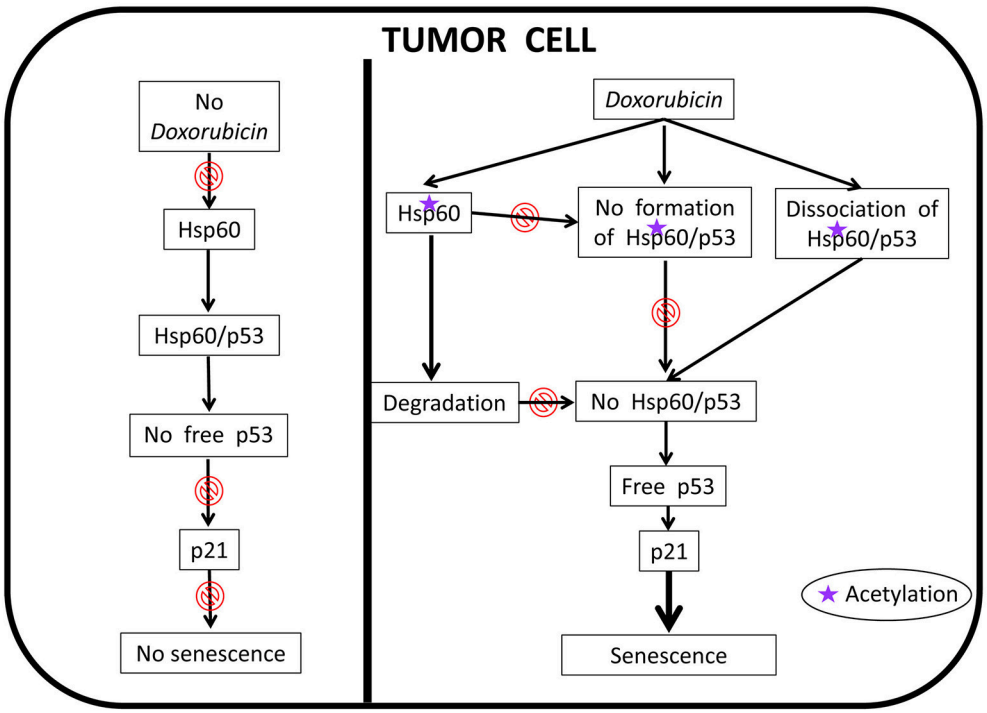

FIGURE 7 | Proposed anti-cancer mechanism of action of doxorubicin involving human HSP60. In the absence of doxorubicin, HSP60 (shown as Hsp60 to encompass not only the human chaperonin but also any other ortholog from animal experimental models) can form complexes with p53 thereby removing free p53 and, thus, there is no interaction between it and p21, which results in the abolition of senescence; the tumor cell is immortal. In this situation HSP60 has an essential pro-tumor effect. Doxorubicin cancels this effect, an action that is associated with HSP60 acetylation. The modified HSP60 is degraded, dissociates from HSP60/p53 complexes, and cannot form de novo these complexes, all of which leads to the occurrence of free p53 that interacts with p21 leading to senescence; the tumor cell now is no longer immortal.

cell compartments other than mitochondria and outside the organelle (Soltys and Gupta, 1998; Cechetto et al., 2000; Cappello et al., 2008, 2014; Wick et al., 2014; Wick, 2016; Rahman et al., 2017; van Eden et al., 2017; Calderwood, 2018; Pockley and Henderson, 2018; see other references at http://hsp60.com/localization/). By Electron Microscopy, it has been demonstrated that in normal conditions, 15–20% of Hsp60 is located at extra-mitochondrial sites, namely, in the mitochondrial outer membrane, cytosolic vesicles plasma membrane, endoplasmic reticulum, and peroxisomes (Soltys and Gupta, 1998). These locations seem to correspond to specific physiological functions. As an example, in mature insulin secretory vesicles of pancreatic beta-cells, Hsp60, according to its canonical function, could have a role in insulin core condensation necessary for the hormone release (Soltys and Gupta, 1998). Hsp60 is also involved in assembly of membrane proteins and in the condensation of urate oxidase crystalline core of rat liver peroxisomes. It is especially in pathologic situations such as cancer and autoimmune and inflammatory diseases that HSP60 accumulates in the cytosol, and in extramitochondrial sites (Czarnecka et al., 2006; Desmetz et al., 2008; Cappello et al., 2011, 2014; Macario et al., 2013; Wick et al., 2014; Macario and Conway de Macario, 2016; Rahman et al., 2017; van Eden et al., 2017; Calderwood, 2018; Pockley and Henderson, 2018). The question still open is how the protein reaches these sites, and, consequentially, which forms of Hsp60 can be found in the various locations. One hypothesis is that cytosolic accumulation of Hsp60 could occur via a mitochondrial export mechanism, which would release Hsp60 devoid of MTS into the cytosol (Soltys and Gupta, 1998). In this regard, several possibilities can be considered, such as reverse operation of the mitochondrial import channel, or an as yet undefined export pathway, or a movement through lipids, or an export mechanism involving vesicles. Also, in some cases, Hsp60 can reside and accumulate in the cytosol without being imported into mitochondria and, therefore, this Hsp60 would bear MTS. An example is provided by the LNCaP cells, in which exposure to apoptosis inducers, such as serum starvation or Dox treatment, causes HSP60 accumulation in the absence of mitochondrial release (Chandra et al., 2007). Moreover, an antibody against the MTS crossreacted with a protein that is present only in the cytoplasm of rat liver cell (Itoh et al., 2002) and, although not explicitly commented in the original article, two bands are present in the Western blot (with anti-Hsp60 monoclonal antibody) of the cytoplasmic fraction from adult cardiac myocytes (Kirchhoff et al., 2002). It has been demonstrated that in some apoptotic systems mtHsp60 directly interacts with procaspase-3 in the cytosol, enhancing caspase-3 maturation and activation as part of a pro-apoptotic mechanism (Samali et al., 1999; Xanthoudakis et al., 1999; Chandra et al., 2007). In other systems characterized by naïve

Hsp60 accumulation in the cytosol, an anti-apoptotic, pro-survival role is believed to occur, since Hsp60 knockdown or inhibition causes cell death (Kirchhoff et al., 2002; Chandra et al., 2007; Caruso Bavisotto et al., 2017b). In this case, Hsp60 binds procaspase-3 and thereby blocks the apoptotic cascade. In summary, mature mtHsp60 would activate pro-apoptotic mechanisms and, thus, in certain types of cancer it would interfere with cancer cell growth, whereas naïve Hsp60 would be anti-apoptotic and ensure survival of cancer cells. Moreover, it was found that from the cytosol, HSP60 was released by tumor cells via exosomes into the extracellular space (Merendino et al., 2010; Campanella et al., 2012). In this case, by specific immunoprecipitation experiments, two HSP60 forms were found, suggesting the coexistence of mature and naïve forms of the chaperonin. In conclusion, either one or the other, or both forms of HSP60, naïve and mitochondrial, may potentially occur at the various locations in which the chaperonin has been detected in pathological conditions, and this is an issue deserving more investigation. Also, elucidation of the oligomeric organization of the chaperonin in all those locations in which it has been detected in pathological situations will no doubt provide new insights into the molecular basis of disease. For instance, it has been demonstrated that a single mutation in HSP60 found in MitCHAP-60 destabilizes the chaperonin oligomers (Parnas et al., 2009). This is why in view of the potentially key roles of naïve HSP60 in cancer and other diseases, several studies have focused on its oligomeric organization and structure (Vilasi et al., 2014; Ricci et al., 2016, 2017; Enriquez et al., 2017). A detailed study of the structure and self-organization of naïve cytosolic recombinant His-tag HSP60 in solution was performed, using biophysical methods such as Light and X-Ray Scattering, Single Molecule Spectroscopy, and hydrodynamics measurements (Vilasi et al., 2014). *In vitro* experiments were carried out under conditions approximating as much as possible those occurring *in vivo*, using HSP60 at a range of concentrations encompassing those believed to occur *in vivo*: from 10 nM to 79.5 μM. In *E. coli*, the GroEL concentration is estimated to be 35 μM of monomers (Lorimer, 1996). Even if there are no data from direct measurements on the Hsp60 concentrations in the eukaryotic-cell cytosol or mitochondria, we can assume that the range of concentrations described above should include those found *in vivo*, in all cell compartments, under physiological, and stress conditions. Our results showed that HSP60 oligomerizes at all the concentration tested, forming both tetradecamers and heptamers with a prevalence of the former and no detectable monomers (Vilasi et al., 2014). This is illustrated by data from Native Gel Electrophoresis and Dynamic Light Scattering, **Figure 5**. HSP60 at higher concentrations was analyzed by Small Angle X-Ray Scattering and, at lower concentrations was analyzed by Fluorescence Correlation Spectroscopy (Vilasi et al., 2014). In another laboratory, HSP60 was purified applying a protocol that yields HSP60 without the His6-tag (Enriquez et al., 2017). The results were similar to those described in the preceding lines, although a more marked difference between tetradecamer and heptamer concentrations was found. In this case, the HSP60-His6-tag purification via Affinity Column Chromatography yielded a protein unable to oligomerize and occurring exclusively as monomers. Instead, the protein without His6-tag, studied by EM, Native Gel Electrophoresis, and Light Scattering appeared as tetradecamers with a minor part of heptamers. It has not yet been established what form, monomer, or single or double ring occurs in the cytosol. However, based on the findings described above, we can conclude that naïve HSP60 has biochemical features like those of the mitochondrial mature HSP60 and monomers associate to form the classical toroidal form. We hypothesize that this form does not disassemble before entering, as monomer, into mitochondria. It is likely that cytosolic chaperones, such as Hsp70 and Hsp90, bind the Hsp60 precursor and usher it into mitochondria thus preventing oligomerization in the cytosol. However, we can only say at this time, that in the case of HSP60 accumulation resulting from the failure of the chaperonin precursor to enter into mitochondria, the protein has the ability to form the toroidal structure, probably as necessary to perform its functions in those specific conditions. Future studies should also focus on determining ATPase and in vitro folding activities of naïve HSP60 to establish the extent of its functionality in comparison with the mature molecule.

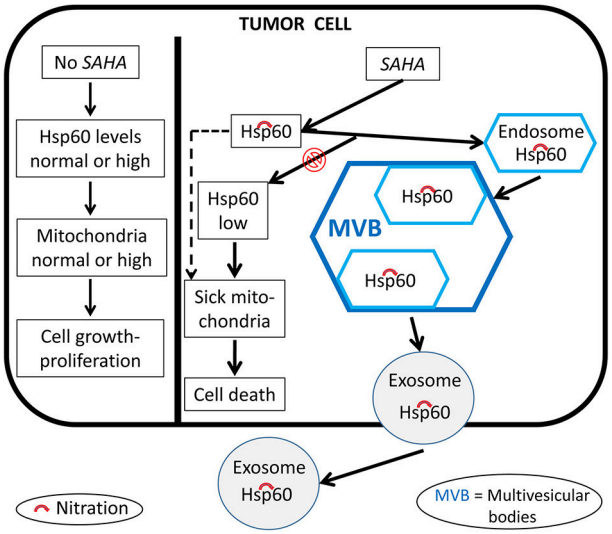

FIGURE 8 | Proposed mechanism of the anti-cancer effects of SAHA involving human HSP60. In the absence of SAHA, the levels and quality of HSP60 (shown as Hsp60 to encompass not only the human chaperonin but also any other ortholog from animal experimental models) and mitochondria are those required by the tumor cell to grow and proliferate. The anti-tumor effect of SAHA modifies these HSP60 parameters. HSP60 levels decrease, the protein is nitrated, i.e., functionally impaired, which leads to sick mitochondria and its capture by endosomes and multivesicular bodies and, ultimately, secretion out of the cell via exosomes; all these events contribute to a decrease of normal HSP60 inside the tumor cell and to impairment of mitochondrial physiology, leading to tumor-cell death.

It is worth noting that mature HSP60 produced without His6-tag occurs predominantly as single rings (Nielsen and Cowan, 1998; Parnas et al., 2009), whereas for naïve HSP60 the equilibrium seems to shift toward double rings. Structural differences between the two HSP60 forms can also be inferred from the studies on the chemical stability of the two proteins,

(**Figure 6**) (Ricci et al., 2016, 2017). In order to corroborate this suggestion, further studies are needed to directly compare the two proteins, possibly purified under the same conditions, also in relation to their different activity.

HSP60 POST-TRANSLATIONAL MODIFICATIONS

The functions of Hsp60 are closely related to its structure and, therefore, any changes in composition and conformation due to mutations or aberrant post translational modification (PTM) may cause a chaperonopathy.

Most likely, some PTMs occur during the synthesis of the Hsp60 peptide at or near the ribosome and also later, but before the folding process necessary to yield a mature, functional Hsp60 monomer, ready to display its functions alone or as part of a heptamer or tetradecamer. Several lines of research are currently underway aimed to: (a) clarify how PTM change Hsp60 properties and functions and, thereby, its physiological roles; and (b) determine its etiopathogenic activity in chaperonopathies. For instance, a recent study examined HSP60 hyperacetylation during anticancer-drug treatment in human osteosarcoma cells (Gorska et al., 2013). The results lead to the working hypothesis that the post-translational hyperacetylation of HSP60 associated with administration of geldanamycin, contributes to the death of cancer cells.

More recently, it was reported that HSP60 hyperacetylation and ubiquitination are associated with the response of cancer cells to administration of the anticancer-drug doxorubicin (Marino Gammazza et al., 2017). Hyperacetylated HSP60 would be directed via ubiquitination to the proteasome system, which would cause a decrease or loss of HSP60 functions, leading to the re-instauration of cellular senescence in cancer cells followed by tumor-cell growth arrest, **Figure 7**. The HSP60 PTM may lead to disruption of its interaction with other molecules such as p53. These results are in agreement with the observation that HSP60 O-GlcNAcylation impairs its complexing with Bax, leading to cell death (Kim et al., 2006). Also, in line with these data is the finding that HSP60 modifications have an impact on its trafficking, favoring its secretion into the extracellular space (Campanella et al., 2016).

It was found that the histone deacetylase inhibitor, suberoylanilide hydroxamic acid (SAHA) is cytotoxic for tumor cells, an effect associated with changes in the levels of concentration and nitration of HSP60, **Figure 8** (Campanella et al., 2016). The nitrated protein could be exported via extracellular vesicles, such as exosomes (Campanella et al., 2016; Caruso Bavisotto et al., 2017a). Since exosomes are extracellular vehicles that transport factors associated with cancer progression and factors that can modulate the immune response, the presence of HSP60 in them suggests involvement of this chaperonin in inflammation, immune system modulation, and regulation of tumor microenvironment and growth.

In summary, our most recent work has provided new insights, supporting the idea that post-translational modification of HSP60 are associated with key changes inside and outside cells. For instance (i) acetylation is accompanied by a decrease of HSP60 levels and functions such as interaction with p53, and re-instauration of senescence in tumor cells; (ii) acetylation and ubiquitination most likely leads to HSP60 degradation in the proteasome; and (iii) HSP60 nitration affects its trafficking, favoring its translocation into exosomes and subsequent secretion into the circulation, a situation that allows HSP60 to reach target cells, near or far, and thus exercise, for instance, a regulatory action on the immune system. Working hypotheses for studying the effect of PTM on Hsp60 in tumor cells treated with anti-cancer drugs are depicted in **Figures 7**, **8**.

CONCLUSIONS AND PERSPECTIVES

Hsp60 monomers in solution tend to associate into oligomers and form heptameric rings, and double rings, i.e., tetradecamers. The latter seem to be the preferred functional complex. However, single rings may also have functions *in vivo*, without the need for tetradecamer intermediates, under normal and pathologcal conditions. This point deserves more research because single rings may participate in cellular mechanisms which, if elucidated, will enhance our understanding of molecular chaperones and their roles in health and disease. Monomers as such, despite their tendency to oligomerize when in solution, may also play important roles in health and disease. We know that Hsp60 occurs in mitochondria, cytosol, other organelles, the plasma cell membrane, the intercellular space, and in circulation free or attached to corpuscular bodies such as red and white cells, or in exosomes. It is likely that at least in some of these locations Hsp60 is present as monomers, the functions of which deserve active investigation, as much as heptamers and tetradecamers do.

Other structural details of Hsp60 in health and disease that deserve close scrutiny are PTM. These molecular modifications may be crucial for determining: (i) with which of the various possible interactive partners Hsp60 will interact; (ii) the locale in which it will reside and function; (iii); which of the several physiological roles the Hsp60 molecule is able to play will in fact be played; and (iv) whether the chaperonin will be cytoprotective or pathogenic.

AUTHOR CONTRIBUTIONS

All authors listed have made a substantial, direct and intellectual contribution to the work, and approved it for publication.

ACKNOWLEDGMENTS

SV was partially supported by the Italian grant FIRB "Future in research" RBFR12SIPT MIND; and by the Italian 2007–2013 PON grant "Hippocrates-Sviluppo di micro- e nano-tecnologie e sistemi avanzati per la salute dell'uomo" PON02 00355 2964193. CCB, AMG, and FC were partially supported by IEMEST. AJLM and ECdM were partially supported by IMET. This work was done under the agreement between IEMEST (Italy) and IMET (USA) (this is IMET contribution number IMET 18-001).

REFERENCES

Bie, A. S., Fernandez-Guerra, P., Birkler, R. I., Nisemblat, S., Pelnena, D., Lu, X., et al. (2016). Effects of a mutation in the HSPE1 gene encoding the mitochondrial co-chaperonin HSP10 and its potential association with a neurological and developmental disorder. *Front. Mol. Biosci*. 3:65. doi: 10.3389/fmolb.2016.00065

Bross, P., and Fernandez-Guerra, P. (2016). Disease-associated mutations in the hspd1 gene encoding the large subunit of the mitochondrial HSP60/HSP10 chaperonin complex. *Front. Mol. Biosci*. 3:49. doi: 10.3389/fmolb.2016.00049

Bross, P., Naundrup, S., Hansen, J., Nielsen, M. N., Christensen, J. H., Kruhøffer, M., et al. (2008). The Hsp60-(p.V98I) mutation associated with hereditary spastic paraplegia SPG13 compromises chaperonin function both *in vitro* and *in vivo*. *J. Biol. Chem*. 283, 15694–15700. doi: 10.1074/jbc.M800548200

Calderwood, S. K. (2018). Heat shock proteins and cancer: intracellular chaperones or extracellular signalling ligands? *Philos. Trans. R. Soc. Lond. B Biol. Sci*. 373:20160524. doi: 10.1098/rstb.2016.0524

Campanella, C., Bucchieri, F., Merendino, A. M., Fucarino, A., Burgio, G., Corona, D. F., et al. (2012). The odyssey of Hsp60 from tumor cells to other destinations includes plasma membrane-associated stages and Golgi and exosomal protein-trafficking modalities. *PLoS ONE* 7:e42008. doi: 10.1371/journal.pone.0042008

Campanella, C., D'Anneo, A., Marino Gammazza, A., Caruso Bavisotto, C., Barone, R., Emanuele, S., et al. (2016). The histone deacetylase inhibitor SAHA induces HSP60 nitration and its extracellular release by exosomal vesicles in human lung-derived carcinoma cells. *Oncotarget* 7, 28849–28867. doi: 10.18632/oncotarget.6680

Cappello, F., Conway de Macario, E., Marasà, L., Zummo, G., and Macario, A. J. L. (2008). Hsp60 expression, new locations, functions and perspectives for cancer diagnosis and therapy. *Cancer Biol. Ther*. 7, 801–809. doi: 10.4161/cbt.7.6.6281

Cappello, F., Conway de Macario, E., Zummo, G., and Macario, A. J. L. (2011). Immunohistochemistry of human Hsp60 in health and disease: from autoimmunity to cancer. *Methods Mol. Biol*. 787, 245–254. doi: 10.1007/978-1-61779-295-3_18

Cappello, F., Marino Gammazza, A., Palumbo Piccionello, A., Campanella, C., Pace, A., Conway de Macario, E., et al. (2014). Hsp60 chaperonopathies and chaperonotherapy: targets and agents. *Expert Opin. Ther. Targets* 18, 185–208. doi: 10.1517/14728222.2014.856417

Caruso Bavisotto, C., Cappello, F., Macario, A. J. L., Conway de Macario, E., Logozzi, M., Fais, S., et al. (2017a). Exosomal HSP60: a potentially useful biomarker for diagnosis, assessing prognosis, and monitoring response to treatment. *Exp. Rev. Mol. Diag*. 17, 815–822. doi: 10.1080/14737159.2017.1356230

Caruso Bavisotto, C., Nikolic, D., Marino Gammazza, A., Barone, R., Lo Cascio, F., Mocciaro, E., et al. (2017b). The dissociation of the Hsp60/pro-Caspase-3 complex by bis(pyridyl)oxadiazole copper complex (CubipyOXA) leads to cell death in NCI-H292 cancer cells. *J. Inorg. Biochem*. 170, 8–16. doi: 10.1016/j.jinorgbio.2017.02.004

Cechetto, J. D., Soltys, B. J., and Gupta, R. S. (2000). Localization of mitochondrial 60-kD heat shock chaperonin protein (Hsp60) in pituitary growth hormone secretory granules and pancreatic zymogen granules. *J. Histochem. Cytochem*. 48, 45–56. doi: 10.1177/002215540004800105

Chandra, D., Choy, G., and Tang, D. G. (2007). Cytosolic accumulation of HSP60 during apoptosis with or without apparent mitochondrial release: evidence that its pro-apoptotic or pro-survival functions involve differential interactions with caspase-3. *J. Biol. Chem*. 282, 31289–31301. doi: 10.1074/jbc.M702777200

Chen, J., Zhang, Q., Ren, W., and Li, W. (2017). Piecing together the allosteric patterns of chaperonin GroEL. *J. Phys. Chem. B* 121, 4987–4996. doi: 10.1021/acs.jpcb.7b01992

Cheng, M. Y., Hartl, F. U., and Horwich, A. L. (1990). The mitochondrial chaperonin hsp60 is required for its own assembly. *Nature* 348, 455–458. doi: 10.1038/348455a0

Clare, D. K., Vasishtan, D., Stagg, S., Quispe, J., Farr, G. W., Topf, M., et al. (2012). ATP-triggered conformational changes delineate substrate-binding and -folding mechanics of the GroEL chaperonin. *Cell* 149, 113–123. doi: 10.1016/j.cell.2012.02.047

Coluzza, I., De Simone, A., Fraternali, F., and Frenkel, D. (2008). Multi-scale simulations provide supporting evidence for the hypothesis of intramolecular protein translocation in GroEL/GroES complexes. *PLoS Comput. Biol*. 4:e1000006. doi: 10.1371/journal.pcbi.1000006

Conway de Macario, E., Maeder, D. L., and Macario, A. J. L. (2003). Breaking the mould: archaea with all four chaperoning systems. *Biochem. Biophys. Res. Commun*. 301, 811–812. doi: 10.1016/S0006-291X(03)00047-0

Czarnecka, A. M., Campanella, C., Zummo, G., and Cappello, F. (2006). Mitochondrial chaperones in cancer: from molecular biology to clinical diagnostics. *Cancer Biol. Ther*. 5, 714–720 doi: 10.4161/cbt.5.7.2975

Desmetz, C., Bibeau, F., Boissière, F., Bellet, V., Rouanet, P., Maudelonde, T., et al. (2008). Proteomics-based identification of HSP60 as a tumor-associated antigen in early stage breast cancer and ductal carcinoma in situ. *J. Proteome Res*. 7, 3830–3837. doi: 10.1021/pr800130d

Dickson, R., Weiss, C., Howard, R. J., Alldrick, S. P., Ellis, R. J., Lorimer, G., et al. (2000). Reconstitution of higher plant chloroplast chaperonin 60 tetradecamers active in protein folding. *J. Biol. Chem*. 275, 11829–11835. doi: 10.1074/jbc.275.16.11829

Ellis, R. J., and van der Vies, S. M. (1988). The Rubisco subunit binding protein. *Photosyn. Res*. 16, 101–115. doi: 10.1007/BF00039488

Ellis, R. J., van der Vies, S. M., and Hemmingsen, S. M. (1989). The molecular chaperone concept. *Biochem. Soc. Symp*. 55, 145–153.

Enriquez, A. S., Rojo, H. M., Bhatt, J. M., Molugu, S. K., Hildenbrand, Z. L., and Bernal, R. A. (2017). The human mitochondrial Hsp60 in the APO conformation forms a stable tetradecameric complex. *Cell Cycle* 16, 1309–1319. doi: 10.1080/15384101.2017.1321180

Fei, X., Ye, X., LaRonde, N. A., and Lorimer, G. H. (2014). Formation and structures of GroEL:GroES2 chaperonin footballs, the protein-folding functional form. *Proc. Natl. Acad. Sci. U.S.A*. 111, 12775–12780. doi: 10.1073/pnas.1412922111

Georgopoulos, C. P., and Hohn, B. (1978). Identification of a host protein necessary for bacteriophage morphogenesis (the groE gene product). *Proc. Natl. Acad. Sci. U.S.A*. 75, 131–135 doi: 10.1073/pnas.75.1.131

Goloubinoff, P., Christeller, J. T., Gatenby, A. A., and Lorimer, G. H. (1989). Reconstitution of active dimeric ribulose bisphosphate carboxylase from an unfolded state depends on two chaperonin proteins and Mg-ATP. *Nature* 342, 884–889. doi: 10.1038/342884a0

Gorska, M., Marino Gammazza, A., Zmijewski, M. A., Campanella, C., Cappello, F., Wasiewicz, T., et al. (2013). Geldanamycin-induced osteosarcoma cell death is associated with hyperacetylation and loss of mitochondrial pool of heat shock protein 60 (hsp60). *PLoS ONE* 8:e71135. doi: 10.1371/journal.pone.0071135

Gupta, R. S. (1995). Evolution of the chaperonin families (Hsp60, Hsp10 and Tcp-1) of proteins and the origin of eukaryotic cells. *Mol. Microbiol*. 15, 1–11. doi: 10.1111/j.1365-2958.1995.tb02216.x

Gupta, R. S., and Austin, R. C. (1987). Mitochondrial matrix localization of a protein altered in mutants resistant to the microtubule inhibitor podophyllotoxin. *Eur. J. Cell Biol*. 45, 170–176.

Hansen, J. J., Bross, P., Westergaard, M., Nielsen, M. N., Eiberg, H., Børglum, A. D., et al. (2003). Genomic structure of the human mitochondrial chaperonin genes: HSP60 and HSP10 are localised head to head on chromosome 2 separated by a bidirectional promoter. *Hum. Genet*. 112, 71–77. doi: 10.1007/s00439-002-0837-9

Hemmingsen, S. M., Woolford, C., van der Vies, S. M., Tilly, K., Dennis, D. T., Georgopoulos, C. P., et al. (1988). Homologous plant and bacterial proteins chaperone oligomeric protein assembly. *Nature* 333, 330–334. doi: 10.1038/333330a0

Hohn, T., Hohn, B., Engel, A., Wurtz, M., and Smith, P. R. (1979). Isolation and characterization of the host protein groE involved in bacteriophage lambda assembly. *J. Mol. Biol*. 129, 359–373. doi: 10.1016/0022-2836(79)90501-1

Horwich, A. L. (2011). Protein folding in the cell: an inside story. *Nat. Med*. 17, 1211–1216. doi: 10.1038/nm.2468

Horwich, A. L., Fenton, W. A., Chapman, E., and Farr, G. W. (2007). Two families of chaperonin: physiology and mechanism. *Annu. Rev. Cell Dev. Biol*. 23, 115–145. doi: 10.1146/annurev.cellbio.23.090506.123555

Hutchinson, E. G., Tichelaar, W., Hofhaus, G., Weiss, H., and Leonard, K. R. (1989). Identification and electron microscopic analysis of a chaperonin oligomer from *Neurospora crassa*. *EMBO J*. 8, 1485–1490.

Illingworth, M., Ellis, H., and Chen, L. (2017). Creating the functional single-ring GroEL-GroES chaperonin systems via modulating GroEL-GroES interaction. *Sci. Rep*. 7:9710. doi: 10.1038/s41598-017-10499-4

Ishii, N. (2017). GroEL and the GroEL-GroES complex. *Subcell. Biochem*. 83, 483–504. doi: 10.1007/978-3-319-46503-6_17

Ishii, N., Taguchi, H., Sasabe, H., and Yoshida, M. (1995). Equatorial split of holo-chaperonin from *Thermus thermophilus* by ATP and K^+. *FEBS Lett*. 362, 121–125. doi: 10.1016/0014-5793(95)00222-U

Itoh, H., Komatsuda, A., Ohtani, H., Wakui, H., Imai, H., Sawada, K., et al. (2002). Mammalian Hsp60 is quickly sorted into mitochondria under conditions of dehydration. *Eur. J. Biochem*. 269, 5931–5938. doi: 10.1046/j.1432-1033.2002.03317.x

Jindal, S., Dudani, A. K., Singh, B., Harley, C. B., and Gupta, R. S. (1989). Primary structure of a human mitochondrial protein homologous to the bacterial and plant chaperonins and to the 65-kilodalton mycobacterial antigen. *Mol. Cell. Biol.* 9, 2279–2283. doi: 10.1128/MCB.9.5.2279

Kalderon, B., Kogan, G., Bubis, E., and Pines, O. (2015). Cytosolic Hsp60 can modulate proteasome activity in yeast. *J. Biol. Chem*. 290, 3542–3551. doi: 10.1074/jbc.M114.626622

Kim, H. S., Kim, E. M., Lee, J., Yang, W. H., Park, T. Y., Kim, Y. M., et al. (2006). Heat shock protein 60 modified with O-linked N-acetylglucosamine is involved in pancreatic beta-cell death under hyperglycemic conditions. *FEBS Lett*. 580, 2311–2316. doi: 10.1016/j.febslet.2006.03.043

Kirchhoff, S. R., Gupta, S., and Knowlton, A. A. (2002). Cytosolic heat shock protein 60, apoptosis, and myocardial injury. *Circ. J*. 195, 2899–2904 doi: 10.1161/01.CIR.0000019403.35847.23

Koike-Takeshita, A., Arakawa, T., Taguchi, H., and Shimamura, T. (2014). Crystal structure of a symmetric football-shaped GroEL:GroES2-ATP14 complex determined at 3.8Å reveals rearrangement between two GroEL rings. *J. Mol. Biol.* 426, 3634–3641. doi: 10.1016/j.jmb.2014.08.017

Levy-Rimler, G., Viitanen, P., Weiss, C., Sharkia, R., Greenberg, A., Niv, A., et al. (2001). The effect of nucleotides and mitochondrial chaperonin 10 on the structure and chaperone activity of mitochondrial chaperonin 60. *Eur. J. Biochem.* 268, 3465–3472. doi: 10.1046/j.1432-1327.2001.02243.x

Liu, J., Sankar, K., Wang, Y., Jia, K., and Jernigan, R. L. (2017). Directional force originating from ATP hydrolysis drives the GroEL conformational change. *Biophys. J*. 112, 1561–1570. doi: 10.1016/j.bpj.2017.03.004

Lorimer, G. H. (1996). A quantitative assessment of the role of the chaperonin proteins in protein folding *in vivo*. *FASEB J*. 10, 5–9.

Macario, A. J. L., and Conway de Macario, E. (2005). Sick chaperones, cellular stress, and disease. *New Engl. J. Med.* 353, 1489–1501. doi: 10.1056/NEJMra050111

Macario, A. J. L., and Conway de Macario, E. (2016). The chaperoning and the immune systems with the microbiome integrate a matrix that supports health: when one of them is disturbed the others suffer and disease ensues. *Life Saf. Secur.* 4, 101–123. doi: 10.12882/2283-7604.2016.4.6

Macario, A. J. L., Conway de Macario, E., and Cappello, F. (2013). *The Chaperonopathies Diseases with Defective Molecular Chaperones*. Heidelberg; New York, NY; London: Springer Dordrecht: Library of Congress.

Marino Gammazza, A., Campanella, C., Barone, R., Caruso Bavisotto, C., Gorska, M., Wozniak, M., et al. (2017). Doxorubicin anti-tumor mechanisms include Hsp60 post-translational modifications leading to the Hsp60/p53 complex dissociation and instauration of replicative senescence. *Cancer Lett*. 385, 75–86. doi: 10.1016/j.canlet.2016.10.045

McMullin, T. W., and Hallberg, R. L. (1988). A highly evolutionarily conserved mitochondrial protein is structurally related to the protein encoded by the *Escherichia coli* groEL gene. *Mol. Cell. Biol*. 8, 371–380. doi: 10.1128/MCB.8.1.371

Merendino, A. M., Bucchieri, F., Campanella, C., Marcianò, V., Ribbene, A., David, S., et al. (2010). Hsp60 is actively secreted by human tumor cells. *PLoS ONE* 5:e9247. doi: 10.1371/journal.pone.0009247

Mukherjee, K., Conway de Macario, E., Macario, A. J. L., and Brocchieri, L. (2010). Chaperonin genes on the rise: new divergent classes and intense duplication in human and other vertebrate genomes. *BMC Evol. Biol*. 10:64. doi: 10.1186/1471-2148-10-64

Nielsen, K. L., and Cowan, N. J. (1998). A single ring is sufficient for productive chaperonin mediated folding *in vivo*. *Mol. Cell* 2, 93–99. doi: 10.1016/S1097-2765(00)80117-3

Nisemblat, S., Parnas, A., Yaniv, O., Azem, A., and Frolow, F. (2014). Crystallization and structure determination of a symmetrical 'football' complex of the mammalian mitochondrial Hsp60-Hsp10 chaperonins. *Acta Crystallogr. F Struct. Biol. Commun.* 70(Pt 1), 116–119. doi: 10.1107/S2053230X1303389X.

Nisemblat, S., Yaniv, O., Parnas, A., Frolow, F., and Azem, A. (2015). Crystal structure of the human mitochondrial chaperonin symmetrical football complex. *Proc. Natl. Acad. Sci. U.S.A*. 112, 6044–6049. doi: 10.1073/pnas.1411718112

Okamoto, T., Ishida, R., Yamamoto, H., Tanabe-Ishida, M., Haga, A., Takahashi, H., et al. (2015). Functional structure and physiological functions of mammalian wild-type HSP60. *Arch. Biochem. Biophys.* 586, 10–19. doi: 10.1016/j.abb.2015.09.022

Ostermann, J., Horwich, A. L., Neupert, W., and Hartl, F. U. (1989). Protein folding in mitochondria requires complex formation with hsp60 and ATP hydrolysis. *Nature* 341, 125–130. doi: 10.1038/341125a0

Parnas, A., Nadler, M., Nisemblat, S., Horovitz, A., Mandel, H., and Azem, A. (2009). The MitCHAP-60 disease is due to entropic destabilization of the human mitochondrial Hsp60 oligomer. *J. Biol. Chem*. 284, 28198–28203. doi: 10.1074/jbc.M109.031997

Picketts, D. J., Mayanil, C. S., and Gupta, R. S. (1989). Molecular cloning of a Chinese hamster mitochondrial protein related to the "chaperonin" family of bacterial and plant proteins. *J. Biol. Chem*. 264, 12001–12008.

Pockley, A. G., and Henderson, B. (2018). Extracellular cell stress (heat shock) proteins-immune responses and disease: an overview. *Philos. Trans. R. Soc. Lond. B Biol. Sci.* 373:20160522. doi: 10.1098/rstb.2016.0522

Rahman, M., Steuer, J., Gillgren, P., Hayderi, A., Liu, A., and Frostegård, J. (2017). Induction of dendritic cell-mediated activation of T cells from atherosclerotic plaques by human heat shock protein 60. *J. Am. Heart Assoc*. 6:e006778. doi: 10.1161/JAHA.117.006778

Ricci, C., Carrotta, R., Rappa, G. C., Mangione, M. R., Librizzi, F., San Biagio, P. L., et al. (2017). Investigation on different chemical stability of mitochondrial Hsp60 and its precursor. *Biophys. Chem*. 229, 31–38. doi: 10.1016/j.bpc.2017.07.008

Ricci, C., Ortore, M. G., Vilasi, S., Carrotta, R., Mangione, M. R., Bulone, D., et al. (2016). Stability and disassembly properties of human naïve Hsp60 and bacterial GroEL chaperonins. *Biophys. Chem*. 208, 68–75. doi: 10.1016/j.bpc.2015.07.006

Roh, S. H., Hryc, C. F., Jeong, H. H., Fei, X., Jakana, J., Lorimer, G. H., et al. (2017). Subunit conformational variation within individual GroEL oligomers resolved by Cryo-EM. *Proc. Natl. Acad. Sci. U.S.A*. 114, 8259–8264. doi: 10.1073/pnas.1704725114

Saibil, H. R., Fenton, W. A., Clare, D. K., and Horwich, A. L. (2013). Structure and allostery of the chaperonin GroEL. *J. Mol. Biol.* 425, 1476–1487. doi: 10.1016/j.jmb.2012.11.028

Samali, A., Cai, J., Zhivotovsky, B., Jones, D. P., and Orrenius, S. (1999). Presence of a pre-apoptotic complex of pro-caspase-3, Hsp60 and Hsp10 in the mitochondrial fraction of Jurkat cells. *EMBO J*. 18, 2040–2048 doi: 10.1093/emboj/18.8.2040

Sameshima, T., Iizuka, R., Ueno, T., and Funatsu, T. (2010). Denatured proteins facilitate the formation of the football-shaped GroEL-(GroES)2 complex. *Biochem. J*. 427, 247–254. doi: 10.1042/BJ20091845

Soltys, B. J., and Gupta, R. S. (1998). "Mitochondrial molecular chaperones hsp60 and mhsp70: are their role restricted to mitochondria?" in *Stress Proteins Handbook of Experimental Pharmacology*, ed D. S. Latchman (Berlin; Heidelberg: Springer), 69–100.

Spinello, A., Ortore, M. G., Spinozzi, F., Ricci, C., Barone, G., Marino Gammazza, A., et al. (2015). Quaternary structures of GroEL and naïve-Hsp60 chaperonins in solution: a combined SAXS-MD study. *RSC Adv*. 5, 49871–49879. doi: 10.1039/C5RA05144D

Taguchi, H. (2015). Reaction cycle of chaperonin GroEL via symmetric "football" intermediate. *J. Mol. Biol.* 427, 2912–2918. doi: 10.1016/j.jmb.2015.04.007

van Eden, W., Jansen, M. A. A., Ludwig, I., van Kooten, P., van der Zee, R., and Broere, F. (2017). The enigma of heat shock proteins in immune tolerance. *Front. Immunol.* 8:1599. doi: 10.3389/fimmu.2017.01599

Viitanen, P. V., Lorimer, G. H., Seetharam, R., Gupta, R. S., Oppenheim, J., Thomas, J. O., et al. (1992). Mammalian mitochondrial chaperonin 60 functions as a single toroidal ring. *J. Biol. Chem.* 267, 695–698.

Vilasi, S., Carrotta, R., Mangione, M. R., Campanella, C., Librizzi, F., Randazzo, L., et al. (2014). Human Hsp60 with its mitochondrial import signal occurs in solution as heptamers and tetradecamers remarkably stable over a wide range of concentrations. *PLoS ONE* 9:e97657. doi: 10.1371/journal.pone.0097657

Weiss, C., Jebara, F., Nisemblat, S., and Azem, A. (2016). Dynamic complexes in the chaperonin-mediated protein folding cycle. *Front. Mol. Biosci.* 3:80. doi: 10.3389/fmolb.2016.00080

Wick, C. (2016). Tolerization against atherosclerosis using heat shock protein 60. *Cell Stress Chaper.* 21, 201–211. doi: 10.1007/s12192-015-0659-z

Wick, G., Jakic, B., Buszko, M., Wick, M. C., and Grundtman, C. (2014). The role of heat shock proteins in atherosclerosis. *Nat. Rev. Cardiol.* 11, 516–529. doi: 10.1038/nrcardio.2014.91

Xanthoudakis, S., Roy, S., Rasper, D., Hennessey, T., Aubin, Y., Cassady, R., et al. (1999). Hsp60 accelerates the maturation of pro-caspase-3 by upstream activator proteases during apoptosis. *EMBO J.* 18, 2049–2056. doi: 10.1093/emboj/18.8.2049

Conflict of Interest Statement: The authors declare that the research was conducted in the absence of any commercial or financial relationships that could be construed as a potential conflict of interest.

frontiers in Molecular Biosciences

REVIEW
published: 11 April 2018
doi: 10.3389/fmolb.2018.00031

A Glimpse Into the Structure and Function of Atypical Type I Chaperonins

*Mohammed Y. Ansari and Shekhar C. Mande**

National Centre for Cell Science, Pune, India

Chaperonins are a subclass of molecular chaperones that assist cellular proteins to fold and assemble into their native shape. Much work has been done on Type I chaperonins, which has elucidated their elegant mechanism. Some debate remains about the details in these mechanisms, but nonetheless the roles of these in helping protein folding have been understood in great depth. In this review we discuss the known functions of atypical Type I chaperonins, highlighting evolutionary aspects that might lead chaperonins to perform alternate functions.

Keywords: Type I chaperonins, GroEL, GroES, *Mycobacterium tuberculosis*, protein folding, gene duplication

OPEN ACCESS

Edited by:
Abdussalam Azem,
Tel Aviv University, Israel

Reviewed by:
David A. Dougan,
La Trobe University, Australia
Anat Ben-Zvi,
Ben-Gurion University of the Negev, Israel

****Correspondence:***
Shekhar C. Mande
shekhar@nccs.res.in;
director@nccs.res.in

Specialty section:
This article was submitted to Protein Folding, Misfolding and Degradation, a section of the journal Frontiers in Molecular Biosciences

Received: *04 January 2018*
Accepted: *21 March 2018*
Published: *11 April 2018*

Citation:
Ansari MY and Mande SC (2018) A Glimpse Into the Structure and Function of Atypical Type I Chaperonins. Front. Mol. Biosci. 5:31. doi: 10.3389/fmolb.2018.00031

MOLECULAR CHAPERONES

Molecular chaperones comprise of a wide range of proteins playing key roles in cellular homeostasis and are responsible for assisting in protein folding, assembly of multimeric proteins, translocation of proteins within and across cell, degradation of unwanted, or misfolded proteins during normal cellular processes and stabilization of proteins by preventing aggregation and assisting in refolding under stress conditions (Lindquist, 1986; Lindquist and Craig, 1988).

Proteins reported to have chaperone activity were initially discovered as those overexpressed during heat shock and hence were named as the heat shock proteins (Hsp). Apart from heat shock, other stress condition such as carbon, nitrogen, or phosphate limiting conditions were also known to induce molecular chaperones. These proteins are classified according to their molecular weight into five major families: (a) Hsp100 family, (b) Hsp90 family, (c) Hsp70 family, (d) Hsp60 family, and (e) small heat shock protein family (sHsp) (Bohen et al., 1995; Schirmer et al., 1996; Bukau and Horwich, 1998). The chaperones are also classified based on their mode of action into: (a) Foldases, Chaperones that assist refolding of unfolded proteins by using ATP, e.g., Hsp70 and Hsp60, (b) Holdases, Chaperones that bind folding intermediates and prevent aggregation, e.g., sHsp and Hsp40, and (c) Disaggregases, Chaperones which actively disaggregate the harmful protein aggregates, which might lead to their small fragments, e.g., members of AAA + ATPase superfamily and Hsp100. This type of classification holds true with few exceptions (Richter et al., 2010; Kim et al., 2013). Much of our understanding on the mechanisms of chaperone-assisted protein folding has been derived from work on Hsp60 and Hsp70 families of chaperones. This review focuses on Hsp60 class of molecular chaperones, highlighting Hsp60 with atypical structure and function.

Hsp60 Family/Chaperonins

The 60 kDa chaperones form large oligomeric rings, and are also referred to as the chaperonins. Chaperonins can be further sub-classified into two groups on the basis of requirement of co-chaperonins and their cellular location. Type I chaperonins are found in the cytoplasm of prokaryotes and in the mitochondrion and chloroplast of eukaryotes. They require the assistance

of the co-chaperonin i.e., Hsp10, which acts as a cap on the ring. The well-studied Type I chaperonin is known as the GroEL-GroES system in *Escherichia coli*. Its homologs are Cpn60/Cpn20 in chloroplasts, and mtHsp60/mtHsp10 in mitochondrion (Cheng et al., 1989; Hayer-Hartl et al., 1995; Dickson et al., 2000). Type II chaperonins are found in the cytoplasm of eukaryotes and in the archaebacterial micro-organisms. They have an in-built lid and hence do not require co-chaperonins for their function (Ranson et al., 1998). Example of Type II chaperonin includes eukaryotic TriC/CCT machinery (TCP-1 ring complex/chaperonin containing TCP-1 complex), which is made up of 8 subunits and the thermosome in archaebacteria. Contrary to Type I chaperonins, substrate independent capture of Type II chaperonins require the assistance of prefoldin and Hsp70 homologs (Iizuka et al., 2004; Cuéllar et al., 2008). Recently, a third group known as Type III chaperonins was reported which are structurally similar to Type II chaperonins but mechanistically and phylogenetically distinct from both Type I and Type II chaperonins e.g., *Carboxydothermus hydrogenoformans* chaperonin (Ch-CPN) (Techtmann and Robb, 2010; An et al., 2017; **Figure 1**). The Type I, II, and III chaperonins are also known as Group I, II, and III chaperonins.

Structure-Function of Type I Chaperonins: Prokaryotic Cytosol

E. coli GroEL-GroES

Structural and functional studies on *E. coli* GroEL have shown that it forms a tetradecameric structure composed of two heptameric rings stacked on each other forming a cavity, which changes its character from being predominantly hydrophobic to hydrophilic upon binding GroES. Substrate protein folding takes place in this cavity with the assistance of co-chaperonin GroES, which is a cap-like heptameric structure (Mande et al., 1996). Each GroES monomer is of 10 kDa size. The GroEL monomer is demarcated into three domains namely apical, intermediate, and equatorial domain. Each monomer is ∼57 kDa in size.

There are two models proposed for the GroEL-GroES mediated substrate protein folding. Asymmetric/sequential model, which is accepted widely. In this model the GroEL and GroES are present stoichiometrically in 2:1 ratio (14:7 subunit ratio). In the other model known as the symmetric/simultaneous model, which is based on the recently observed GroEL-GroES complex, both rings of GroEL are capped by co-chaperonin GroES in the stoichiometric ratio of 1:1 i.e., $(GroEL\text{-}GroES)_2$, and subunit ratio of 14:14 (Sameshima et al., 2008; Ye and Lorimer, 2013; Fei et al., 2014). Symmetric $(GroEL\text{-}GroES)_2$ complex has been observed both in the presence and absence of substrate protein suggesting a transient intermediate state in the folding reaction cycle.

Structure-Function of Type I Chaperonins: Endosymbiotic Organelles

Chloroplast and Mitochondrial Chaperonins

The chloroplast chaperonins are typically referred to as Cpn60 (GroEL homologs) and Cpn10 (GroES homologs). The Cpn60 chaperonins are made up of multiple subunits which are diverged into two related but distinct α and β types (Dickson et al., 2000; Hill and Hemmingsen, 2001). Contrary to bacterial chaperonins, which contain multiple subunits and prefer homo-oligomerization (Ojha et al., 2005; Gould et al., 2007), chloroplast chaperonins form hetero-oligomers with its two types of chaperonin α and β subunits. Heterogeneity also exists in the co-chaperonin structure. Cpn10 is similar to the standard co-chaperonin, forming heptameric single ring of 10 kDa subunits (Koumoto et al., 2001; Sharkia et al., 2003). Cpn20 has two Cpn10-like polypeptide sequences joined in tandem. The purified Cpn20 exists as a tetramer ring-like structure containing 20 kDa subunit. It is fully functional *in vitro*, helping refolding of denatured protein in presence of both chloroplast Cpn60 and *E. coli* GroEL (Tang et al., 2006). Moreover, the *Chlamydomonas reinhardtii* Cpn10 assist GroEL only in presence of Cpn20 (Tsai et al., 2012). Thus, a considerable heterogeneity exists in the oligomeric assembly of chloroplast chaperonins.

The human mitochondrial chaperonin, mtHsp60 is known to have a protein-folding mechanism (mitochondrial protein) distinct from GroEL-GroES system and requires a single heptameric ring to carry out its protein folding function along with its co-chaperonin, mtHsp10 (Viitanen et al., 1992; Nielsen and Cowan, 1998). However, the crystal structure of mitochondrial chaperonin in complex with its co-chaperonin, mtHsp60-mtHsp10 depicts a unique intermediate stage where mtHsp60-mtHsp10 forms a symmetric double-ring football-like structure, $(mtHsp60)_{14} + 2\ (mtHsp10)_7$.

Type I Chaperonins: Non-canonical Features

Multiple Chaperonins Across Species

Analysis of completely sequenced genomes suggest that about 30% of all the genomic sequence data possess multiple copies of gene sequences encoding chaperonins (Lund, 2009; Kumar et al., 2015). Distribution of these multiple chaperonins based on extensive phylogenetic analysis suggest that multiple copies of chaperonin genes exist predominantly in five phyla, namely, (a) phylum *Actinobacteria*, (b) phylum *Firmicutes*, (c) phylum *Cyanobacteria*, (d) phylum *Chlamydia,* and (e) *α-Proteobacteria* phylum (Kumar et al., 2015).

Actinobacteria

Actinobacteria are Gram-positive bacteria and possess high G + C content in their genomes, e.g., *Mycobacterium tuberculosis*, *Mycobacterium leprae,* and *Bifidobacterium longum*. These species typically possess two copies of chaperonin genes, with one of the copies being present on an operon-like structure. The other copy of Cpn60 exists as an independent gene without the presence of Cpn10 gene (Rinke de Wit et al., 1992). The actinobacterial chaperonin genes are under the regulatory control of HrcA transcription factor which binds to upstream CIRCE (controlling inverted repeat of chaperone expression) sequence (Duchêne et al., 1994; Grandvalet et al., 1998). In some cases regulation is mediated through HspR transcription factor binding to upstream HAIR (HspR Associated Inverted Repeat) sequence (Barreiro et al., 2004).

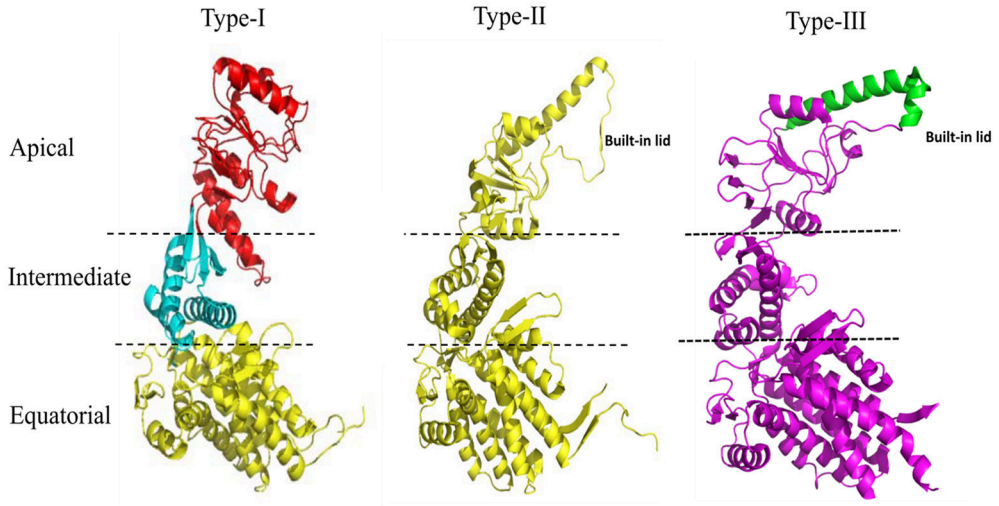

FIGURE 1 | Structural features of the Type I, Type II, and Type III chaperonins. The comparative structure analysis of Type I, Type II, and Type III chaperonins. Structures were downloaded from the RCSB with codes of PDB: 1AON, 3RUW, and 5X9U, respectively. Type I chaperonin is demarcated into Apical, Intermediate, and Equatorial domains, analogous regions of which are shown in Type II and III chaperonins using dotted lines. Type II chaperonin has a characteristic built-in lid in the structure that plays the role of co-chaperonin GroES of Type I chaperonin. Type III chaperonins are structurally similar to Type II chaperonins in having built-in-lid. However, the sequence, structure and function of the lid are distinct in Type II and Type III chaperonins (An et al., 2017). The PyMOL program (PyMOL Molecular Graphics System, version 1.3) was used to generate this figure.

Firmicutes

Firmicutes are Gram-positive bacteria and possess low G + C content in their genomes, e.g., *Staphylococcus aureus*, *Desulfitobacterium dehalogenans,* and *C. hydrogenoformans*. *Firmicutes* are known to possess both prokaryotic-like Type I chaperonin genes and archael-like chaperonin genes classified as Type III chaperonin. Type I chaperonins are arranged in an operonic arrangement with the co-chaperonin, while Type III chaperonin gene is located in the *dnaK* operon. Both the Type 1 and Type III chaperonin genes are regulated by HrcA transcription factor (Techtmann and Robb, 2010).

Chlamydiae

Chlamydiae are mostly obligate intracellular pathogens, e.g., *Chlamydia trachomatis*, *Chlamydia pneumonia,* and *Chlamydia psittaci*. Chlamydial species possess three copies of chaperonin genes (McNally and Fares, 2007). Operonic arrangement suggests that only one copy of the chaperonin genes exists along with its co-chaperonin. However, other chaperonin genes are located separately. Regulation of chlamydial chaperonin genes is complex. The first copy of the chaperonin gene is induced by heat shock and regulated by HrcA-CIRCE system. The second copy of the chaperonin gene is induced when *Chlamydia* are inside monocyte or macrophages (Kol et al., 1999), and the third copy of the chaperonin gene is induced when *Chlamydia* are in Hep-2 cells (Gérard et al., 2004). Such types of expression and regulation of chaperonin genes suggest life-cycle specific patterns and independent functional roles for them.

α-proteobacteria

Rhizobia, which belong to the *α-proteobacteria* class, are symbiotic organisms living in association with leguminous plants in the root nodules and are involved in nitrogen fixation, e.g., *Bradyrhizobium japonicum*, *Rhizobium leguminosarum*. *Rhizobia* contain most number of copies of chaperonins. *B. japonicum* has seven copies of chaperonin genes (Fischer et al., 1993). *R. leguminosarum* is a well-characterized organism and has three copies of chaperonin genes. Gene arrangement in all these organisms suggests that the three copies of the chaperonin gene form separate operons with their respective co-chaperonin genes (George et al., 2004). One of the chaperonin operons is located on the genomic island that contains genes involved in nitrogen fixation. It is regulated by NiF factors that regulate nitrogen fixation genes (Ogawa and Long, 1995). The second copy of the chaperonin gene is not well-studied and is known to be involved in chaperoning property of several model substrate proteins (George et al., 2004).

Cyanobacteria

Cyanobacteria are largely photosynthetic bacteria, e.g., *Synechococcus platensis*, *Prochlorococcus marinus,* and *Anabaena variabilis*. About 90% of the genomic sequences of the cyanobacterial species contain two copies of chaperonin genes with one of them being arranged on an operon while the other chaperonin gene coded separately. Some cyanobacterial species containing three copies of chaperonin genes, where two of its chaperonin genes being located with respective co-chaperonins in the operon while the third copy of chaperonin genes is independent (Lund, 2009; Kumar et al., 2015). Chaperonin genes existing in the operonic arrangement with their co-chaperonins are essential genes while the ones which exist independent of the co-chaperonin are non-essential (Sato et al., 2008).

The two cyanobacterial chaperonin genes are positively regulated by RpoH and negatively regulated by HrcA proteins. Upon heat shock, one of the chaperonin genes is induced rapidly while the other chaperonin gene is gradually induced (Kojima and Nakamoto, 2007; Rajaram and Apte, 2010). The chaperonin gene that is gradually induced on heat shock is known to be directly involved in photosynthesis.

Evolutionary Lineage

As more genomic sequences are becoming available, analysis of chaperonin genes suggests that distribution and frequency of multiple copies of chaperonin genes across phyla and organisms continues to increase (Lund, 2009; Kumar et al., 2015). In order to understand the cause of multiplicity of chaperonin genes is either due to horizontal gene transfer or gene duplication, phylogenetic analysis was carried on GroEL proteins across species, which revealed that the causes of existence of multiple copies of GroELs are non-uniform. In a few cases there is gene duplication event followed by evolutionary selection such as that observed in myxobacterial GroELs, mycobacterial first and second copy of GroEL and few rhizobial GroELs. In the case of the third mycobacterial GroEL homolog, few rhizobial GroELs and methanosarcinal GroELs, horizontal gene transfer occurred (Goyal et al., 2006; Kumar et al., 2015).

It has been proposed earlier in our lab that mycobacterial GroEL has been duplicated and undergone various selective pressures to perform distinctive structural and functional role during the course of evolution (Goyal et al., 2006). Biophysical and biochemical studies on recombinantly purified *M. tuberculosis* GroELs have shown that GroEL1 and GroEL2 exist as lower oligomeric species contrary to tetradecameric GroEL structure of *E. coli* (Qamra et al., 2004). The crystal structure of *M. tuberculosis* GroEL2 in its dimeric form highlighted the presence of distinct residues at the interface region, probably responsible for the change in oligomerization (**Figure 2**; Qamra and Mande, 2004). Gene shuffling and domain swapping studies on *M. tuberculosis* GroEL1 suggest that the equatorial domain is responsible for failed oligomerization. The apical domain can withstand large insertions and deletions (Kumar et al., 2009). Around the same time it was shown that GroEL1 has evolved to promiscuously bind nucleic acids (Basu et al., 2009) and oligomerization is facilitated by phosphorylation of serine residues (Kumar et al., 2009). Since GroEL2 is known to be essential chaperonin in *Mycobacteria*, whereas the oligomeric assembly of GroEL1 is regulated post-translationally, it was

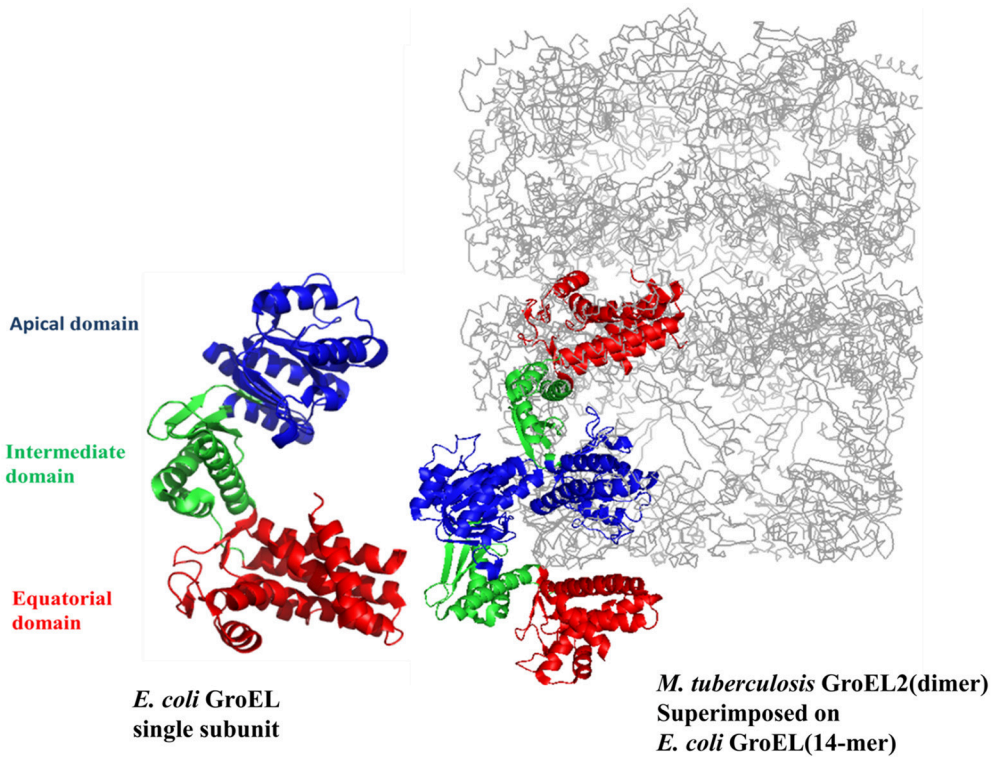

FIGURE 2 | The crystal structure of *M. tuberculosis* GroEL2 superimposed on *E. coli* GroEL-ES structure. The structure of *M. tuberculosis* GroEL2 (PDB ID:1SJP) shows lower oligomeric status (dimer). Colored in blue, green, and red are the Apical, Intermediate and Equatorial domain, respectively. Compared to *E. coli* GroEL (PDB ID: 1AON) shown in gray color, the inter-subunit interaction is mediated through Apical domain in *M. tuberculosis* GroEL2 structure whereas inter-subunit interaction is through Equatorial domain in *E. coli* GroEL. Single subunit of *M. tuberculosis* GroEL2 is aligned to *E. coli* GroES bound GroEL ring representing asymmetric model. GroES structure has been removed for simplicity. A single subunit of *E. coli* GroEL has been shown with the same color-coded domains compared to *M. tuberculosis* GroEL2 for comparative analysis. The PyMOL program (PyMOL Molecular Graphics System, version 1.3) was used to generate this figure.

reported that tetradecameric assembly and precise inter-domain communication are prerequisite for chaperonin activity (Chilukoti et al., 2015).

Functional Diversity

It is important to examine whether the presence of multiple copies of chaperonins are responsible for behaving as canonical chaperonins or they have diverged to carry out novel functions. It is also important to note whether these multiple chaperonins act on common substrates or on distinct pool of substrates. GroELs are highly conserved across different species and it has been shown that homologs of chaperonins from other bacteria are able to function in *E. coli* suggesting overlapping of substrate proteins and common mechanism of GroEL function. The interactions of substrate proteins with GroEL are hydrophobic in nature, so conformational change mediated exposure of the apical and the equatorial domains in the cavity plays a key role in substrate recognition and assists protein folding. Binding of substrate proteins to GroEL is through α/β domains of proteins with no sequence similarity (Kerner et al., 2005; Kumar and Mande, 2011) and further studies suggest that GroEL selectively binds globular substrates rather than extended polypeptides (Robinson et al., 1994; Goldberg et al., 1997). Multiple copies of chaperonins in an organism have also been reported to have evolved to carry out novel functions. GroEL homolog in an insect symbiont, *Xenorhabdus nematophila* has been shown to be toxic to insects which is mediated through binding to alpha-chitin. Mutational analysis on these GroEL homologs suggests that the amino acid critical for this kind of activity is distinct from the essential chaperonin (Joshi et al., 2008). In *M. tuberculosis*, GroEL2 acts as a generalist chaperonin (Hu et al., 2008) while GroEL1 is reported to be associated with nucleoids (Basu et al., 2009). Thus, it is apparent that gene duplication of *groEL* genes has led to the functional diversity of chaperonins and/or distinct substrate spectrum for intracellular protein folding.

Post-translational Modifications/Biofilm Formation

Post-translational modifications in proteins are employed by organisms to modulate their physiological processes and adapt to constantly changing environment (Bernal et al., 2014). Chaperonins have been reported to be post-translationally modified in certain organisms, and this modification has been reported to gain/loss of their function. For example, fractionation of *M. tuberculosis* cell lysate has shown that tetradecameric form of GroEL1 is attained only upon phosphorylation at serine residues (Kumar et al., 2009). Similarly in another report it has been shown that phosphorylation occurs at threonine residues (Canova et al., 2009). Both of these observations suggest that oligomerization of GroEL1 is a result of post-translational modification.

Many pathogens evade innate immune response and become resistant to antibiotics by forming biofilms on epithelial cells (Hall-Stoodley and Stoodley, 2005). The role of GroEL in biofilm formation has been elucidated in a few organisms. For example, GroEL1 mutant of *M. smegmatis* fails to form biofilm. Mechanistic studies revealed that *M. smegmatis* GroEL1 interacts with the KasA enzyme, which is critical for mycolic acid biosynthesis involved in biofilm formation (Ojha et al., 2005). Interestingly, it has been recently reported that GroEL in pathogenic strain *B. anthracis* gets phosphorylated and thereby modulates biofilm formation. These findings highlight that phosphorylation of GroEL has functional implications (Arora et al., 2017). Acetylation is another post-translational modification associated with *E. coli* and *M. tuberculosis* chaperonins, however a functional role has not yet been ascribed to this modification (Liu et al., 2014). Similarly, mitochondrial co-chaperonin (mtHsp10) undergoes acetyl modification and controls folding of mitochondrial proteins under excess nutrient condition (Lu et al., 2015).

C-Terminal Diversity

Various studies highlight the importance of the C-terminal residues of GroEL in the overall functioning of the chaperonin (Tang et al., 2006; Chen et al., 2013). In cases pertaining to multiple copies of chaperonins, they have distinct pattern of C-terminal residues. While the C-terminus of GroEL (from *E. coli*) has a 13 residue motif $(GGM)_4M$, GroEL homologs from other organisms (which contain multiple copies of chaperonins) have distinct C-terminal motifs, such as:

a) Histidine-rich C-terminal, e.g., *Mycobacteria* (Colaco and MacDougall, 2014)

b) Pattern-less C-terminus, e.g., *Rhizobia* (George et al., 2004)

c) Similar $(GGM)_4M$ repeats, e.g., *Myxobacteria* (Wang et al., 2013)

d) Lack of GGM-like tail, e.g., *Methanosarcina* (Figueiredo et al., 2004)

It is clearly seen that many chaperonin paralogs in different organisms have GGM-like C-terminus. A wide range of genomic organization is seen in these chaperonins. Moreover, differences are also seen in their co-expression with co-chaperonin and essentiality of their function. Thus, these paralogs are perplexingly observed to be either essential or non-essential, co-expressed with their co-chaperonin or not co-expressed, and possibly function as housekeeping chaperonins. On the other hand chaperonins not possessing the GGM-like C-terminus have possibly evolved to carry out novel functions (Ojha et al., 2005; Wang et al., 2013; **Figure 3**).

CONCLUDING REMARKS

Type I chaperonins are important by virtue of their role in intracellular protein folding. GroEL-GroES system in bacteria helps folding of about 10–15% of cytosolic proteins. Various structures of GroEL solved in apo-form, nucleotide-bound form as well as in complex with co-chaperonin GroES attempt to explain the role of these chaperonins in protein folding (Saibil et al., 2013). The existence of multiple chaperonins and their role in varied functions hints evolutionary pressure toward adapting to different environmental conditions. The structure of *M. tuberculosis* GroEL2 highlights lower oligomeric state and more exposed hydrophobic surfaces, probably to

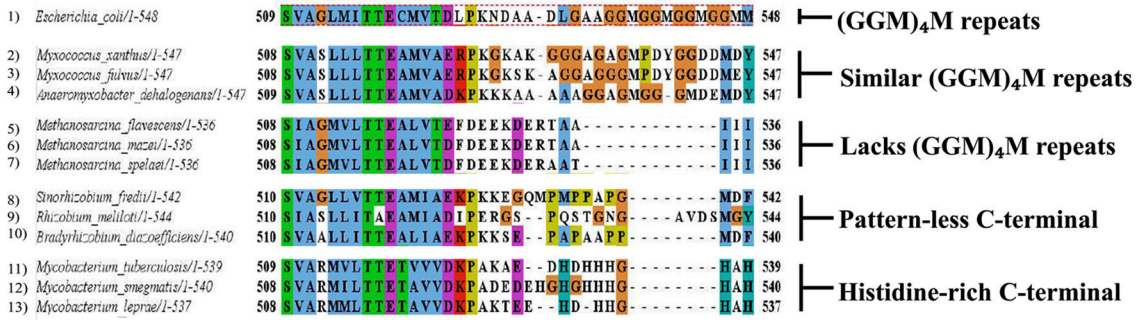

FIGURE 3 | Multiple chaperonins in bacteria displaying diversity at C-terminal. Sequence alignment highlighting C-terminal regions of the representative bacterial GroEL homologs with the *E. coli* GroEL. The last C-terminal residues of selected multiple GroELs in different bacteria show divergence from the canonical (GGM)4M motif of the *E. coli* GroEL shown in dotted red box. Sequences were retrieved from www.uniprot.org and aligned in MEGA6 using MUSCLE algorithm (www.megasoftware.net). Formatting of aligned sequences were done in Jalview alignment viewer (www.jalview.org). Residues in the alignment follow the default Clustal color scheme of Jalview.

increase substrate pool and energy conservation (Qamra and Mande, 2004; Qamra et al., 2004; Kumar and Mande, 2011). Owing to the presence of Histidine-rich C-terminal in multiple chaperonins, these have been proposed to help in alternate biological functions. *M. smegmatis* GroEL1 binding to iron may help in biofilm formation (Ojha et al., 2005). Survival defect of M. tuberculosis *groEL1* knockout strain under low aeration condition might help in oxygen sensing by directly binding to metals or help certain metalloproteins in folding (Sharma et al., 2016). The structure of other homologous chaperonin proteins will probably answer the myriad of questions associated with the novel functions of chaperonin homologs.

AUTHOR CONTRIBUTIONS

All authors listed have made a substantial, direct, and intellectual contribution to the work, and approved it for publication.

ACKNOWLEDGMENTS

MYA thanks the financial support for Senior Research Fellowship of the Department of Biotechnology (DBT), Ministry of Science and Technology, Government of India. The authors would like to gratefully acknowledge the financial support for work in the SCM laboratory through grants BT/PR15450/COE/34/46/2016 and BT/PR3260/BRB/10/967/2011 of the DBT.

REFERENCES

An, Y. J., Rowland, S. E., Na, J. H., Spigolon, D., Hong, S. K., Yoon, Y. J., et al. (2017). Structural and mechanistic characterization of an archaeal-like chaperonin from a thermophilic bacterium. *Nat. Commun.* 8:827. doi: 10.1038/s41467-017-00980-z

Arora, G., Sajid, A., Virmani, R., Singhal, A., Kumar, C. M. S., Dhasmana, N., et al. (2017). Ser/Thr protein kinase PrkC-mediated regulation of GroEL is critical for biofilm formation in *Bacillus anthracis*. *NPJ Biofilms Microbiomes* 3:7. doi: 10.1038/s41522-017-0015-4

Barreiro, C., González-Lavado, E., Pátek, M., and Martín, J. F. (2004). Transcriptional analysis of the groES-groEL1, groEL2, and dnaK genes in *Corynebacterium glutamicum*: characterization of heat shock-induced promoters. *J. Bacteriol.* 186, 4813–4817. doi: 10.1128/JB.186.14.4813-4817.2004

Basu, D., Khare, G., Singh, S., Tyagi, A., Khosla, S., and Mande, S. C. (2009). A novel nucleoid-associated protein of *Mycobacterium tuberculosis* is a sequence homolog of GroEL. *Nucleic Acids Res.* 37, 4944–4954. doi: 10.1093/nar/gkp502

Bernal, V., Castaño-Cerezo, S., Gallego-Jara, J., Écija-Conesa, A., de Diego, T., Iborra, J. L., et al. (2014). Regulation of bacterial physiology by lysine acetylation of proteins. *N. Biotechnol.* 31, 586–595. doi: 10.1016/j.nbt.2014.03.002

Bohen, S. P., Kralli, A., and Yamamoto, K. R. (1995). Hold 'em and fold' em: chaperones and signal transduction. *Science* 268, 1303–1304.

Bukau, B., and Horwich, A. L. (1998). The Hsp70 and Hsp60 chaperone machines. *Cell* 92, 351–366. doi: 10.1016/S0092-8674(00)80928-9

Canova, M. J., Kremer, L., and Molle, V. (2009). The *Mycobacterium tuberculosis* GroEL1 chaperone is a substrate of Ser/Thr protein kinases. *J. Bacteriol.* 191, 2876–2883. doi: 10.1128/JB.01569-08

Chen, D. H., Madan, D., Weaver, J., Lin, Z., Schröder, G. F., Chiu, W., et al. (2013). Visualizing GroEL/ES in the act of encapsulating a folding protein. *Cell* 153, 1354–1365. doi: 10.1016/j.cell.2013.04.052

Cheng, M. Y., Hartl, F. U., Martin, J., Pollock, R. A., Kalousek, F., Neupert, W., et al. (1989). Mitochondrial heat-shock protein hsp60 is essential for assembly of proteins imported into yeast mitochondria. *Nature* 337, 620–625. doi: 10.1038/337620a0

Chilukoti, N., Kumar, C. M., and Mande, S. C. (2015). GroEL2 of *Mycobacterium tuberculosis* reveals the importance of structural pliability in chaperonin function. *J. Bacteriol.* 198, 486–497. doi: 10.1128/JB.00844-15

Colaco, C. A., and MacDougall, A. (2014). Mycobacterial chaperonins: the tail wags the dog. *FEMS Microbiol. Lett.* 350, 20–24. doi: 10.1111/1574-6968.12276

Cuéllar, J., Martín-Benito, J., Scheres, S. H., Sousa, R., Moro, F., López-Viñas, E., et al. (2008). The structure of CCT-Hsc70 NBD suggests a mechanism for Hsp70 delivery of substrates to the chaperonin. *Nat. Struct. Mol. Biol.* 15, 858–864. doi: 10.1038/nsmb.1464

Dickson, R., Weiss, C., Howard, R. J., Alldrick, S. P., Ellis, R. J., Lorimer, G., et al. (2000). Reconstitution of higher plant chloroplast chaperonin 60 tetradecamers active in protein folding. *J. Biol. Chem.* 275, 11829–11835. doi: 10.1074/jbc.275.16.11829

Duchêne, A. M., Thompson, C. J., and Mazodier, P. (1994). Transcriptional analysis of groEL genes in Streptomyces coelicolor A3(2). *Mol. Gen. Genet.* 245, 61–68. doi: 10.1007/BF00279751

Fei, X., Ye, X., LaRonde, N. A., and Lorimer, G. H. (2014). Formation and structures of GroEL:GroES2 chaperonin footballs, the protein-folding functional form. *Proc. Natl. Acad. Sci. U.S.A.* 111, 12775–12780. doi: 10.1073/pnas.1412922111

Figueiredo, L., Klunker, D., Ang, D., Naylor, D. J., Kerner, M. J., Georgopoulos, C., et al. (2004). Functional characterization of an archaeal GroEL/GroES chaperonin system: significance of substrate encapsulation. *J. Biol. Chem.* 279, 1090–1099. doi: 10.1074/jbc.M310914200

Fischer, H. M., Babst, M., Kaspar, T., Acuña, G., Arigoni, F., and Hennecke, H. (1993). One member of a gro-ESL-like chaperonin multigene family in *Bradyrhizobium japonicum* is co-regulated with symbiotic nitrogen fixation genes. *EMBO J.* 12, 2901–2912.

George, R., Kelly, S. M., Price, N. C., Erbse, A., Fisher, M., and Lund, P. A. (2004). Three GroEL homologues from *Rhizobium leguminosarum* have distinct *in vitro* properties. *Biochem. Biophys. Res. Commun.* 324, 822–828. doi: 10.1016/j.bbrc.2004.09.140

Gérard, H. C., Whittum-Hudson, J. A., Schumacher, H. R., and Hudson, A. P. (2004). Differential expression of three *Chlamydia trachomatis* hsp60-encoding genes in active vs. persistent infections. *Microb. Pathog.* 36, 35–39. doi: 10.1016/j.micpath.2003.08.005

Goldberg, M. S., Zhang, J., Sondek, S., Matthews, C. R., Fox, R. O., and Horwich, A. L. (1997). Native-like structure of a protein-folding intermediate bound to the chaperonin GroEL. *Proc. Natl. Acad. Sci. U.S.A.* 94, 1080–1085. doi: 10.1073/pnas.94.4.1080

Gould, P. S., Burgar, H. R., and Lund, P. A. (2007). Homologous cpn60 genes in *Rhizobium leguminosarum* are not functionally equivalent. *Cell Stress Chaperones* 12, 123–131. doi: 10.1379/CSC-227R.1

Goyal, K., Qamra, R., and Mande, S. C. (2006). Multiple gene duplication and rapid evolution in the groEL gene: functional implications. *J. Mol. Evol.* 63, 781–787. doi: 10.1007/s00239-006-0037-7

Grandvalet, C., Rapoport, G., and Mazodier, P. (1998). hrcA, encoding the repressor of the groEL genes in Streptomyces albus G, is associated with a second dnaJ gene. *J. Bacteriol.* 180, 5129–5134.

Hall-Stoodley, L., and Stoodley, P. (2005). Biofilm formation and dispersal and the transmission of human pathogens. *Trends Microbiol.* 13, 7–10. doi: 10.1016/j.tim.2004.11.004

Hayer-Hartl, M. K., Martin, J., and Hartl, F. U. (1995). Asymmetrical interaction of GroEL and GroES in the ATPase cycle of assisted protein folding. *Science* 269, 836–841. doi: 10.1126/science.7638601

Hill, J. E., and Hemmingsen, S. M. (2001). *Arabidopsis thaliana* type I and II chaperonins. *Cell Stress Chaperones* 6, 190–200. doi: 10.1379/1466-1268(2001)006<0190:ATTIAI>2.0.CO;2

Hu, Y., Henderson, B., Lund, P. A., Tormay, P., Ahmed, M. T., Gurcha, S. S., et al. (2008). A *Mycobacterium tuberculosis* mutant lacking the groEL homologue cpn60.1 is viable but fails to induce an inflammatory response in animal models of infection. *Infect. Immun.* 76, 1535–1546. doi: 10.1128/IAI.01078-07

Iizuka, R., So, S., Inobe, T., Yoshida, T., Zako, T., Kuwajima, K., et al. (2004). Role of the helical protrusion in the conformational change and molecular chaperone activity of the archaeal group II chaperonin. *J. Biol. Chem.* 279, 18834–18839. doi: 10.1074/jbc.M400839200

Joshi, M. C., Sharma, A., Kant, S., Birah, A., Gupta, G. P., Khan, S. R., et al. (2008). An insecticidal GroEL protein with chitin binding activity from *Xenorhabdus nematophila*. *J. Biol. Chem.* 283, 28287–28296. doi: 10.1074/jbc.M804416200

Kerner, M. J., Naylor, D. J., Ishihama, Y., Maier, T., Chang, H. C., Stines, A. P., et al. (2005). Proteome-wide analysis of chaperonin-dependent protein folding in *Escherichia coli*. *Cell* 122, 209–220. doi: 10.1016/j.cell.2005.05.028

Kim, Y. E., Hipp, M. S., Bracher, A., Hayer-Hartl, M., and Hartl, F. U. (2013). Molecular chaperone functions in protein folding and proteostasis. *Annu. Rev. Biochem.* 82, 323–355. doi: 10.1146/annurev-biochem-060208-092442

Kojima, K., and Nakamoto, H. (2007). A novel light- and heat-responsive regulation of the groE transcription in the absence of HrcA or CIRCE in cyanobacteria. *FEBS Lett.* 581, 1871–1880. doi: 10.1016/j.febslet.2007.03.084

Kol, A., Bourcier, T., Lichtman, A. H., and Libby, P. (1999). Chlamydial and human heat shock protein 60s activate human vascular endothelium, smooth muscle cells, and macrophages. *J. Clin. Invest.* 103, 571–577. doi: 10.1172/JCI5310

Koumoto, Y., Shimada, T., Kondo, M., Hara-Nishimura, I., and Nishimura, M. (2001). Chloroplasts have a novel Cpn10 in addition to Cpn20 as co-chaperonins in *Arabidopsis thaliana*. *J. Biol. Chem.* 276, 29688–29694. doi: 10.1074/jbc.M102330200

Kumar, C. M., Khare, G., Srikanth, C. V., Tyagi, A. K., Sardesai, A. A., and Mande, S. C. (2009). Facilitated oligomerization of mycobacterial GroEL: evidence for phosphorylation-mediated oligomerization. *J. Bacteriol.* 191, 6525–6538. doi: 10.1128/JB.00652-09

Kumar, S., and Mande, S. (2011). Protein chaperones and non-protein substrates: on substrate promiscuity of GroEL. *Curr. Sci.* 100, 1646–1653.

Kumar, C. M., Mande, S. C., and Mahajan, G. (2015). Multiple chaperonins in bacteria—novel functions and non-canonical behaviors. *Cell Stress Chaperones* 20, 555–574. doi: 10.1007/s12192-015-0598-8

Lindquist, S. (1986). The heat-shock response. *Annu. Rev. Biochem.* 55, 1151–1191. doi: 10.1146/annurev.bi.55.070186.005443

Lindquist, S., and Craig, E. A. (1988). The heat-shock proteins. *Annu. Rev. Genet.* 22, 631–677. doi: 10.1146/annurev.ge.22.120188.003215

Liu, F., Yang, M., Wang, X., Yang, S., Gu, J., Zhou, J., et al. (2014). Acetylome analysis reveals diverse functions of lysine acetylation in *Mycobacterium tuberculosis*. *Mol. Cell. Proteomics* 13, 3352–3366. doi: 10.1074/mcp.M114.041962

Lu, Z., Chen, Y., Aponte, A. M., Battaglia, V., Gucek, M., and Sack, M. N. (2015). Prolonged fasting identifies heat shock protein 10 as a Sirtuin 3 substrate elucidating a new mechanism linking mitochondrial protein acetylation to fatty acid oxidation enzyme folding and function. *J. Biol. Chem.* 290, 2466–2476. doi: 10.1074/jbc.M114.606228

Lund, P. A. (2009). Multiple chaperonins in bacteria–why so many? *FEMS Microbiol. Rev.* 33, 785–800. doi: 10.1111/j.1574-6976.2009.00178.x

Mande, S. C., Mehra, V., Bloom, B. R., and Hol, W. G. (1996). Structure of the heat shock protein chaperonin-10 of *Mycobacterium leprae*. *Science* 271, 203–207. doi: 10.1126/science.271.5246.203

McNally, D., and Fares, M. A. (2007). *In silico* identification of functional divergence between the multiple groEL gene paralogs in Chlamydiae. *BMC Evol. Biol.* 7:81. doi: 10.1186/1471-2148-7-81

Nielsen, K. L., and Cowan, N. J. (1998). A single ring is sufficient for productive chaperonin-mediated folding *in vivo*. *Mol. Cell* 2, 93–99. doi: 10.1016/S1097-2765(00)80117-3

Ogawa, J., and Long, S. R. (1995). The Rhizobium meliloti groELc locus is required for regulation of early nod genes by the transcription activator NodD. *Genes Dev.* 9, 714–729. doi: 10.1101/gad.9.6.714

Ojha, A., Anand, M., Bhatt, A., Kremer, L., Jacobs, W. R., and Hatfull, G. F. (2005). GroEL1: a dedicated chaperone involved in mycolic acid biosynthesis during biofilm formation in mycobacteria. *Cell* 123, 861–873. doi: 10.1016/j.cell.2005.09.012

Qamra, R., and Mande, S. C. (2004). Crystal structure of the 65-kilodalton heat shock protein, chaperonin 60.2, of *Mycobacterium tuberculosis*. *J. Bacteriol.* 186, 8105–8113. doi: 10.1128/JB.186.23.8105-8113.2004

Qamra, R., Srinivas, V., and Mande, S. C. (2004). *Mycobacterium tuberculosis* GroEL homologues unusually exist as lower oligomers and retain the ability to suppress aggregation of substrate proteins. *J. Mol. Biol.* 342, 605–617. doi: 10.1016/j.jmb.2004.07.066

Rajaram, H., and Apte, S. K. (2010). Differential regulation of groESL operon expression in response to heat and light in Anabaena. *Arch. Microbiol.* 192, 729–738. doi: 10.1007/s00203-010-0601-9

Ranson, N. A., White, H. E., and Saibil, H. R. (1998). Chaperonins. *Biochem. J.* 333(Pt 2), 233–242. doi: 10.1042/bj3330233

Richter, K., Haslbeck, M., and Buchner, J. (2010). The heat shock response: life on the verge of death. *Mol. Cell* 40, 253–266. doi: 10.1016/j.molcel.2010.10.006

Rinke de Wit, T. F., Bekelie, S., Osland, A., Miko, T. L., Hermans, P. W., van Soolingen, D., et al. (1992). Mycobacteria contain two groEL genes: the second *Mycobacterium leprae* groEL gene is arranged in an operon with groES. *Mol. Microbiol.* 6, 1995–2007. doi: 10.1111/j.1365-2958.1992.tb01372.x

Robinson, C. V., Gross, M., Eyles, S. J., Ewbank, J. J., Mayhew, M., Hartl, F. U., et al. (1994). Conformation of GroEL-bound alpha-lactalbumin probed by mass spectrometry. *Nature* 372, 646–651. doi: 10.1038/372646a0

Saibil, H. R., Fenton, W. A., Clare, D. K., and Horwich, A. L. (2013). Structure and allostery of the chaperonin GroEL. *J. Mol. Biol.* 425, 1476–1487. doi: 10.1016/j.jmb.2012.11.028

Sameshima, T., Ueno, T., Iizuka, R., Ishii, N., Terada, N., Okabe, K., et al. (2008). Football- and bullet-shaped GroEL-GroES complexes coexist during the reaction cycle. *J. Biol. Chem*. 283, 23765–23773. doi: 10.1074/jbc.M802541200

Sato, S., Ikeuchi, M., and Nakamoto, H. (2008). Expression and function of a groEL paralog in the thermophilic cyanobacterium Thermosynechococcus elongatus under heat and cold stress. *FEBS Lett*. 582, 3389–3395. doi: 10.1016/j.febslet.2008.08.034

Schirmer, E. C., Glover, J. R., Singer, M. A., and Lindquist, S. (1996). HSP100/Clp proteins: a common mechanism explains diverse functions. *Trends Biochem. Sci*. 21, 289–296. doi: 10.1016/S0968-0004(96)10038-4

Sharkia, R., Bonshtien, A. L., Mizrahi, I., Weiss, C., Niv, A., Lustig, A., et al. (2003). On the oligomeric state of chloroplast chaperonin 10 and chaperonin 20. *Biochim. Biophys. Acta* 1651, 76–84. doi: 10.1016/S1570-9639(03)00237-1

Sharma, A., Rustad, T., Mahajan, G., Kumar, A., Rao, K. V., Banerjee, S., et al. (2016). Towards understanding the biological function of the unusual chaperonin Cpn60.1 (GroEL1) of *Mycobacterium tuberculosis*. *Tuberc. Edinb. Scotl*. 97, 137–146. doi: 10.1016/j.tube.2015.11.003

Tang, Y. C., Chang, H. C., Roeben, A., Wischnewski, D., Wischnewski, N., Kerner, M. J., et al. (2006). Structural features of the GroEL-GroES nano-cage required for rapid folding of encapsulated protein. *Cell* 125, 903–914. doi: 10.1016/j.cell.2006.04.027

Techtmann, S. M., and Robb, F. T. (2010). Archaeal-like chaperonins in bacteria. *Proc. Natl. Acad. Sci. U.S.A*. 107, 20269–20274. doi: 10.1073/pnas.1004783107

Tsai, Y. C., Mueller-Cajar, O., Saschenbrecker, S., Hartl, F. U., and Hayer-Hartl, M. (2012). Chaperonin cofactors, Cpn10 and Cpn20, of green algae and plants function as hetero-oligomeric ring complexes. *J. Biol. Chem*. 287, 20471–20481. doi: 10.1074/jbc.M112.365411

Viitanen, P. V., Lorimer, G. H., Seetharam, R., Gupta, R. S., Oppenheim, J., Thomas, J. O., et al. (1992). Mammalian mitochondrial chaperonin 60 functions as a single toroidal ring. *J. Biol. Chem*. 267, 695–698.

Wang, Y., Zhang, W. Y., Zhang, Z., Li, J., Li, Z. F., Tan, Z. G., et al. (2013). Mechanisms involved in the functional divergence of duplicated GroEL chaperonins in *Myxococcus xanthus* DK1622. *PLoS Genet*. 9:e1003306. doi: 10.1371/journal.pgen.1003306

Ye, X., and Lorimer, G. H. (2013). Substrate protein switches GroE chaperonins from asymmetric to symmetric cycling by catalyzing nucleotide exchange. *Proc. Natl. Acad. Sci. U.S.A*. 110, E4289–E4297. doi: 10.1073/pnas.13177 02110

Conflict of Interest Statement: The authors declare that the research was conducted in the absence of any commercial or financial relationships that could be construed as a potential conflict of interest.

frontiers in Molecular Biosciences

PERSPECTIVE
published: 27 April 2018
doi: 10.3389/fmolb.2018.00042

Single-Ring Intermediates Are Essential for Some Chaperonins

*Jay M. Bhatt[1], Adrian S. Enriquez[1], Jinliang Wang[1], Humberto M. Rojo[1], Sudheer K. Molugu[2], Zacariah L. Hildenbrand[3] and Ricardo A. Bernal[1]**

[1] Department of Chemistry, The University of Texas at El Paso, El Paso, TX, United States, [2] Department of Pharmacology, School of Medicine, Case Western Reserve University, Cleveland, OH, United States, [3] Inform Environmental, Dallas, TX, United States

Chaperonins are macromolecular complexes found throughout all kingdoms of life that assist unfolded proteins reach a biologically active state. Historically, chaperonins have been classified into two groups based on sequence, subunit structure, and the requirement for a co-chaperonin. Here, we present a brief review of chaperonins that can form double- and single-ring conformational intermediates in their protein-folding catalytic pathway. To date, the bacteriophage encoded chaperonins ϕ-EL and OBP, human mitochondrial chaperonin and most recently, the bacterial groEL/ES systems, have been reported to form single-ring intermediates as part of their normal protein-folding activity. These double-ring chaperonins separate into single-ring intermediates that have the ability to independently fold a protein. We discuss the structural and functional features along with the biological relevance of single-ring intermediates in cellular protein folding. Of special interest are the ϕ-EL and OBP chaperonins which demonstrate features of both group I and II chaperonins in addition to their ability to function via single-ring intermediates.

Keywords: chaperonins, GroEL, phiEL, HSP60, protein folding, single-ring chaperonins

OPEN ACCESS

Edited by:
Abdussalam Azem, Tel Aviv University, Israel

Reviewed by:
Marc Jamin, Université Grenoble Alpes, France
Krzysztof Liberek, University of Gdansk, Poland

****Correspondence:***
Ricardo A. Bernal
rbernal@utep.edu

Specialty section:
This article was submitted to Protein Folding, Misfolding and Degradation, a section of the journal Frontiers in Molecular Biosciences

Received: *17 November 2017*
Accepted: *13 April 2018*
Published: *27 April 2018*

Citation:
Bhatt JM, Enriquez AS, Wang J, Rojo HM, Molugu SK, Hildenbrand ZL and Bernal RA (2018) Single-Ring Intermediates Are Essential for Some Chaperonins. Front. Mol. Biosci. 5:42. doi: 10.3389/fmolb.2018.00042

INTRODUCTION

All the information required for macromolecules to acquire their correct three-dimensional structure and to undergo large conformational changes is found in the primary structure. Some proteins can refold on their own while others require assistance in regaining structural integrity and biological activity in the event of misfolding. Chaperonins are large complexes that are responsible for refolding these misfolded proteins. They constitute a highly conserved family of functionally and structurally related protein complexes that assist in the proper folding of non-native proteins involved in a wide variety of cellular processes (Brocchieri and Karlin, 2000; Henderson et al., 2010). In the absence of protein-folding assistance, cells accumulate misfolded protein and protein aggregates that eventually lead to cell death (Dekker et al., 2008; Sukhanova et al., 2012). Chaperonins are multi-subunit assemblies that form an internal protein-folding chamber that segregates misfolded substrate proteins from cytoplasmic constituents that can interfere with correct protein-folding. The general structure of chaperonins includes three separate domains that execute specific functions (Schoehn et al., 2000; Iizuka et al., 2004; Spiess et al., 2004). The apical domain is a highly flexible domain that interacts with the substrate protein and with a co-chaperonin that closes the opening to the protein-folding chamber after the substrate has entered (Saibil et al., 1993; Booth et al., 2008; Zhang et al., 2010). The intermediate domain acts as a hinge between the apical and the equatorial domain which is responsible for contacts between

the two rings. The equatorial domain contains the nucleotide binding pocket and is responsible for conformational changes that drive the protein-folding cycle (Braig et al., 1994; Ditzel et al., 1998; Zhang et al., 2010).

Historically, chaperonins have been categorized into two groups according to their sequence similarity, the number of subunits and their arrangement, and their need for a co-chaperonin (Cheng et al., 1990; Reissmann et al., 2007; Techtmann and Robb, 2010; Lopez et al., 2015; An et al., 2017). Over the years, chaperonins with single-ring intermediates have been identified in eukaryotes and more recently in viruses (Horwich et al., 1993; Shaburova et al., 2006; Cornelissen et al., 2012; Hildenbrand and Bernal, 2012; Molugu et al., 2016; Semenyuk et al., 2016; An et al., 2017; Marine et al., 2017). Their protein-folding mechanisms, however, were poorly understood because they were largely based on knowledge obtained from studies of the bacterial groEL/ES chaperonin or its respective single-ring mutants (Sun et al., 2003; Liu et al., 2009; Kovács et al., 2010; Illingworth et al., 2011, 2015; Enriquez et al., 2017). Recent cryo-EM structural analyses on the ϕ-EL phage-encoded chaperonin revealed that it undergoes ring dissociation to form single-ring intermediates upon ATP hydrolysis (Hertveldt et al., 2005; Kurochkina et al., 2012; Semenyuk et al., 2015; Molugu et al., 2016). The novel single-ring intermediates of the ϕ-EL and OBP chaperonin are like those reported for the human mitochondrial chaperonin (Viitanen et al., 1992; Levy-Rimler et al., 2001). These single ring intermediates, along with other structural and functional features, differentiate ϕ-EL and OBP from commonly described group I and group II chaperonins.

CHARACTERISTICS OF GROUP I AND II CHAPERONINS

Group I chaperonins like the *Escherichia coli* chaperonin groEL and its co-chaperonin GroES (together denoted as groEL/ES), are typically found in eubacteria with the exception of the eukaryotic mitochondrial heat shock protein 60 (hsp60) and its co-chaperonin heat shock protein 10 (hsp60/10) (Fenton and Horwich, 1997). They are characterized as homo-tetradecamers composed of two stacked seven-membered rings (see **Table 1**) (Horwich et al., 2009; Enriquez et al., 2017). In addition, group I chaperonins possess a staggered (1:2) inter-ring subunit organization where one subunit in one ring directly contacts two subunits in the opposite ring (Braig et al., 1994; Ditzel et al., 1998; Hildenbrand and Bernal, 2012). The defining feature of group I chaperonins is that they require the assistance of an additional co-chaperonin protein that acts as a lid to isolate the central protein-folding chamber (Hayer-Hartl et al., 2016). In the absence of co-chaperonin, group I chaperonins can prevent non-native protein aggregation but are unable to fold them (Ellis, 2003; Horwich et al., 2009).

Group II members include chaperonins from archaeal (Mm-cpn) and eukaryotic cells (TriC). These chaperonins can be homo or hetero-oligomers consisting of 7–9 subunits per ring (see **Table 1**). These group II complexes have an in-register (1:1) inter-ring subunit arrangement where each subunit contacts only one subunit in the opposite ring (Braig et al., 1994; Ditzel et al., 1998; Hildenbrand and Bernal, 2012). Group II chaperonins do not require a co-chaperonin for proper protein-folding due to an extra structural protrusion atop the apical domain that rearranges itself upon ATP hydrolysis to form a built-in lid that seals the central cavity (Ditzel et al., 1998; Kusmierczyk and Martin, 2003; Joachimiak et al., 2014).

THE ϕ-EL SINGLE-RING ATPASE CYCLE

Typically, bacteriophages will utilize the host chaperonin to process nascent viral polypeptides. However, the ϕ-EL chaperonin encoded by the *Pseudomonas aeruginosa* is unique in that it is the first of only two chaperonin groEL orthologs that have been identified in the phage genome (phage OBP being the other, see below). Chaperonin ϕ-EL possesses structural features of both group I and II (Molugu et al., 2016). The ϕ-EL chaperonin is like group I chaperonins in that it forms a homo-oligomeric tetradecameric complex and does not have substrate specificity. On the other hand, the similarities between ϕ-EL and group II chaperonins include the lack of a co-chaperonin and an in-register (1:1) subunit arrangement at the inter-ring interface (**Table 1**).

Recent electron microscope reconstructions have demonstrated that nucleotides control the conformational state of the chaperonin and that the substrate is the trigger that allows progression of the chaperonin along the catalytic protein-folding cycle (Molugu et al., 2016). In the absence of substrate and presence of ATP, the ϕ-EL chaperonin forms an open double-ring conformation that is primed for substrate binding (**Figure 1**). This conformation is stable until the substrate binds and triggers ATP hydrolysis. This *in-vitro* behavior makes sense because the chaperonin without substrate would deplete ATP reserves in futile hydrolysis reactions. ATP hydrolysis by both rings simultaneously triggers ring separation resulting in a more than two-fold enlargement in volume of the internal cavity (**Figure 1**). The enlarged protein-folding chamber enables the encapsulation of the 116 kDa denatured β-galactosidase protein, a substrate too large to be folded by groEL/ES (Ayling and Baneyx, 1996; Molugu et al., 2016). Interestingly, hydrolysis of ATP simultaneously triggers an extreme downward tilt of the equatorial domains that result in ring dissociation into two single-ring complexes (Molugu et al., 2016). This contributes in large part to the expansion of the internal chamber. At the apical end, ATP hydrolysis also induces closure of the internal chamber in what appears to be an iris-like rearrangement of the apical domains, circumventing the need for a co-chaperonin to act as a lid to create an isolated internal chamber. The two rings then re-associate to form a closed double-ring complex that then relies on the binding of ATP to release folded substrate and initiate another iteration of protein-folding (Molugu et al., 2016). The ϕ-EL chaperonin probably operates via a one-stroke protein-folding mechanism due to the simultaneous activity of both rings, as depicted in **Figure 1**. Furthermore, inter-ring negative cooperativity is likely eliminated since both rings appear to fold proteins

TABLE 1 | Features of group I and II chaperonins compared to ϕ-EL.

	Group I	**Group II**	**ϕ-EL**
Source	Bacteria, *Homo sapiens*	Archaea and eukaryotes	Bacteriophage
Location	Cytoplasmic and endosymbiotic organelles	Cytoplasmic	Cytoplasmic
Substrate	**Promiscuous**	Substrate-specific	**Promiscuous**
Subunits per ring	7	7–9	7
Oligomeric organization	**Homo-oligomeric**	Hetero-oligomeric	**Homo-oligomeric**
Co-chaperonin	Required	**Not Required**	**Not Required**
Inter-ring Interactions	Out of register (1:2)	**In-register (1:1)**	**In-register (1:1)**
Ring separation	No	No	Yes

Items in bold demonstrate similarities between ϕ-EL chaperonin and Group I and II chaperonins.

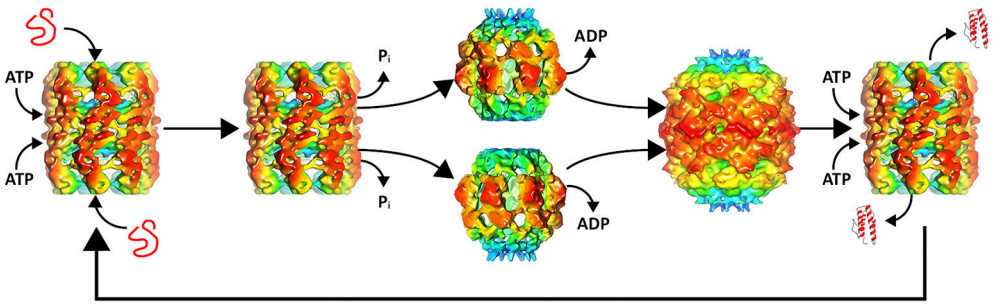

FIGURE 1 | ϕ-EL protein-folding catalytic cycle. A misfolded substrate enters each of the two ATP bound chaperonin internal chambers. ATP hydrolysis induces apical domain rearrangement resulting in the closure of the internal chamber as well as ring separation. ADP removal allows the rings to reassemble to form the APO conformation. Renewed binding of ATP opens the protein-folding chamber allowing the folded substrate to exit and the cycle to begin again. Structures of intermediates were generated with chimera using the deposited maps EMD-6492, EMD-6493, and EMD-6494.

simultaneously and therefore also must bind ATP to both rings (Molugu et al., 2016).

Most of what is known about single-ring chaperonins is largely based on studies of the ϕ-EL chaperonin and gro-EL single-ring mutant (SR1) (Weissman et al., 1995; Chen et al., 2006; Molugu et al., 2016). Cryo-EM structural analysis of the SR1-D398A groEL/ES revealed an 80% expansion of the volume of the central cavity compared to the expanded double-ring conformation (Chen et al., 2006). This expanded protein-folding cavity is also observed in ϕ-EL where it probably evolved to accommodate large viral proteins that cannot be encapsulated by the host double-ring chaperonin (Wolf, 2006; Molugu et al., 2016). Again, this was proven to be the case because the ϕ-EL chaperonin was able to effectively fold β-galactosidase, a protein that is not accommodated by groEL (Molugu et al., 2016).

THE OBP PHAGE CHAPERONIN

In addition to the ϕ-EL chaperonin, there is emerging evidence that many chaperonins may share the single-ring intermediate in their protein-folding catalytic cycle. Recently, another viral encoded chaperonin in the genome of *Pseudomonas* phage OBP has been purified as a single-ring complex (Semenyuk et al., 2016). The OBP gene product 246 (gp246) has been shown to form heptameric single-rings by electron microscopy. Although it was purified exclusively as a single-ring, this single-ring is likely an intermediate conformation in the protein-folding cycle of the OBP chaperonin. Like ϕ-EL, it does not require a co-chaperonin for its biological activity in *in-vitro* experiments (Semenyuk et al., 2016). All single-ring forming chaperonins studied to date form the single-ring as a conformational intermediate in the protein-folding cycle and do not function as a single-ring complex exclusively. It is anticipated that OBP gp246 will behave similarly and future X-ray structures or cryo-EM reconstructions will shed more light on the details about the OBP gp246 protein-folding cycle.

THE HUMAN MITOCHONDRIAL HSP60/10 PROTEIN-FOLDING MECHANISM

Naturally occurring single-ring chaperonins like hsp60/10 were not well studied due to the instability of the functional complex *in-vitro* (Levy-Rimler et al., 2002; Vilasi et al., 2014). This lack of knowledge led researchers to make assumptions about single-ring chaperonins based on studies performed on groEL/ES single-ring mutants (Viitanen et al., 1998; Chen et al., 2006; Liu et al., 2009; Kovács et al., 2010). The human mitochondrial hsp60/10 chaperonin is the eukaryotic homolog of the bacterial groEL/ES complex and assists in maintaining the proper folding of newly imported and

stress denatured mitochondrial proteins (Cheng et al., 1990; Horwich, 1990; Lubben et al., 1990; Dickson et al., 1994). Although the majority of hsp60 chaperonin resides in the mitochondrial matrix, numerous studies have now implicated its involvement in a variety of cellular processes at extra-mitochondrial locations (Singh et al., 1990; Soltys and Gupta, 1996, 1997, 1999; Itoh et al., 2002; Hildenbrand and Bernal, 2012; Henderson et al., 2013; Cappello et al., 2014). A functionally compromised hsp60/10 chaperonin complex in humans can lead to mitochondrial dysfunction and has been implicated in various neurodegenerative disorders (Magen et al., 2008; Parnas et al., 2009).

Early studies using chimeric groEL/hsp60 chaperonins revealed a single-ring hsp60 complex that retained the ability to fold target proteins *in-vitro* nearly identical to its wild-type counterpart (Nielsen and Cowan, 1998; Nielsen et al., 1999). This observation led to the conclusion that the mitochondrial single-ring chaperonin can maintain productive protein-folding without the use of double-ring complexes. Additionally, the expression of hsp60/10 proteins in an *E. coli* strain devoid of groEL/ES demonstrated that the hsp60/10 can compensate for the loss of groEL/ES (Nielsen et al., 1999).

More recent TEM and X-ray crystallographic investigations have provided strong evidence that the human mitochondrial chaperonin utilizes both double- and single-ring intermediates during its ATPase cycle (Levy-Rimler et al., 2001; Nisemblat et al., 2014, 2015; Vilasi et al., 2014; Enriquez et al., 2017). A mutant human hsp60 complexed with mouse hsp10 was crystallized resulting in a symmetric "American football" shaped structure (Hartman et al., 1992; Nisemblat et al., 2015). In addition, a 100° rotation of one subunit in each ring of the crystal structure indicated the intra-ring positive cooperativity observed in groEL is also not conserved in the mitochondrial chaperonin. Negative stain electron-microscopy on the nucleotide free wild-type human mitochondrial hsp60 complex revealed it forms a symmetrical, and stable tetradecameric complex that requires the presence of substrate to initiate ATPase activity (Enriquez et al., 2017). Negative stain electron microscope investigations of hsp60 have also demonstrated that it favors a tetradecameric complex in the presence of ATP, and a football complex in the presence of ATP and hsp10 (Levy-Rimler et al., 2001). It is still unclear whether ring-expansion occurs in the hsp60/10 single-ring complex and whether it allows for the folding of large proteins or if it simply doubles the protein-folding capacity when under stressful mitochondrial conditions.

The *in-vitro* analysis of the hsp60/10 ADP complex is difficult because biochemical studies indicate that hsp60 has an affinity for hsp10 that is so low in the presence of ADP that the affinity is nearly immeasurable (Nielsen and Cowan, 1998). Subsequent investigations demonstrated that the addition of ADP has little effect on the ATPase activity of hsp60/10 (Nielsen and Cowan, 1998; Levy-Rimler et al., 2001). Despite the evidence for hsp60/10 single-ring activity, the exact cellular conditions that coerce the formation of the hsp60/10 single-complex have yet to be elucidated (Viitanen et al., 1992; Nielsen et al., 1999; Nisemblat et al., 2015). Clearly, additional studies that include high resolution structural information of the single-ring intermediate are required to get a better understanding of how the hsp60/10 chaperonin folds a substrate protein.

GROEL/ES COMPLEX AND SINGLE-RING INTERMEDIATES

Recently, Yan et al. (2018) suggested that the groEL/ES complex may also be forming single-ring intermediates (Yan et al., 2018). This was observed in groEL mutants in the presence of the ATP analog ADP·BeFx which is supposed to mimic the ATP bound state, the ADP·Fx that mimics the transition state of ATP hydrolysis, and ADP·VO_4 that mimics the post-hydrolysis state. ADP·BeFx binding to the *trans* ring of the asymmetric groEL/ES complex triggers ring separation. The separated rings reassemble after groES and ADP dissociate from the former *cis* ring. Preventing ring separation via mutagenesis led to complexes with reduced activity *in-vitro* and *in-vivo*. In our hands, these nucleotide analogs yielded off-pathway intermediates suggesting that the analogs were not behaving as predicted compared to the natural nucleotides (ATP and ADP) (unpublished data). The absence of a substrate prevented progression of the chaperonin to the next conformational intermediate and so we decided to simply use the natural nucleotides to avoid structural artifacts.

CONCLUSION

Single-ring intermediates have been identified for ϕ-EL, OBP and hsp60/10 chaperonin complexes. Recently, groEL/ES complexes have also been suggested to operate via single-ring intermediates although further data is required to prove that single-rings are relevant. The naturally occurring single-ring intermediates are an integral part of bacteriophage and human mitochondrial chaperonin protein-folding catalytic pathways. The exact sequence, structural and cellular conditions that regulate the formation of these single-ring intermediates in still unknown. Further insight into single-ring chaperonins is important since the human hsp60 is now implicated in the onset of a wide variety of diseases including arthritis, cancer, and neurodegenerative disorders (Hansen et al., 2002; Parnas et al., 2009; Ghosh et al., 2010; Campanella et al., 2012; Henderson and Martin, 2013).

AUTHOR CONTRIBUTIONS

JB, AE, ZH, JW, and RB: contributed to the writing of the manuscript; JW and SM: performed all of the bioinformatics calculations and generated **Figure 1**; HR: generated **Figure 1**. All of the authors contributed to the editing of various versions of the manuscript and all read the final version.

ACKNOWLEDGMENTS

This work was made possible by the Welch Foundation award (AH-1649) and NIH-NIGMS (SC3GM113805) awarded to RB.

We would also like to acknowledge the UTEP BBRC and grant 5G12MD007592 from the National Institutes on Minority Health and Health Disparities (NIMHD), a component of the National Institutes of Health (NIH). JB was supported by the NIH-NIGMS under linked Award Numbers RL5GM118969, TL4GM118971, and UL1GM118970.

REFERENCES

An, Y. J., Rowland, S. E., Na, J. H., Spigolon, D., Hong, S. K., Yoon, Y. J., et al. (2017). Structural and mechanistic characterization of an archaeal-like chaperonin from a thermophilic bacterium. *Nat. Commun.* 8:827. doi: 10.1038/s41467-017-00980-z

Ayling, A., and Baneyx, F. (1996). Influence of the GroE molecular chaperone machine on the *in vitro* refolding of *Escherichia coli* beta-galactosidase. *Protein Sci.* 5, 478–487.

Booth, C. R., Meyer, A. S., Cong, Y., Topf, M., Sali, A., Ludtke, S. J., et al. (2008). Mechanism of lid closure in the eukaryotic chaperonin TRiC/CCT. *Nat. Struct. Mol. Biol.* 15, 746–753. doi: 10.1038/nsmb.1436

Braig, K., Otwinowski, Z., Hegde, R., Boisvert, D. C., Joachimiak, A., Horwich, A. L., et al. (1994). The crystal structure of the bacterial chaperonin GroEL at 2.8 A. *Nature* 371, 578–586.

Brocchieri, L., and Karlin, S. (2000). Conservation among HSP60 sequences in relation to structure, function, and evolution. *Protein Sci.* 9, 476–486. doi: 10.1110/ps.9.3.476

Campanella, C., Bucchieri, F., Merendino, A. M., Fucarino, A., Burgio, G., Corona, D. F., et al. (2012). The odyssey of Hsp60 from tumor cells to other destinations includes plasma membrane-associated stages and Golgi and exosomal protein-trafficking modalities. *PLoS ONE* 7:e42008. doi: 10.1371/journal.pone.0042008

Cappello, F., Marino Gammazza, A., Palumbo Piccionello, A., Campanella, C., Pace, A., Conway de Macario, E., et al. (2014). Hsp60 chaperonopathies and chaperonotherapy: targets and agents. *Expert Opin. Ther. Targets* 18, 185–208. doi: 10.1517/14728222.2014.856417

Chen, D. H., Song, J. L., Chuang, D. T., Chiu, W., and Ludtke, S. J. (2006). An expanded conformation of single-ring GroEL-GroES complex encapsulates an 86 kDa substrate. *Structure* 14, 1711–1722. doi: 10.1016/j.str.2006.09.010

Cheng, M. Y., Hartl, F. U., and Horwich, A. L. (1990). The mitochondrial chaperonin hsp60 is required for its own assembly. *Nature* 348, 455–458. doi: 10.1038/348455a0

Cornelissen, A., Hardies, S. C., Shaburova, O. V., Krylov, V. N., Mattheus, W., Kropinski, A. M., et al. (2012). Complete genome sequence of the giant virus OBP and comparative genome analysis of the diverse KZ-related phages. *J. Virol.* 86, 1844–1852. doi: 10.1128/JVI.06330-11

Dekker, C., Stirling, P. C., McCormack, E. A., Filmore, H., Paul, A., Brost, R. L., et al. (2008). The interaction network of the chaperonin CCT. *EMBO J.* 27, 1827–1839. doi: 10.1038/emboj.2008.108

Dickson, R., Larsen, B., Viitanen, P. V., Tormey, M. B., Geske, J., Strange, R., et al. (1994). Cloning, expression, and purification of a functional nonacetylated mammalian mitochondrial chaperonin 10. *J. Biol. Chem.* 269, 26858–26864.

Ditzel, L., Löwe, J., Stock, D., Stetter, K. O., Huber, H., Huber, R., et al. (1998). Crystal structure of the thermosome, the archaeal chaperonin and homolog of CCT. *Cell* 93, 125–138.

Ellis, R. J. (2003). Protein folding: importance of the Anfinsen cage. *Curr. Biol.* 13, R881–R883. doi: 10.1016/j.cub.2003.10.051

Enriquez, A. S., Rojo, H. M., Bhatt, J. M., Molugu, S. K., Hildenbrand, Z. L., and Bernal, R. A. (2017). The human mitochondrial Hsp60 in the APO conformation forms a stable tetradecameric complex. *Cell Cycle* 16, 1309–1319. doi: 10.1080/15384101.2017.1321180

Fenton, W. A., and Horwich, A. L. (1997). GroEL-mediated protein folding. *Protein Sci.* 6, 743–760. doi: 10.1002/pro.5560060401

Ghosh, J. C., Siegelin, M. D., Dohi, T., and Altieri, D. C. (2010). Heat shock protein 60 regulation of the mitochondrial permeability transition pore in tumor cells. *Cancer Res.* 70, 8988–8993. doi: 10.1158/0008-5472.CAN-10-2225

Hansen, J. J., Dürr, A., Cournu-Rebeix, I., Georgopoulos, C., Ang, D., Nielsen, M. N., et al. (2002). Hereditary spastic paraplegia SPG13 is associated with a mutation in the gene encoding the mitochondrial chaperonin Hsp60. *Am. J. Hum. Genet.* 70, 1328–1332. doi: 10.1086/339935

Hartman, D. J., Hoogenraad, N. J., Condron, R., and Høj, P. B. (1992). Identification of a mammalian 10-kDa heat shock protein, a mitochondrial chaperonin 10 homologue essential for assisted folding of trimeric ornithine transcarbamoylase *in vitro*. *Proc. Natl. Acad. Sci. U.S.A.* 89, 3394–3398. doi: 10.1073/pnas.89.8.3394

Hayer-Hartl, M., Bracher, A., and Hartl, F. U. (2016). The GroEL-GroES chaperonin machine, a nano-cage for protein folding. *Trends Biochem. Sci.* 41, 62–76. doi: 10.1016/j.tibs.2015.07.009

Henderson, B., Fares, M. A., and Lund, P. A. (2013). Chaperonin 60: a paradoxical, evolutionarily conserved protein family with multiple moonlighting functions. *Biol. Rev. Camb. Philos. Soc.* 88, 955–987. doi: 10.1111/brv.12037

Henderson, B., Lund, P. A., and Coates, A. R. (2010). Multiple moonlighting functions of mycobacterial molecular chaperones. *Tuberculosis* 90, 119–124. doi: 10.1016/j.tube.2010.01.004

Henderson, B., and Martin, A. (2013). Bacterial moonlighting proteins and bacterial virulence. *Curr. Top. Microbiol. Immunol.* 358, 155–213. doi: 10.1007/82_2011_188

Hertveldt, K., Lavigne, R., Pleteneva, E., Sernova, N., Kurochkina, L., Korchevskii, R., et al. (2005). Genome comparison of *Pseudomonas aeruginosa* large phages. *J. Mol. Biol.* 354, 536–545. doi: 10.1016/j.jmb.2005.08.075

Hildenbrand, Z. L., and Bernal, R. A. (2012). Chaperonin-mediated folding of viral proteins. *Adv. Exp. Med. Biol.* 726, 307–324. doi: 10.1007/978-1-4614-0980-9_13

Horwich, A. (1990). Protein import into mitochondria and peroxisomes. *Curr. Opin. Cell Biol.* 2, 625–633 doi: 10.1016/0955-0674(90)90103-L

Horwich, A. L., Apetri, A. C., and Fenton, W. A. (2009). The GroEL/GroES cis cavity as a passive anti-aggregation device. *FEBS Lett.* 583, 2654–2662. doi: 10.1016/j.febslet.2009.06.049

Horwich, A. L., Low, K. B., Fenton, W. A., Hirshfield, I. N., and Furtak, K. (1993). Folding *in vivo* of bacterial cytoplasmic proteins: role of GroEL. *Cell* 74, 909–917 doi: 10.1016/0092-8674(93)90470-B

Iizuka, R., So, S., Inobe, T., Yoshida, T., Zako, T., Kuwajima, K., et al. (2004). Role of the helical protrusion in the conformational change and molecular chaperone activity of the archaeal group II chaperonin. *J. Biol. Chem.* 279, 18834–18839. doi: 10.1074/jbc.M400839200

Illingworth, M., Ramsey, A., Zheng, Z., and Chen, L. (2011). Stimulating the substrate folding activity of a single ring GroEL variant by modulating the cochaperonin GroES. *J. Biol. Chem.* 286, 30401–30408. doi: 10.1074/jbc.M111.255935

Illingworth, M., Salisbury, J., Li, W., Lin, D., and Chen, L. (2015). Effective ATPase activity and moderate chaperonin-cochaperonin interaction are important for the functional single-ring chaperonin system. *Biochem. Biophys. Res. Commun.* 466, 15–20. doi: 10.1016/j.bbrc.2015.08.034

Itoh, H., Komatsuda, A., Ohtani, H., Wakui, H., Imai, H., Sawada, K., et al. (2002). Mammalian HSP60 is quickly sorted into the mitochondria under conditions of dehydration. *Eur. J. Biochem.* 269, 5931–5938 doi: 10.1046/j.1432-1033.2002.03317.x

Joachimiak, L. A., Walzthoeni, T., Liu, C. W., Aebersold, R., and Frydman, J. (2014). The structural basis of substrate recognition by the eukaryotic chaperonin TRiC/CCT. *Cell* 159, 1042–1055. doi: 10.1016/j.cell.2014.10.042

Kovács, E., Sun, Z., Liu, H., Scott, D. J., Karsisiotis, A. I., Clarke, A. R., et al. (2010). Characterisation of a GroEL single-ring mutant that supports growth of *Escherichia coli* and has GroES-dependent ATPase activity. *J. Mol. Biol.* 396, 1271–1283. doi: 10.1016/j.jmb.2009.11.074

Kurochkina, L. P., Semenyuk, P. I., Orlov, V. N., Robben, J., Sykilinda, N. N., and Mesyanzhinov, V. V. (2012). Expression and functional characterization of the first bacteriophage-encoded chaperonin. *J. Virol.* 86, 10103–10111. doi: 10.1128/JVI.00940-12

Kusmierczyk, A. R., and Martin, J. (2003). Nucleotide-dependent protein folding in the type II chaperonin from the mesophilic archaeon *Methanococcus maripaludis*. *Biochem. J.* 371(Pt 3), 669–673. doi: 10.1042/bj20030230

Levy-Rimler, G., Bell, R. E., Ben-Tal, N., and Azem, A. (2002). Type I chaperonins: not all are created equal. *FEBS Lett.* 529, 1–5. doi: 10.1016/S0014-5793(02)03178-2

Levy-Rimler, G., Viitanen, P., Weiss, C., Sharkia, R., Greenberg, A., Niv, A., et al. (2001). The effect of nucleotides and mitochondrial chaperonin 10 on the structure and chaperone activity of mitochondrial chaperonin 60. *Eur. J. Biochem.* 268, 3465–3472. doi: 10.1046/j.1432-1327.2001.02243.x

Liu, H., Kovács, E., and Lund, P. A. (2009). Characterisation of mutations in GroES that allow GroEL to function as a single ring. *FEBS Lett.* 583, 2365–2371. doi: 10.1016/j.febslet.2009.06.027

Lopez, T., Dalton, K., and Frydman, J. (2015). The mechanism and function of group II chaperonins. *J. Mol. Biol.* 427, 2919–2930. doi: 10.1016/j.jmb.2015.04.013

Lubben, T. H., Gatenby, A. A., Donaldson, G. K., Lorimer, G. H., and Viitanen, P. V. (1990). Identification of a groES-like chaperonin in mitochondria that facilitates protein folding. *Proc. Natl. Acad. Sci. U.S.A.* 87, 7683–7687 doi: 10.1073/pnas.87.19.7683

Magen, D., Georgopoulos, C., Bross, P., Ang, D., Segev, Y., Goldsher, D., et al. (2008). Mitochondrial hsp60 chaperonopathy causes an autosomal-recessive neurodegenerative disorder linked to brain hypomyelination and leukodystrophy. *Am. J. Hum. Genet.* 83, 30–42. doi: 10.1016/j.ajhg.2008.05.016

Marine, R. L., Nasko, D. J., Wray, J., Polson, S. W., and Wommack, K. E. (2017). Novel chaperonins are prevalent in the virioplankton and demonstrate links to viral biology and ecology. *ISME J.* 11, 2479–2491. doi: 10.1038/ismej.2017.102

Molugu, S. K., Hildenbrand, Z. L., Morgan, D. G., Sherman, M. B., He, L., Georgopoulos, C., et al. (2016). Ring separation highlights the protein-folding mechanism used by the phage EL-encoded chaperonin. *Structure* 24, 537–546. doi: 10.1016/j.str.2016.02.006

Nielsen, K. L., and Cowan, N. J. (1998). A single ring is sufficient for productive chaperonin-mediated folding *in vivo*. *Mol. Cell* 2, 93–99 doi: 10.1016/S1097-2765(00)80117-3

Nielsen, K. L., McLennan, N., Masters, M., and Cowan, N. J. (1999). A single-ring mitochondrial chaperonin (Hsp60-Hsp10) can substitute for GroEL-GroES *in vivo*. *J. Bacteriol.* 181, 5871–5875.

Nisemblat, S., Parnas, A., Yaniv, O., Azem, A., and Frolow, F. (2014). Crystallization and structure determination of a symmetrical 'football' complex of the mammalian mitochondrial Hsp60-Hsp10 chaperonins. *Acta Crystallogr. F Struct. Biol. Commun.* 70(Pt 1), 116–119. doi: 10.1107/S2053230X1303389X

Nisemblat, S., Yaniv, O., Parnas, A., Frolow, F., and Azem, A. (2015). Crystal structure of the human mitochondrial chaperonin symmetrical football complex. *Proc. Natl. Acad. Sci. U.S.A.* 112, 6044–6049. doi: 10.1073/pnas.1411718112

Parnas, A., Nadler, M., Nisemblat, S., Horovitz, A., Mandel, H., and Azem, A. (2009). The MitCHAP-60 disease is due to entropic destabilization of the human mitochondrial Hsp60 oligomer. *J. Biol. Chem.* 284, 28198–28203. doi: 10.1074/jbc.M109.031997

Reissmann, S., Parnot, C., Booth, C. R., Chiu, W., and Frydman, J. (2007). Essential function of the built-in lid in the allosteric regulation of eukaryotic and archaeal chaperonins. *Nat. Struct. Mol. Biol.* 14, 432–440. doi: 10.1038/nsmb1236

Saibil, H. R., Zheng, D., Roseman, A. M., Hunter, A. S., Watson, G. M. F., Chen, S., et al. (1993). Atp induces large quaternary rearrangements in a cage-like chaperonin structure. *Curr. Biol.* 3, 265–273. doi: 10.1016/0960-9822(93)90176-O

Schoehn, G., Quaite-Randall, E., Jiménez, J. L., Joachimiak, A., and Saibil, H. R. (2000). Three conformations of an archaeal chaperonin, TF55 from Sulfolobus shibatae. *J. Mol. Biol.* 296, 813–819 doi: 10.1006/jmbi.2000.3505

Semenyuk, P. I., Orlov, V. N., and Kurochkina, L. P. (2015). Effect of chaperonin encoded by gene 146 on thermal aggregation of lytic proteins of bacteriophage EL *Pseudomonas aeruginosa*. *Biochem. Mosc.* 80, 172–179. doi: 10.1134/S0006297915020042

Semenyuk, P. I., Orlov, V. N., Sokolova, O. S., and Kurochkina, L. P. (2016). New GroEL-like chaperonin of bacteriophage OBP *Pseudomonas fluorescens* suppresses thermal protein aggregation in an ATP-dependent manner. *Biochem. J.* 473, 2383–2393. doi: 10.1042/BCJ201 60367

Shaburova, O. V., Hertveldt, K. D. M., de la Crus, Krylov, S. V., Pleteneva, E. A., Burkaltseva, M. V., et al. (2006). [Comparison of new giant bacteriophages OBP and Lu11 of soil pseudomonads with bacteriophages of phiKZ-supergroup of *Pseudomonas aeruginosa*]. *Genetika* 42, 1065–1074. doi: 10.1134/S1022795406080059

Singh, B., Patel, H. V., Ridley, R. G., Freeman, K. B., and Gupta, R. S. (1990). Mitochondrial import of the human chaperonin (HSP60) protein. *Biochem. Biophys. Res. Commun.* 169, 391–396 doi: 10.1016/0006-291X(90)90344-M

Soltys, B. J., and Gupta, R. S. (1996). Immunoelectron microscopic localization of the 60-kDa heat shock chaperonin protein (Hsp60) in mammalian cells. *Exp. Cell Res.* 222, 16–27. doi: 10.1006/excr.1996.0003

Soltys, B. J., and Gupta, R. S. (1997). Cell surface localization of the 60 kDa heat shock chaperonin protein (hsp60) in mammalian cells. *Cell Biol. Int.* 21, 315–320. doi: 10.1006/cbir.1997.0144

Soltys, B. J., and Gupta, R. S. (1999). Mitochondrial-matrix proteins at unexpected locations: are they exported? *Trends Biochem. Sci.* 24, 174–177.

Spiess, C., Meyer, A. S., Reissmann, S., and Frydman, J. (2004). Mechanism of the eukaryotic chaperonin, protein folding in the chamber of secrets. *Trends Cell Biol.* 14, 598–604. doi: 10.1016/j.tcb.2004.09.015

Sukhanova, A., Poly, S., Shemetov, A., Bronstein, I., and Nabiev, I. (2012). Implications of protein structure instability, from physiological to pathological secondary structure. *Biopolymers* 97, 577–588. doi: 10.1002/bip.22055

Sun, Z., Scott, D. J., and Lund, P. A. (2003). Isolation and characterisation of mutants of GroEL that are fully functional as single rings. *J. Mol. Biol.* 332, 715–728 doi: 10.1016/S0022-2836(03)00830-1

Techtmann, S. M., and Robb, F. T. (2010). Archaeal-like chaperonins in bacteria. *Proc. Natl. Acad. Sci. U.S.A.* 107, 20269–20274. doi: 10.1073/pnas.1004783107

Viitanen, P. V., Lorimer, G., Bergmeier, W., Weiss, C., Kessel, M., and Goloubinoff, P. (1998). Purification of mammalian mitochondrial chaperonin 60 through *in vitro* reconstitution of active oligomers. *Meth. Enzymol.* 290, 203–217 doi: 10.1016/S0076-6879(98)90020-9

Viitanen, P. V., Lorimer, G. H., Seetharam, R., Gupta, R. S., Oppenheim, J., Thomas, J. O., et al. (1992). Mammalian mitochondrial chaperonin 60 functions as a single toroidal ring. *J. Biol. Chem.* 267, 695–698.

Vilasi, S., Carrotta, R., Mangione, M. R., Campanella, C., Librizzi, F., Randazzo, L., et al. (2014). Human Hsp60 with its mitochondrial import signal occurs in solution as heptamers and tetradecamers remarkably stable over a wide range of concentrations. *PLoS ONE* 9:e97657. doi: 10.1371/journal.pone.0097657

Weissman, J. S., Hohl, C. M., Kovalenko, O., Kashi, Y., Chen, S., Braig, K., et al. (1995). Mechanism of GroEL action: productive release of polypeptide from a sequestered position under GroES. *Cell* 83, 577–587 doi: 10.1016/0092-8674(95)90098-5

Wolf, S. G. (2006). Single-ring GroEL: an expanded view. *Structure* 14, 1599–1600. doi: 10.1016/j.str.2006.10.007

Yan, X., Shi, Q., Bracher, A., Milicić, G., Singh, A. K., Hartl, F. U., et al. (2018). GroEL ring separation and exchange in the chaperonin reaction. *Cell* 172, 605.e11–617.e11. doi: 10.1016/j.cell.2017.12.010

Zhang, J., Baker, M. L., Schroder, G. F., Douglas, N. R., Reissmann, S., Jakana, J., et al. (2010). Mechanism of folding chamber closure in a group II chaperonin. *Nature* 463, 379–383. doi: 10.1038/nature08701

Conflict of Interest Statement: ZH is employed by the company Inform Environmental, LLC.

The other authors declare that the research was conducted in the absence of any commercial or financial relationships that could be construed as a potential conflict of interest.

frontiers in Molecular Biosciences

REVIEW
published: 19 January 2018
doi: 10.3389/fmolb.2017.00098

Chloroplast Chaperonin: An Intricate Protein Folding Machine for Photosynthesis

Qian Zhao [1,2] *and Cuimin Liu* [1]*

[1] State Key Laboratory of Plant Cell and Chromosome Engineering, Institute of Genetics and Developmental Biology, Chinese Academy of Sciences, Beijing, China, [2] University of Chinese Academy of Sciences, Beijing, China

Group I chaperonins are large cylindrical-shaped nano-machines that function as a central hub in the protein quality control system in the bacterial cytosol, mitochondria and chloroplasts. In chloroplasts, proteins newly synthesized by chloroplast ribosomes, unfolded by diverse stresses, or translocated from the cytosol run the risk of aberrant folding and aggregation. The chloroplast chaperonin system assists these proteins in folding into their native states. A widely known protein folded by chloroplast chaperonin is the large subunit of ribulose 1,5-bisphosphate carboxylase/oxygenase (Rubisco), an enzyme responsible for the fixation of inorganic CO_2 into organic carbohydrates during photosynthesis. Chloroplast chaperonin was initially identified as a Rubisco-binding protein. All photosynthetic eucaryotes genomes encode multiple chaperonin genes which can be divided into α and β subtypes. Unlike the homo-oligomeric chaperonins from bacteria and mitochondria, chloroplast chaperonins are more complex and exists as intricate hetero-oligomers containing both subtypes. The Group I chaperonin requires proper interaction with a detachable lid-like co-chaperonin in the presence of ATP and Mg^{2+} for substrate encapsulation and conformational transition. Besides the typical Cpn10-like co-chaperonin, a unique co-chaperonin consisting of two tandem Cpn10-like domains joined head-to-tail exists in chloroplasts. Since chloroplasts were proposed as sensors to various environmental stresses, this diversified chloroplast chaperonin system has the potential to adapt to complex conditions by accommodating specific substrates or through regulation at both the transcriptional and post-translational levels. In this review, we discuss recent progress on the unique structure and function of the chloroplast chaperonin system based on model organisms *Chlamydomonas reinhardtii* and *Arabidopsis thaliana*. Knowledge of the chloroplast chaperonin system may ultimately lead to successful reconstitution of eukaryotic Rubisco *in vitro*.

Keywords: chaperonin, Rubisco, chloroplast, photosynthesis, protein folding

OPEN ACCESS

Edited by:
Abdussalam Azem, Tel Aviv University, Israel

Reviewed by:
Celeste Elyona Weiss, Tel Aviv University, Israel
Johannes Herrmann, Kaiserslautern University of Technology, Germany

***Correspondence:**
Cuimin Liu
cmliu@genetics.ac.cn

Specialty section:
This article was submitted to Protein Folding, Misfolding and Degradation, a section of the journal Frontiers in Molecular Biosciences

Received: *10 November 2017*
Accepted: *28 December 2017*
Published: *19 January 2018*

Citation:
Zhao Q and Liu C (2018) Chloroplast Chaperonin: An Intricate Protein Folding Machine for Photosynthesis. Front. Mol. Biosci. 4:98. doi: 10.3389/fmolb.2017.00098

INTRODUCTION

Proteins are involved in almost all cellular processes. To attain biologically active functionality, newly-translated proteins must fold into a well-defined three-dimensional structure with high efficiency and fidelity. How proteins find folding trajectory to reach their native conformation is a fundamental question (Bartlett and Radford, 2009; Dill and MacCallum, 2012). Anfinsen's

exquisite ribonuclease A renaturation assay reveals that the physical driving force of protein folding is encoded in its amino acid sequence, which suggests newly translated proteins are able to fold spontaneously *in vitro* (Anfinsen et al., 1954). However, proteins may expose unburied hydrophobic regions to a highly crowded environment during synthesis and folding, resulting in susceptibility to nonnative interaction that ultimately leads to misfolding and aggregation. Moreover, cells often encounter stresses such as high temperature, reactive oxygen species, and osmotic pressure, which may trap newly translated proteins in partially folded and aggregation-prone intermediates, or even terminally misfolded states (Ellis and Minton, 2006; Powers et al., 2009).

To counteract these stresses, cells have evolved a network of molecular chaperones as part of the protein homeostasis system to assist in protein *de novo* folding and maintain mature proteins in their native conformation (Hartl and Hayer-Hartl, 2002; Bukau et al., 2006; Hartl et al., 2011; Kim et al., 2013b; Saibil, 2013). The definition of molecular chaperone covers a wide range of proteins, including those accompanying proteins during synthesis and translocation, helping proteins cope with stress-induced misfolding and aggregation, or assisting protein complex assembly without being retained as part of the final structure of the protein. Chaperones also play an initiating role in protein unfolding and disaggregation or targeting misfolded proteins for degradation. Several families of ATP-dependent molecular chaperones exist in cells, with many of them classified as heat shock proteins (Hsps) since their expression is induced under conditions of high temperature. These chaperones are classified into four basic groups according to their molecular weight: Hsp60, Hsp70, Hsp90, and Hsp100. In addition to well-studied ATP-dependent molecular chaperones, a number of chaperones that assist in protein folding independent of ATP hydrolysis have also been identified (Suss and Reichmann, 2015; Horowitz et al., 2017). The entire cellular chaperone network composed of various molecular chaperones functions in diverse aspects of the protein quality control system to maintain protein homeostasis.

Chaperonins are one of the most important molecular chaperones that can be found in both prokaryotes and eukaryotes (Yébenes et al., 2011). They are large oligomeric protein complexes comprised of two rings stacked back to back, each of which creates a central cavity, known as the Anfinsen cage, for encapsulating substrate proteins. Two distantly related subgroups of chaperonins can be distinguished based on structure and functional dependence on co-chaperonin. Group I chaperonins, also known as Hsp60s, are present in bacteria and endosymbiotic organelles of eukaryotes: chloroplasts and mitochondria. They functionally cooperate in an ATP dependent manner with Hsp10 family proteins, which form the lid of the protein folding cage. This cooperation between Hsp60 and Hsp10 prevents substrate proteins from escaping and expands the folding chamber to accommodate larger proteins (Thirumalai and Lorimer, 2001; Horwich, 2013). Group II chaperonins, known as thermosome and TRiC, are found in archaea and the eukaryotic cytosol respectively. In contrast to Group I chaperonins, they contain a built-in lid instead of an obligate co-chaperonin that closes the folding chamber upon ATP binding. Accumulative studies of structure and function of Group II chaperonins from *Thermoplasma acidophilum*, *Saccharomyces cerevisiae*, and *Homo sapiens* revealed how exactly these protein machines work (Horwich et al., 2007; Lopez et al., 2015).

Knowledge about the functional mechanism of Group I chaperonins is mainly derived from the stable and simplified archetype GroEL/ES from *Escherichia coli* (Chan and Dill, 1996; Sigler et al., 1998; Hayer-Hartl et al., 2016). Compared to its counterpart in bacteria, the chloroplast chaperonin system is far more complicated due to its subunit diversification and dynamic nature (Hill and Hemmingsen, 2001; Weiss et al., 2009; Vitlin Gruber et al., 2013a; Trösch et al., 2015). Further investigation of the chloroplast chaperonin system will enhance our knowledge of chaperonins and may provide clues to remold this protein folding machine for specific purposes in synthetic biology.

GROUP I CHAPERONIN PARADIGM GROEL-GROES

GroEL and its cofactor GroES from *Escherichia coli* are the archetype of Group I chaperonin protein folding machines. Detailed structures of GroEL/GroES have been well studied over the last two decades by X-ray crystallography and cryo-electron microscopy. Like all Group I chaperonins, GroEL is a cylindrical tetradecamer composed of two heptameric rings which contain seven identical ∼57 kD subunits. Each subunit is folded into three distinct domains: an equatorial domain haboring ATPase activity and providing almost all inter-ring and intra-ring contacts (Braig et al., 1994; Boisvert et al., 1996), an apical domain that binds co-chaperonin GroES and non-native substrate protein, and a hinge-like intermediate domain which connects the above two domains and is responsible for the allosteric signal transmission triggered by nucleotide binding and hydrolysis in the individual GroEL subunit (Xu et al., 1997; Ranson et al., 2006) (Sigler et al., 1998; Hayer-Hartl et al., 2016). The co-chaperonin, GroES, is a dome-shaped heptameric ring consisting of seven ∼10 kD subunits (Hunt et al., 1996). Through its mobile loop region, GroES functionally interacts with helix H and helix I of the GroEL apical domain in the presence of nucleotide. The interaction between GroES and GroEL drives the conformational change of GroEL, mainly via twisting and elevating the apical domains, resulting in a two-fold increase in volume, which is sufficient to accomodate ∼60 kDa protein substrates. The interaction also creates a protective hydrophilic cavity with a negatively-charged inner wall conducive to protein folding (Xu et al., 1997; Clare et al., 2012).

In addition to the static point-in-time structures of GroEL, the dynamic process of GroEL-GroES assisted protein folding has also been established by structural and biochemical studies. The protein folding reaction cycle driven by ATP binding and hydrolysis is governed by a precise cooperative network including inner-ring positive cooperativity and inter-ring negative cooperativity (Gray and Fersht, 1991; Bochkareva et al., 1992; Bochkareva and Girshovich, 1994) (**Figure 1**). In the apo-state, GroEL subunits switch back and forth between a tense T state (low affinity for ATP) and a relaxed R state (high

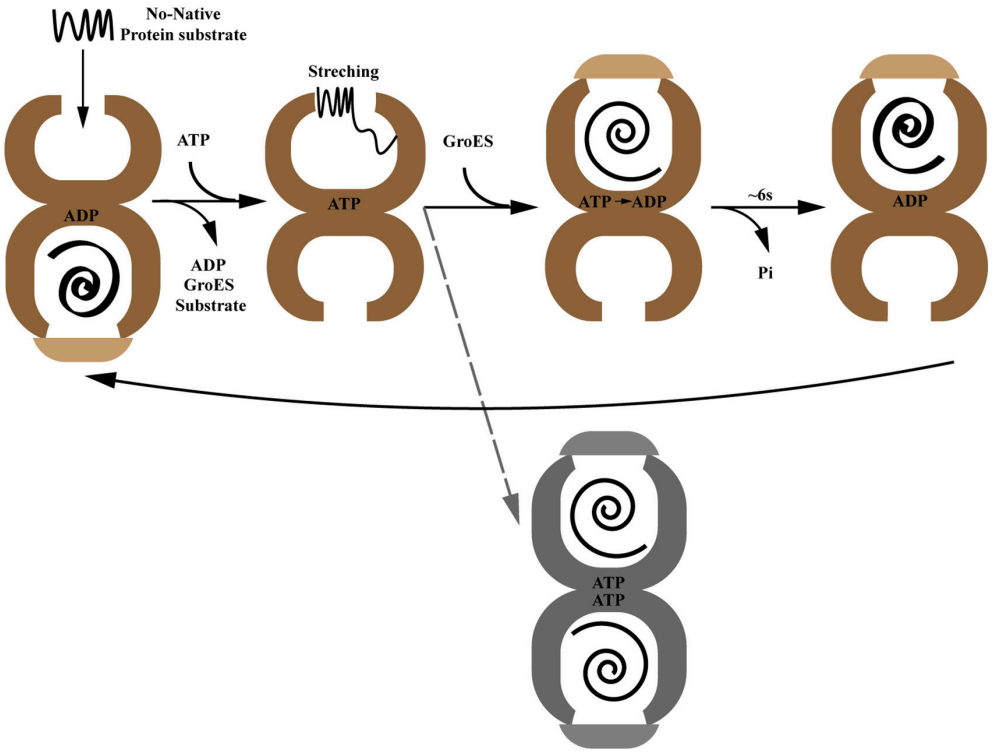

FIGURE 1 | The paradigmatic chaperonin GroES/GroEL reaction cycle. The gray dotted line indicates the controversial GroEL/(GroES)2 folding active intermediate.

affinity for ATP) (Ranson et al., 2006; Clare et al., 2012). In the protein folding state, the open nucleotide-free trans-ring captures non-native polypeptides with exposed hydrophobic surfaces. This interaction involves 3 or 4 GroEL apical domains which account for their overlap binding with both substrate protein and GroES. Followed by ATP binding, the substrate protein experiences a mechanical stretching by the conformational change of apical domains, which leads to unfolding of misfolded protein intermediates (Farr et al., 2000; Ashcroft et al., 2002; Horst et al., 2005; Elad et al., 2007; Lin et al., 2008). Then GroES collides with this ATP-occupied substrate-bound GroEL ring, called the cis-ring, forming a ternary structure. This triggers a large rigid body elevation and twist of apical domains that propels non-native polypeptide into a GroES-capped, hydrophilic chamber for folding (Chen et al., 2013). The process time of this step depends on the ATP hydrolysis rate, ∼6 s at 25°C (Sharma et al., 2008). Subsequent binding of ATP in the opposite trans-ring results in GroES dissociation, as well as substrate protein and ADP release. At the same time, the opposite trans-ring becomes the new folding-active cis-ring (Ranson et al., 2006). For substrate proteins that are too large to be encapsulated (usually in excess of 60 kD), GroEL/GroES may still assist them in folding through binding and release from the trans-ring (Farr et al., 2003; Chaudhuri et al., 2009). Although the classical reaction cycle presented above depicts a perfect asymmetrical working model of the GroEL/GroES system, symmetrical football shaped GroEL/$(GroES)_2$ complexes have also been observed in extensive studies suggesting the presence of GroEL with both chambers simultaneously active in folding substrates *in vivo* (Azem et al., 1994; Harris et al., 1994; Llorca et al., 1994; Sameshima et al., 2008, 2010). Recent crystal structures of symmetrical GroEL/$(GroES)_2$ and mitochondrial Hsp60-$(Hsp10)_2$ indicate this may be a conserved mechanism (Fei et al., 2014; Koike-Takeshita et al., 2014; Nisemblat et al., 2015). However, a fluorescence cross-correlation study showed that the GroEL/$(GroES)_2$ structure is not likely to exist in the presence of physiological levels of ATP which leaves this mechanism still under debate (Haldar et al., 2015).

Despite the study of the GroEL/ES paradigm providing an insightful perspective on how Group I chaperonin functions as a protein folding machine, several key problems remain elusive. What structural features of a protein determine whether or not it is GroEL-dependent? How can GroEL balance its capability between specialization and generalization? What is the co-evolutionary process of Group I chaperonin and protein substrates? The study of organelle chaperonin systems may give us hints toward answering these questions.

CHLOROPLAST CHAPERONIN AND CO-CHAPERONIN PROTEINS

Dating back to the 1980s when John Ellis at the University of Warwick studied light-driven protein synthesis in isolated intact chloroplasts, he observed the unexpected phenomenon that radioactive Rubisco large subunit (RbcL) co-migrates

with another prominently stained band of protein before it interacts with transmembrane imported Rubisco small subunit (RbcS) to form Rubisco holoenzyme (Barraclough and Ellis, 1980). This Rubisco large subunit-binding protein was the first identified protein that binds to newly-synthesized polypeptides and subsequently became widely known as chaperonin Cpn60 (Hemmingsen and Ellis, 1986; Hemmingsen et al., 1988). Now we know that newly translated Rubisco large subunit was captured by chaperonin to prevent aggregation as a transient intermediate. Despite Cpn60 important role in folding Rubisco, its counterpart from *E. coli*, the GroEL/ES system, with the advantages of high stability and simple components eventually became a research paradigm that established the current model of the mechanism of chaperonin function as described above.

Since chloroplast chaperonin subunits share ∼50% sequence similarity with GroEL, it is reasonable to assume the functional mechanism of chloroplast chaperonin assisted protein folding is parallel to that of GroEL-ES mediated folding in bacteria. However, chloroplast chaperonins possess a unique feature that is not shared with chaperonins from bacteria and mitochondria; namely, multiple copies of two chaperonin subunit subtypes, α type and β type, which share ∼50% sequence similarity with each other, are combined into hetero-oligomeric species (Musgrove et al., 1987). For example, the unicellular green algae *Chlamydomonas reinhardtii* encodes three CPN60 subunits, termed CPN60α1, CPN60β2, and CPN60β2 (Thompson et al., 1995; Schroda, 2004). Furthermore, the situation becomes even more complex in higher plants, such as monocotyledon and dicotyledon model organisms *Oryza sativa* and *Arabidopsis thaliana,* which both have six Cpn60 paralogs (**Figure 2**; **Table 1**) (*Arabidopsis* Cpn60 nomenclature in this review is according to the TAIR database) (Hill and Hemmingsen, 2001; Kim et al., 2013a). The recombinantly-expressed Cpn60β subunit from *Brassica napus* is able to assemble efficiently into a tetradecamer and fold the cyanobacterial Rubisco large subunit in *E. coli* cells, while the Cpn60α subunit is only capable of assembling into an oligomeric state and supporting folding in the presence of Cpn60β (Cloney et al., 1992a,b). An *in vitro* assay of Cpn60β1, Cpn60β2, Cpn60β3 from *Arabidopsis thaliana* (note: the protein nomenclature is in accordance with TAIR) showed that all three Cpn60β subunits assembled into β-type homo-oligomers and displayed refolding activity when cooperating with authentic chloroplast co-chaperonins (Vitlin et al., 2011). Each homo-oligomeric Cpn60β complex has its specific properties and preferences for co-chaperonin partners. Similarly, CPN60β2 and CPN60β1 from *Chlamydomonas* could be reconstituted into homo-oligomeric species *in vitro*, however, only CPN60β2 disassembled into monomer upon ATP hydrolysis (Bai et al., 2015). These results suggested that the Cpn60β subunits from one organism are functionally diverse though they share very high homology. Chloroplast chaperonins isolated from different organisms suggested they are α/β mixed hetero-oligomers, even though the arrangement of different subunits in the Cpn60 complex remains elusive (Cook et al., 1987; Musgrove et al., 1987; Hernan and Sligar, 1995; Nishio et al., 1999; Bai et al., 2015). *In vitro* reconstitution experiments with *E. coli* expressing Cpn60α and Cpn60β subunits from *Pisum sativum* generated two kinds of tetradecamers, α/β mixed hetero-oligomers and β homo-oligomers. Despite β subunits being able to assemble into homo-oligomers, they are preferentially incorporated into α/β mixed hetero-oligomers in the presence of α subunits. This provided strong support for the viewpoint that α/β mixed hetero-oligomers are predominant *in vivo* (Dickson et al., 2000). A recent study of CPN60 from *Chlamydomonas reinhardtii* also suggested that even though CPN60 monomers and homo-oligomers both possessed ATPase activity, only protein complexes containing all three subunits, the CPN60αβ1β2 oligomeric complex, have functional cooperation with GroES in refolding a model substrate (Bai et al., 2015). Thus, overwhelming evidence suggests that the major functional species *in vitro* is a hetero-oligomer composed of α and β subunits.

Another feature that is unique to hetero-oligomeric chloroplast chaperonins is their notorious instability in the presence of ATP, that is, the purified Cpn60 complex from *Pisum sativum* and recombinantly expressed CPN60αβ1β2 of *Chlamydomonas reinhardtii* display ATP-dependent dissociation (Dickson et al., 2000; Bai et al., 2015). The oligomer dissociation largely results from the interaction of equatorial domains.

Electron micrographs of the Cpn60αβ hetero-oligomer reveal that chloroplast chaperonin exhibits the well-known double-ring cylindrical shape, indicating a conserved structure in the Group I chaperonin kingdom (Dickson et al., 2000). Recently, the first crystal structure of the homo-oligomer CPN60β1, which shows partial functionality in the presence of Hsp10, was solved at 3.8 Å. The overall architecture of CPN60β1 displays a typical type I chaperonin structure, with a 7-fold symmetrical cylinder structure consisting of two stacked rings composed of seven subunits. Each subunit is also composed of an equatorial, intermediate, and apical domain. In Cpn60 subunits, the equatorial domain directs oligomer formation and the C-terminus (484-547) in this domain determines oligomer disassembly properties driven by ATP hydrolysis (Bai et al., 2015; Zhang et al., 2016a). However, Apo CPN60β1 resembles the intermediate state of allosteric GroEL, with a central cavity 6 Å larger than GroEL in diameter (Zhang et al., 2016a) (**Figure 3**). Moreover, the compaction in CPN60β1 is looser relative to GroEL, with less inter-subunit interface area and fewer amino acids involved in inter-subunit contacts. One distinguishing feature of CPN60β1 is that it has a wider ATP binding pocket compared to apo GroEL. These structural features may explain Cpn60 specific dissociation driven by ATP hydrolysis.

Compared to their bacterial and mitochondrial homologs, chloroplast co-chaperonin subunits also exhibit interesting difference. In 1992, the first chloroplast co-chaperonin was identified by a pull-down assay using pea chloroplast lysate with GroEL as bait. This chloroplast co-chaperonin is capable of assisting GroEL in folding a chemically denatured dimeric Rubisco, similar to GroES. But a fascinating aspect of this chloroplast co-chaperonin is that its molecular weight is ∼24 kD, twice the size of GroES (Bertsch et al., 1992). Similarly, co-chaperonin AtCpn21 with a molecular weight of ∼21 kD has also been observed in chloroplasts of *Arabidopsis thaliana*. The AtCpn21 precursor protein deduced by cDNA sequence contains a typical chloroplast transit peptide at its amino-terminus

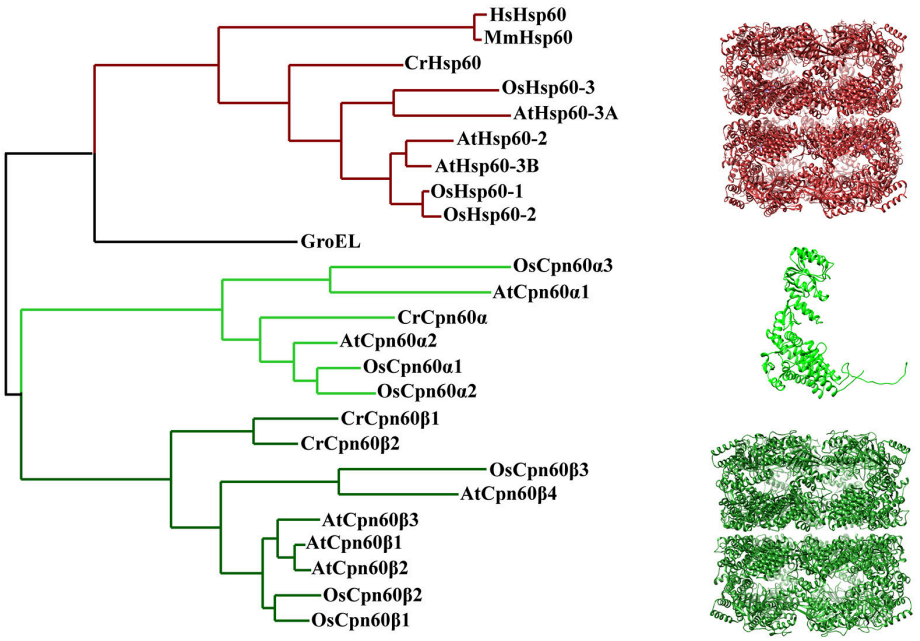

FIGURE 2 | Phylogenetic relationships of chaperonin proteins from bacteria, chloroplasts, and mitochondria. The tree was generated using Phylogeny (http://www.phylogeny.fr/). Protein sequences of *E. coli*, *H. sapiens*, and *M. musculus* chaperonin are from UniProt database [GroEL (P0A6F5), HsHsp60 (P108090), MmHsp60 (P63038)]. Protein sequence of plant mitochondria and chloroplast chaperonins are from Phytozome, TAIR and RGAP [CrHsp60 (Cre06.g309100), AtHsp60-2 (AT2G33210), AtHsp60-3A (AT3G13860), AtHsp60-3B (AT3G23990), OsHsp60-1 (Os10g32550), OsHsp60-2 (Os03g04970), OsHsp60-3 (Os05g46290), CrCpn60α (Cre04.g231222), CrCpn60β1(Cre17.g741450), CrCpn60β2 (Cre07.g339150), AtCpn60α1 (At5g18820), AtCpn60α2 (At2g28000), AtCpn60β1 (At5g56500), AtCpn60β2 (At3g13470), AtCpn60β3 (At1g55490), AtCpn60β4 (At1g26230), OsCpn60α1 (Os12g17910), OsCpn60α2 (Os03g64210), OsCpn60α3 (Os09g38980), OsCpn60β1 (Os06g02380), OsCpn60β2 (Os02g01280), OsCpn60β3 (ChrSy.fgenesh.gene.28)]. The molecular structure was generated by UCSF Chimera (Pettersen et al., 2004) using CrCpn60β1coodinates 5CDI from Protein Data Bank.

and two GroES-like domains joined together head-to-tail (Hirohashi et al., 1999). Mature AtCpn21 protein formed tetrameric structures as revealed by gel-filtration and cross-linking analysis (Koumoto et al., 1999). In addition to Cpn20s, classical GroES-like co-chaperonins have also been found in chloroplasts of several organisms (Schlicher and Soll, 1996; Hill and Hemmingsen, 2001). Since whole genome information of multiple plant species is available, it is known that there are two types of co-chaperonin subunits present in chloroplasts: a conventional GroES-like Cpn10 type, and a chloroplast-specific Cpn20 type that contains two tandem GroES-like domains (**Figure 4**). *Chlamydomonas reinhardtii* encodes three chloroplast co-chaperonin subunits named according to their molecular weights as CrCPN11, CrCPN20, and CrCPN23, while *Arabidopsis thaliana* and *Oryza sativa* both have three paralogs as listed in **Table 1**. Though chloroplast co-chaperonin subunits seem conserved among species, each subunit has unique biochemical properties. In *Arabidopsis*, AtCpn10-2 and AtCpn20 form functional homo-oligomers on their own, while AtCpn10-1 subunit is functional only upon formation of hetero-oligomers with other co-chaperonins (Vitlin Gruber et al., 2014). The case is similar in *Chlamydomonas*, that is, CrCPN20 and/or CrCPN23 tend to combine with CrCPN10 to form functional hetero-oligomers composed of seven GroES-like domains (Tsai et al., 2012).

Although some mitochondria and bacteria also possess more than one chaperonin subunit, it is still a fascinating question why the chloroplast uniquely contains divergent Cpn60 α/β chaperonin subunits as well as Cpn10/20 co-chaperonin types (Kumar et al., 2015). Transcriptome and proteome studies in *Arabidopisis* indicated expression levels of chaperonin and co-chaperonin genes differ according to developmental stage (Weiss et al., 2009), which increases the complex potential of the chaperonin system for regulation on both transcriptional and post-translational levels. In different tissues or developmental stages, or even facing different environmental stimuli, it is plausible that the functional chaperonin system is composed of various combinations of chloroplast chaperonin and its co-chaperonins to strategically deal with specific situations. From an evolutionary perspective, the chloroplast is an endosymbiotic organelle where the most important chemical reaction of photosynthesis takes place. It is also reasonable to deduce that chloroplasts developed a chaperonin system with several features that adapt to accommodate different photosynthetic proteins. Our knowledge from the Group I chaperonin paradigm, the GroEL-ES system, is insufficient to explain the multiformity of the chloroplast chaperonin system. Therefore, genetic, biochemical and structural data directly obtained from chloroplast chaperonins will be needed to shed light on the mechanism of this protein folding machine in photosynthesis.

TABLE 1 | Chloroplast chaperonins and co-chaperonins in model species: nomenclature and function.

Protein name	Organism	Gene number	Mutant line	Phenotype	References
CrCpn60α	*Chlamydomonas reinhardtii*	Cre04.g231222	Unknown	Unknown	
CrCpn60β1	*Chlamydomonas reinhardtii*	Cre17.g741450	Unknown	Unknown	
CrCpn60β2	*Chlamydomonas reinhardtii*	Cre07.g339150	Unknown	Unknown	
AtCpn60α1	*Arabidopsis thaliana*	At2g28000	T-DNA insertion (*slp1*)	Retardation of embryo development before the heart stage	Apuya et al., 2001
AtCpn60α2	*Arabidopsis thaliana*	At5g18820	T-DNA insertion (*emb3007*)	Embryo development arrested at the globular stage	Ke et al., 2017
AtCpn60β1	*Arabidopsis thaliana*	At1g55490	T-DNA insertion (*len1*)	Impaired leaves and showed systemic acquired resistance (SAR) under short-day condition	Ishikawa et al., 2003
AtCpn60β2	*Arabidopsis thaliana*	At3g13470	T-DNA insertion	No obvious phenotype	Suzuki et al., 2009
AtCpn60β3	*Arabidopsis thaliana*	At5g56500	Unknown	Unknown	
AtCpn60β4	*Arabidopsis thaliana*	At1g26230	Ds transposon-tagged lines(*crr27)*	Defective in NDH activity	Peng et al., 2011
OsCpn60α1	*Oryza Sativa*	Os12g17910	T-DNA insertion	Pale-green phenotype at the seedling stage	Kim et al., 2013a
OsCpn60α2	*Oryza Sativa*	Os03g64210	Natural mutation	Albino phenotype before the 3-leaf stage grown below 24°C	Jiang et al., 2014
OsCpn60α3	*Oryza Sativa*	Os09g38980	Unknown	Unknown	
OsCpn60β1	*Oryza Sativa*	Os06g02380	Unknown	Unknown	
OsCpn60β2	*Oryza Sativa*	Os02g01280	Unknown	Unknown	
OsCpn60β3	*Oryza Sativa*	ChrSy.fgenesh.gene.28	Unknown	Unknown	
CrCpn11	*Chlamydomonas reinhardtii*	Cre16.g673729	Unknown	Unknown	
CrCpn20	*Chlamydomonas reinhardtii*	Cre08.g358562	Unknown	Unknown	
CrCpn23	*Chlamydomonas reinhardtii*	Cre12.g505850	Unknown	Unknown	
AtCpn10-1	*Arabidopsis thaliana*	At3g60210	Unknown	Unknown	
AtCpn10-2	*Arabidopsis thaliana*	At2g44650	Unknown	Unknown	
AtCpn20	*Arabidopsis thaliana*	At5g20720	T-DNA insertion	Increased ABA sensitivity, homozygous lethal	Zhang et al., 2013
OsCpn10	*Oryza Sativa*	Os10g41710	Unknown	Unknown	
OsCpn20-1	*Oryza Sativa*	Os02g54060	Unknown	Unknown	
OsCpn20-2	*Oryza Sativa*	Os09g26730	Unknown	Unknown	
OsCpn20-3	*Oryza Sativa*	Os06g09679	Unknown	Unknown	
OsCpn20-4	*Oryza Sativa*	Os06g09688	Unknown	Unknown	

Chloroplast chaperonin names from Chlamydomonas reinhardtii, Arabidopsis thaliana, are according to Phytozome, TAIR, while those from Oryza Sativa are based on the original names described in Kim et al. (2013a). Chloroplast co-chaperonin names from Chlamydomonas reinhardtii, Arabidopsis thaliana are based on the original names described in Tsai et al. (2012) and Vitlin Gruber et al. (2013a). Chloroplast co-chaperonins from Oryza Sativa are named in this review.

FUNCTIONAL DIVERGENCE OF CHLOROPLAST CHAPERONIN AND CO-CHAPERONIN SUBUNITS

Chloroplast chaperonins are extremely labile protein complexes, and therefore conventional biochemical methods may fall short to when it comes to explaining the nature of their multiplicity. Genetic analysis of chloroplast chaperonin and co-chaperonin mutants and the study of their roles in specific tissues or developmental stages provide a global view on how this dynamic chaperonin system works and the possible significance of its divergence. The first phenotypic dissection of Cpn60 mutants was conducted in *cpn60α1* (At2g28000) which was generated by T-DNA insertion in *Arabidopsis*. This *atcpn60α1* mutant was termed *schlepperless* due to its highly reduced embryonic cotyledons. Compared to wild-type, the entire embryo of *Atcpn60α1* remains white during maturation, suggesting photosynthesis incompetence. Further analysis of this mutant indicates that the absence of functional AtCpn60α1 disrupts the development of the chloroplast which results in defective development of the embryo (Apuya et al., 2001). A similar function of Cpn60α has also been demonstrated in rice according to a study using forward genetics. Map based cloning of the thermo-sensitive chloroplast development 9 (tcd9) rice mutant revealed that the mutation is located in a gene encoding a Cpn60α protein. Genetic complementation demonstrated that the *OsCpn60α* gene is precisely responsible for the albino phenotype before the 3-leaf stage grown below 20°C (Jiang et al., 2014). These two studies suggest a conserved function of Cpn60α members in chloroplast development.

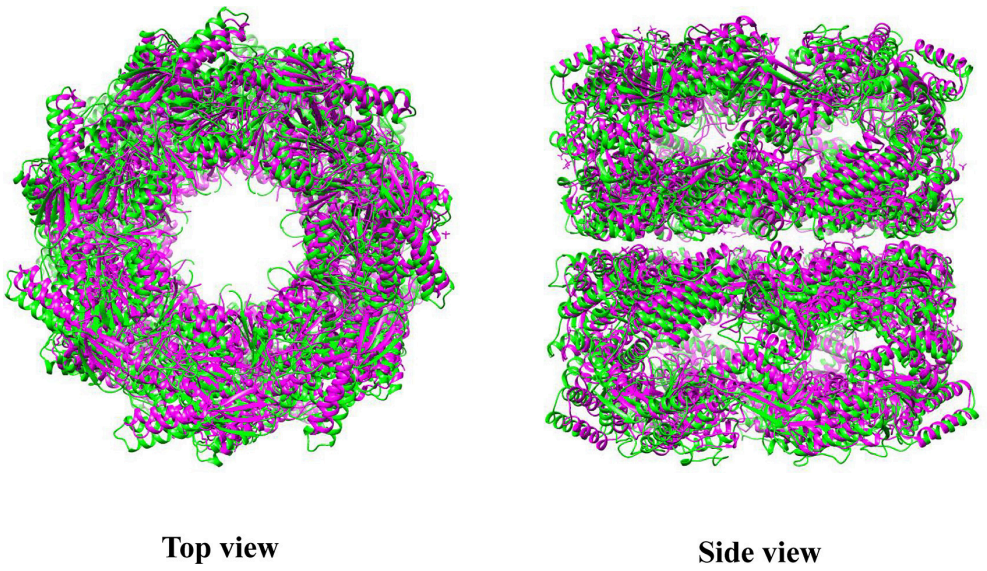

FIGURE 3 | Superposition of CrCpn60β1 with GroEL. Green represents CrCpn60β1 and magenta represents GroEL. The molecular structure was generated by UCSF Chimera (Pettersen et al., 2004) using CrCpn60β1 coordinates 5CDI and GroEL coordinates 1XCK from Protein Data Bank.

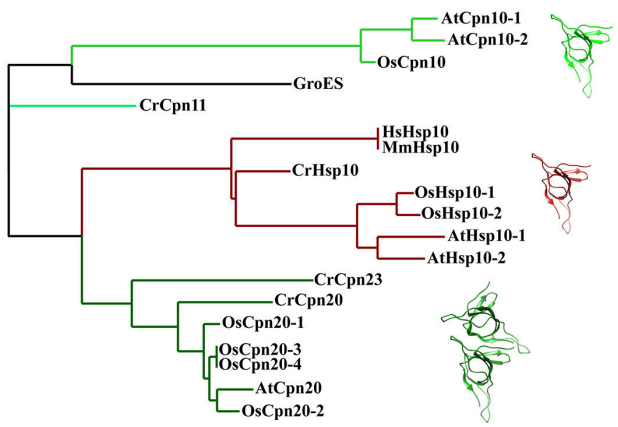

FIGURE 4 | Phylogenetic relationships of co-chaperonin proteins from bacteria, chloroplasts and mitochondria. The tree was generated using Phylogeny (http://www.phylogeny.fr/). Protein sequences of *E. coli*, *H. sapiens*, and *M. musculus* chaperonin are from UniProt database Protein sequence of plant mitochondria and chloroplast co-chaperonins are from Phytozome, TA Protein sequences of mitochondria chaperonin are from IR and RGAP [AtHsp10-1 (AT1G14980), AtHsp10-2 (AT1G23100), CrHsp10 (Cre03.g178450), OsHsp10-1(Os03g25050), OsHsp10-2 (Os07g44740), CrCpn11 (Cre16.g673729), CrCpn20 (Cre08.g358562), CrCpn23 (Cre12.g505850), AtCpn10-1 (At3g60210), AtCpn10-2 (At2g44650), AtCpn20 (At5g20720), OsCpn10 (Os10g41710), OsCpn20-1 (Os02g54060), OsCpn20-2 (Os09g26730), OsCpn20-3 (Os06g09679), OsCpn20-4 (Os06g09688)]. The molecular structure was generated by UCSF Chimera (Pettersen et al., 2004) using GroES coordinates 1AON from Protein Data Bank.

Additional Cpn60 mutants including *atcpn60α1* (At2g28000), *atcpn60β1* (At1g55490), and *atcpn60β2* (At3g13470) have been isolated in research focusing on chloroplast division in *Arabidopsis* (Suzuki et al., 2009). This work showed that AtCpn60α1, AtCpn60β1, and AtCpn60β2 are required for formation of a normal chloroplast division apparatus, especially by influencing folding of chloroplast division related proteins and regulating FtsZ polymer dynamics. The *atcpn60β1atcpn60β2* double mutant exhibited an albino phenotype, similar to the *atcpn60α1* single mutant. However, *atcpn60β1* and *atcpn60β2* single mutants did not show an albino phenotype but had slightly reduced chlorophyll. These results suggest that the phylogenetically closely related AtCpn60β1 and AtCpn60β2 are functionally redundant. Another notable observation is that although the *atcpn60α1* single mutant and *atcpn60β1atcpn60β2* showed a similar albino phenotype, *atcpn60β1atcpn60β2* was able to germinate while *cpn60α1* arrested at the embryo stage (Apuya et al., 2001; Suzuki et al., 2009). This supports the hypothesis that different Cpn60 subunits may incorporate into one major pathway; However, these subunits may also be individually responsible for folding specific protein substrates.

The hypothesis raised above was supported by a study identifying Rubisco activase interacting proteins during heat stress. A 60 kD protein with a N-terminal signal sequence simultaneously corresponding to both AtCpn60β1 and AtCpn60β2 was captured. Cpn60β was associated with Rubisco activase in a high molecular mass complex, and the dynamic regulation of their association depended on heat stress. This suggested AtCpn60β1 and/or AtCpn60β2 play a role in preventing Rubisco activase from thermal denaturation. The study of *Cpn60α1* mutant from *Oryza sativa* provided another example; the amount of Rubisco large subunit (rbcL) was severely reduced in the *osCpn60α1* mutant, while some imported proteins remained unchanged. This demonstrated that Rubisco large subunit may depend on OsCpn60α1 for proper folding (Kim et al., 2013a). The direct evidence for the assumption

came from the study of Cpn60β4 in *Arabidopsis*. When the *Cpn60β4* (At1g26230) gene is defective, the chloroplast fails to accumulate the NADH dehydrogenase-like complex (NDH), and the other three Cpn60β subunits cannot replace the function of Cpn60β4. Co-immunoprecipitation data revealed that Cpn60β4 forms a hetero-oligomeric complex with other Cpn60 α and β subunits and this complex is essential for the folding of the NDH subunit NdhH. Furthermore, the unique C-terminus of Cpn60β4 is required for the refolding activity of NdhH in the chaperonin complex (Peng et al., 2011). A very recent study about the function of Cpn60α2 (At5g18820) during *Arabidopsis* embryo development provided another example of subunit specific folding of protein substrates. A co-immunoprecipitation assay coupled with LC-MS/MS identified KASI, a protein important for the formation of heart-shaped embryos, as a specific interactor of Cpn60α2. A genetic study showed that KASI protein levels were largely reduced in the *atcpn60α2* mutant. Further studies demonstrated that Cpn60α2, Cpn60β2, and Cpn60β3 were able to assemble into a functional chaperonin complex and specifically assist in folding of KASI. It is plausible that these three subunits form functional oligomers in certain developmental stages. However, a detailed biochemical characterization remains elusive (Ke et al., 2017).

A biochemical study of chloroplast chaperonins from *Chlamydomonas reinhardtii* provided additional insight into the divergence of CPN60 subunits. Specifically, domain swapping between GroEL and CPN60 subunits demonstrated that in the functional hetero-oligomeric complex CPN60αβ1β2, the CPN60α apical domain could not functionally cooperate with co-chaperonin GroES, but recognized its cognate substrate CrRubisco large subunit more efficiently than CPN60β apical domain and vice versa. This implied chloroplast chaperonin adopts a different strategy than GroEL to cope with the paradox that the same region of apical domains is responsible for simultaneous binding of co-chaperonin and protein substrates (Chen et al., 2013; Zhang et al., 2016b). Though functionality of two types of subunits is divergent, they are highly cooperative in oligomer formation. The equatorial domain of CPN60α could not direct self-assembly, but cooperated with CPN60β1 to form fully functional oligomers (Zhang et al., 2016a).

It has long been accepted that specific co-chaperonins would endow the chaperonin system with uncommon ability to accommodate diverse protein substrates. An interesting example is the T4 phage encoded protein, GP31, which is homologous to GroES. Structural and biochemical studies of GP31 proved that an expanded folding chamber was formed with GroEL-GP31 and these heterologous partners are able to fold the capsid protein GP23. Similar mechanisms may exist in chloroplast considering that there are two kinds of co-chaperonin isoforms (**Figure 4**). A study characterizing chloroplast co-chaperonin subunits of both *Arabidopsis* and *Chlamydomonas* indicated that different combinations of Cpn10/20 subunits create diverse hetero-oligomers with various refolding activities, perhaps adapting the chaperonin system to specific protein substrates (Tsai et al., 2012).

Study of chloroplast co-chaperonin gene mutants in *Arabidopsis* addressed the unique importance of Cpn20 type co-chaperonin. Cpn10 type co-chaperonin null mutants such as *atcpn10-1* and *atcpn10-2* were able to germinate normally, whereas knock out of Cpn20 in Arabidopsis is lethal (Zhang et al., 2013). It has been demonstrated that Cpn20 homo-oligomer is able to cooperate with chaperonin, which also raises the symmetry dilemma. Namely, how does hexameric or octameric Cpn20 oligomer interact with a chaperonin complex with seven-fold symmetry? Two studies suggested this is a simple obstacle that the chaperonin system overcomes. Cpn20 from *Plasmodium falciparum* apicoplast, a degenerate chloroplast, is fully functional *in vitro* and able to replace GroES in *E. coli* at both normal and heat-shock temperatures. Since *Plasmodium falciparum* apicoplast contains only one Cpn20 type co-chaperonin, PfCpn20 may also function similarly *in vivo* (Vitlin Gruber et al., 2013b). In another *in vitro* biochemical study, GroES and Cpn20 concatamers, consisting of six to eight covalently linked 10 kD GroES domains, cooperatively function with GroEL similar to the native heptameric GroES form. The cooperation between chaperonin and co-chaperonin results from asymmetrical interaction by leaving one chaperonin subunit unbounded (six GroES domain) or excluding one co-chaperonin from the interaction (eight GroES domain) (**Figure 5**) (Guo et al., 2015). These results showed how chloroplast Cpn20, with even-numbered GroES-like domains, cooperated with odd-numbered chaperonin oligomers. However, though concatamers composed of six or eight GroES domains are functional, it seems that the native form of co-chaperonin in *Arabidopsis* and *Chlamydomonas* is most likely a hetero-oligomer with seven-fold symmetry (Tsai et al., 2012; Vitlin Gruber et al., 2014).

Another deduction on why chloroplasts have so many chaperonin and co-chaperonin genes points to their additional functions other than folding proteins as molecular chaperones, so-called moonlighting function. For example, CPN60α was previously reported to exhibit a novel function as a group II intron-specific binding protein and was presumed to be a general chloroplast RNA splicing factor (Balczun et al., 2006). Chloroplast proteomic studies in *Arabidopsis* showed that Cpn20 is much more abundant than other subunits in the chloroplast chaperonin system, which suggested Cpn20 has additional moonlighting function (Peltier et al., 2006). Cpn20 overexpressing mutants and mutants with defective co-chaperonin activity were reported to increase FeSOD activity by functioning as probable Fe chaperones (Kuo et al., 2013a,b). Analysis of Cpn20 knock down mutants showed that Cpn20 functions negatively in the ABAR-WRKY40 coupled ABA signaling pathway by antagonizing Mg-chelatase H subunit to derepress the ABA-responsive WRKY40 transcription repressor (Zhang et al., 2013, 2014). To clarify the moonlighting function of different chloroplast chaperonin and co-chaperonin proteins, more studies are still needed.

CHLOROPLAST CHAPERONIN ASSISTED RUBISCO FOLDING AND ASSEMBLY

Ribulose-1,5-bisphosphate carboxylase/oxygenase (Rubisco), the most important chloroplast chaperonin substrate, catalyzes the chemical reaction by which inorganic carbon enters the organic

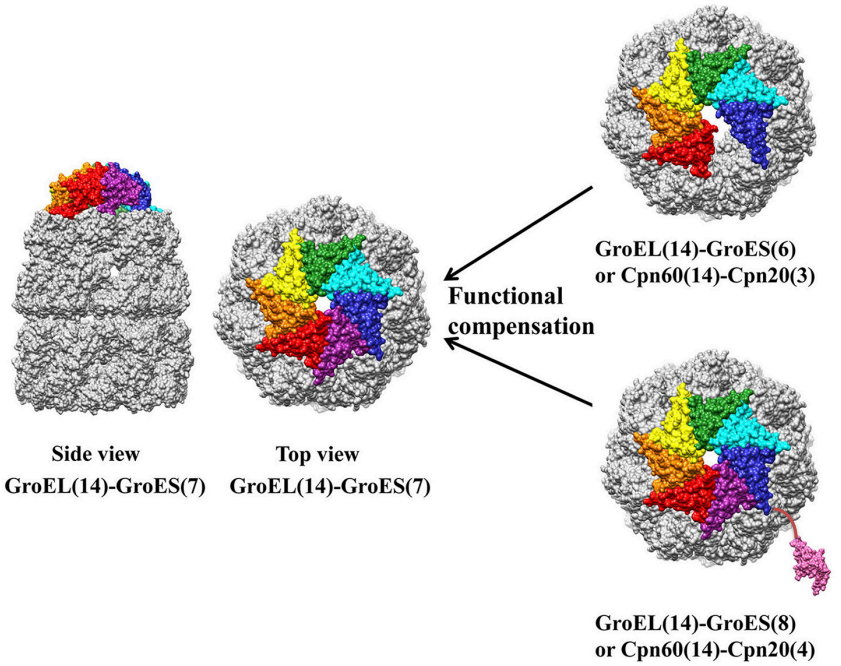

FIGURE 5 | Asymmetric functional interaction between chloroplast chaperonin and co-chaperonin. GroEL is colored in gold, and seven GroES subunits are colored in red, orange, yellow, green, cyan, blue, and pink. Co-chaperonins consisting of six or eight GroES like domains function equally as well as heptameric GroES. The molecular structure was generated by UCSF Chimera (Pettersen et al., 2004) using GroES-GroEL-ADP coordinates 1AON from Protein Data Bank.

biosphere. As a key enzyme that catalyzes the rate-limiting step of photosynthetic carbon fixation in the Calvin–Benson–Bassham cycle as well as an ancient enzyme that evolved from a high CO_2 atmospheric environment, Rubisco is widely known for its abundance and inefficiency. Therefore, numerous efforts have been undertaken to engineer Rubisco to improve carbon fixation efficiency with reduced amounts of Rubisco at the expense of less nitrogen. However, a high throughput Rubisco mutant screening platform is so far infeasible due to the lack of assembly of Form I Rubisco outside chloroplasts.

Form I Rubisco, a hexadecameric protein complex consisting of eight large (RbcL) and eight small (RbcS) subunits, exists in plants, green algae, cyanobacteria and proteobacteria. Even though it has been widely accepted that newly-translated RbcL would be captured by chloroplast chaperonin to avoid aggregation, how RbcS is coupled with RbcL and assembled into Rubisco holoenzyme had remained unknown. The breakthrough came from the study of RbcX protein which was first identified in *Anabaena* and *Synechococcus*. Co-expression of RbcX in *E. coli* facilitated the production of active Rubisco, suggesting RbcX is involved in the Rubisco assembly pathway (Li and Tabita, 1997; Onizuka et al., 2004; Emlyn-Jones et al., 2006). Functional analysis revealed that RbcX acts as an assembly chaperone, downstream of chaperonin-mediated RbcL folding, to promote the formation of RbcL(8) core complexes. The crystal structure showed that the 15 kD RbcX forms a homodimer containing a hydrophobic central groove that binds the peptide motif EIKFEFD present at the C-terminus of RbcL subunits. The subsequent cryo-electron microscopy structure of $RbcL_{(8)}$-$(RbcX_2)_{(8)}$ assembly intermediate revealed $RbcX_{(2)}$ acts as a molecular stapler in stabilizing the RbcL subunits and facilitates $RbcL_{(8)}$ core assembly. Finally, replacement of RbcX by RbcS results in holoenzyme formation (Saschenbrecker et al., 2007; Liu et al., 2010). Highly homologous RbcX proteins exist in *Thermosynechococcus elongates* and *Arabidopsis thaliana* as revealed by their structures, implying this may be a conserved mechanism for Rubisco assembly across species (Tarnawski et al., 2011; Kolesinski et al., 2013).

In addition to RbcX, other Rubisco assembly associated factors have also been discovered in recent years. For example, analysis of *Zea mays* mutants showed that Bundle Sheath Defective 2 (Bsd2), Rubisco Accumulation Factor 1 (Raf1), and Rubisco Accumulation Factor 2 (Raf2) are responsible for proper assembly of Rubisco (Brutnell et al., 1999; Feiz et al., 2012, 2014). Co-transformation of Raf1 and RbcL from Arabidopsis into tobacco chloroplast results in improved production of hybrid Rubisco, suggesting Raf1 protein co-evolved with RbcL (Whitney et al., 2015). Just like RbcX, Raf1 also functions downstream of chaperonin-assisted RbcL folding by stabilizing RbcL dimers for assembly into $(RbcL)_8$ core complexes, suggesting diverse Rubisco assembly factors have functional redundancy (Hauser et al., 2015).

Despite more and more Rubisco assembly factors being identified, recombinant production of plant Rubisco in *E. coli* or reconstitution of Rubisco holoenzyme in test tubes has not been achieved so far. From the perspective of evolution, it is noteworthy that α/β type divergence of chaperonin subunits appeared after the endosymbiotic event involving cyanobacteria

with only GroEL-type chaperonin. Given the fact that Rubisco is the most abundant protein in the world, the chaperonin system responsible for Rubisco biogenesis must have specially adapted to cope with the burdensome task of folding and assembling such large quantities of protein. According to the classic Rubisco folding and assembly pathway described above, the chaperonin system is believed to function in RbcL folding, upstream of holoenzyme assembly, where GroEL could have done the job in prokaryotic organisms. However, the protein folding machine for plant Rubisco is the chloroplast chaperonin system, which we believe it has special properties cannot be replaced by GroEL system. Maybe it is time to set up an *in vitro* system containing the chloroplast chaperonin system and currently known Rubisco assembly factors to make plant Rubisco reconstitution a reality.

CONCLUDING REMARKS

Genetic and biochemical studies emphasize the regulatory role of chloroplast chaperonin in photosynthesis, and some photosynthetic proteins are identified as substrates of chloroplast chaperonin, such as Rubisco large subunit, NDH subunit NdhH and ATPase synthase γ subunits (Mao et al., 2015). The protein substrates involved in embryo development and chloroplast division, as well as the processes affected by Cpn60 subunit mutation are not yet clarified. Sophisticated studies are needed to identify the substrates specifically folded by certain chaperonin subunits. The crystal structure of CPN60β1 resembles that of GroEL (Zhang et al., 2016a), but the composition and arrangement of the *in vivo* chaperonin complex, which might vary under different conditions, remains elusive. Elucidating the functional mechanism of chloroplast chaperonin will be of special importance in the context of efforts to assemble eukaryotic Rubisco *in vitro*.

AUTHOR CONTRIBUTIONS

All authors listed, have made substantial, direct and intellectual contribution to the work, and approved it for publication.

ACKNOWLEDGMENTS

This work was supported by the National Natural Science Foundation of China (31671262).

REFERENCES

Anfinsen, C. B., Redfield, R. R., Choate, W. L., Page, J., and Carroll, W. R. (1954). Studies on the gross structure, cross-linkages, and terminal sequences in ribonuclease. *J. Biol. Chem.* 207, 201–210.

Apuya, N. R., Yadegari, R., Fischer, R. L., Harada, J. J., Zimmerman, J. L., and Goldberg, R. B. (2001). The Arabidopsis embryo mutant schlepperless has a defect in the chaperonin-60alpha gene. *Plant Physiol.* 126, 717–730. doi: 10.1104/pp.126.2.717

Ashcroft, A. E., Brinker, A., Coyle, J. E., Weber, F., Kaiser, M., Moroder, L., et al. (2002). Structural plasticity and noncovalent substrate binding in the GroEL apical domain. A study using electrospay ionization mass spectrometry and fluorescence binding studies. *J. Biol. Chem.* 277, 33115–33126. doi: 10.1074/jbc.M203398200

Azem, A., Kessel, M., and Goloubinoff, P. (1994). Characterization of a functional GroEL14(GroES7)2 chaperonin hetero-oligomer. *Science* 265, 653–656. doi: 10.1126/science.7913553

Bai, C., Guo, P., Zhao, Q., Lv, Z., Zhang, S., Gao, F., et al. (2015). Protomer roles in chloroplast chaperonin assembly and function. *Mol. Plant* 8, 1478–1492. doi: 10.1016/j.molp.2015.06.002

Balczun, C., Bunse, A., Schwarz, C., Piotrowski, M., and Kuck, U. (2006). Chloroplast heat shock protein Cpn60 from *Chlamydomonas reinhardtii* exhibits a novel function as a group II intron-specific RNA-binding protein. *FEBS Lett.* 580, 4527–4532. doi: 10.1016/j.febslet.2006.07.030

Barraclough, R., and Ellis, R. J. (1980). Protein synthesis in chloroplasts. IX. Assembly of newly-synthesized large subunits into ribulose bisphosphate carboxylase in isolated intact pea chloroplasts. *Biochim. Biophys. Acta* 608, 19–31. doi: 10.1016/0005-2787(80)90129-X

Bartlett, A. I., and Radford, S. E. (2009). An expanding arsenal of experimental methods yields an explosion of insights into protein folding mechanisms. *Nat. Struct. Mol. Biol.* 16, 582–588. doi: 10.1038/nsmb.1592

Bertsch, U., Soll, J., Seetharam, R., and Viitanen, P. V. (1992). Identification, characterization, and DNA sequence of a functional "double" groES-like chaperonin from chloroplasts of higher plants. *Proc. Natl. Acad. Sci. U.S.A.* 89, 8696–8700. doi: 10.1073/pnas.89.18.8696

Bochkareva, E. S., and Girshovich, A. S. (1994). ATP induces non-identity of two rings in chaperonin GroEL. *J. Biol. Chem.* 269, 23869–23871.

Bochkareva, E. S., Lissin, N. M., Flynn, G. C., Rothman, J. E., and Girshovich, A. S. (1992). Positive cooperativity in the functioning of molecular chaperone GroEL. *J. Biol. Chem.* 267, 6796–6800.

Boisvert, D. C., Wang, J., Otwinowski, Z., Horwich, A. L., and Sigler, P. B. (1996). The 2.4 A crystal structure of the bacterial chaperonin GroEL complexed with ATP gamma S. *Nat. Struct. Biol.* 3, 170–177. doi: 10.1038/nsb0296-170

Braig, K., Otwinowski, Z., Hegde, R., Boisvert, D. C., Joachimiak, A., Horwich, A. L., et al. (1994). The crystal structure of the bacterial chaperonin GroEL at 2.8 A. *Nature* 371, 578–586. doi: 10.1038/371578a0

Brutnell, T. P., Sawers, R. J., Mant, A., and Langdale, J. A. (1999). BUNDLE SHEATH DEFECTIVE2, a novel protein required for post-translational regulation of the rbcL gene of maize. *Plant Cell* 11, 849–864. doi: 10.1105/tpc.11.5.849

Bukau, B., Weissman, J., and Horwich, A. (2006). Molecular chaperones and protein quality control. *Cell* 125, 443–451. doi: 10.1016/j.cell.2006.04.014

Chan, H. S., and Dill, K. A. (1996). A simple model of chaperonin-mediated protein folding. *Proteins* 24, 345–351. doi: 10.1002/(SICI)1097-0134(199603)24:3<345::AID-PROT7>3.0.CO;2-F

Chaudhuri, T. K., Verma, V. K., and Maheshwari, A. (2009). GroEL assisted folding of large polypeptide substrates in Escherichia coli: Present scenario and assignments for the future. *Prog. Biophys. Mol. Biol.* 99, 42–50. doi: 10.1016/j.pbiomolbio.2008.10.007

Chen, D. H., Madan, D., Weaver, J., Lin, Z., Schroder, G. F., Chiu, W., et al. (2013). Visualizing GroEL/ES in the act of encapsulating a folding protein. *Cell* 153, 1354–1365. doi: 10.1016/j.cell.2013.04.052

Clare, D. K., Vasishtan, D., Stagg, S., Quispe, J., Farr, G. W., Topf, M., et al. (2012). ATP-triggered conformational changes delineate substrate-binding and -folding mechanics of the GroEL chaperonin. *Cell* 149, 113–123. doi: 10.1016/j.cell.2012.02.047

Cloney, L. P., Bekkaoui, D. R., Wood, M. G., and Hemmingsen, S. M. (1992a). Assessment of plant chaperonin-60 gene function in Escherichia coli. *J. Biol. Chem.* 267, 23333–23336.

Cloney, L. P., Wu, H. B., and Hemmingsen, S. M. (1992b). Expression of plant chaperonin-60 genes in Escherichia coli. *J. Biol. Chem.* 267, 23327–23332.

Cook, R. M., Ashworth, R. F., and Musgrove, N. R. (1987). Eosinophil- and neutrophil-mediated injury of human lung fibroblast cells. *Int. Arch. Allergy Appl. Immunol.* 83, 428–431. doi: 10.1159/000234380

Dickson, R., Weiss, C., Howard, R. J., Alldrick, S. P., Ellis, R. J., Lorimer, G., et al. (2000). Reconstitution of higher plant chloroplast chaperonin 60 tetradecamers active in protein folding. *J. Biol. Chem.* 275, 11829–11835. doi: 10.1074/jbc.275.16.11829

Dill, K. A., and MacCallum, J. L. (2012). The protein-folding problem, 50 years on. *Science* 338, 1042–1046. doi: 10.1126/science.1219021

Elad, N., Farr, G. W., Clare, D. K., Orlova, E. V., Horwich, A. L., and Saibil, H. R. (2007). Topologies of a substrate protein bound to the chaperonin GroEL. *Mol. Cell* 26, 415–426. doi: 10.1016/j.molcel.2007.04.004

Ellis, R. J., and Minton, A. P. (2006). Protein aggregation in crowded environments. *Biol. Chem.* 387, 485–497. doi: 10.1515/BC.2006.064

Emlyn-Jones, D., Woodger, F. J., Price, G. D., and Whitney, S. M. (2006). RbcX can function as a rubisco chaperonin, but is non-essential in Synechococcus PCC7942. *Plant Cell Physiol.* 47, 1630–1640. doi: 10.1093/pcp/pcl028

Farr, G. W., Fenton, W. A., Chaudhuri, T. K., Clare, D. K., Saibil, H. R., and Horwich, A. L. (2003). Folding with and without encapsulation by cis- and trans-only GroEL-GroES complexes. *EMBO J.* 22, 3220–3230. doi: 10.1093/emboj/cdg313

Farr, G. W., Furtak, K., Rowland, M. B., Ranson, N. A., Saibil, H. R., Kirchhausen, T., et al. (2000). Multivalent binding of nonnative substrate proteins by the chaperonin GroEL. *Cell* 100, 561–573. doi: 10.1016/S0092-8674(00)80692-3

Fei, X., Ye, X., LaRonde, N. A., and Lorimer, G. H. (2014). Formation and structures of GroEL:GroES2 chaperonin footballs, the protein-folding functional form. *Proc. Natl. Acad. Sci. U.S.A.* 111, 12775–12780. doi: 10.1073/pnas.1412922111

Feiz, L., Williams-Carrier, R., Belcher, S., Montano, M., Barkan, A., and Stern, D. B. (2014). A protein with an inactive pterin-4a-carbinolamine dehydratase domain is required for Rubisco biogenesis in plants. *Plant J.* 80, 862–869. doi: 10.1111/tpj.12686

Feiz, L., Williams-Carrier, R., Wostrikoff, K., Belcher, S., Barkan, A., and Stern, D. B. (2012). Ribulose-1,5-bis-phosphate carboxylase/oxygenase accumulation factor1 is required for holoenzyme assembly in maize. *Plant Cell* 24, 3435–3446. doi: 10.1105/tpc.112.102012

Gray, T. E., and Fersht, A. R. (1991). Cooperativity in ATP hydrolysis by GroEL is increased by GroES. *FEBS Lett.* 292, 254–258. doi: 10.1016/0014-5793(91)80878-7

Guo, P., Jiang, S., Bai, C., Zhang, W., Zhao, Q., and Liu, C. (2015). Asymmetric functional interaction between chaperonin and its plastidic cofactors. *FEBS J.* 282, 3959–3970. doi: 10.1111/febs.13390

Haldar, S., Gupta, A. J., Yan, X., Milicic, G., Hartl, F. U., and Hayer-Hartl, M. (2015). Chaperonin-assisted protein folding: relative population of asymmetric and symmetric GroEL:GroES complexes. *J. Mol. Biol.* 427, 2244–2255. doi: 10.1016/j.jmb.2015.04.009

Harris, J. R., Pluckthun, A., and Zahn, R. (1994). Transmission electron microscopy of GroEL, GroES, and the symmetrical GroEL/ES complex. *J. Struct. Biol.* 112, 216–230. doi: 10.1006/jsbi.1994.1022

Hartl, F. U., Bracher, A., and Hayer-Hartl, M. (2011). Molecular chaperones in protein folding and proteostasis. *Nature* 475, 324–332. doi: 10.1038/nature10317

Hartl, F. U., and Hayer-Hartl, M. (2002). Molecular chaperones in the cytosol: from nascent chain to folded protein. *Science* 295, 1852–1858. doi: 10.1126/science.1068408

Hauser, T., Bhat, J. Y., Milicic, G., Wendler, P., Hartl, F. U., Bracher, A., et al. (2015). Structure and mechanism of the Rubisco-assembly chaperone Raf1. *Nat. Struct. Mol. Biol.* 22, 720–728. doi: 10.1038/nsmb.3062

Hayer-Hartl, M., Bracher, A., and Hartl, F. U. (2016). The GroEL-GroES chaperonin machine: a nano-cage for protein folding. *Trends Biochem. Sci.* 41, 62–76. doi: 10.1016/j.tibs.2015.07.009

Hemmingsen, S. M., and Ellis, R. J. (1986). Purification and properties of ribulosebisphosphate carboxylase large subunit binding protein. *Plant Physiol.* 80, 269–276. doi: 10.1104/pp.80.1.269

Hemmingsen, S. M., Woolford, C., van der Vies, S. M., Tilly, K., Dennis, D. T., Georgopoulos, C. P., et al. (1988). Homologous plant and bacterial proteins chaperone oligomeric protein assembly. *Nature* 333, 330–334. doi: 10.1038/333330a0

Hernan, R. A., and Sligar, S. G. (1995). Tetrameric hemoglobin expressed in Escherichia coli. Evidence of heterogeneous subunit assembly. *J. Biol. Chem.* 270, 26257–26264. doi: 10.1074/jbc.270.44.26257

Hill, J. E., and Hemmingsen, S. M. (2001). *Arabidopsis thaliana* type I and II chaperonins. *Cell Stress Chaperones* 6, 190–200. doi: 10.1379/1466-1268(2001)006<0190:ATTIAI>2.0.CO;2

Hirohashi, T., Nishio, K., and Nakai, M. (1999). cDNA sequence and overexpression of chloroplast chaperonin 21 from *Arabidopsis thaliana*. *Biochim. Biophys. Acta* 1429, 512–515. doi: 10.1016/S0167-4838(98)00268-4

Horowitz, S., Koldewey, P., Stull, F., and Bardwell, J. C. (2017). Folding while bound to chaperones. *Curr. Opin. Struct. Biol.* 48, 1–5. doi: 10.1016/j.sbi.2017.06.009

Horst, R., Bertelsen, E. B., Fiaux, J., Wider, G., Horwich, A. L., and Wuthrich, K. (2005). Direct NMR observation of a substrate protein bound to the chaperonin GroEL. *Proc. Natl. Acad. Sci. U.S.A.* 102, 12748–12753. doi: 10.1073/pnas.0505642102

Horwich, A. L. (2013). Chaperonin-mediated protein folding. *J. Biol. Chem.* 288, 23622–23632. doi: 10.1074/jbc.X113.497321

Horwich, A. L., Fenton, W. A., Chapman, E., and Farr, G. W. (2007). Two families of chaperonin: physiology and mechanism. *Annu. Rev. Cell Dev. Biol.* 23, 115–145. doi: 10.1146/annurev.cellbio.23.090506.123555

Hunt, J. F., Weaver, A. J., Landry, S. J., Gierasch, L., and Deisenhofer, J. (1996). The crystal structure of the GroES co-chaperonin at 2.8 A resolution. *Nature* 379, 37–45. doi: 10.1038/379037a0

Ishikawa, A., Tanaka, H., Nakai, M., and Asahi, T. (2003). Deletion of a chaperonin 60 beta gene leads to cell death in the Arabidopsis lesion initiation 1 mutant. *Plant Cell Physiol.* 44, 255–261. doi: 10.1093/pcp/pcg031

Jiang, Q., Mei, J., Gong, X. D., Xu, J. L., Zhang, J. H., Teng, S., et al. (2014). Importance of the rice TCD9 encoding alpha subunit of chaperonin protein 60 (Cpn60alpha) for the chloroplast development during the early leaf stage. *Plant Sci.* 215–216, 172–179. doi: 10.1016/j.plantsci.2013.11.003

Ke, X., Zou, W., Ren, Y., Wang, Z., Li, J., Wu, X., et al. (2017). Functional divergence of chloroplast Cpn60alpha subunits during Arabidopsis embryo development. *PLoS Genet.* 13:e1007036. doi: 10.1371/journal.pgen.1007036

Kim, S. R., Yang, J. I., and An, G. (2013a). OsCpn60alpha1, encoding the plastid chaperonin 60alpha subunit, is essential for folding of rbcL. *Mol. Cells* 35, 402–409. doi: 10.1007/s10059-013-2337-2

Kim, Y. E., Hipp, M. S., Bracher, A., Hayer-Hartl, M., and Hartl, F. U. (2013b). Molecular chaperone functions in protein folding and proteostasis. *Annu. Rev. Biochem.* 82, 323–355. doi: 10.1146/annurev-biochem-060208-092442

Koike-Takeshita, A., Arakawa, T., Taguchi, H., and Shimamura, T. (2014). Crystal structure of a symmetric football-shaped GroEL:GroES2-ATP14 complex determined at 3.8A reveals rearrangement between two GroEL rings. *J. Mol. Biol.* 426, 3634–3641. doi: 10.1016/j.jmb.2014.08.017

Kolesinski, P., Golik, P., Grudnik, P., Piechota, J., Markiewicz, M., Tarnawski, M., et al. (2013). Insights into eukaryotic Rubisco assembly - crystal structures of RbcX chaperones from *Arabidopsis thaliana*. *Biochim. Biophys. Acta* 1830, 2899–2906. doi: 10.1016/j.bbagen.2012.12.025

Koumoto, Y., Shimada, T., Kondo, M., Takao, T., Shimonishi, Y., Hara-Nishimura, I., et al. (1999). Chloroplast Cpn20 forms a tetrameric structure in *Arabidopsis thaliana*. *Plant J.* 17, 467–477. doi: 10.1046/j.1365-313X.1999.00388.x

Kumar, C. M., Mande, S. C., and Mahajan, G. (2015). Multiple chaperonins in bacteria–novel functions and non-canonical behaviors. *Cell Stress Chaperones* 20, 555–574. doi: 10.1007/s12192-015-0598-8

Kuo, W. Y., Huang, C. H., and Jinn, T. L. (2013a). Chaperonin 20 might be an iron chaperone for superoxide dismutase in activating iron superoxide dismutase (FeSOD). *Plant Signal. Behav.* 8:e23074. doi: 10.4161/psb.23074

Kuo, W. Y., Huang, C. H., Liu, A. C., Cheng, C. P., Li, S. H., Chang, W. C., et al. (2013b). CHAPERONIN 20 mediates iron superoxide dismutase (FeSOD) activity independent of its co-chaperonin role in Arabidopsis chloroplasts. *New Phytol.* 197, 99–110. doi: 10.1111/j.1469-8137.2012.04369.x

Li, L. A., and Tabita, F. R. (1997). Maximum activity of recombinant ribulose 1,5-bisphosphate carboxylase/oxygenase of Anabaena sp. strain CA requires the product of the rbcX gene. *J. Bacteriol.* 179, 3793–3796. doi: 10.1128/jb.179.11.3793-3796.1997

Lin, Z., Madan, D., and Rye, H. S. (2008). GroEL stimulates protein folding through forced unfolding. *Nat. Struct. Mol. Biol.* 15, 303–311. doi: 10.1038/nsmb.1394

Liu, C., Young, A. L., Starling-Windhof, A., Bracher, A., Saschenbrecker, S., Rao, B. V., et al. (2010). Coupled chaperone action in folding and assembly of hexadecameric Rubisco. *Nature* 463, 197–202. doi: 10.1038/nature08651

Llorca, O., Marco, S., Carrascosa, J. L., and Valpuesta, J. M. (1994). The formation of symmetrical GroEL-GroES complexes in the presence of ATP. *FEBS Lett.* 345, 181–186. doi: 10.1016/0014-5793(94)00432-3

Lopez, T., Dalton, K., and Frydman, J. (2015). The Mechanism and Function of Group II Chaperonins. *J. Mol. Biol.* 427, 2919–2930. doi: 10.1016/j.jmb.2015.04.013

Mao, J., Chi, W., Ouyang, M., He, B., Chen, F., and Zhang, L. (2015). PAB is an assembly chaperone that functions downstream of chaperonin 60 in the assembly of chloroplast ATP synthase coupling factor 1. *Proc. Natl. Acad. Sci. U.S.A.* 112, 4152–4157. doi: 10.1073/pnas.1413392111

Musgrove, J. E., Johnson, R. A., and Ellis, R. J. (1987). Dissociation of the ribulosebisphosphate-carboxylase large-subunit binding protein into dissimilar subunits. *Eur. J. Biochem.* 163, 529–534. doi: 10.1111/j.1432-1033.1987.tb10900.x

Nisemblat, S., Yaniv, O., Parnas, A., Frolow, F., and Azem, A. (2015). Crystal structure of the human mitochondrial chaperonin symmetrical football complex. *Proc. Natl. Acad. Sci. U.S.A.* 112, 6044–6049. doi: 10.1073/pnas.1411718112

Nishio, K., Hirohashi, T., and Nakai, M. (1999). Chloroplast chaperonins: evidence for heterogeneous assembly of alpha and beta Cpn60 polypeptides into a chaperonin oligomer. *Biochem. Biophys. Res. Commun.* 266, 584–587. doi: 10.1006/bbrc.1999.1868

Onizuka, T., Endo, S., Akiyama, H., Kanai, S., Hirano, M., Yokota, A., et al. (2004). The rbcX gene product promotes the production and assembly of ribulose-1,5-bisphosphate carboxylase/oxygenase of Synechococcus sp. PCC7002 in *Escherichia coli*. *Plant Cell Physiol.* 45, 1390–1395. doi: 10.1093/pcp/pch160

Peltier, J. B., Cai, Y., Sun, Q., Zabrouskov, V., Giacomelli, L., Rudella, A., et al. (2006). The oligomeric stromal proteome of *Arabidopsis thaliana* chloroplasts. *Mol. Cell. Proteomics* 5, 114–133. doi: 10.1074/mcp.M500180-MCP200

Peng, L., Fukao, Y., Myouga, F., Motohashi, R., Shinozaki, K., and Shikanai, T. (2011). A chaperonin subunit with unique structures is essential for folding of a specific substrate. *PLoS Biol.* 9:e1001040. doi: 10.1371/journal.pbio.1001040

Pettersen, E. F., Goddard, T. D., Huang, C. C., Couch, G. S., Greenblatt, D. M., Meng, E. C., et al. (2004). UCSF Chimera–a visualization system for exploratory research and analysis. *J. Comput. Chem.* 25, 1605–1612. doi: 10.1002/jcc.20084

Powers, E. T., Morimoto, R. I., Dillin, A., Kelly, J. W., and Balch, W. E. (2009). Biological and chemical approaches to diseases of proteostasis deficiency. *Annu. Rev. Biochem.* 78, 959–991. doi: 10.1146/annurev.biochem.052308.114844

Ranson, N. A., Clare, D. K., Farr, G. W., Houldershaw, D., Horwich, A. L., and Saibil, H. R. (2006). Allosteric signaling of ATP hydrolysis in GroEL-GroES complexes. *Nat. Struct. Mol. Biol.* 13, 147–152. doi: 10.1038/nsmb1046

Saibil, H. (2013). Chaperone machines for protein folding, unfolding and disaggregation. *Nat. Rev. Mol. Cell Biol.* 14, 630–642. doi: 10.1038/nrm3658

Sameshima, T., Iizuka, R., Ueno, T., and Funatsu, T. (2010). Denatured proteins facilitate the formation of the football-shaped GroEL-(GroES)2 complex. *Biochem. J.* 427, 247–254. doi: 10.1042/BJ20091845

Sameshima, T., Ueno, T., Iizuka, R., Ishii, N., Terada, N., Okabe, K., et al. (2008). Football- and bullet-shaped GroEL-GroES complexes coexist during the reaction cycle. *J. Biol. Chem.* 283, 23765–23773. doi: 10.1074/jbc.M802541200

Saschenbrecker, S., Bracher, A., Rao, K. V., Rao, B. V., Hartl, F. U., and Hayer-Hartl, M. (2007). Structure and function of RbcX, an assembly chaperone for hexadecameric Rubisco. *Cell* 129, 1189–1200. doi: 10.1016/j.cell.2007.04.025

Schlicher, T., and Soll, J. (1996). Molecular chaperones are present in the thylakoid lumen of pea chloroplasts. *FEBS Lett.* 379, 302–304. doi: 10.1016/0014-5793(95)01534-5

Schroda, M. (2004). The Chlamydomonas genome reveals its secrets: chaperone genes and the potential roles of their gene products in the chloroplast. *Photosyn. Res.* 82, 221–240. doi: 10.1007/s11120-004-2216-y

Sharma, S., Chakraborty, K., Muller, B. K., Astola, N., Tang, Y. C., Lamb, D. C., et al. (2008). Monitoring protein conformation along the pathway of chaperonin-assisted folding. *Cell* 133, 142–153. doi: 10.1016/j.cell.2008.01.048

Sigler, P. B., Xu, Z., Rye, H. S., Burston, S. G., Fenton, W. A., and Horwich, A. L. (1998). Structure and function in GroEL-mediated protein folding. *Annu. Rev. Biochem.* 67, 581–608. doi: 10.1146/annurev.biochem.67.1.581

Suss, O., and Reichmann, D. (2015). Protein plasticity underlines activation and function of ATP-independent chaperones. *Front. Mol. Biosci.* 2:43. doi: 10.3389/fmolb.2015.00043

Suzuki, K., Nakanishi, H., Bower, J., Yoder, D. W., Osteryoung, K. W., and Miyagishima, S. Y. (2009). Plastid chaperonin proteins Cpn60 alpha and Cpn60 beta are required for plastid division in *Arabidopsis thaliana*. *BMC Plant Biol.* 9:38. doi: 10.1186/1471-2229-9-38

Tarnawski, M., Krzywda, S., Bialek, W., Jaskolski, M., and Szczepaniak, A. (2011). Structure of the RuBisCO chaperone RbcX from the thermophilic cyanobacterium *Thermosynechococcus elongatus*. *Acta Crystallogr. Sect. F Struct. Biol. Cryst. Commun.* 67, 851–857. doi: 10.1107/S1744309111018860

Thirumalai, D., and Lorimer, G. H. (2001). Chaperonin-mediated protein folding. *Annu. Rev. Biophys. Biomol. Struct.* 30, 245–269. doi: 10.1146/annurev.biophys.30.1.245

Thompson, M. D., Paavola, C. D., Lenvik, T. R., and Gantt, J. S. (1995). Chlamydomonas transcripts encoding three divergent plastid chaperonins are heat-inducible. *Plant Mol. Biol.* 27, 1031–1035. doi: 10.1007/BF00037029

Trösch, R., Mühlhaus, T., Schroda, M., and Willmund, F. (2015). ATP-dependent molecular chaperones in plastids–More complex than expected. *Biochim. Biophys. Acta* 1847, 872–888. doi: 10.1016/j.bbabio.2015.01.002

Tsai, Y. C., Mueller-Cajar, O., Saschenbrecker, S., Hartl, F. U., and Hayer-Hartl, M. (2012). Chaperonin cofactors, Cpn10 and Cpn20, of green algae and plants function as hetero-oligomeric ring complexes. *J. Biol. Chem.* 287, 20471–20481. doi: 10.1074/jbc.M112.365411

Vitlin, A., Weiss, C., Demishtein-Zohary, K., Rasouly, A., Levin, D., Pisanty-Farchi, O., et al. (2011). Chloroplast beta chaperonins from A. thaliana function with endogenous cpn10 homologs *in vitro*. *Plant Mol. Biol.* 77, 105–115. doi: 10.1007/s11103-011-9797-6

Vitlin Gruber, A., Nisemblat, S., Azem, A., and Weiss, C. (2013a). The complexity of chloroplast chaperonins. *Trends Plant Sci.* 18, 688–694. doi: 10.1016/j.tplants.2013.08.001

Vitlin Gruber, A., Nisemblat, S., Zizelski, G., Parnas, A., Dzikowski, R., Azem, A., et al. (2013b). *P. falciparum* cpn20 is a bona fide co-chaperonin that can replace GroES in *E. coli*. *PLoS ONE* 8:e53909. doi: 10.1371/journal.pone.0053909

Vitlin Gruber, A., Zizelski, G., Azem, A., and Weiss, C. (2014). The Cpn10(1) co-chaperonin of *A. thaliana* functions only as a hetero-oligomer with Cpn20. *PLoS ONE* 9:e113835. doi: 10.1371/journal.pone.0113835

Weiss, C., Bonshtien, A., Farchi-Pisanty, O., Vitlin, A., and Azem, A. (2009). Cpn20: siamese twins of the chaperonin world. *Plant Mol. Biol.* 69, 227–238. doi: 10.1007/s11103-008-9432-3

Whitney, S. M., Birch, R., Kelso, C., Beck, J. L., and Kapralov, M. V. (2015). Improving recombinant Rubisco biogenesis, plant photosynthesis and growth by coexpressing its ancillary RAF1 chaperone. *Proc. Natl. Acad. Sci. U.S.A.* 112, 3564–3569. doi: 10.1073/pnas.1420536112

Xu, Z., Horwich, A. L., and Sigler, P. B. (1997). The crystal structure of the asymmetric GroEL-GroES-(ADP)7 chaperonin complex. *Nature* 388, 741–750. doi: 10.1038/41944

Yébenes, H., Mesa, P., Munoz, I. G., Montoya, G., and Valpuesta, J. M. (2011). Chaperonins: two rings for folding. *Trends Biochem. Sci.* 36, 424–432. doi: 10.1016/j.tibs.2011.05.003

Zhang, S., Zhou, H., Yu, F., Bai, C., Zhao, Q., He, J., et al. (2016a). Structural insight into the cooperation of chloroplast chaperonin subunits. *BMC Biol.* 14:29. doi: 10.1186/s12915-016-0251-8

Zhang, S., Zhou, H., Yu, F., Gao, F., He, J., and Liu, C. (2016b). Functional partition of Cpn60alpha and Cpn60beta subunits in substrate recognition and cooperation with co-chaperonins. *Mol. Plant* 9, 1210–1213. doi: 10.1016/j.molp.2016.04.019

Zhang, X. F., Jiang, T., Wu, Z., Du, S. Y., Yu, Y. T., Jiang, S. C., et al. (2013). Cochaperonin CPN20 negatively regulates abscisic acid signaling in Arabidopsis. *Plant Mol. Biol.* 83, 205–218. doi: 10.1007/s11103-013-0082-8

Zhang, X., Jiang, T., Yu, Y., Wu, Z., Jiang, S., Lu, K., et al. (2014). Arabidopsis co-chaperonin CPN20 antagonizes Mg-chelatase H subunit to derepress ABA-responsive WRKY40 transcription repressor. *Sci. China Life Sci.* 57, 11–21. doi: 10.1007/s11427-013-4587-9

Conflict of Interest Statement: The authors declare that the research was conducted in the absence of any commercial or financial relationships that could be construed as a potential conflict of interest.

The reviewer CW and handling Editor declared their shared affiliation.

frontiers in Molecular Biosciences

REVIEW
published: 13 March 2018
doi: 10.3389/fmolb.2018.00024

Rubisco Assembly in the Chloroplast

Anna Vitlin Gruber[1*†] *and Leila Feiz*[2*†]

[1] *Department of Molecular, Cell and Developmental Biology, University of California, Los Angeles, Los Angeles, CA, United States,* [2] *Boyce Thompson Institute, Cornell University, Ithaca, NY, United States*

Ribulose-1,5-bisphosphate carboxylase/oxygenase (Rubisco) catalyzes the rate-limiting step in the Calvin-Benson cycle, which transforms atmospheric carbon into a biologically useful carbon source. The slow catalytic rate of Rubisco and low substrate specificity necessitate the production of high levels of this enzyme. In order to engineer a more efficient plant Rubisco, we need to better understand its folding and assembly process. Form I Rubisco, found in green algae and vascular plants, is a hexadecamer composed of 8 large subunits (RbcL), encoded by the chloroplast genome and 8 small, nuclear-encoded subunits (RbcS). Unlike its cyanobacterial homolog, which can be reconstituted *in vitro* or in *E. coli*, assisted by bacterial chaperonins (GroEL-GroES) and the RbcX chaperone, biogenesis of functional chloroplast Rubisco requires Cpn60-Cpn20, the chloroplast homologs of GroEL-GroES, and additional auxiliary factors, including Rubisco accumulation factor 1 (Raf1), Rubisco accumulation factor 2 (Raf2) and Bundle sheath defective 2 (Bsd2). The discovery and characterization of these factors paved the way for *Arabidopsis* Rubisco assembly in *E. coli*. In the present review, we discuss the uniqueness of hetero-oligomeric chaperonin complex for RbcL folding, as well as the sequential or concurrent actions of the post-chaperonin chaperones in holoenzyme assembly. The exact stages at which each assembly factor functions are yet to be determined. Expression of *Arabidopsis* Rubisco in *E. coli* provided some insight regarding the potential roles for Raf1 and RbcX in facilitating RbcL oligomerization, for Bsd2 in stabilizing the oligomeric core prior to holoenzyme assembly, and for Raf2 in interacting with both RbcL and RbcS. In the long term, functional characterization of each known factor along with the potential discovery and characterization of additional factors will set the stage for designing more efficient plants, with a greater biomass, for use in biofuels and sustenance.

Keywords: Rubisco, folding, assembly, chaperone, chaperonin, chloroplast

OPEN ACCESS

Edited by:
Adina Breiman,
Tel Aviv University, Israel

Reviewed by:
Eilika Weber-Ban,
ETH Zurich, Switzerland
Cuimin Liu,
Institute of Genetics and Developmental Biology (CAS), China

***Correspondence:**
Anna Vitlin Gruber
annavitlin@gmail.com
Leila Feiz
lf259@cornell.edu

[†]*Co-first author.*

Specialty section:
This article was submitted to Protein Folding, Misfolding and Degradation, a section of the journal Frontiers in Molecular Biosciences

Received: *22 November 2017*
Accepted: *27 February 2018*
Published: *13 March 2018*

Citation:
Vitlin Gruber A and Feiz L (2018) Rubisco Assembly in the Chloroplast. Front. Mol. Biosci. 5:24. doi: 10.3389/fmolb.2018.00024

INTRODUCTION

Ribulose-1,5-bisphosphate carboxylase/oxygenase (Rubisco) is Earth's most abundant enzyme, used by autotrophic organisms to convert CO_2 into organic compounds via the Calvin-Benson pathway (Andersson and Backlund, 2008). Rubisco catalyzes photosynthetic carbon reduction and photorespiratory carbon oxidation upon reaction with its substrates riboluse-1,5-bisphosphate, and CO_2 or O_2, respectively. The poor catalytic properties of Rubisco CO_2 fixation necessitate a high abundance of this enzyme. Hence, Rubisco constitutes ~30–50% of the soluble protein in C_3 plant leaves (Feller et al., 2008; Phillips and Milo, 2009). This enormous investment of energy, water and nitrogen limits biomass and crop yields.

Since all biomass results from the act of Rubisco in photosynthesis, increasing crop yields ultimately depends on improving the efficiency of carbon fixation. Although the catalytic performance of bacterial and archaeal Rubisco was successfully enhanced (Durão et al., 2015; Wilson et al., 2016), efforts to engineer a more catalytically efficient plant Rubisco remain unsuccessful (Parry et al., 2013). Consequently, not only has Rubisco become an intriguing model for studying protein folding and assembly, but also, elucidating the process of its biogenesis should allow researchers to improve its efficiency.

In order to engineer plant Rubisco or transplant a more productive version into hosts of agricultural or biotechnological interest, this protein should be viewed as a multi enzyme complex, in which all the parts work together and cannot be excluded (John Andrews and Whitney, 2003; Erb and Zarzycki, 2018). This review focuses on what is known about the folding and assembly of plant Rubisco. The chloroplast system supporting Rubisco biogenesis is unique in its complexity, and only the precise orchestration of folding and assembly leads to functional protein.

RUBISCO: AN EVOLUTIONARY PERSPECTIVE

Why is Rubisco so inefficient? Rubisco evolved before the oxygenation of the atmosphere, conditions under which there was no need to discriminate between O_2 and CO_2. In addition to the carboxylation, Rubisco catalyzes a non-productive oxygenation reaction that results in the formation of 2-phosphoglycolate (2PG). 2PG being a toxic compound, is recycled in plants in an energy-wasteful process called photorespiration (Zhu et al., 2010; Walker et al., 2016). The rise of atmospheric O_2 concentration resulted in an increased error rate and forced Rubisco to lower its catalytic rate, reaching the Pareto optimality of enzyme activity and specificity (Tcherkez et al., 2006; Savir et al., 2010; Studer et al., 2014; Tawfik, 2014; Shih et al., 2016). The evolutionary adaptations eventually led to the formation of what is known as the "Rubiscosome"—a multifaceted complex of proteins which support Rubisco formation and function (Erb and Zarzycki, 2018). During this process, Rubisco evolved to form complex oligomeric structures and to collaborate with specific chaperones and activases.

Proteins belonging to the Rubisco family can be classified into 3 forms. The most ancient form III Rubisco, which is found in archaea, catalyzes regeneration of Ribulose-1,5-bisphosphate (RuBP), produced during nucleotide metabolism (Tabita et al., 2008a,b). In contrast, forms II and I evolved to catalyze RuBP carboxylation or oxygenation in an autotrophic, photosynthetic context. Form II Rubiscos are present in bacteria and dinoflagellates, while form I exists in plants, algae, cyanobacteria and proteobacteria (Andersson and Backlund, 2008). Form I Rubiscos are classified into red-type (in photosynthetic bacteria and non-green algae) and green-type (in proteobacteria, cyanobacteria, green algae and land plants) (Tabita, 1999; Badger and Bek, 2008; Tabita et al., 2008b). The green-type Rubiscos are further classified as forms IA and IB (Bracher et al., 2017). A phylogenetic tree of green-type Rubisco large subunits from various organisms mentioned in this review is presented in **Figure 1**, together with the factors participating in the assembly process.

The common feature of all Rubiscos is the formation of the active site at the interface between L_2 - two Rubisco large subunits (RbcL, 50–55 kDa). Form II and III Rubiscos have $(L_2)_n$ stoichiometry (with n up to 5) while form I Rubisco is organized in four L_2 dimers that assemble together with eight small subunits (RbcS, 12–18 kDa) to form a hetero-hexadecameric complex—L_8S_8. Rubiscos structure and function is extensively reviewed in Andersson and Backlund (2008) and Bracher et al. (2017). This higher-order oligomerization and presence of small subunits allowed for an increase in catalytic efficiency and substrate specificity. The increase in specificity for CO_2 over O_2 made Rubisco more vulnerable to inhibition by naturally occurring sugar phosphates, including RuBP (Mueller-Cajar, 2017). Evolutionary compensation took place in the form of Rubisco activases, which evolved to overcome this obstacle

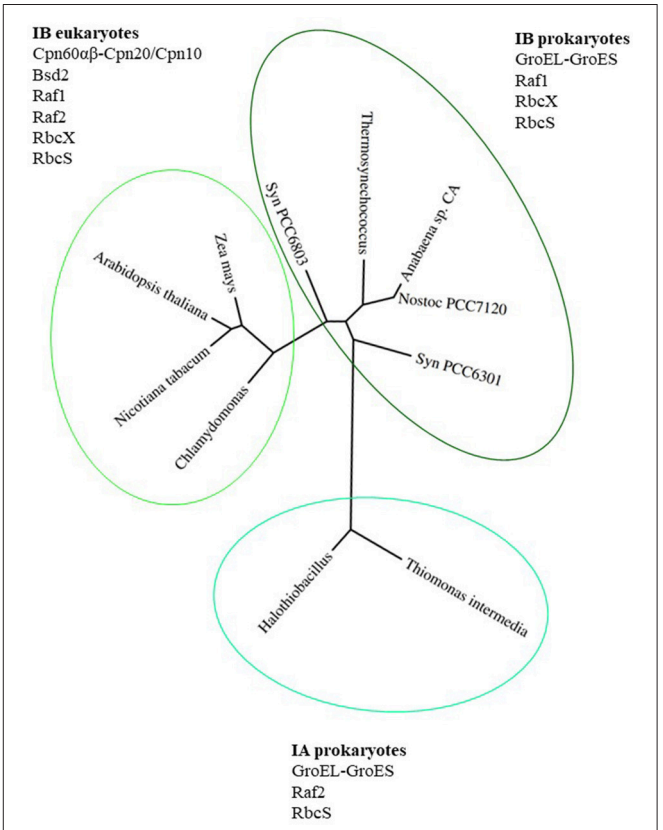

FIGURE 1 | Phylogenetic tree of green-type RbcL subunits together with factors involved in Rubisco holoenzyme formation. Phylogenetic tree of RbcL sequences represents organisms mentioned in this review. The variety of folding and assembly factors and their involvement in Rubisco biogenesis are shown for each clade and discussed in the text. Species full names: *Thiomonas intermedia K 12, Halothiobacillus neapolitanus, Synechococcus PCC6301, Nostoc* sp. *PCC7120, Anabaena* sp. CA, *Thermosynechococcus elongatus, Synechocystis PCC 6803, Chlamydomonas reinhardtii, Arabidopsis thaliana, Zea mays, Nicotiana tabacum*. The phylogenetic tree was created using phylogeny.fr (http://www.phylogeny.fr; Dereeper et al., 2008, 2010).

by releasing the inhibitory sugars (Salvucci et al., 1987; Mueller-Cajar et al., 2011; Tsai et al., 2015; Loganathan et al., 2016).

Form II Rubisco, which is composed only of two large subunits, can undergo spontaneous assembly in *E. coli* or *in vitro* without the assistance of GroEL and GroES (Goloubinoff et al., 1989a). Co-expression of the Rubisco subunits from *Rhodospirillum rubrum* along with GroEL-GroES in *E. coli*, however, significantly increased the assembly yield, suggesting that the folding machinery was a rate limiting factor (Goloubinoff et al., 1989b). In contrast, reconstitution of the cyanobacterial form I Rubisco from *Synechococcus PCC6301* (*Syn 6301*) with the assistance of GroEL-GroES chaperonins, yielded only small amount of holoenzyme until the assembly chaperone, RbcX was added, following RbcL folding (Liu et al., 2010).

Similar to their endosymbiont cyanobacterial ancestor, chloroplasts contain a form I Rubisco. Nevertheless, assembly of the chloroplast Rubisco has emerged as one of the most complicated assembly processes that is known for oligomeric proteins. Spontaneous assembly of the eight small and eight large subunits of form I Rubisco from any plant by random collision proved inefficient, both in *E. coli* and in a test tube, regardless of chaperonins and RbcX presence (Feiz et al., 2012; Hauser et al., 2015a, reviewed in Bracher et al., 2017). Bundle sheath defective 2 (Bsd2) was the first Rubisco specific factor that was shown to have an indispensable role in plant Rubisco assembly (Brutnell et al., 1999). Recently, forward genetics was used to identify two novel factors involved in plastid Rubisco biogenesis, Rubisco accumulation factor 1 (Raf1) (Feiz et al., 2012) and Rubisco accumulation factor 2 (Raf2) (Feiz et al., 2014). Structural and molecular characterization of these factors paved the road to elucidation of their role in Rubisco assembly, resulting in a successful expression of plant Rubisco holoenzyme in *E. coli* (Aigner et al., 2017). In the following chapters each factor will be described and its role in Rubisco biogenesis will be discussed.

CHLOROPLAST CHAPERONINS

In eukaryotes, Rubisco large subunit is universally encoded by the chloroplast genome. The small subunits are encoded in the nucleus in plants and green algae and in the chloroplast genome in non-green algae (Tabita, 1999). Once transcribed and translated, the small subunit is imported into the chloroplast and folded to its functional form (Dobberstein et al., 1977; Highfield and Ellis, 1978). The large subunit is transcribed in the chloroplast, but to keep up a tight stoichiometry with its nucleus-encoded partner, its translation undergoes an assembly-dependent autoregulation (Wostrikoff and Stern, 2007).

One of the early post-translational chaperones in the process of Rubisco holoenzyme folding and assembly is the chloroplast chaperonin machinery. Chaperonins were initially discovered as a high-molecular-weight complex associated with RbcL, following its synthesis in isolated intact chloroplasts, prior to formation of holoenzyme (Barraclough and Ellis, 1980; Roy et al., 1982; Roy, 1989; Ellis, 1990). Early studies demonstrated that the protein was an oligomer composed of two subunit types, which reversibly dissociated into monomers in the presence of ATP, and was homologous to certain bacterial proteins that were crucial for phage morphogenesis (Hemmingsen et al., 1988). The general concept of a chaperone protein was born from these discoveries, and most research in the field focused on the extremely stable *E. coli* chaperonin system (GroEL-GroES).

Chloroplast homologs together with bacterial and mitochondrial chaperonins belong to the type I category. The type I chaperonin system consists of 2 oligomeric partners, working together to bind and fold partially denatured proteins. In *E. coli*, the binding partner is a tetradecamer of 60 kDa Cpn60 subunits (GroEL) while the co-chaperonin partner is a heptamer of 10 kDa Cpn10 subunits (GroES).

Though chloroplast chaperonins diverge from the bacterial system in several aspects, the most intriguing is the broad array of subunit types and the complexity of their oligomeric arrangements. Two GroEL-like subtypes are found in chloroplast, Cpn60α and Cpn60β, that can form homo- or hetero-oligomeric chaperonin species (Musgrove et al., 1987; Martel et al., 1990; Nishio et al., 1999). These subtypes are ∼50% homologous to each other as well as to GroEL. Several paralogous forms of each type can be found in most plants (Hill and Hemmingsen, 2001; Schroda, 2004; Friso et al., 2010; Trösch et al., 2015). Similarly, chloroplasts harbor two types of co-chaperonin homologs. The first is a typical, GroES-like Cpn10, while the second gene is unique to chloroplast and consists of two Cpn10-like sequences joined head-to-tail with molecular weight of 20–23 kDa (Cpn20) (Bertsch et al., 1992). Similar to the 60 kDa partner, each chloroplast co-chaperonin also exists in several paralogous forms (Hill and Hemmingsen, 2001; Tsai et al., 2012). The entire cohort of Rubisco folding and assembly factors from *Arabidopsis thaliana* (*At—Arabidopsis*), *Zea mays* (*Zm—*maize), and *Chlamydomonas reinhardtii* (*Cr—Chlamydomonas*) are summarized in **Table 1**.

Two oligomeric forms of Cpn60 were reconstituted *in vitro* from purified Cpn60α and Cpn60β monomers of several species (Dickson et al., 2000; Vitlin et al., 2011; Tsai et al., 2012; Bai et al., 2015) and were shown to form oligomers when expressed in *E. coli* (Cloney et al., 1992a,b; Bai et al., 2015). The reconstituted oligomers included the αβ hetero-oligomers, consisting of an approximate 1:1 ratio of α:β (Tsai et al., 2012) and all β homo-oligomers (Dickson et al., 2000; Vitlin et al., 2011; Bai et al., 2015). The αβ hetero-oligomers were further demonstrated to contain complicated mixtures of α and β paralogs (Peng et al., 2011; Bai et al., 2015; Ke et al., 2017).

By way of contrast, Cpn60α subunits expressed alone in *E. coli*, were not capable of assembling into a tetradecamer, nor were they able to form functional oligomers *in vitro* (Cloney et al., 1992a,b; Dickson et al., 2000; Bai et al., 2015). Domain swapping analysis in *Chlamydomonas* chaperonins demonstrated that equatorial domain controls the Cpn60α monomeric state. ATP hydrolysis drives allosteric rearrangement and promotes oligomer disassembly through Cpn60β C-terminal fragment, and cooperation from both subunits is needed to form active hetero-oligomers (Zhang et al., 2016a). Furthermore, functional divergence between the three *Chlamydomonas* subunits was attributed to both the apical and the equatorial domains, with both types of subunits evolved to have substrate specificity as

TABLE 1 | Paralogs of Rubisco folding and assembly chaperones*.

Subunit	MW (kDa)	*Arabidopsis*	Maize	*Chlamydomonas*
RbcL	50–55	**AtCg00490**	GRMZM2G448344	CreCp.g007100
RbcS	12–18	**At5g38410** At1g67090 At5g38420 At5g38430	GRMZM2G113033 GRMZM2G098520	Cre02.g120150 Cre02.g120100
Cpn60α	~60	**At2g28000(α1)**	AC215201.3 GRMZM2G434173	Cre04.g231222
		At5g18820(α2)	GRMZM2G321767	Cre06.g309100
Cpn60β	~60	**At1g55490(β1)** At3g13470(β2)	GRMZM2G083716	Cre07.g339150
		At5g56500(β3)	GRMZM2G015989	Cre17.g741450
		At1g26230(β4)	GRMZM2G042253	
Cpn10	~10	At2g44650(1) At3g60210(2)	GRMZM2G050961 GRMZM2G035063 GRMZM2G013652	Cre16.g673729
Cpn20	20–23	**At5g20720**	GRMZM2G091189 GRMZM2G127609 GRMZM2G399284	Cre08.g358562 Cre12.g505850
RbcX	~15	At4g04330(1)	GRMZM2G115476 NM_001149531	Cre07.g339000 Cre01.g030350
		At5g19855(2)		
Raf1	40–46	At5g28500(1) **At3g04550(2)**	GRMZM2G457621	Cre06.g308450
Raf2	~18	**At5g51110**	GRMZM2G139123	Cre01.g049000
Bsd2	~8	**At3g47650**	GRMZM2G062788	Cre06.g251716

Highlighted in bold are the subunits supporting Arabidopsis Rubisco expression and assembly in E. coli (Aigner et al., 2017).

well as co-chaperonin preference (Zhang et al., 2016b). Overall, Cpn60 complex formation from protomers *in vitro* depends critically on the presence of Mg-ATP, subunit concentration, temperature and Cpn60β protomer presence, suggesting that Cpn60β subunits likely initiate the oligomerization (Bloom et al., 1983; Lissin, 1995; Viitanen et al., 1998; Dickson et al., 2000; Bonshtien et al., 2009; Bai et al., 2015; Vitlin Gruber et al., 2018).

Significant heterogeneity was demonstrated for co-chaperonins as well. Cpn20 proteins from various organisms were shown to form tetrameric ring-like structures *in vitro* (Bertsch et al., 1992; Baneyx et al., 1995; Viitanen et al., 1995; Koumoto et al., 1999; Bonshtien et al., 2007; Tsai et al., 2012; Vitlin Gruber et al., 2013b, 2014; Bai et al., 2015). It was also demonstrated that *Arabidopsis* Cpn10(1) (At2g44650) organized into a ring of seven 10-kDa subunits, similar to GroES (Koumoto et al., 2001; Sharkia et al., 2003). In contrast, *Chlamydomonas* Cpn10 and Cpn23 proteins were purified as monomers (Tsai et al., 2012), and the third co-chaperonin from *Arabidopsis* Cpn10(2) (At3g60210), was purified as inactive, low molecular weight species (monomers or dimers) (Vitlin Gruber et al., 2014). Upon mixing Cpn10 with Cpn20 subunits, different active hetero-oligomeric species are produced *in vitro*. Interestingly, co-chaperonin subunits that are unable to support chaperonin function on their own, contributed to activity when incorporated into hetero-oligomer (Tsai et al., 2012; Vitlin Gruber et al., 2014; Guo et al., 2015). Even more interesting was the fact that co-chaperonins designed to contain either 6, 7, or 8 domains were fully functional with GroEL and Cpn60 oligomers, indicating that a symmetrical match is not stringently required for chaperonin function in general (Guo et al., 2015), though each co-chaperonin paralog might be crucial for folding of specific substrate. The latest progress in chloroplast chaperonin field is reviewed in Zhao and Liu (2018).

CHAPERONIN SUBUNIT SPECIFICITY AND RBCL FOLDING

The ability of Cpn60 and Cpn10 subunits to oligomerize in different combinations imply on a tremendous number of potential combinatorial Cpn60-Cpn10 pairs in the chloroplast, which could allow for a large number of substrates and modes of regulation (Vitlin Gruber et al., 2013a). Considering the heterogeneity, plasticity and asymmetry of the chloroplast chaperonin system, one can imagine chaperonin machines that

are custom-made in a kind of substrate-directed organization. The importance of various subunits for folding of specific substrates is slowly being unraveled (reviewed in Vitlin Gruber et al., 2013a). Recent works in *Arabidopsis* demonstrated the specific role of Cpn60α2 (At5g18820) in folding of KASI (β-ketoacyl-[acyl carrier protein] synthase I) (Ke et al., 2017), and Cpn60β4 (At1g26230) was shown to be specifically required for the folding of NdhH, a subunit of the NADH dehydrogenase-like complex (NDH) (Peng et al., 2011).

But what do we know about chaperonin specificity for the most abundant chloroplast protein, RbcL? In maize, RbcL was found in association with a chaperonin complex composed of the two most abundant Cpn60 subunits, ZmCpn60α1 (Cps2 encoded by AC215201.3) and ZmCpn60β1 (GRMZM2G083716) (Feiz et al., 2012). Similarly, hetero-oligomer containing the most highly expressed Cpn60 subunits from *Arabidopsis* chloroplast (Cpn60α1—At2g28000 and Cpn60β1—At1g55490) efficiently folded the cognate AtRbcL subunit expressed in *E. coli*. Chaperonin activity could be facilitated by chloroplast tetrameric AtCpn20, as well as bacterial heptameric GroES, but not by chloroplast heptameric AtCpn10(1), suggesting a specificity of the later co-chaperonin in folding chloroplast substrates other than RbcL (Aigner et al., 2017). AtCpn60β1, which easily oligomerizes to form homo-tetradecamers (Cloney et al., 1992b; Vitlin et al., 2011), mediated RbcL folding in *E. coli* assisted by AtCpn20, albeit with lower efficiency in comparison to hetero-oligomer (Aigner et al., 2017). In the future it will be interesting to investigate the substrate specificity of additional chloroplast chaperonin paralogs and whether other Cpn60-Cpn10 pairs with various combination of subunits will be able to efficiently fold RbcL.

Numerous mutational analyses suggest that the Cpn60α subunit has a specific significance for the folding of RbcL. Examination of the data in the literature shows a correlation between down-regulation of specific chloroplast Cpn60α subunits and the amount of Rubisco (Vitlin Gruber et al., 2013a). It should be noted that unfolded or unassembled Rubisco cannot accumulate in plants and is completely prone to degradation, so Rubisco content in alpha mutants is not only the indicator of Rubisco synthesis, but of its folding and assembly as well. For example, the maize *cps2* mutant exhibited a pale green and seedling-lethal phenotype with 95% less Rubisco than wild type, while the level of other chloroplast proteins remained intact (Feiz et al., 2012), suggesting Rubisco specificity of this ZmCpn60α1. Mutation in the *cps2* ortholog of rice (Os12g17910), also resulted in drastically reduced levels of RbcL in a pale green seedling, without a decrease in the levels of other important proteins (Kim et al., 2013). A single amino acid substitution (D335A) at a conserved position in *Arabidopsis* ortholog Cpn60α1, caused retarded growth and pale green-leaf phenotype. Although the total levels of Cpn60α and Cpn60β were increased in this mutant, possibly due to compensation effects, the levels of RbcL were reduced (Peng et al., 2011). Recently, two new *Arabidopsis* and rice mutants carrying mutations in Cpn60αs were described. In *Arabidopsis*, mutation in Cpn60α1 (At5g18820) caused embryo development arrest at the globular stage (Ke et al., 2017). Rice thermo-sensitive chloroplast development 9 (*tcd9*) mutant grown below 24°C, had an albino phenotype at the 3-leaf stage (Jiang et al., 2014). It remains to be determined whether these Cpn60α subunits are involved in Rubisco folding.

What is the precise role of the Cpn60α subunit in RbcL folding? Structural studies in *Chlamydomonas* indicated that the Cpn60α apical domain recognizes CrRbcL with higher efficiency in comparison to Cpn60β, but it comes with the price of hindered functional co-operation of Cpn60α with different co-chaperonins (Zhang et al., 2016b). Based on these results we could hypothesize that Cpn60α evolved to specifically recognize and perhaps prioritize RbcL binding in the chloroplast, while Cpn60β maintained the responsibility for oligomerization and productive interaction with co-chaperonins. Characterization of additional chaperonin mutants will reveal the list of chaperonin subunits specifically required for Rubisco folding, as well as their specificity for other chloroplast substrates, while additional biochemical studies will help uncovering the precise mode of function of chloroplast chaperonins.

RBCX ENHANCES $RBCL_8$ ASSEMBLY BY STABILIZING FOLDED $RBCL_2$

RbcX gene was first described in cyanobacterium *Anabaena 7120* (*Nostoc* sp. *PCC7120*) (Larimer and Soper, 1993) and its role was gradually revealed in subsequent studies. RbcX is conserved from the cyanobacteria to plants (Hauser et al., 2015b). Co-expression of the RbcX genes from various cyanobacteria as well as from *C. reinhartii* or *A. thaliana*, was shown to enhance the assembly of cyanobacterial Rubisco in *E. coli* (Li and Tabita, 1997; Onizuka et al., 2004; Saschenbrecker et al., 2007; Kolesinski et al., 2011; Bracher et al., 2015), suggesting a conserved mode of function for all the homologs. Insertional inactivation of RbcX genes that were located in or outside of the Rubisco operons in two cyanobacteria strains, suggested that the RbcX protein may be essential for Rubisco biogenesis only when it is expressed from the Rubisco operon (Li and Tabita, 1997; Emlyn-Jones et al., 2006). Considering the large diversity of RbcL genes from different cyanobacterial strains, as presented in **Figure 1**, it seems that some developed dependence on RbcX assistance, while others are RbcX independent, or in need of other assembly factors.

RbcX is a homodimer of a ∼15 kDa subunits, mostly α-helical. In *Syn 6301*, each RbcX subunit binds to a motif at the C-terminus of a folded large subunit, thereby clamping together the RbcL antiparallel dimer. The term assembly chaperone was coined for RbcX because of the mechanism by which this protein mediates the oligomeric assembly. By stabilizing the RbcL dimeric core, $RbcX_2$ prevents rebinding of the labile, partially folded RbcL monomers to GroEL-GroES, and facilitate their assembly into the $RbcL_8$ core complex. Finally, RbcS binding to $RbcL_8$ triggers a conformational change that results in RbcX release and formation of the holoenzyme (Saschenbrecker et al., 2007; Liu et al., 2010). The ease by which RbcS replaces RbcX during assembly originates from the dynamic nature of the RbcX interaction with RbcL. When high affinity, heterologous RbcX (from *Anabaena* sp. CA) was co-expressed with RbcL in *E. coli*,

the RbcX could not be replaced by RbcS. This phenomenon originally facilitated determination of the RbcX-RbcL structure (Saschenbrecker et al., 2007), and led to successful reconstitution of the holoenzyme from *Syn 6301* (Liu et al., 2010).

Arabidopsis contains two RbcX genes. AtRbcX2, encoded by the At5g19855 gene is closely related to the cyanobacterial homolog, and was found in the stromal fraction, while AtRbcX1, encoded by the At4g04330 gene, is a more distant homolog and was shown to localize in the thylakoid fraction (Kolesinski et al., 2011). Both proteins were crystallized and shown to have different affinities for the RbcL C-terminus (Kolesinski et al., 2013). AtRbcX2 was one of the assembly factors that when expressed with chaperonins and other assembly chaperones in *E. coli*, resulted in the *Arabidopsis* Rubisco formation. This protein, however, was suggested to be more of an enhancer than an essential chaperone, since in its absence, around 50% of recombinant Rubisco was formed (Aigner et al., 2017). The evolutionary perspective of the RbcX gene duplication in plants and the relevance of this duplication to Rubisco biogenesis is another intriguing question. The thylakoid localization of AtRbcX1 together with its lower affinity toward RbcL (Kolesinski et al., 2013), may suggest a divergent role for this homolog. Interestingly, *Chlamydomonas* encodes only the AtRbcX1 homologs, CrRbcXA and CrRbcXB. CrRbcXA was structurally and functionally characterized and shown to support cyanobacterial Rubisco assembly (Bracher et al., 2015). In the future, characterization of RbcX mutants as well as additional biochemical studies could reveal their precise role in Rubisco assembly and the unique properties of each homolog.

RAF1 IS ESSENTIAL FOR RBCL ASSEMBLY, DOWNSTREAM OF CHAPERONIN FOLDING

Rubisco accumulation factor 1 (Raf1), the first factor characterized as an assembly chaperone involved in Rubisco biogenesis in chloroplasts (Feiz et al., 2012), was found by screening the maize Photosynthetic Mutant Library (PML), a collection of ∼2,000 photosynthetic mutants, for Rubisco-specific deficiencies (Belcher et al., 2015). The maize *raf1* mutants are pale green, unable to accumulate Rubisco and are lethal at the seedling stage. Characterization of the mutant indicated that in the absence of Raf1, newly-synthesized RbcL subunits are not assembled into the holoenzyme, but instead are trapped in an ∼800 kDa chaperonin complex (Feiz et al., 2012). Even though co-immunoprecipitation of RbcL with Raf1 indicated that Rubisco is the primary protein client of the Raf1, these experiments could not reveal a detailed mode of action of Raf1 in the chloroplast.

Functional characterization of cyanobacterial Raf1 from *Thermosynechococcus elongatus* (*Te*) indicated that it forms intermediate complexes with RbcL, resembling the RbcX role (Kolesinski et al., 2014; Hauser et al., 2015a). *In vitro* reconstitution showed that two RbcL-Raf1 complexes, $Raf1_2$-$RbcL_2$ and $Raf1_8$-$RbcL_8$, were formed in the presence of the GroEL and GroES. Similar to RbcX, Raf1 in the octameric complex was displaced by RbcS to complete the assembly of the holoenzyme (Hauser et al., 2015a). Mutational analysis of the C- and N- terminal domains of the cyanobacterial Raf1 showed that Raf1 binds to RbcL at different interaction sites than RbcX. It was also shown that unlike RbcX, the Raf1 α-domain and RbcS share overlapping binding sites on RbcL, causing the highly dynamic Raf1-RbcL interaction to allow RbcS binding (Hauser et al., 2015a). This could be the reason behind the difficulty of capturing the Raf1-RbcL intermediates in chloroplast lysate. Taking into consideration that RbcX was reported as being fully capable of assembling the cyanobacterial Rubisco (Saschenbrecker et al., 2007; Liu et al., 2010), the most plausible hypothesis for the Raf1 function in cyanobacteria is that it is redundant with RbcX in the assembly pathway. Indeed, a recent finding showed that similar to RbcX deletion in some cyanobacteria, Raf1 deletion in *Synechocystis PCC 6803* (*Syn 6803*) did not cause any growth defect (Kolesinski et al., 2017), suggesting that these factors might have overlapping functions.

Crystal structures of the N- and C-terminal domains of the *Arabidopsis* Raf1 suggested that plant Raf1 has a different structure than plant RbcX and consists of an N-terminal α-helical domain, and a C-terminal β-sheet domain connected by a flexible linker segment (Hauser et al., 2015a). In addition, plant Raf1 is essential for Rubisco assembly, while RbcX was shown to only enhance the assembly process (Aigner et al., 2017), suggesting that these chaperones might act sequentially, in parallel or in cooperation, rather than being redundant as in cyanobacteria.

A direct application of Raf1 discovery in crop improvement was implemented by taking advantage of Raf1 co-evolution with RbcL (Whitney et al., 2015). In this study transplastomic expression of AtRaf1 in the *Nicotiana tabacum* (*Nt*) host, which was deficient in native NtRbcL, but expressing a heterologous Rubisco, composed of the AtRbcL and NtRbcS, resulted in quicker production and increased levels of Rubisco, bigger plants and improved photosynthesis, relative to the same host expressing only the endogenous NtRaf1. The two-fold increase in Rubisco content in the presence of AtRaf1 was still half the level of holoenzyme in WT tobacco plants. Even though this was attributed to a five-fold lower AtRbcL transcript levels relative to the endogenous NtRbcL in the WT, it is likely that co-expression of the other cognate factors that have co-evolved with RbcL, including Raf2, Bsd2, RbcX, and chaperonin homologous, was essential for a full assembly of the heterologous Rubisco. The importance of Raf1 and RbcL co-evolution was demonstrated again, when *Arabidopsis* assembly factors were not compatible for folding recombinant NtRubisco, until Raf1 replacement with the cognate protein slightly improved the holoenzyme assembly (Aigner et al., 2017), suggesting the co-evolution of not only Raf1 but other members of the Rubiscosome, unique to each plant.

RAF2 IS ESSENTIAL FOR RUBISCO BIOGENESIS

The other Rubisco deficient mutant that was found in the maize PML was *raf2* (*rubisco accumulation factor* 2), which carries a loss of function mutation in the GRMZM2G139123 locus

encoding a chloroplast-targeted protein with an inactive pterin-4a-carbinolamine dehydratase (PCD) domain (Feiz et al., 2014). Raf2 homologs are found in vascular plants, green algae and in bacteria that accumulate form IA Rubisco in their CO_2-concentrating organelles called α-carboxysomes. Raf2 has not been found in the cyanobacterial strains that contain the plant-like form IB Rubisco, nor in red algae (Hauser et al., 2015b). Loss of Raf2 function results in a weaker phenotype than disruption of Raf1 in maize, nevertheless *raf2* is also seedling-lethal (Feiz et al., 2014). In the absence of Raf2, newly synthetized RbcL is associated with the chaperonin complex, suggesting that like Raf1, Raf2 functions at a post-chaperonin assembly stage (Feiz et al., 2014; Aigner et al., 2017).

Chemical cross-linking followed by co-immunoprecipitation showed that maize Raf2 interacts with RbcS and to a lesser extent with RbcL in the chloroplast stroma (Feiz et al., 2014). Recombinant maize Raf2 (∼18 kDa) migrates as dimers and tetramers on native gels (Feiz et al., 2014), consistent with animal PCD proteins (Hevel et al., 2008), and with the Raf2 homolog from *Thiomonas intermedia* K12, which was crystallized as a dimer (Wheatley et al., 2014). In α-carboxysome-containing bacteria, such as chemoautotrophic bacterium *Thiomonas intermedia* K 12 and *Halothiobacillus neapolitanus*, Raf2 is expressed from the Rubisco operon and does not show PCD activity. Heterologous co-expression of Raf2 from the latter strain with Rubisco, GroEL and GroES in *E. coli*, increased the amount of assembled Rubisco (Wheatley et al., 2014). AtRaf2 was one of the assembly chaperones whose presence proved essential in assembling AtRubisco in *E. coli* (Aigner et al., 2017).

The mechanism by which Raf2 plays role(s) in Rubisco biogenesis has yet to be studied in detail. It has been known that animal PCD dimers mediate dimerization of the HNFα homeodomain transcription factor, a key step in HNFα activation (Endrizzi et al., 1995; Rose et al., 2004). Structural modeling of plant Raf2 indicated the conservation of an α-helical stretch of 17 amino acids that was proposed to function in both dimerization of the PCD and its interaction with HNFα, perhaps suggesting a dimerization or oligomerization role for Raf2 in Rubisco holoenzyme assembly (Feiz et al., 2014).

BSD2 IS ESSENTIAL FOR RUBISCO ASSEMBLY BY STABILIZING $RBCL_8$ INTERMEDIATE

Bsd2 was identified as a plastid-localized DnaJ-like Zn finger-containing protein with a role in post-translational biogenesis of maize Rubisco. Like *raf1* and *raf2*, the *bsd2* mutant is Rubisco-deficient and seedling lethal. Originally, Bsd2 was proposed to be part of a complex containing DnaJ-like (Hsp40) and Dna-K like (Hsp70) proteins, hypothetically transferring the newly-synthesized RbcL to the chaperonin folding apparatus (Brutnell et al., 1999). However, there is no evidence to support this model or to suggest that chaperonin-assisted folding of RbcL is preceded by a Dna-J/Hsp70-mediated complex that can bind the emerging RbcL nascent chain and protect it from aggregation. Overall, Bsd2 similarity to Hsp40 is limited to the hairpin structure of the Zn finger domain general architecture (Aigner et al., 2017).

Bsd2 homologs are limited to the plant and algae lineages (Hauser et al., 2015b), suggesting their emergence after the endosymbiotic event and chloroplast evolution. Pulse-labeling of chloroplast proteins in the maize *bsd2* mutant showed that the newly synthesized RbcL is associated with the chaperonin complex, suggesting that like Raf1 and Raf2, Bsd2 functions at a post-chaperonin stage of Rubisco assembly (Feiz et al., 2014). Co-immunoprecipitation with maize Bsd2 occurred for RbcS and to a lesser extent with RbcL and occurred reciprocally with Raf1 (Feiz et al., 2014).

In some of the experiments that were conducted during in *E. coli* biogenesis of the chloroplast Rubisco (Aigner et al., 2017), two higher order complexes migrated above the Rubisco holoenzyme on native gel. Whereas none of these bands showed any trace of Raf1, Raf2, or RbcX, the higher band contained RbcL and Bsd2 and the lower contained RbcL, Bsd2, and RbcS. The disappearance of both bands along with the promotion in $RbcL_8S_8$ formation, after an increase in RbcS expression, suggested that the higher order Bsd2-bound complexes might have formed due to RbcS insufficiency. Interestingly, when RbcS was deleted from the co-expression experiment, only the higher band was observed and when both RbcS and Raf2 were omitted, none of complexes were detected (Aigner et al., 2017), suggesting that Raf2 mediates the Bsd2-RbcL interaction.

AtBsd2 alone crystallized as monomer of ∼8 kDa (Aigner et al., 2017). In the center of its hairpin structure two Zn atoms were found, each coordinated by four cysteines. Because plant $RbcL_2$ or $RbcL_8$ intermediates have not been detected in *E coli*, cyanobacterial TeRbcL (from *Thermosynechococcus elongatus* BP-1) was co-expressed with AtBsd2 and the crystal structure of the $TeRbcL_8AtBsd2_8$ complex was obtained. In the complex, Bsd2 join RbcL dimers to form an $RbcL_8$ core surrounded by eight Bsd2 proteins. The relevance of the AtBsd2-TeRbcL interacting residues was further validated by mutational analysis of AtBsd2 and testing its competency in assembling AtRubisco in *E. coli*. No overlap was observed for Bsd2 and RbcS binding sites on RbcL (Aigner et al., 2017). Cyanobacterial RbcX and Raf1 were also shown to bind to either $TeRbcL_8$ or $SeRbcL_8$ (from *Synechococcus elongatus*) (Bracher et al., 2011; Hauser et al., 2015a). The $TeRbcL_8AtBsd2_8$ complex, however, was suggested to be the last assembly intermediate before holoenzyme formation with RbcS (Aigner et al., 2017).

DETAILING THE ASSEMBLY PATHWAY BY *IN VITRO* RECONSTITUTION OF PLANT RUBISCO

Elucidation of the assembly steps of cyanobacterial Rubisco and identification of the essential chloroplast factors helped with partial depiction of the assembly pathway for plant Rubisco and led to successful expression of *Arabidopsis* Rubisco in *E. coli* (Aigner et al., 2017). A proposed path, leading to holoenzyme formation in chloroplasts, is described in **Figure 2**. In short, newly-synthesized RbcS (S) is imported into the chloroplast

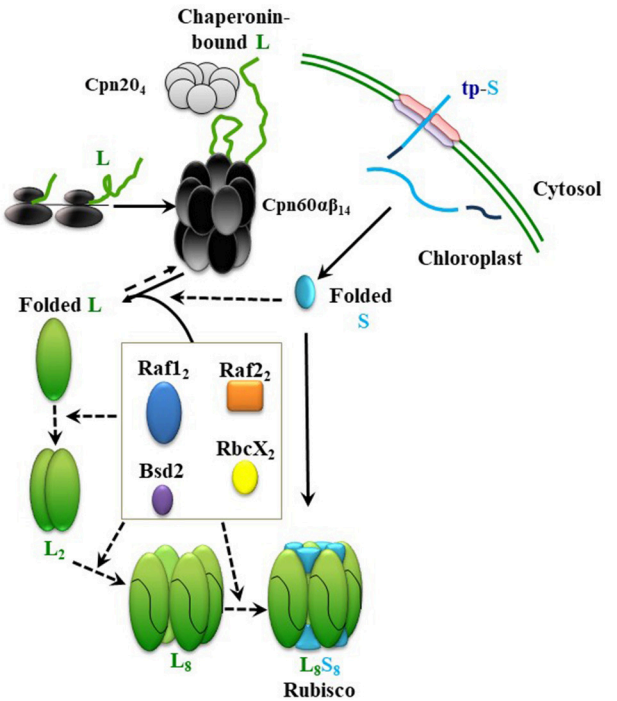

FIGURE 2 | Model summarizing the roles of different chaperones in Rubisco assembly. From top; Newly-synthesized RbcL (L) interacts with the chaperonin complex, which leads to correct folding (Native L). After import into chloroplast and cleavage of its transit peptide, RbcS (S) folds spontaneously, or with the help of a chaperone. Raf1, Raf2, RbcX, and Bsd2 form dynamic intermediates with the folded RbcL. RbcS subunits could either displace the chaperones in a final chaperone-RbcL intermediate to form the holoenzyme (L_8S_8), or interact with chaperones and RbcL in earlier stages of the assembly. Continuous and dashed arrows indicate certain and speculative nature of each step, respectively.

and folded, independently or with the help of chaperones, to the native state, after cleavage of its transit peptide. Newly-synthesized RbcL (L) in chloroplast is folded by the chaperonin hetero-complex assisted by Cpn20. In the absence of assembly factors, RbcL would not be able to escape from the chaperonin cycle, ultimately leading to aggregation and proteolysis. Raf1, Raf2, and RbcX dimers and Bsd2 monomers mediate formation of intermediates from folded RbcL, leading to their displacement by the RbcS and formation of the holoenzyme. So far, we have no evidence for the presence of any distinct post-chaperonin RbcL-containing intermediates, such as $RbcL_2$ and $RbcL_8$, that can be formed prior to biogenesis of the chloroplast holoenzyme. Putative intermediate complexes containing RbcS, RbcL, Raf1, Raf2, and Bsd2 were co-immunoprecipitated from plant lysates, following *in vivo* crosslinking, but their size, composition and stoichiometry remained to be determined (Feiz et al., 2014).

Using cyanobacterial RbcL, similar roles in dimerization and octamerization of the chloroplast RbcL have been proposed for RbcX, Raf1, and Bsd2 (Bracher et al., 2011; Hauser et al., 2015a; Aigner et al., 2017). In the most recent model, however, sequential functions have been proposed, during which Raf1 and RbcX are involved in the earlier RbcL oligomerization steps, and their replacement by Bsd2 mediates a later stabilization step of the $RbcL_8$ core. According to this model, RbcS may only have to replace Bsd2 before formation of the holoenzyme (Aigner et al., 2017).

Many question marks surround this model. What is the precise role of Raf2? Is RbcS folded spontaneously or in need of chaperone assistance to reach conformation compatible for RbcL binding? Do RbcX and Raf1 act in parallel or cooperatively? How Bsd2 displaces Raf1/RbcX? How RbcS displaces Bsd2? Are there additional factors involved in Rubisco biogenesis? Revealing the sequential steps of assembly, as well as the precise role of different chaperone paralogs is the next challenge. Further *in vitro* and *in vivo* experiments seem essential in unraveling the assembly steps and characterizing the unique structural and functional properties of the different factors.

Reconstitution of *Arabidopsis* Rubisco *in vitro* was previously attempted. The results showed that RbcL subunits stayed bound to chaperonins and did not assemble into any type of oligomers or holoenzyme despite the presence of all assembly factors except Bsd2 (Hauser, 2016), as one would expect in light of the recent work. Whether the entire cohort of assembly factors, their exact levels, and an accurate timing of theirs functions, would be sufficient for *in vitro* assembly, is yet to be determined. Evolution has invested tremendous resources in the fine-tuning of various folding and assembly factors and their compatibility with RbcL and RbcS in chloroplast. Further genetic and biochemical studies are necessary for complete, in detail understanding of this complex pathway.

AUTHOR CONTRIBUTIONS

All authors listed have made a substantial, direct and intellectual contribution to the work, and approved it for publication.

ACKNOWLEDGMENTS

We thank Dr. Celeste Weiss and Prof. David Stern for critically reading the manuscript. This material is based upon work that is supported by the Agriculture and Food Research Initiative (AFRI) from the National Institute of Food and Agriculture, U.S. Department of Agriculture, under award number 2016-67013-24464.

REFERENCES

Aigner, H., Wilson, R. H., Bracher, A., Calisse, L., Bhat, J. Y., Hartl, F. U., et al. (2017). Plant RuBisCo assembly in *E. coli* with five chloroplast chaperones including BSD2. *Science* 358, 1272–1278. doi: 10.1126/science.aap9221

Andersson, I., and Backlund, A. (2008). Structure and function of Rubisco. *Plant Physiol. Biochem.* 46, 275–291. doi: 10.1016/j.plaphy.2008.01.001

Badger, M. R., and Bek, E. J. (2008). Multiple Rubisco forms in proteobacteria: their functional significance in relation to CO_2 acquisition by the CBB cycle. *J. Exp. Bot.* 59, 1525–1541. doi: 10.1093/jxb/erm297

Bai, C., Guo, P., Zhao, Q., Lv, Z., Zhang, S., Gao, F., et al. (2015). Protomer roles in chloroplast chaperonin assembly and function. *Mol. Plant* 8, 1478–1492. doi: 10.1016/j.molp.2015.06.002

Baneyx, F., Bertsch, U., Kalbach, C. E., Van der Vies, S. M., Soll, J., and Gatenby, A. A. (1995). Spinach chloroplast cpn21 co-chaperonin possesses two functional domains fused together in a toroidal structure and exhibits nucleotide-dependent binding to plastid chaperonin 60. *J. Biol. Chem.* 270, 10695–10702. doi: 10.1074/jbc.270.18.10695

Barraclough, R., and Ellis, R. J. (1980). Protein synthesis in chloroplasts IX. Assembly of newly-synthesized large subunits into ribulose bishopshate carboxylase in isolated intact pea chloroplasts. *BBA Sect. Nucleic Acids Protein Synth*. 608, 19–31. doi: 10.1016/0005-2787(80)90129-X

Belcher, S., Williams-Carrier, R., Stiffler, N., and Barkan, A. (2015). Large-scale genetic analysis of chloroplast biogenesis in maize. *Biochim. Biophys. Acta Bioenerg.* 1847, 1004–1016. doi: 10.1016/j.bbabio.2015.02.014

Bertsch, U., Soll, J., Seetharam, R., and Viitanen, P. V. (1992). Identification, characterization, and DNA sequence of a functional "double" groES-like chaperonin from chloroplasts of higher plants. *Proc. Natl. Acad. Sci. U.S.A.* 89, 8696–8700.

Bloom, M. V., Milos, P., and Roy, H. (1983). Light-dependent assembly of ribulose-1,5-bisphosphate carboxylase. *Cell Biol.* 80, 1013–1017. doi: 10.1073/pnas.80.4.1013

Bonshtien, A. L., Parnas, A., Sharkia, R., Niv, A., Mizrahi, I., Azem, A., et al. (2009). Differential effects of co-chaperonin homologs on cpn60 oligomers. *Cell Stress Chaperones* 14, 509–519. doi: 10.1007/s12192-009-0104-2

Bonshtien, A. L., Weiss, C., Vitlin, A., Niv, A., Lorimer, G. H., and Azem, A. (2007). Significance of the N-terminal domain for the function of chloroplast cpn20 chaperonin. *J. Biol. Chem.* 282, 4463–4469. doi: 10.1074/jbc.M606433200

Bracher, A., Hauser, T., Liu, C., Hartl, F. U., and Hayer-Hartl, M. (2015). structural analysis of the rubisco-assembly chaperone RbcX-II from *Chlamydomonas reinhardtii*. *PLoS ONE* 10:e0135448. doi: 10.1371/journal.pone.0135448

Bracher, A., Starling-Windhof, A., Hartl, F. U., and Hayer-Hartl, M. (2011). Crystal structure of a chaperone-bound assembly intermediate of form I Rubisco. *Nat. Struct. Mol. Biol.* 18, 875–880. doi: 10.1038/nsmb.2090

Bracher, A., Whitney, S. M., Hartl, F. U., and Hayer-Hartl, M. (2017). Biogenesis and metabolic maintenance of Rubisco. *Annu. Rev. Plant Biol.* 68, 29–60. doi: 10.1146/annurev-arplant-043015-111633

Brutnell, T. P., Sawers, R. J., Mant, A., and Langdale, J. A. (1999). BUNDLE SHEATH DEFECTIVE2, a novel protein required for post-translational regulation of the rbcL gene of maize. *Plant Cell* 11, 849–864. doi: 10.1105/tpc.11.5.849

Cloney, L. P., Bekkaoui, D. R., Wood, M. G., and Hemmingsen, S. M. (1992a). Assessment of plant chaperonin-60 gene function in *Escherichia coli*. *J. Biol. Chem.* 267, 23333–23336.

Cloney, L. P., Wu, H. B., and Hemmingsen, S. M. (1992b). Expression of plant chaperonin-60 genes in *Escherichia coli*. *J. Biol. Chem.* 267, 23327–23332.

Dereeper, A., Audic, S., Claverie, J.-M., and Blanc, G. (2010). BLAST-EXPLORER helps you building datasets for phylogenetic analysis. *BMC Evol. Biol.* 10:8. doi: 10.1186/1471-2148-10-8

Dereeper, A., Guignon, V., Blanc, G., Audic, S., Buffet, S., Chevenet, F., et al. (2008). Phylogeny.fr: robust phylogenetic analysis for the non-specialist. *Nucleic Acids Res.* 36, W465–W469. doi: 10.1093/nar/gkn180

Dickson, R., Weiss, C., Howard, R. J., Alldrick, S. P., Ellis, R. J., Lorimer, G., et al. (2000). Reconstitution of higher plant chloroplast chaperonin 60 tetradecamers active in protein folding. *J. Biol. Chem.* 275, 11829–11835. doi: 10.1074/jbc.275.16.11829

Dobberstein, B., Blobel, G., and Chua, N. H. (1977). *In vitro* synthesis and processing of a putative precursor for the small subunit of ribulose-1,5-bisphosphate carboxylase of *Chlamydomonas reinhardtii*. *Proc. Natl. Acad. Sci. U.S.A.* 74, 1082–1085. doi: 10.1073/pnas.74.3.1082

Durão, P., Aigner, H., Nagy, P., Mueller-Cajar, O., Hartl, F. U., and Hayer-Hartl, M. (2015). Opposing effects of folding and assembly chaperones on evolvability of Rubisco. *Nat. Chem. Biol.* 11, 148–155. doi: 10.1038/nchembio.1715

Ellis, R. J. (1990). Molecular chaperones: the plant connection. *Science* 250, 954–959. doi: 10.1126/science.250.4983.954

Emlyn-Jones, D., Woodger, F. J., Price, G. D., and Whitney, S. M. (2006). RbcX can function as a Rubisco chaperonin, but is non-essential in Synechococcus PCC7942. *Plant Cell Physiol.* 47, 1630–1640. doi: 10.1093/pcp/pcl028

Endrizzi, J. A., Cronk, J. D., Wang, W., Crabtree, G. R., and Alber, T. (1995). Crystal structure of DCoH, a bifunctional, protein-binding transcriptional coactivator. *Science* 268, 556–559. doi: 10.1126/science.7725101

Erb, T. J., and Zarzycki, J. (2018). A short history of RubisCO: the rise and fall (?) of Nature's predominant CO_2 fixing enzyme. *Curr. Opin. Biotechnol.* 49, 100–107. doi: 10.1016/j.copbio.2017.07.017

Feiz, L., Williams-Carrier, R., Belcher, S., Montano, M., Barkan, A., and Stern, D. B. (2014). A protein with an inactive pterin-4a-carbinolamine dehydratase domain is required for Rubisco biogenesis in plants. *Plant J.* 80, 862–869. doi: 10.1111/tpj.12686

Feiz, L., Williams-Carrier, R., Wostrikoff, K., Belcher, S., Barkan, A., and Stern, D. B. (2012). Ribulose-1,5-bis-phosphate carboxylase/oxygenase accumulation factor1 is required for holoenzyme assembly in maize. *Plant Cell* 24, 3435–3446. doi: 10.1105/tpc.112.102012

Feller, U., Anders, I., and Mae, T. (2008). Rubiscolytics: fate of rubisco after its enzymatic function in a cell is terminated. *J. Exp. Bot.* 59, 1615–1624. doi: 10.1093/jxb/erm242

Friso, G., Majeran, W., Huang, M., Sun, Q., and van Wijk, K. J. (2010). Reconstruction of metabolic pathways, protein expression, and homeostasis machineries across maize bundle sheath and mesophyll chloroplasts: large-scale quantitative proteomics using the first maize genome assembly. *Plant Physiol.* 152, 1219–1250. doi: 10.1104/pp.109.152694

Goloubinoff, P., Christeller, J. T., Gatenby, A. A., and Lorimer, G. H. (1989a). Reconstitution of active dimeric ribulose bisphosphate carboxylase from an unfolded state depends on two chaperonin proteins and Mg-ATP. *Nature* 342, 884–889. doi: 10.1038/342884a0

Goloubinoff, P., Gatenby, A. A., and Lorimer, G. H. (1989b). GroE heat-shock proteins promote assembly of foreign prokaryotic ribulose bisphosphate carboxylase oligomers in *Escherichia coli*. *Nature* 337, 44–47. doi: 10.1038/337044a0

Guo, P., Jiang, S., Bai, C., Zhang, W., Zhao, Q., and Liu, C. (2015). Asymmetric functional interaction between chaperonin and its plastidic cofactors. *FEBS J.* 282, 3959–3970. doi: 10.1111/febs.13390

Hauser, T. (2016). *Structural and Functional Characterization of Rubisco Assembly Chaperones*. Available online at: https://edoc.ub.uni-muenchen.de/19416/1/Hauser_Thomas.pdf

Hauser, T., Bhat, J. Y., Milicić, G., Wendler, P., Hartl, F. U., Bracher, A., et al. (2015a). Structure and mechanism of the Rubisco-assembly chaperone Raf1. *Nat. Struct. Mol. Biol.* 22, 720–728. doi: 10.1038/nsmb.3062

Hauser, T., Popilka, L., Hartl, F. U., and Hayer-Hartl, M. (2015b). Role of auxiliary proteins in Rubisco biogenesis and function. *Nat. Plants* 1:15065. doi: 10.1038/nplants.2015.65

Hemmingsen, S. M., Woolford, C., van der Vies, S. M., Tilly, K., Dennis, D. T., Georgopoulos, C. P., et al. (1988). Homologous plant and bacterial proteins chaperone oligomeric protein assembly. *Nature* 333, 330–334. doi: 10.1038/333330a0

Hevel, J. M., Pande, P., Viera-Oveson, S., Sudweeks, T. J., Jaffree, L. S., Hansen, C. M., et al. (2008). Determinants of oligomerization of the bifunctional protein DCoHα and the effect on its enzymatic and transcriptional coactivator activities. *Arch. Biochem. Biophys.* 477, 356–362. doi: 10.1016/j.abb.2008.06.023

Highfield, P. E., and Ellis, R. J. (1978). Synthesis and transport of the small subunit of chloroplast ribulose bisphosphate carboxylase. *Nature* 271, 420–424. doi: 10.1038/271420a0

Hill, J. E., and Hemmingsen, S. M. (2001). *Arabidopsis thaliana* type I and II chaperonins. *Cell Stress Chaperones* 6, 190–200. doi: 10.1379/1466-1268(2001)006<0190:ATTIAI>2.0.CO;2

Jiang, Q., Mei, J., Gong, X. D., Xu, J. L., Zhang, J. H., Teng, S., et al. (2014). Importance of the rice TCD9 encoding α subunit of chaperonin protein 60 (Cpn60α) for the chloroplast development during the early leaf stage. *Plant Sci.* 215–216, 172–179. doi: 10.1016/j.plantsci.2013.11.003

John Andrews, T., and Whitney, S. M. (2003). Manipulating ribulose bisphosphate carboxylase/oxygenase in the chloroplasts of higher plants. *Arch. Biochem. Biophys.* 414, 159–169. doi: 10.1016/S0003-9861(03)00100-0

Ke, X., Zou, W., Ren, Y., Wang, Z., Li, J., Wu, X., et al. (2017). Functional divergence of chloroplast Cpn60α subunits during Arabidopsis embryo development. *PLoS Genet.* 13:e1007036. doi: 10.1371/journal.pgen.1007036

Kim, S.-R., Yang, J.-I., and An, G. (2013). OsCpn60α1, encoding the plastid chaperonin 60α subunit, is essential for folding of rbcL. *Mol. Cells* 35, 402–409. doi: 10.1007/s10059-013-2337-2

Kolesinski, P., Belusiak, I., Czarnocki-Cieciura, M., and Szczepaniak, A. (2014). Rubisco Accumulation Factor 1 from *Thermosynechococcus elongatus* participates in the final stages of ribulose-1,5-bisphosphate carboxylase/oxygenase assembly in *Escherichia coli* cells and *in vitro*. *FEBS J.* 281, 3920–3932. doi: 10.1111/febs.12928

Kolesinski, P., Golik, P., Grudnik, P., Piechota, J., Markiewicz, M., Tarnawski, M., et al. (2013). Insights into eukaryotic Rubisco assembly - Crystal structures of RbcX chaperones from *Arabidopsis thaliana*. *Biochim. Biophys. Acta Gen. Subj.* 1830, 2899–2906. doi: 10.1016/j.bbagen.2012.12.025

Kolesinski, P., Piechota, J., and Szczepaniak, A. (2011). Initial characteristics of RbcX proteins from *Arabidopsis thaliana*. *Plant Mol. Biol.* 77, 447–459. doi: 10.1007/s11103-011-9823-8

Kolesinski, P., Rydzy, M., and Szczepaniak, A. (2017). Is RAF1 protein from *Synechocystis* sp. PCC 6803 really needed in the cyanobacterial Rubisco assembly process? *Photosynth. Res.* 132, 135–148. doi: 10.1007/s11120-017-0336-4

Koumoto, Y., Shimada, T., Kondo, M., Hara-Nishimura, I., and Nishimura, M. (2001). Chloroplasts have a novel Cpn10 in addition to Cpn20 as Co-chaperonins in *Arabidopsis thaliana*. *J. Biol. Chem.* 276, 29688–29694. doi: 10.1074/jbc.M102330200

Koumoto, Y., Shimada, T., Kondo, M., Takao, T., Shimonishi, Y., Hara-Nishimura, I., et al. (1999). Chloroplast Cpn20 forms a tetrameric structure in *Arabidopsis thaliana*. *Plant J.* 17, 467–477. doi: 10.1046/j.1365-313X.1999.00388.x

Larimer, F. W., and Soper, T. S. (1993). Overproduction of Anabaena 7120 ribulose-bisphosphate carboxylase/oxygenase in *Escherichia coli*. *Gene* 126, 85–92. doi: 10.1016/0378-1119(93)90593-R

Li, L. A., and Tabita, F. R. (1997). Maximum activity of recombinant ribulose 1,5-bisphosphate carboxylase/oxygenase of *Anabaena* sp. strain CA requires the product of the rbcX gene. *J. Bacteriol.* 179, 3793–3796. doi: 10.1128/jb.179.11.3793-3796.1997

Lissin, N. M. (1995). *In vitro* dissociation and self-assembly of three chaperonin 60s: the role of ATP. *FEBS Lett.* 361, 55–60. doi: 10.1016/0014-5793(95)00151-X

Liu, C., Young, A. L., Starling-Windhof, A., Bracher, A., Saschenbrecker, S., Rao, B. V., et al. (2010). Coupled chaperone action in folding and assembly of hexadecameric Rubisco. *Nature* 463, 197–202. doi: 10.1038/nature08651

Loganathan, N., Tsai, Y.-C., and Mueller-Cajar, O. (2016). Characterization of the heterooligomeric red-type rubisco activase from red algae. *Proc. Natl. Acad. Sci. U.S.A.* 113, 14019–14024. doi: 10.1073/pnas.1610758113

Martel, R., Cloney, L. P., Pelcher, L. E., and Hemmingsen, S. M. (1990). Unique composition of plastid chaperonin-60: α and β polypeptide-encoding genes are highly divergent. *Gene* 94, 181–187. doi: 10.1016/0378-1119(90)90385-5

Mueller-Cajar, O. (2017). The Diverse AAA+ Machines that repair inhibited rubisco active sites. *Front. Mol. Biosci.* 4, 1–17. doi: 10.3389/fmolb.2017.00031

Mueller-Cajar, O., Stotz, M., Wendler, P., Hartl, F. U., Bracher, A., and Hayer-Hartl, M. (2011). Structure and function of the AAA+ protein CbbX, a red-type Rubisco activase. *Nature* 479, 194–199. doi: 10.1038/nature10568

Musgrove, J. E., Johnson, R. A., and Ellis, R. J. (1987). Dissociation of the ribulosebisphosphate-carboxylase large-subunit binding protein into dissimilar subunits. *Eur. J. Biochem.* 163, 529–534. doi: 10.1111/j.1432-1033.1987.tb10900.x

Nishio, K., Hirohashi, T., and Nakai, M. (1999). Chloroplast chaperonins: evidence for heterogeneous assembly of alpha and beta Cpn60 polypeptides into a chaperonin oligomer. *Biochem. Biophys. Res. Commun.* 266, 584–587. doi: 10.1006/bbrc.1999.1868

Onizuka, T., Endo, S., Akiyama, H., Kanai, S., Hirano, M., Yokota, A., et al. (2004). The rbcX gene product promotes the production and assembly of ribulose-1,5-bisphosphate carboxylase/oxygenase of Synechococcus sp. PCC7002 in *Escherichia coli*. *Plant Cell Physiol.* 45, 1390–1395. doi: 10.1093/pcp/pch160

Parry, M. A. J., Andralojc, P. J., Scales, J. C., Salvucci, M. E., Carmo-Silva, A. E., Alonso, H., et al. (2013). Rubisco activity and regulation as targets for crop improvement. *J. Exp. Bot.* 64, 717–730. doi: 10.1093/jxb/ers336

Peng, L., Fukao, Y., Myouga, F., Motohashi, R., Shinozaki, K., and Shikanai, T. (2011). A chaperonin subunit with unique structures is essential for folding of a specific substrate. *PLoS Biol.* 9:e1001040. doi: 10.1371/journal.pbio.1001040

Phillips, R., and Milo, R. (2009). A feeling for the numbers in biology. *Proc. Natl. Acad. Sci. U.S.A.* 106, 21465–21471. doi: 10.1073/pnas.0907732106

Rose, R. B., Pullen, K. E., Bayle, J. H., Crabtree, G. R., and Alber, T. (2004). Biochemical and structural basis for partially redundant enzymatic and transcriptional functions of DCoH and DCoH2. *Biochemistry* 43, 7345–7355. doi: 10.1021/bi049620t

Roy, H. (1989). Rubisco assembly: a model system for studying the mechanism of chaperonin action. *Plant Cell* 1, 1035–1042. doi: 10.1105/tpc.1.11.1035

Roy, H., Bloom, M., Milos, P., and Monroe, M. (1982). Studies on the assembly of large subunits of ribulose bisphosphate carboxylase in isolated pea chloroplasts. *J. Cell Biol.* 94, 20–27. doi: 10.1083/jcb.94.1.20

Salvucci, M. E., Werneke, J. M., Ogren, W. L., and Portis, A. R. (1987). Purification and species distribution of rubisco activase. *Plant Physiol.* 84, 930–936. doi: 10.1104/pp.84.3.930

Saschenbrecker, S., Bracher, A., Rao, K. V., Rao, B. V., Hartl, F. U., and Hayer-Hartl, M. (2007). Structure and Function of RbcX, an assembly chaperone for hexadecameric rubisco. *Cell* 129, 1189–1200. doi: 10.1016/j.cell.2007.04.025

Savir, Y., Noor, E., Milo, R., and Tlusty, T. (2010). Cross-species analysis traces adaptation of Rubisco toward optimality in a low-dimensional landscape. *Proc. Natl. Acad. Sci. U.S.A.* 107, 3475–3480. doi: 10.1073/pnas.0911663107

Schroda, M. (2004). The Chlamydomonas genome reveals its secrets: chaperone genes and the potential roles of their gene products in the chloroplast. *Photosyn. Res.* 82, 221–240. doi: 10.1007/s11120-004-2216-y

Sharkia, R., Bonshtien, A. L., Mizrahi, I., Weiss, C., Niv, A., Lustig, A., et al. (2003). On the oligomeric state of chloroplast chaperonin 10 and chaperonin 20. *Biochim. Biophys. Acta Prot. Proteom.* 1651, 76–84. doi: 10.1016/S1570-9639(03)00237-1

Shih, P. M., Occhialini, A., Cameron, J. C., Andralojc, P. J., Parry, M. A. J., and Kerfeld, C. A. (2016). Biochemical characterization of predicted Precambrian RuBisCO. *Nat. Commun.* 7:10382. doi: 10.1038/ncomms10382

Studer, R. A., Christin, P.-A., Williams, M. A., and Orengo, C. A. (2014). Stability-activity tradeoffs constrain the adaptive evolution of RubisCO. *Proc. Natl. Acad. Sci. U.S.A.* 111, 2223–2228. doi: 10.1073/pnas.1310811111

Tabita, F. R. (1999). Microbial ribulose 1,5-bisphosphate carboxylase/oxygenase: a different perspective. *Photosyn. Res.* 60, 1–28. doi: 10.1023/A:1006211417981

Tabita, F. R., Hanson, T. E., Satagopan, S., Witte, B. H., and Kreel, N. E. (2008a). Phylogenetic and evolutionary relationships of RubisCO and the RubisCO-like proteins and the functional lessons provided by diverse molecular forms. *Philos. Trans. R. Soc. B Biol. Sci.* 363, 2629–2640. doi: 10.1098/rstb.2008.0023

Tabita, F. R., Satagopan, S., Hanson, T. E., Kreel, N. E., and Scott, S. S. (2008b). Distinct form I, II, III, and IV Rubisco proteins from the three kingdoms of life provide clues about Rubisco evolution and structure/function relationships. *J. Exp. Bot.* 59, 1515–1524. doi: 10.1093/jxb/erm361

Tawfik, D. S. (2014). Accuracy-rate tradeoffs: how do enzymes meet demands of selectivity and catalytic efficiency? *Curr. Opin. Chem. Biol.* 21, 73–80. doi: 10.1016/j.cbpa.2014.05.008

Tcherkez, G. G., Farquhar, G. D., and Andrews, T. J. (2006). Despite slow catalysis and confused substrate specificity, all ribulose bisphosphate carboxylases may be nearly perfectly optimized. *Proc. Natl. Acad. Sci. U.S.A.* 103, 7246–7251. doi: 10.1073/pnas.0600605103

Trösch, R., Mühlhaus, T., Schroda, M., and Willmund, F. (2015). ATP-dependent molecular chaperones in plastids–More complex than expected. *Biochim. Biophys. Acta* 1847, 872–888. doi: 10.1016/j.bbabio.2015.01.002

Tsai, Y.-C., Lapina, M. C., Bhushan, S., and Mueller-Cajar, O. (2015). Identification and characterization of multiple rubisco activases in chemoautotrophic bacteria. *Nat. Commun.* 6:8883. doi: 10.1038/ncomms9883

Tsai, Y. C., Mueller-Cajar, O., Saschenbrecker, S., Hartl, F. U., and Hayer-Hartl, M. (2012). Chaperonin cofactors, Cpn10 and Cpn20, of green algae and plants function as hetero-oligomeric ring complexes. *J. Biol. Chem.* 287, 20471–20481. doi: 10.1074/jbc.M112.365411

Viitanen, P. V., Bacot, K., Dickson, R., and Webb, T. (1998). Purification of recombinant plant and animal GroES homologs: chloroplast and mitochondrial chaperonin. *Meth. Enzymol.* 290, 218–230. doi: 10.1016/S0076-6879(98)90021-0

Viitanen, P. V., Schmidt, M., Buchner, J., Suzuki, T., Vierling, E., Dickson, R., et al. (1995). Functional characterization of the higher plant chloroplast chaperonins. *J. Biol. Chem.* 270, 18158–18164. doi: 10.1074/jbc.270.30.18158

Vitlin, A., Weiss, C., Demishtein-Zohary, K., Rasouly, A., Levin, D., Pisanty-Farchi, O., et al. (2011). Chloroplast β chaperonins from *A. thaliana* function with endogenous cpn10 homologs *in vitro*. *Plant Mol. Biol.* 77, 105–115. doi: 10.1007/s11103-011-9797-6

Vitlin Gruber, A., Nisemblat, S., Azem, A., and Weiss, C. (2013a). The complexity of chloroplast chaperonins. *Trends Plant Sci.* 18, 688–694. doi: 10.1016/j.tplants.2013.08.001

Vitlin Gruber, A., Nisemblat, S., Zizelski, G., Parnas, A., Dzikowski, R., Azem, A., et al. (2013b). *P. falciparum* cpn20 is a bona fide co-chaperonin that can replace GroES in *E. coli*. *PLoS ONE* 8:e53909. doi: 10.1371/journal.pone.0053909

Vitlin Gruber, A., Vugman, M., Azem, A., and Weiss, C. E. (2018). Reconstitution of pure chaperonin hetero-oligomer preparations *in vitro* by temperature modulation. *Front. Mol. Biosci.* 5:5. doi: 10.3389/fmolb.2018.00005

Vitlin Gruber, A., Zizelski, G., Azem, A., and Weiss, C. (2014). The Cpn10(1) co-chaperonin of *A. thaliana* functions only as a hetero-oligomer with Cpn20. *PLoS ONE* 9:e113835. doi: 10.1371/journal.pone.0113835

Walker, B. J., VanLoocke, A., Bernacchi, C. J., and Ort, D. R. (2016). The costs of photorespiration to food production now and in the future. *Annu. Rev. Plant Biol.* 67, 107–129. doi: 10.1146/annurev-arplant-043015-111709

Wheatley, N. M., Sundberg, C. D., Gidaniyan, S. D., Cascio, D., and Yeates, T. O. (2014). Structure and identification of a pterin dehydratase-like protein as a RuBisCO assembly factor in the alpha-carboxysome. *J. Biol. Chem.* 289, 7973–7981. doi: 10.1074/jbc.M113.531236

Whitney, S. M., Birch, R., Kelso, C., Beck, J. L., and Kapralov, M., V (2015). Improving recombinant Rubisco biogenesis, plant photosynthesis and growth by coexpressing its ancillary RAF1 chaperone. *Proc. Natl. Acad. Sci. U.S.A.* 112, 3564–3569. doi: 10.1073/pnas.1420536112

Wilson, R. H., Alonso, H., and Whitney, S. M. (2016). Evolving Methanococcoides burtonii archaeal Rubisco for improved photosynthesis and plant growth. *Sci. Rep.* 6:22284. doi: 10.1038/srep22284

Wostrikoff, K., and Stern, D. (2007). Rubisco large-subunit translation is autoregulated in response to its assembly state in tobacco chloroplasts. *Proc. Natl. Acad. Sci. U.S.A.* 104, 6466–6471. doi: 10.1073/pnas.0610586104

Zhang, S., Zhou, H., Yu, F., Bai, C., Zhao, Q., He, J., et al. (2016a). Structural insight into the cooperation of chloroplast chaperonin subunits. *BMC Biol.* 14:29. doi: 10.1186/s12915-016-0251-8

Zhang, S., Zhou, H., Yu, F., Gao, F., He, J., and Liu, C. (2016b). Functional partition of Cpn60α and Cpn60β subunits in substrate recognition and cooperation with co-chaperonins. *Mol. Plant* 9, 1210–1213. doi: 10.1016/j.molp.2016.04.019

Zhao, Q., and Liu, C. (2018). Chloroplast chaperonin: an intricate protein folding machine for photosynthesis. *Front. Mol. Biosci.* 4:98. doi: 10.3389/fmolb.2017.00098

Zhu, X.-G., Long, S. P., and Ort, D. R. (2010). Improving photosynthetic efficiency for greater yield. *Annu. Rev. Plant Biol.* 61, 235–261. doi: 10.1146/annurev-arplant-042809-112206

Conflict of Interest Statement: The authors declare that the research was conducted in the absence of any commercial or financial relationships that could be construed as a potential conflict of interest.

frontiers in Molecular Biosciences

ORIGINAL RESEARCH
published: 26 January 2018
doi: 10.3389/fmolb.2018.00005

Reconstitution of Pure Chaperonin Hetero-Oligomer Preparations *in Vitro* by Temperature Modulation

Anna Vitlin Gruber[1], *Milena Vugman*[2], *Abdussalam Azem*[2] *and Celeste E. Weiss*[2]*

[1] Department of Molecular, Cell and Developmental Biology, University of California, Los Angeles, Los Angeles, CA, United States, [2] Department of Biochemistry and Molecular Biology, George S. Wise Faculty of Life Sciences, Tel Aviv University, Tel Aviv, Israel

Chaperonins are large, essential, oligomers that facilitate protein folding in chloroplasts, mitochondria, and eubacteria. Plant chloroplast chaperonins are comprised of multiple homologous subunits that exhibit unique properties. We previously characterized homogeneous, reconstituted, chloroplast-chaperonin oligomers *in vitro*, each composed of one of three highly homologous beta subunits from *A. thaliana*. In the current work, we describe alpha-type subunits from the same species and investigate their interaction with β subtypes. Neither alpha subunit was capable of forming higher-order oligomers on its own. When combined with β subunits in the presence of Mg-ATP, only the α2 subunit was able to form stable functional hetero-oligomers, which were capable of refolding denatured protein with native chloroplast co-chaperonins. Since β oligomers were able to oligomerize in the absence of α, we sought conditions under which αβ hetero-oligomers could be produced without contamination of β homo-oligomers. We found that β2 subunits are unable to oligomerize at low temperatures and used this property to obtain homogenous preparations of functional α2β2 hetero-oligomers. The results of this study highlight the importance of reaction conditions such as temperature and concentration for the reconstitution of chloroplast chaperonin oligomers *in vitro*.

Keywords: chaperone, chaperonin, chloroplast, *A. thaliana*, oligomer, *in vitro*, temperature

OPEN ACCESS

Edited by:
Ophry Pines,
Hebrew University of Jerusalem, Israel

Reviewed by:
Eyal Gur,
Ben-Gurion University of the Negev, Beersheba, Israel
Hideki Taguchi,
Tokyo Institute of Technology, Japan

***Correspondence:**
Celeste E. Weiss
celeste@tauex.tau.ac.il

Specialty section:
This article was submitted to Protein Folding, Misfolding and Degradation, a section of the journal Frontiers in Molecular Biosciences

Received: *22 November 2017*
Accepted: *11 January 2018*
Published: *26 January 2018*

Citation:
Vitlin Gruber A, Vugman M, Azem A and Weiss CE (2018) Reconstitution of Pure Chaperonin Hetero-Oligomer Preparations in Vitro by Temperature Modulation. Front. Mol. Biosci. 5:5. doi: 10.3389/fmolb.2018.00005

INTRODUCTION

Chaperonins are a subfamily of chaperone proteins found in bacteria and bacteria-derived organelles. In contrast to the well-studied GroEL of *Escherichia coli*, which has one Cpn60 gene product (Johnson et al., 1989), that forms functional homo-oligomers composed of 14 subunits, chloroplasts contain two Cpn60 subtypes, Cpn60α and Cpn60β (Musgrove et al., 1987; Martel et al., 1990; Cloney et al., 1992a,b, 1993, 1994; Nishio et al., 1999). These subtypes exhibit ∼50% homology to each other, similar to their respective homologies to GroEL, and are each present in two or more paralogous forms in most higher plants (Hemmingsen et al., 1988; Cloney et al., 1994; Hill and Hemmingsen, 2001). These subunits combine to form extremely labile hetero-oligomeric chaperonin species, which dissociate into monomeric form upon dilution, particularly in the presence of ATP (Musgrove et al., 1987; Roy et al., 1988; Lissin, 1995; Viitanen et al., 1998; Dickson et al., 2000; Bonshtien et al., 2009).

Arabidopsis chloroplast contains six Cpn60 homologs: two Cpn60α subunits and four Cpn60β subunits (Hill and Hemmingsen, 2001). Unlike Cpn60β proteins which share a high level of

sequence similarity (Vitlin et al., 2011), significant divergence of primary structure is apparent between the two Cpn60α paralogs. The two *Arabidopsis* Cpn60α proteins are similar in length (543 and 541 amino acids) and share 60% identity of peptide sequence (excluding the putative transit peptide). The sequence differences are evenly distributed along the length of the proteins (Hill and Hemmingsen, 2001).

Many species contain orthologs of both Cpn60α1 (At5g18820) and Cpn60α2 (At2g28000). Several groups characterized knockout or point mutants of Cpn60α2 orthologs, all resulting in severe impairment of plant development (Apuya et al., 2001; Suzuki et al., 2009; Peng et al., 2011; Feiz et al., 2012; Kim et al., 2013; Jiang et al., 2014; Ke et al., 2017). A knockout strain of α1 was arrested at the globular embryo stage (Ke et al., 2017), while an α2 knockout was arrested at the heart stage (Apuya et al., 2001). Cpn60α1 and Cpn60α2 vary greatly in their expression levels. Cpn60α2 was shown to be the most highly expressed of the Cpn60 homologs in all tissues and during all developmental stages in comparison with other chaperonins (Weiss et al., 2009). In contrast, Cpn60α1 subunit expression is barely detectable at the RNA level (Weiss et al., 2009) although recent studies reported that this protein is highly expressed in the SAM of early seedlings and embryonic cotyledons (Ke et al., 2017).

Several groups have investigated the oligomerization of chloroplast Cpn60 subunits from different plants *in vitro*. Attempts to reconstitute oligomers from purified *P. sativum* α monomers alone were unsuccessful. However, upon addition of β subunits, hetero-oligomers were formed, composed of α and β subunits (αβ hetero-oligomer) (Dickson et al., 2000). These results were consistent with studies on chaperonins from *Brassica napus* and *C. reinhardtii*, which produced functional αβ oligomers when over-expressed together in *E. coli* (Cloney et al., 1992a,b; Bai et al., 2015). Similar to GroEL, reconstituted αβ hetero-oligomers from *P. sativum* could mediate the refolding of denatured substrate when assisted with co-chaperonin from any source: bacteria (GroES), mitochondria (mt-cpn10) or chloroplast (Cpn20) (Dickson et al., 2000), whereas beta homo-oligomers were functional *in vitro* with native chloroplast co-chaperonins and with heterologous mt-cpn10 (Dickson et al., 2000; Vitlin et al., 2011).

In this work we used a well-established method for Cpn60 monomer purification and oligomer reconstitution, that was developed in our lab (Vitlin et al., 2011), in order to study both *Arabidopsis* Cpn60α subunits as monomers, as well as the hetero-oligomers that are formed together with Cpn60β subunits. We show that the α2 subunit can form functional oligomers with β subunits, while the α1 subunit is unable to oligomerize under any conditions that we tested *in vitro*. Since β subunits oligomerize on their own, production of pure αβ hetero-oligomer is liable to be contaminated by β homo-oligomer. The dependence of reconstitution on temperature and concentration can be manipulated to ensure that the resulting hetero-oligomeric preparations are homogeneous. In this work, we present a method for reconstitution of hetero-oligomers, composed of α2 and β2 subunits that are free of contaminating β2 homo-oligomers.

RESULTS

Purification and Structural Characterization of Alpha Subunits

We have cloned and purified both Cpn60α homologs using a strategy that was developed and described for Cpn60β subunits (Vitlin et al., 2011). The final step of the purification process hinted at the physico-chemical differences between these two proteins. As can be seen in **Figure 1A** and Figure S1A, α1 eluted from the gel filtration column earlier than α2, suggesting that the α1 form is larger than α2. In addition, α1 eluted as a single sharp peak, while the α2 elution profile displayed several peaks. In order to further investigate these differences, we subjected the proteins to crosslinking with glutaraldehyde, to analyze their oligomeric state. The crosslinking pattern of both subunits exhibited several high molecular-weight bands (**Figure 1B** and Figure S1B). However, one major difference stood out between the α1 and the α2 samples: while the main band in the α2 samples represented the monomeric form, no monomer was observed for α1, but rather a lower mobility species consistent with that of a dimer.

In order to determine the molecular weight of these proteins, we carried out analytical ultracentrifugation. Two variations of this method, sedimentation velocity and sedimentation equilibrium, were used to analyze the α homologs. Using sedimentation velocity, we found that both subunits were characterized by a single peak, with average sedimentation coefficients of ∼4 S and 5 S for α2 and α1, respectively. The sedimentation co-efficient of α2 is similar to the previously published coefficient for GroES (70 kDa), 4 S (Seale et al., 1996), indicating that this subunit is mainly monomeric while α1 is larger and most likely a dimer. Analysis of sedimentation equilibrium (**Figure 1C**) corroborated this observation, with a calculated molecular weight of 100,400 Da for α1 and of 64,900 Da for α2. The expected monomer weight for these proteins is ∼57,000 Dalton. Thus, the results of sedimentation equilibrium indicate that α1 is best modeled as a dimer and α2 is primarily monomeric.

Reconstitution and Functional Characterization of αβ Hetero-Oligomers

Since their discovery, chaperonin tetradecamers composed of Cpn60α and Cpn60β subunits have been considered to be the native form of chaperonin oligomers that are active in chloroplasts (Musgrove et al., 1987), although functional β homo-oligomers were described *in vitro* (Dickson et al., 2000; Vitlin et al., 2011; Bai et al., 2015). To our surprise, attempts to reconstitute hetero-oligomers containing α1 were not successful. Reconstitution mixtures containing α1 alone or in combination with any individual β subunit eluted from the gel filtration column as inactive, low molecular weight species (not shown). The fact that no Cpn60β oligomer was formed in the presence of Cpn60α1 was intriguing, since Cpn60β subunits alone generally tend to form oligomers under the same conditions. This suggests that an interaction is taking place between the monomers but it is not productive in furthering formation of a tetradecamer. A similar phenomenon was described for the α subunit of

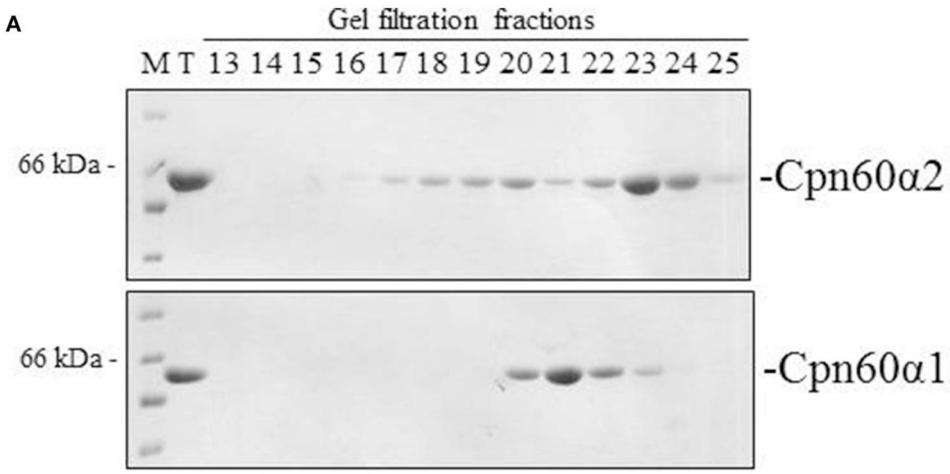

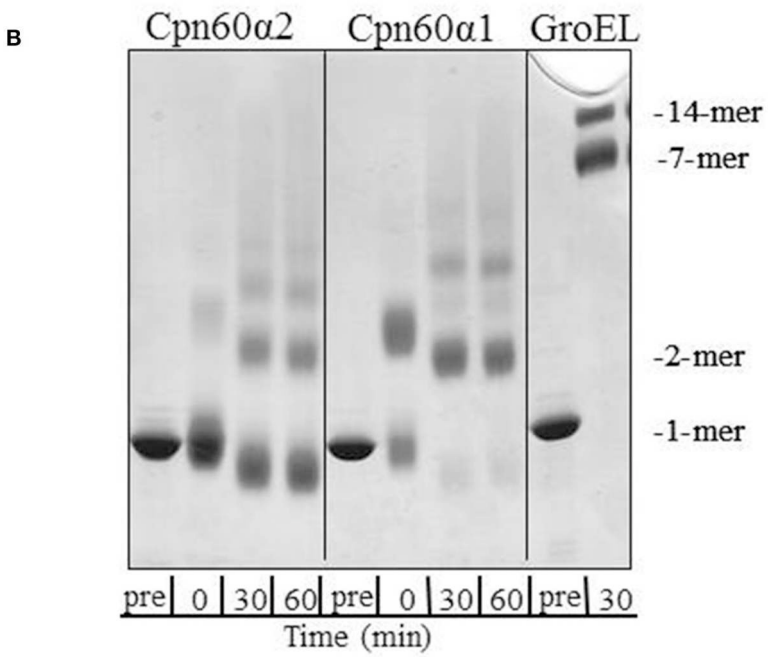

C

Protein	Molecular Mass (kDa)	s value (S)
Cpn60α1	100.4	5
Cpn60α2	64.9	4

FIGURE 1 | The oligomeric state of Cpn60α1 and Cpn60α2 subtypes. **(A)** Elution profile of α1 and α2 from Superdex 200 gel filtration column. 1 mg protein was injected into a Superdex 200 gel filtration column pre-equilibrated with 50 mM Tris-HCl pH 8, 300 mM NaCl, 5% (v/v) glycerol and run at a rate of 1 ml/min for 120 min. Fractions of 3 ml were collected. Five microliters of each fraction was run on an SDS-PAGE mini-gel. M, molecular weight marker; T, total. **(B)** Cross linking pattern of α1 and α2. Twenty micromolar of purified protein was subjected to cross-linking with 0.1% glutaraldehyde, for the indicated times at RT, in a buffer containing 50 mM Na-HEPES pH 8, 10 mM $MgCl_2$ and 100 mM KCl. Samples were analyzed by SDS-PAGE in a 2.4–12% gradient gel and stained with Coomassie Brilliant Blue. **(C)** Analytical ultracentrifugation values for α1 and α2. The data was obtained as described in the Materials and Methods section in buffer: 50 mM Tris-HCl pH 8, 200 mM NaCl, 10 mM $MgCl_2$ and 100 mM KCl.

Chlamydomonas (Bai et al., 2015), which was incapable of forming mixed oligomers with any individual Cpn60β subunit. Interestingly, in Bai et al. these species composed of one α subunit and one β subunit were still capable of complementing a GroEL deletion strain of *E. coli*.

We next examined the ability of α2 to form mixed oligomers with each of the three β subunits. Initially we followed oligomer formation using native gel electrophoresis. As can be seen in **Figure 2** and Figure S2, α2 does not oligomerize on its own, but is able to form mixed oligomers with β1, β2, or β3 homologs.

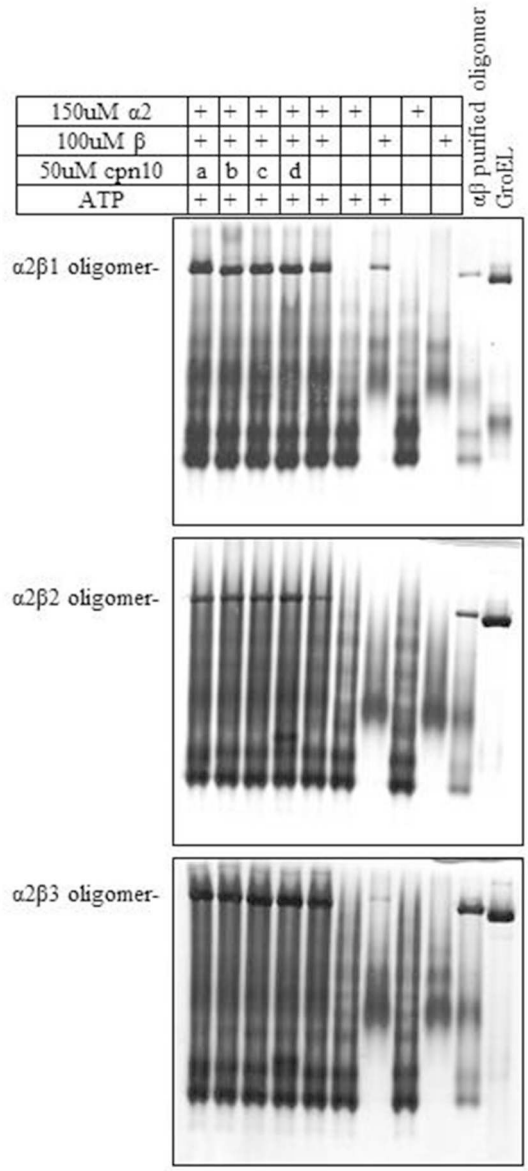

FIGURE 2 | Effect of various Cpn10 homologs on reconstitution of hetero-oligomers. Reconstitution reactions were prepared by incubating 150 μM Cpn60α2 with 100 μM of different Cpn60β subunits and 50 μM of different Cpn10s: a. GroES, b. mt-cpn10, c. Cpn20, d. Cpn10(2), as described in the Materials and Methods section. 1.5 μl of reconstitution product was loaded on a 6% native polyacrylamide gel. Type of oligomeric species formed during the incubation is indicated to the left of the gel.

The oligomerization was induced in the presence of Mg^{2+}-ATP, however, the presence of different Cpn10s slightly improved the reconstitution efficiency, as was shown previously for Cpn60s from other plant, animal and bacterial sources (Dickson et al., 2000; Bai et al., 2015).

Upon scaling up the oligomerization process, we considered several additional factors. On the one hand, Cpn60α and Cpn60β subunits were shown to be organized in the oligomer in an ∼1:1 ratio (Musgrove et al., 1987; Nishio et al., 1999; Dickson et al., 2000). On the other hand, we wanted to ensure that no self-oligomerization of Cpn60β would occur in the reconstitution experiment (when we prepared the mixed Cpn60α2β oligomers). Initially, we were not able to exclude the possibility that a small amount of Cpn60β homo-oligomer was formed during the oligomerization process, together with the hetero-oligomer. The most significant result of this section was the fact that α2β2 hetero-oligomers were found to be stable when separated using gel filtration at 4°C (**Figure 3A** and Figure S3A). This is in comparison to β2 homo-oligomers, which dissociate to monomeric form when exposed to the same temperature (**Figure 3B** and Figure S3B), yet remain stable at room temperature (**Figure 3C** and Figure S3C), as reported in Vitlin et al. (2011). This enabled us to ensure homogeneity of the α2β2 hetero-oligomer preparation. Since α2β2 was the only hetero-oligomer for which we could guarantee a homogeneous preparation, we focused our efforts on α2β2 oligomers and carried out the reconstitution reactions at an excess of Cpn60α2 and at 4°C.

We next examined the chaperonin activity of the α2β2 hetero-oligomers. As demonstrated in **Figure 4** and **Table 1**, the activity of this hetero-oligomer in the presence of chloroplast co-chaperonins [Cpn10(2) and Cpn20] was similar to that of GroEL and reached the maximal yield of ∼80%. It can be seen that α2β2 hetero-oligomer was equally functional with both chloroplast co-chaperonins examined and they both had similar effects on the rate ($t_{1/2} = 4$–5 min) as well.

An interesting observation regarding α2β2 hetero-oligomers is the time dependent accumulation of active MDH, observed in the presence of ATP alone without the addition of any co-chaperonin. This is most likely explained by the low stability of the α2β2 oligomer at this concentration, in the presence of destabilizing ATP and the absence of stabilizing co-chaperonin, resulting in dissociation to Cpn60 monomers and release of partly folded MDH, which spontaneously reaches the native folded state as time passes.

We tested the activity of an additional *Arabidopsis* co-chaperonin, Cpn10(1), which was recently characterized (Vitlin Gruber et al., 2014). As can be seen in **Figure 4**, Cpn10(1) alone is not functional with α2β2 hetero-oligomer. This is consistent with the published results with GroEL and α2β3 hetero-oligomer, where Cpn10(1) was shown to be active only as part of hetero-oligomer with Cpn20 (Vitlin Gruber et al., 2014). Although no protein folding activity is observed, Cpn10(1) has some stabilizing effect on the α2β2 oligomeric structure, indicating that an interaction is taking place between chaperonin and co-chaperonin. Cpn10(1) presence in addition to ATP seems to prevent the hetero-oligomer from dissociating to monomers, thus MDH is not released into the solution and spontaneous

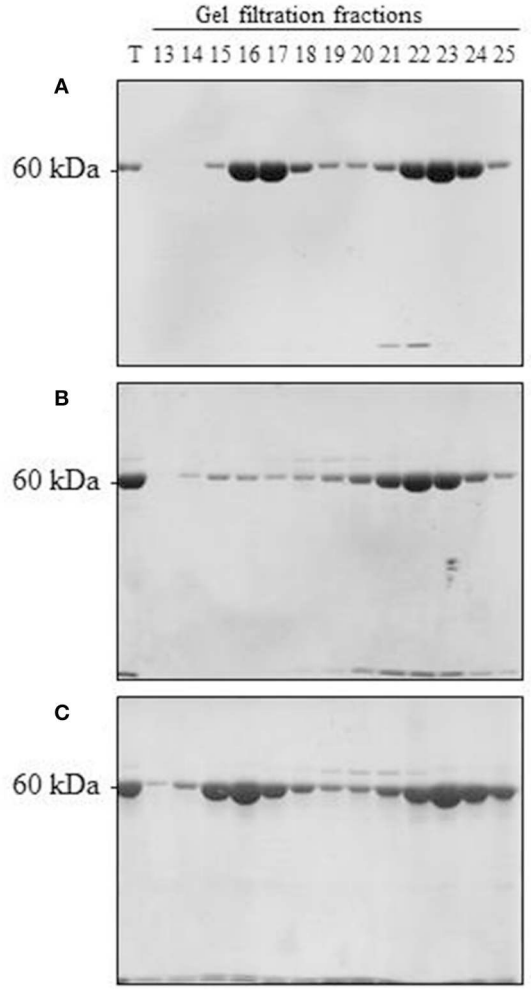

FIGURE 3 | Reconstitution of α2β2 hetero-oligomers and β2 homo-oligomers. **(A)** 150 μM α2, 100 μM β2, and 50 μM mt-cpn10 were reconstituted in a 2 ml reaction mix as indicated in the Materials and Methods section. Samples were then loaded on a Superdex 200 gel filtration column and run at 4°C. Fractions were analyzed by 12 % SDS PAGE and Coomassie Blue staining (7.5 μl was loaded per lane). $T = 0.25$ μl of reconstitution mixture. Oligomer is found in fractions 14–18, monomer is found in fractions 19–25. **(B)** 300 μM β2 and 150 μM mt-cpn10 were reconstituted in a 500 μl reaction and separated by Superdex 200 at 4°C as described in **(A)**. Ten microliters of each fraction was loaded per lane. **(C)** 300 μM β2 and 150 μM mt-cpn10 were reconstituted in a 600 μl reaction and separated by Superdex 200 at room temperature as described in **(B)**.

folding is not detected as it is in the presence of ATP alone. A similar phenomenon was observed in Bonshtien et al. (2009), where Cpn20 from *Arabidopsis* demonstrated similar binding to β homo-oligomers and αβ hetero-oligomers from pea, yet was unable to facilitate refolding of substrate protein with the β homo-oligomers.

DISCUSSION

In this study, we have cloned and purified both types of Cpn60α subunits from *A. thaliana* chloroplast. During the characterization of these subunits, we showed that α1 forms mainly dimers in solution, while α2 formed several low molecular weight oligomeric forms in solution. Neither of these alpha species showed any ability to refold urea-denatured MDH. Monomeric and dimeric forms of Cpn60 are found in a number of bacterial species. For example, evidence of a low molecular weight Cpn60 protein complex exists in *Mycobacterium tuberculosis*, which crystallizes as a dimer (Qamra et al., 2004; Shahar et al., 2011). However, in contrast to the *Arabidopsis* α1, the protein from *M. tuberculosis* exhibits some protein folding activity *in vitro*, oligomerizes to higher order forms in the presence of ammonium sulfate, KCl and ATP, and can replace GroEL *in vivo*, suggesting that the functional form *in vivo* is an oligomer (Fan et al., 2012). Similarly, in cyanobacteria, the GroEL1 protein seems to form unstable, yet functional tetradecamers, while the GroEL2 protein remains monomeric. Both of these species exhibit a low level of protein-refolding activity, which does not depend upon GroES and ATP (Reviewed in Nakamoto and Kojima, 2017). In general, the chloroplast α and β chaperonin subtypes are both thought to have evolved from bacterial GroEL1.

In all studies of chloroplast chaperonins thus far, homologs of the α subunits were incapable of self-assembly to tetradecamers. The foundation for chaperonin oligomerization was consistently shown to be one or more of the β subunits. For *Chlamydomonas* chaperonins, this ability was determined to lie in residues of the equatorial domain and part of the intermediate domain (Zhang et al., 2016). Likewise, for type II chaperonins, it was demonstrated that only CCT4 and CCT5 out of the eight subunits, were capable of oligomerizing on their own, or facilitating oligomerization of a hetero-oligomer (Sergeeva et al., 2013).

In contrast to α1, α2 monomers easily formed mixed oligomers with all types of β subunits tested. An important achievement of this work was our ability to ensure that reconstituted α2β2 hetero-oligomers were not contaminated by β2 homo-oligomers. These pure hetero-tetradecamers were equally and maximally active with authentic *Arabidopsis* chloroplast co-chaperonins: Cpn20 and Cpn10(2). Comparison between the activity pattern of α2β2 hetero-oligomer and the β2 homo-oligomer as published in Vitlin et al. (2011), once again assured us that we are dealing with different species with unique patterns of refolding rate and yield. Although Cpn20 could assist both oligomers to reach a maximal yield, Cpn10(2) served as a functional co-chaperonin only with the α2β2 hetero-oligomer and had a very low activity with β2 homo-oligomer.

Only a limited number of *in vitro* studies have been carried out on chloroplast chaperonin proteins. Starting with the early studies of Roy et al. (1988), it was consistently demonstrated that oligomerization is a very dynamic process and oligomer stability is highly concentration dependent. For example, pea chaperonin in chloroplast lysate preparations was shown to dissociate in the presence of ATP when the lysate was diluted 15-fold (Roy et al., 1988). Successful reconstitution was in general shown to require relatively high concentrations of the protein. This is consistent with an estimated chloroplast chaperonin concentration of 175 μM protomer (Lorimer, 1996).

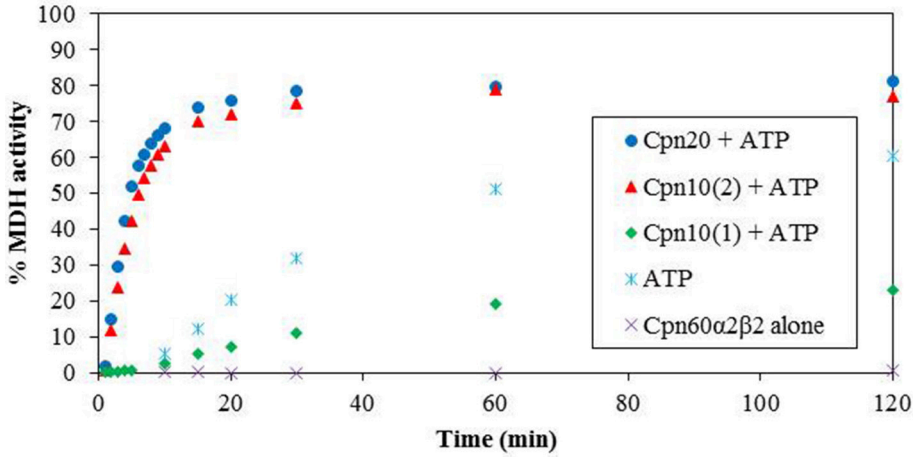

FIGURE 4 | Refolding of denatured MDH by reconstituted α2β2 hetero-oligomers. MDH refolding was carried out by α2β2 hetero-oligomer as described in the Materials and Methods section in 37°C. MDH activity was determined at various time points following the addition of ATP and various Cpn10 homologs. Cpn20: (*filled circle*), Cpn10(2): (*filled triangle*), Cpn10(1): (*filled diamond*), ATP alone: (*asterisk*), α2β2 hetero-oligomer alone: (multi-sign). One hundred percent was taken as the activity of a sample containing a similar amount of native MDH. Values represent the average of two independent experiments.

TABLE 1 | Rates and yields of MDH refolding by αβ hetero-oligomers in the presence of chloroplast co-chaperonins*.

		Cpn20	Cpn10(2)
$t_{½}$ (min)	α2β2	4	4.5
	GroEL	4.5	5
Final refolding yields (%)	α2β2	79.8	78.8
	GroEL	74.7	74.7

Data extracted from **Figure 4 and average of three experiments with GroEL.*

For example, urea-dissociated native pea chloroplast chaperonins were successfully reconstituted at a concentration of 60 μM (Lissin, 1995). Reconstitution of αβ hetero-oligomers cloned from pea was carried out using 30 μM of each protein (Dickson et al., 2000). While reconstitution of *Arabidopsis* β1 and β3 homo-oligomer was achieved at over 50 μM protein, β2 was able to form oligomers only at concentrations >200 μM (Vitlin et al., 2011), near the estimated *in vivo* concentration. In addition, Bonshtien et al. (2009) showed that ATPase activity of reconstituted pea chaperonins reached a stable rate only at 60 μM monomer, presumably representing the concentration at which equilibrium favored the oligomeric state.

In addition to protein concentration, temperature is another factor that was shown to significantly affect the stability of organellar chaperonins *in vitro*. Dissociation of pea chaperonin in the presence of ATP or urea was potentiated by lower temperatures (Lissin, 1995; Viitanen et al., 1995). Dissociation at cold temperature was used by Dickson et al., to obtain a uniform population of β monomers as starting material for oligomeric reconstitution (Dickson et al., 2000). Our previous results showed that β2 oligomers are unable to form at 4°C, although significant oligomerization is observed at 25°C under the same conditions (Vitlin et al., 2011). This is also consistent with the behavior of mitochondrial chaperonins, which were demonstrated to be highly unstable in the presence of ATP at 4°C, yet were stable at 37°C under the same conditions (Weiss, 1997).

In conclusion, we demonstrate a method for reconstituting pure hetero-oligomeric chaperonin particles *in vitro* that are free from contaminating homo-oligomers. This method takes advantage of the difference in oligomeric stability between α2β2 and β2 at 4°C. Our results highlight the complex nature of the chloroplast chaperonin system and emphasize how even the simplest physico-chemical conditions must be taken into account when investigating organellar chaperonins *in vitro*.

MATERIALS AND METHODS

Nomenclature

In this work, we continue with the nomenclature that was established by Hill and Hemmingsen (2001), and which we previously used for *A. thaliana* chloroplast chaperonin subunits (Weiss et al., 2009; Vitlin et al., 2011; Vitlin Gruber et al., 2013a, 2014). It should be noted that different nomenclature is adopted by other groups.

Cpn60 homologs:
At5g18820 (α1 Cpn60)
At2g28000 (α2 Cpn60)
At5g56500 (β1 Cpn60)
At3g13470 (β2 Cpn60)
At1g55490 (β3 Cpn60)
At1g26230 (β4 Cpn60)
Cpn10 homologs
At3g60210 (Cpn10(1))
At2g44650 (Cpn10(2))
At5g20720 (Cpn20)

Cloning and Purification of Chaperonin Subunits

Cpn60α1 (At5g18820) and Cpn60α2 (At2g28000) were cloned between the BamHI-NotI sites of a modified version of pET21d+, which codes for an octa-histidine tag followed by the TEV (Tobacco Etch virus) proteolysis site at the amino terminus of the protein (Opatowsky et al., 2003). The first amino acid of the mature protein was chosen based on presequence predictions (Hill and Hemmingsen, 2001): alanine 33 (α1) and alanine 46 (α2). Due to the nature of the cloning, α1 and α2 contained an additional glycine-serine at the N-terminus of the protein. The constructs were expressed in *E. coli* Rosetta (Novagen) and purified based on the Cpn60β purification protocol (Vitlin et al., 2011).

Previously published protocols were used to purify GroES (Bonshtien et al., 2007), Cpn10(1) (Vitlin Gruber et al., 2014), Cpn10(2) (Sharkia et al., 2003), Cpn20 (Bonshtien et al., 2007), mouse mt-cpn10 (Viitanen et al., 1998), Cpn60β1/2/3 (Vitlin et al., 2011) and GroEL (Bonshtien et al., 2007).

Reconstitution of αβ Hetero-Oligomers

The reconstitution protocols were based on Vitlin et al. (2011). In short, the experiments were carried out in 50 mM Tris-HCl pH 8, 0.3 M NaCl, 10 mM $MgCl_2$, 16 mM KCl, 2 mM dithiothreitol (DTT), 5 mM ATP and different concentrations of Cpn60 and Cpn10 as indicated in the figure legends. The reconstitution mixture was incubated for 5 min at room temperature and then for 1 h at 30°C. For oligomer purification, oligomers and monomers in the reconstitution reaction were separated using a Superdex 200 gel filtration column pre-equilibrated with 50 mM Tris-HCl pH 8, 300 mM NaCl, 5% (v/v) glycerol at 4°C unless stated otherwise. Fractions containing oligomers were pooled, and treated with Ni–NTA-agarose beads in order to remove any traces of his-tagged mt-cpn10 that might have co-purified with the Cpn60. The relevant fractions were concentrated and flash frozen in liquid nitrogen. For oligomerization tests, reconstitution mixtures were run on native 6% polyacrylamide gels.

Cross-Linking

20 μM Cpn60 was cross-linked by 0.1% (v/v) glutaraldehyde (GA—Pierce), at room temperature in 50 mM Na-HEPES (Ph = 7.5), 10 mM $MgCl_2$, 100 mM KCl. The cross-linking reaction was stopped by addition of one-third volume of sample buffer: 62.5 mM Tris-HCl pH 6.8, 2% SDS, 5% β-mercaptoethanol, 20% glycerol, 1 M urea. Samples were boiled for 5 min prior to electrophoresis in a large 2.4–12% gradient SDS-PAGE.

Analytical Ultracentrifugation

All experiments were carried out as described in Vitlin Gruber et al. (2013b).

In Vitro Refolding of Urea-Denatured MDH

RefoldingA experiments were carried out as described in Vitlin et al. (2011).

AUTHOR CONTRIBUTIONS

AV, MV, CW, and AA: conceived the ideas and designed experiments; AV, MV, and CW: performed experiments; AV, MV, CW, and AA: analyzed data; AV, CW, and AA: contributed toward writing the manuscript.

FUNDING

This work was partially funded by a grant from the Israel Science Foundation, grant number ISF-1507/13 to AA.

SUPPLEMENTARY MATERIAL

The Supplementary Material for this article can be found online at: https://www.frontiersin.org/articles/10.3389/fmolb.2018.00005/full#supplementary-material

REFERENCES

Apuya, N. R., Yadegari, R., Fischer, R. L., Harada, J. J., Zimmerman, J. L., and Goldberg, R. B. (2001). The Arabidopsis embryo mutant schlepperless has a defect in the chaperonin-60alpha gene. *Plant Physiol.* 126, 717–730. doi: 10.1104/pp.126.2.717

Bai, C., Guo, P., Zhao, Q., Lv, Z., Zhang, S., Gao, F., et al. (2015). Protomer roles in chloroplast chaperonin assembly and function. *Mol. Plant* 8, 1478–1492. doi: 10.1016/j.molp.2015.06.002

Bonshtien, A. L., Parnas, A., Sharkia, R., Niv, A., Mizrahi, I., Azem, A., et al. (2009). Differential effects of co-chaperonin homologs on cpn60 oligomers. *Cell Stress Chaperones* 14, 509–519. doi: 10.1007/s12192-009-0104-2

Bonshtien, A. L., Weiss, C., Vitlin, A., Niv, A., Lorimer, G. H., and Azem, A. (2007). Significance of the N-terminal domain for the function of chloroplast cpn20 chaperonin. *J. Biol. Chem.* 282, 4463–4469. doi: 10.1074/jbc.M606433200

Cloney, L. P., Bekkaoui, D. R., Feist, G. L., Lane, W. S., and Hemmingsen, S. M. (1994). *Brassica napus* plastid and mitochondrial chaperonin-60 proteins contain multiple distinct polypeptides. *Plant Physiol.* 105, 233–241. doi: 10.1104/pp.105.1.233

Cloney, L. P., Bekkaoui, D. R., and Hemmingsen, S. M. (1993). Co-expression of plastid chaperonin genes and a synthetic plant Rubisco operon in *Escherichia coli*. *Plant Mol. Biol.* 23, 1285–1290. doi: 10.1007/BF00042362

Cloney, L. P., Bekkaoui, D. R., Wood, M. G., and Hemmingsen, S. M. (1992a). Assessment of plant chaperonin-60 gene function in *Escherichia coli*. *J. Biol. Chem.* 267, 23333–23336.

Cloney, L. P., Wu, H. B., and Hemmingsen, S. M. (1992b). Expression of plant chaperonin-60 genes in *Escherichia coli*. *J. Biol. Chem.* 267, 23327–23332.

Dickson, R., Weiss, C., Howard, R. J., Alldrick, S. P., Ellis, R. J., Lorimer, G., et al. (2000). Reconstitution of higher plant chloroplast chaperonin 60 tetradecamers active in protein folding. *J. Biol. Chem.* 275, 11829–11835. doi: 10.1074/jbc.275.16.11829

Fan, M., Rao, T., Zacco, E., Ahmed, M. T., Shukla, A., Ojha, A., et al. (2012). The unusual mycobacterial chaperonins: evidence for *in vivo* oligomerization and specialization of function. *Mol. Microbiol.* 85, 934–944. doi: 10.1111/j.1365-2958.2012.08150.x

Feiz, L., Williams-Carrier, R., Wostrikoff, K., Belcher, S., Barkan, A., and Stern, D. B. (2012). Ribulose-1,5-bis-phosphate carboxylase/oxygenase accumulation

factor1 is required for holoenzyme assembly in maize. *Plant Cell* 24, 3435–3446. doi: 10.1105/tpc.112.102012

Hemmingsen, S. M., Woolford, C., van der Vies, S. M., Tilly, K., Dennis, D. T., Georgopoulos, C. P., et al. (1988). Homologous plant and bacterial proteins chaperone oligomeric protein assembly. *Nature* 333, 330–334. doi: 10.1038/333330a0

Hill, J. E., and Hemmingsen, S. M. (2001). *Arabidopsis thaliana* type I and II chaperonins. *Cell Stress Chaperones* 6, 190–200. doi: 10.1379/1466-1268(2001)006<0190:ATTIAI>2.0.CO;2

Jiang, Q., Mei, J., Gong, X. D., Xu, J. L., Zhang, J. H., Teng, S., et al. (2014). Importance of the rice TCD9 encoding α subunit of chaperonin protein 60 (Cpn60α) for the chloroplast development during the early leaf stage. *Plant Sci.* 215–216, 172–179. doi: 10.1016/j.plantsci.2013.11.003

Johnson, R. B., Fearon, K., Mason, T., and Jindal, S. (1989). Cloning and characterization of the yeast chaperonin HSP60 gene. *Gene* 84, 295–302. doi: 10.1016/0378-1119(89)90503-9

Ke, X., Zou, W., Ren, Y., Wang, Z., Li, J., Wu, X., et al. (2017). Functional divergence of chloroplast Cpn60α subunits during Arabidopsis embryo development. *PLoS Genet.* 13:e1007036. doi: 10.1371/journal.pgen.1007036

Kim, S.-R., Yang, J.-I., and An, G. (2013). OsCpn60α1, encoding the plastid chaperonin 60α subunit, is essential for folding of rbcL. *Mol. Cells* 35, 402–409. doi: 10.1007/s10059-013-2337-2

Lissin, N. M. (1995). *In vitro* dissociation and self-assembly of three chaperonin 60s: the role of ATP. *FEBS Lett.* 361, 55–60. doi: 10.1016/0014-5793(95)00151-X

Lorimer, H. G. (1996). A quantitative assessment of the role of the chaperonin proteins in protein folding *in vivo*. *FASEB J.* 10, 5–9.

Martel, R., Cloney, L. P., Pelcher, L. E., and Hemmingsen, S. M. (1990). Unique composition of plastid chaperonin-60: α and β polypeptide-encoding genes are highly divergent. *Gene* 94, 181–187. doi: 10.1016/0378-1119(90)90385-5

Musgrove, J. E., Johnson, R. A., and Ellis, R. J. (1987). Dissociation of the ribulosebisphosphate-carboxylase large-subunit binding protein into dissimilar subunits. *Eur. J. Biochem.* 163, 529–534. doi: 10.1111/j.1432-1033.1987.tb10900.x

Nakamoto, H., and Kojima, K. (2017). Non-housekeeping, non-essential GroEL (chaperonin) has acquired novel structure and function beneficial under stress in cyanobacteria. *Physiol. Plant.* 161, 296–310. doi: 10.1111/ppl.12595

Nishio, K., Hirohashi, T., and Nakai, M. (1999). Chloroplast chaperonins: evidence for heterogeneous assembly of alpha and beta Cpn60 polypeptides into a chaperonin oligomer. *Biochem. Biophys. Res. Commun.* 266, 584–587. doi: 10.1006/bbrc.1999.1868

Opatowsky, Y., Chomsky-Hecht, O., Kang, M.-G., Campbell, K. P., and Hirsch, J. A. (2003). The voltage-dependent calcium channel beta subunit contains two stable interacting domains. *J. Biol. Chem.* 278, 52323–52332. doi: 10.1074/jbc.M303564200

Peng, L., Fukao, Y., Myouga, F., Motohashi, R., Shinozaki, K., and Shikanai, T. (2011). A chaperonin subunit with unique structures is essential for folding of a specific substrate. *PLoS Biol.* 9:e1001040. doi: 10.1371/journal.pbio.1001040

Qamra, R., Srinivas, V., and Mande, S. C. (2004). *Mycobacterium tuberculosis* GroEL homologues unusually exist as lower oligomers and retain the ability to suppress aggregation of substrate proteins. *J. Mol. Biol.* 342, 605–617. doi: 10.1016/j.jmb.2004.07.066

Roy, H., Hubbs, A., and Cannon, S. (1988). Stability and dissociation of the large subunit RuBisCO binding protein complex *in vitro* and in Organello. *Plant Physiol.* 86, 50–53. doi: 10.1104/pp.86.1.50

Seale, J. W., Gorovits, B. M., Ybarra, J., and Horowitz, P. M. (1996). Reversible oligomerization and denaturation of the chaperonin GroES. *Biochemistry* 35, 4079–4083. doi: 10.1021/bi953087n

Sergeeva, O. A., Chen, B., Haase-Pettingell, C., Ludtke, S. J., Chiu, W., and King, J. A. (2013). Human CCT4 and CCT5 chaperonin subunits expressed in *Escherichia coli* form biologically active homo-oligomers. *J. Biol. Chem.* 288, 17734–17744. doi: 10.1074/jbc.M112.443929

Shahar, A., Melamed-Frank, M., Kashi, Y., Shimon, L., and Adir, N. (2011). The dimeric structure of the Cpn60.2 chaperonin of *Mycobacterium tuberculosis* at 2.8 Å reveals possible modes of function. *J. Mol. Biol.* 412, 192–203. doi: 10.1016/j.jmb.2011.07.026

Sharkia, R., Bonshtien, A. L., Mizrahi, I., Weiss, C., Niv, A., Lustig, A., et al. (2003). On the oligomeric state of chloroplast chaperonin 10 and chaperonin 20. *Biochim. Biophys. Acta Proteins Proteomics* 1651, 76–84. doi: 10.1016/S1570-9639(03)00237-1

Suzuki, K., Nakanishi, H., Bower, J., Yoder, D. W., Osteryoung, K. W., and Miyagishima, S. (2009). Plastid chaperonin proteins Cpn60α and Cpn60β are required for plastid division in *Arabidopsis thaliana*. *BMC Plant Biol.* 9:38. doi: 10.1186/1471-2229-9-38

Viitanen, P. V., Bacot, K., Dickson, R., and Webb, T. (1998). Purification of recombinant plant and animal GroES homologs: chloroplast and mitochondrial chaperonin. *Methods Enzymol.* 290, 218–230. doi: 10.1016/S0076-6879(98)90021-0

Viitanen, P. V., Schmidt, M., Buchner, J., Suzuki, T., Vierling, E., Dickson, R., et al. (1995). Functional characterization of the higher plant chloroplast chaperonins. *J. Biol. Chem.* 270, 18158–18164. doi: 10.1074/jbc.270.30.18158

Vitlin, A., Weiss, C., Demishtein-Zohary, K., Rasouly, A., Levin, D., Pisanty-Farchi, O., et al. (2011). Chloroplast β chaperonins from *A. thaliana* function with endogenous cpn10 homologs *in vitro*. *Plant Mol. Biol.* 77, 105–115. doi: 10.1007/s11103-011-9797-6

Vitlin Gruber, A., Nisemblat, S., Azem, A., and Weiss, C. (2013a). The complexity of chloroplast chaperonins. *Trends Plant Sci.* 18, 688–694. doi: 10.1016/j.tplants.2013.08.001

Vitlin Gruber, A., Nisemblat, S., Zizelski, G., Parnas, A., Dzikowski, R., Azem, A., et al. (2013b). *P. falciparum* cpn20 is a bona fide co-chaperonin that can replace GroES in *E. coli*. *PLoS ONE* 8:e53909. doi: 10.1371/journal.pone.0053909

Vitlin Gruber, A., Zizelski, G., Azem, A., and Weiss, C. (2014). The Cpn10(1) co-chaperonin of *A. thaliana* functions only as a hetero-oligomer with Cpn20. *PLoS ONE* 9:e113835. doi: 10.1371/journal.pone.0113835

Weiss, C. (1997). *Analysis of the Structure-Function Relationship of the GroE Chaperonin*. Available online at: https://huji-primo.hosted.exlibrisgroup.com/primo-explore/fulldisplay?docid=972HUJI_ALMA21164336530003701&context=L&vid=972HUJI_V1&lang=en_US&search_scope=default_scope&adaptor=LocalSearchEngine&tab$=$default_tab&query$=$any,contains,celesteweiss&sortby$=$ra

Weiss, C., Bonshtien, A., Farchi-Pisanty, O., Vitlin, A., and Azem, A. (2009). Cpn20: Siamese twins of the chaperonin world. *Plant Mol. Biol.* 69, 227–238. doi: 10.1007/s11103-008-9432-3

Zhang, S., Zhou, H., Yu, F., Bai, C., Zhao, Q., He, J., et al. (2016). Structural insight into the cooperation of chloroplast chaperonin subunits. *BMC Biol.* 14:29. doi: 10.1186/s12915-016-0251-8

Conflict of Interest Statement: The authors declare that the research was conducted in the absence of any commercial or financial relationships that could be construed as a potential conflict of interest.

frontiers in Molecular Biosciences

REVIEW
published: 20 April 2018
doi: 10.3389/fmolb.2018.00035

Toward Developing Chemical Modulators of Hsp60 as Potential Therapeutics

*Qianli Meng, Bingbing X. Li and Xiangshu Xiao**

Program in Chemical Biology, Department of Physiology and Pharmacology, Oregon Health and Science University, Portland, OR, United States

The 60 kDa heat shock protein (Hsp60) is classically known as a mitochondrial chaperonin protein working together with co-chaperonin 10 kDa heat shock protein (Hsp10). This chaperonin complex is essential for folding proteins newly imported into mitochondria. However, Hsp60, and/or Hsp10 have also been shown to reside in other subcellular compartments including extracellular space, cytosol, and nucleus. The proteins in these extra-mitochondrial compartments may possess a wide range of functions dependent or independent of its chaperoning activity. But the mechanistic details remain unknown. Mutations in *Hsp60* gene have been shown to be associated with neurodegenerative disorders. Abnormality in expression level and/or subcellular localization have also been detected from different diseased tissues including inflammatory diseases and various cancers. Therefore, there is a strong interest in developing small molecule modulators of Hsp60. Most of the reported inhibitors were discovered through various chemoproteomics strategies. In this review, we will describe the recent progress in this area with reported inhibitors from both natural products and synthetic compounds. The former includes mizoribine, epolactaene, myrtucommulone, stephacidin B, and avrainvillamide while the latter includes *o*-carboranylphenoxyacetanilides and gold (III) porphyrins. The potencies of the known inhibitors range from low micromolar to millimolar concentrations. The potential applications of these inhibitors include anti-cancer, anti-inflammatory diseases, and anti-autoimmune diseases.

Keywords: autoimmune, cancer, chaperone, GroEL, GroES, Hsp60, Hsp10, inhibitor

OPEN ACCESS

Edited by:
Abdussalam Azem,
Tel Aviv University, Israel

Reviewed by:
Alberto J. L. Macario,
University of Maryland, United States
Mark Thomas Fisher,
Kansas University of Medical Center Research Institute, United States

****Correspondence:***
Xiangshu Xiao
xiaoxi@ohsu.edu

Specialty section:
This article was submitted to Protein Folding, Misfolding and Degradation, a section of the journal Frontiers in Molecular Biosciences

Received: *03 January 2018*
Accepted: *26 March 2018*
Published: *20 April 2018*

Citation:
Meng Q, Li BX and Xiao X (2018) Toward Developing Chemical Modulators of Hsp60 as Potential Therapeutics. Front. Mol. Biosci. 5:35. doi: 10.3389/fmolb.2018.00035

INTRODUCTION

Anfinsen's pioneering experiments demonstrated that the primary amino acid sequences of small proteins will dictate their final native conformations (Anfinsen, 1973). For larger proteins, however, molecular chaperones are needed in the cells to help achieve their native conformations (Bukau and Horwich, 1998; Finka et al., 2016). The human 60 kDa heat shock protein 60 (Hsp60), which is also known as 60 kDa chaperonin (Cpn60) and was initially cloned by Jindal et al. (1989), is the homolog of bacterial GroEL (Hemmingsen et al., 1988). GroEL, in conjunction with cochaperonin GroES is the major molecular chaperone in bacteria to help unfolded and/or partially folded polypeptides fold into their native conformations. Increasing evidence has also shown that the GroEL-GroES complex plays a critical role in partial unfolding of misfolded

intermediates for further folding (Shtilerman et al., 1999; Lin et al., 2008; Weaver et al., 2017). Structural studies have shown that the GroEL-GroES complex undergoes extensive conformational changes during the folding pathway wherein the hydrophobic patches can initially bind unfolded polypeptides primarily through hydrophobic interactions (Finka et al., 2016). Large conformational changes in GroEL help fold the hydrophobic residues in the substrates into protein interior to facilitate folding. The conformational changes of GroEL are driven by multiple factors including GroES binding, substrate binding, ATP binding and ATP hydrolysis (Horwich and Fenton, 2009).

Hsp60 was initially characterized as a nuclear-encoded mitochondrial protein to help fold proteins newly imported into mitochondria in conjunction with co-chaperonin Hsp10 (10 kDa heat shock protein) (Jindal et al., 1989; Ostermann et al., 1989; Reading et al., 1989). Interestingly, anti-folding activity of Hsp60 has also been reported for certain substrates (e.g., cytochrome b_2) shortly after the discovery of Hsp60 as a molecular chaperone (Koll et al., 1992). While Hsp60 was thought to be only localized in mitochondria, accumulating data support that it is localized in extramitochondrial compartments as well. These include cytosol (Soltys and Gupta, 1996; Kirchhoff et al., 2002; Chun et al., 2010; Campanella et al., 2012; Kalderon et al., 2015), outer mitochondrial surface (Soltys and Gupta, 1996), cell surface (Soltys and Gupta, 1996, 1997; Piselli et al., 2000; Feng et al., 2002), intracellular vesicles (Soltys and Gupta, 1996), nucleus (Itoh et al., 1995), extracellular space (Soltys and Gupta, 1996; Gupta and Knowlton, 2007), and even in blood circulation (Pockley et al., 1999; Lewthwaite et al., 2002; Shamaei-Tousi et al., 2007; Hamelin et al., 2011). While the function of Hsp60 in these extra-mitochondrial compartments might also involve its chaperoning activity, it is unlikely that its functions in these different locations can be explained solely by its chaperoning activity. Therefore, Hsp60 can be considered as a protein with moonlighting functions (Henderson et al., 2013). In this article, we review the development of chemical modulators of Hsp60 as potential therapeutics. We will primarily focus on the mammalian Hsp60 whereas the bacterial counterpart will be provided as necessary background and comparison purposes.

Hsp60 AND HUMAN DISEASES

As a mitochondrial chaperone, Hsp60 is essential for mitochondrial protein homeostasis (Cheng et al., 1989; Ostermann et al., 1989). The significance of Hsp60 in humans is further illustrated by many disease-associated mutations in *Hsp60* (also called *HSPD1*) (Hansen et al., 2002, 2007; Parnas et al., 2009; Christensen et al., 2010; Bross and Fernandez-Guerra, 2016). For example, V98I mutation in Hsp60 was reported to be associated with hereditary spastic paraplegia SPG13, a rare neurodegenerative disorder characterized by spasticity and weakness of the lower limbs (Hansen et al., 2002; Bross et al., 2008). No effective treatment for SPG13 exists. Biochemically, this mutation is accompanied with reduced capacity in refolding Hsp60 client proteins (Bross et al., 2008). Another mutation in Hsp60 (D27G or D3G in the mature form) was identified from a large kindred with 10 patients suffering from MitCHAP-60 disease, which is an autosomal-recessive neurodegenerative disorder (Magen et al., 2008). This debilitating early onset disease is characterized by hypomyelination and leukodystrophy in the brain. In an attempt to understand the mechanism by which this mutation contributes to the disease, it was found that the D3G mutant was less stable in forming heptameric and tetradecameric oligomers than wild type. This is further accompanied with decreased refolding capacity and ATPase activity (Parnas et al., 2009). Despite the clear connection of these Hsp60 mutants with impaired refolding activity, how these mutations and their defects in refolding activity contribute to the disease pathogenesis remains to be determined.

Besides Hsp60 mutations, abnormal expression level of Hsp60 has also been reported to associate with various diseases, which may also underscore the importance of unique localization pattern of Hsp60 as mentioned above. Hsp60 has been reported to be involved in inflammatory responses and immune reactions (Pockley, 2003). Therefore, the expression level of Hsp60 can potentially modulate these pathophysiological pathways. For example, the expression level of Hsp60 in skin allografts could modulate the host rejection toward the allografts where high level of expression leads to enhanced rejection in non-obese diabetic (NOD) mice (Birk et al., 1999). In this regard, Hsp60 has been shown to be able to function as an autoantigen and the Hsp60 autoimmunity can be modulated in NOD mice by subcutaneous injection of mouse Hsp60 peptides (Elias et al., 1990). This vaccination is protective against allograft rejection (Birk et al., 1999). Mechanistically, this Hsp60 vaccination strategy appears to involve a shift in the phenotype of the T cell response to self Hsp60 from a proinflammatory Th1 type of response to a Th2 regulatory type of response (Elias et al., 1997; Birk et al., 1999). The concept that endogenous Hsp60 can function as an autoantigen leading to production of anti-Hsp60 antibody has also been validated in humans. Patients with spondyloarthritis or periodontitis present higher tier of Hsp60 antibody than normal healthy volunteers (Tabeta et al., 2000; Hjelholt et al., 2013). However, human serum anti-Hsp60 level seems to be independent of predicting kidney allograft rejection (Trieb et al., 2000). The autoimmunity against Hsp60 may serve as a protective factor against the development of atherosclerosis upon aging (Wick, 2016; Zhong et al., 2016). The Hsp60's role as an autoantigen has also been illustrated in the development of a range of other autoimmune diseases including Hashimoto's thyroiditis (Marino Gammazza et al., 2014; Tonello et al., 2015), myasthenia gravis (Astarloa and Castrillo, 1996; Cappello et al., 2010; Marino Gammazza et al., 2012), inflammatory bowel diseases (Tomasello et al., 2011; Füst et al., 2012), chronic obstructive pulmonary diseases (COPD) (Cappello et al., 2011). The involvement of Hsp60 in these different autoimmune diseases is very interesting because one of the clinically used immunosuppressant mizoribine targets Hsp60 (see below).

Hsp60 is also implicated in the cell survival and apoptosis signaling pathways (Czarnecka et al., 2006), the balance of which

is the key to the pathogenesis of cancers (Hanahan and Weinberg, 2011). Increased protein level of Hsp60 has been detected from both solid tumor tissues including breast (Bini et al., 1997; Desmetz et al., 2008), colon (Cappello et al., 2003a; He et al., 2007), cervix (Cappello et al., 2002; Hwang et al., 2009), prostate (Cappello et al., 2003b; Castilla et al., 2010), lung (Xu et al., 2011), ovary (Hjerpe et al., 2013), and liquid tumor samples including acute myeloid leukemia (AML) (Thomas et al., 2005). In many of the cases examined, higher expression is correlated with poorer prognosis (Thomas et al., 2005; Xu et al., 2011; Hjerpe et al., 2013). On the other hand, higher expression of Hsp60 was observed in early-stage ovarian cancer than advanced-stage in one other report (Schneider et al., 1999). As mentioned above, Hsp60 has been detected in blood circulation. A few studies have suggested that circulating Hsp60 protein level or the autoantibody against Hsp60 has potential value in early detection of colorectal cancer and breast cancer (He et al., 2007; Desmetz et al., 2008; Hamelin et al., 2011). If proven, this will add significantly to the field of cancer early detection. The extracellular Hsp60 does not seem to be present as a free form. Instead, several studies (Merendino et al., 2010; Campanella et al., 2012; Hayoun et al., 2012; Caruso Bavisotto et al., 2017) have shown that Hsp60 is packaged in exosomes, which are extracellular vesicles involved in intercellular communications (van Niel et al., 2018). The exosome-localized Hsp60 has been proposed to be actively secreted via endoplasmic reticulum-Golgi secretory pathway, which is inhibitable by brefeldin A or monensin (Campanella et al., 2012; Hayoun et al., 2012). The secreted Hsp60 was also found to be glycosylated in the secretory pathway (Hayoun et al., 2012). Interestingly, Hsp60 from normal cells does not seem to be secreted via this mechanism (Hayoun et al., 2012). Furthermore, it was recently found that a human lung-derived carcinoma cell line H292 treated with a histone deacetylase inhibitor vorinostat showed elevated Hsp60 level in exosomes (Campanella et al., 2016) although the potential clinical significance of this finding remains to be established.

Hsp60's exact role during carcinogenesis is not very clear (Cappello and Zummo, 2005) and it is possible that the altered expression in different cancers is due to its moonlighting functions outside mitochondria. In this regard, cytosolic Hsp60 has been shown to directly interact with the inhibitor of κB kinase (IKK) to promote TNFα-mediated activation of NF-κB-dependent gene transcription and survival of cancer cells (Chun et al., 2010). Hsp60 has also been observed to interact with β-catenin to enhance its transcription activity in the Wnt signaling pathway and promote cancer cell metastasis (Tsai et al., 2009). This interaction likely occurs in the cytosol instead of mitochondria.

Hsp60 MODULATORS

As described above, the Hsp60-Hsp10 chaperone complex is very important in maintaining mitochondrial homeostasis and plays a critical role in different diseases including autoimmune diseases and cancers. Developing small molecule modulators that can target Hsp60 is potentially useful as therapeutics in these disease areas (Nakamura and Minegishi, 2013; Cappello et al., 2014). In addition, such small molecule modulators can be powerful chemical tools to further elucidate the biological functions of Hsp60 in different contexts. Although numerous natural and synthetic compounds have been developed to target another chaperone protein Hsp90, relative few have been developed to target Hsp60 (Nakamura and Minegishi, 2013; Pace et al., 2013; Cappello et al., 2014; Radons, 2017). Most the Hsp60 inhibitors developed so far are derived from chemoproteomics studies of known bioactive compounds. The known Hsp60 inhibitors are either from natural products or synthetic compounds. Mechanistically, these inhibitors can be classified into two types. Type I inhibitors are found to block ATP binding and hydrolysis. Because the ATP-dependent conformational changes are affected, the Hsp60-Hsp10's refolding activity is inhibited by these inhibitors. Type II inhibitors include compounds that covalently react with certain cysteine residues in Hsp60. However, the details of these inhibitors' binding sites have not been revealed definitely. The following section will summarize the known Hsp60 modulators. We classify the inhibitors based on their sources of discovery, i.e., natural products or synthetic compounds.

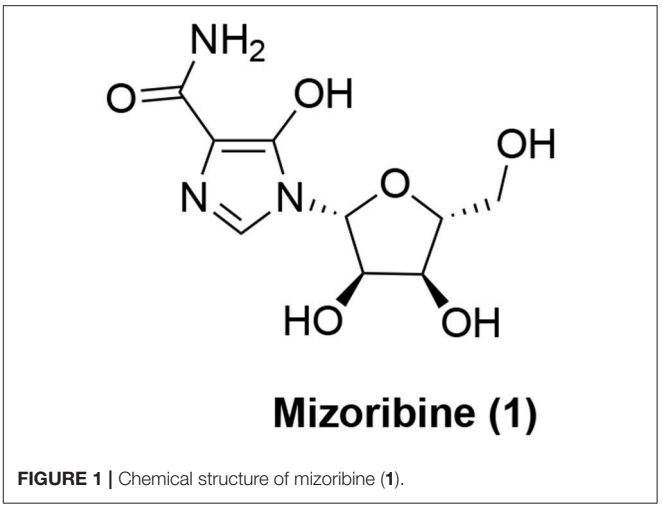

FIGURE 1 | Chemical structure of mizoribine (**1**).

Natural Products-Based Hsp60 Inhibitors

The search for small molecule inhibitors of Hsp60 started with natural products. The first small organic molecule to be known as an Hsp60 inhibitor is mizoribine (**1**, **Figure 1**). Mizoribine is an imidazole nucleoside antibiotics and was isolated from *Eupenicillium brefeldianum* (Mizuno et al., 1974). Mizoribine is devoid of anti-microbial activity, but has potent immunosuppressive activity (Mizuno et al., 1974) and has been used clinically after renal transplantation (Tajima et al., 1984). Its immunosuppressive activity is postulated to be related to mizoribine monophosphate derived from adenosine kinase reaction after cellular uptake. Mizoribine monophosphate inhibits inosine monophosphate (IMP) dehydrogenase and guanosine monophosphate (GMP) synthase resulting in depletion of intracellular GTP level to block T cell proliferation (Turka et al., 1991). In an effort to identify the direct binding

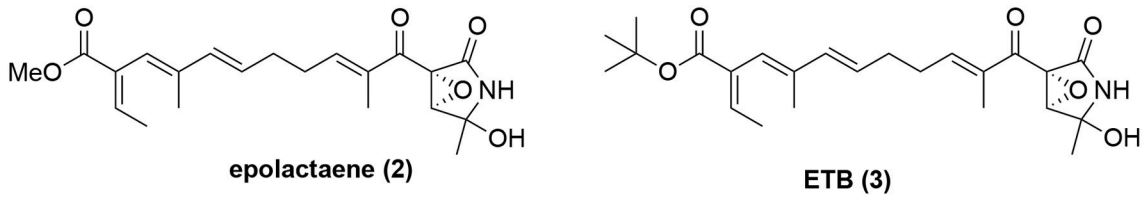

FIGURE 2 | Chemical structures of epolactaene (**2**) and its *tert*-butyl ester ETB (**3**).

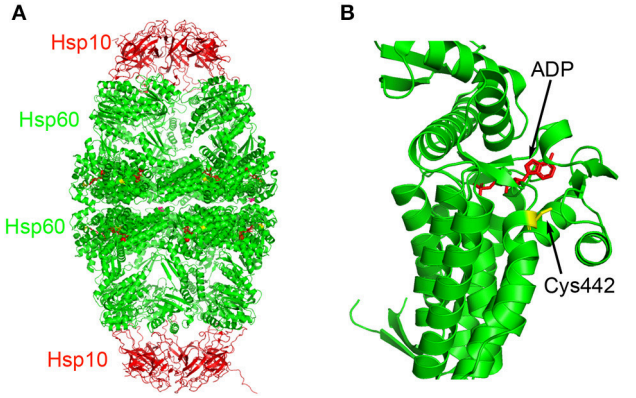

FIGURE 3 | Binding site of ETB on Hsp60. **(A)** The Hsp60-Hsp10 complex (PDB: 4PJ1) is color-coded in red (Hsp10) and green (Hsp60) cartoons. The ADP molecules are presented in stick model in red and Cys442 residues are presented in stick model in yellow. **(B)** Close-up of the ADP binding pocket along with Cys442 in Hsp60.

proteins of mizoribine, an affinity reagent was prepared based on mizoribine and found that it bound to Hsp60 (Itoh et al., 1999). This direct binding led to inhibition of the chaperone activity of the Hsp60-Hsp10 complex. The ATPase activity of Hsp60 was also inhibited by mizoribine, which was accompanied with more stable association of Hsp10 with Hsp60 (Tanabe et al., 2012). Interestingly, the effect of mizoribine on the bacterial GroEL-GroES complex is much less pronounced (Tanabe et al., 2012), suggesting that selective targeting can be achieved even with the highly homologous proteins. As mentioned above, Hsp60 is also involved in autoimmunity, it is tentative to speculate that mizoribine's activity on the Hsp60-Hsp10 complex or Hsp60 alone may also contribute to its immunosuppressive effect although supplementing GTP could reverse mizoribine's immunosuppressive effect (Turka et al., 1991). In this respect, it is of note that mM concentrations of mizoribine are needed to inhibit Hsp60's activity (Tanabe et al., 2012) while the clinically achievable plasma concentrations of mizoribine were only ∼30 μM (Honda et al., 2006). However, further medicinal chemistry optimization of mizoribine to improve its Hsp60-targeting activity has not been reported.

Another natural product known to inhibit Hsp60 is epolactaene (**2**, **Figure 2**), which was originally isolated from the fungal strain *Penicillium* sp. BM 1689-P and was shown to be able to promote neurite outgrowth in SH-SY5Y cells (Kakeya et al., 1995). Its *tert*-butyl ester ETB (**3**, **Figure 2**) was shown to be as active as epolactaene (Nagumo et al., 2004). However, it had an unknown mechanism of action. To identify the direct molecular targets of ETB, a biotinylated ETB was synthesized for pulldown experiments (Nagumo et al., 2005). Mass spectrometry identification of the precipitated proteins identified that ETB bound to Hsp60. In a competition experiment, ETB was shown to selectively bind to Hsp60 without appreciable binding to other chaperone proteins including Hsp70 and Hsp90 (Nagumo et al., 2005). This binding interaction also led to inhibition of Hsp60-Hsp10's chaperoning activity. Further biochemical studies showed that ETB covalently reacted with Cys442 of Hsp60 (Nagumo et al., 2005). Mapping this residue to the recently solved X-ray crystal structure of human Hsp60-Hsp10 complex (Nisemblat et al., 2015) revealed that it is located at a site in close proximity to the ATP binding pocket (**Figure 3**), suggesting potential allosteric modulation. Although there are multiple reactive electrophilic centers in ETB, the α,β-unsaturated ketone is the most likely conjugation site for ETB based on additional structure-activity relationship (SAR) studies (Nagumo et al., 2004). Interestingly, ETB does not inhibit the ATPase activity of Hsp60 (Ban et al., 2010), suggesting that the covalent interaction between ETB and Cys442 may allosterically modulate Hsp60-Hsp10's chaperoning activity without interfering with its ATPase activity. While Cys442 modification does not modulate Hsp60's ATPase activity, Cys138 alkylation in GroEL significantly enhances its ATPase activity although these Cys residues are not conserved (Martin, 1998; Parnas et al., 2012). Despite the clear biochemical evidence to support that ETB targets Hsp60, it remains to be established how this binding and modulation of Hsp60 are linked to ETB's activity in promoting neurite outgrowth in SH-SY5Y cells.

Recently, myrtucommulone A (MC, **4**, **Figure 4**) was identified as yet another natural product to inhibit Hsp60 (Wiechmann et al., 2017). MC is a non-prenylated acylphloroglucinol with multiple reported bioactivities, including antibacterial (Rotstein et al., 1974; Appendino et al., 2002), antioxidant (Rosa et al., 2003), anti-inflammatory (Feisst et al., 2005; Rossi et al., 2009), and anti-tumor properties (Tretiakova et al., 2008; Grandjenette et al., 2015; Izgi et al., 2015). MC was found to act on isolated mitochondria from human leukemia cells, and to affect mitochondrial functions at submicromolar concentrations, including loss of mitochondrial

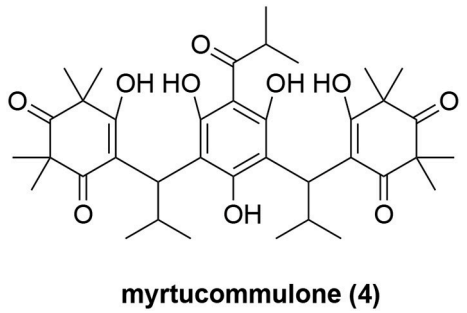

myrtucommulone (4)

FIGURE 4 | Chemical structure of myrtucommulone A (MC, **4**).

membrane potential ($\Delta\psi$m), reduction of mitochondrial viability and inhibition of mitochondrial ATP synthesis (Wiechmann et al., 2015). But the exact molecular targets of MC within mitochondria were unknown. Toward this end, MC was immobilized onto sepharose resin to pulldown cellular proteins that might bind to MC (Wiechmann et al., 2017). Although multiple protein bands were observed to bind to MC, Hsp60 was the most prominent one. Further biochemical validation experiments showed that Hsp60 is a direct mitochondrial protein target of MC and MC inhibited the refolding activity of the Hsp60-Hsp10 complex. Moreover, the authors also proposed that Hsp60 is likely to protect the mitochondrial proteins Lon protease-like protein (LONP) and leucine-rich protein 130 (LRP130) against heat-shock-induced aggregation because they are both significantly influenced by MC (Wiechmann et al., 2017). While MC clearly can modulate Hsp60's activity, it was reported that MC also targets microsomal prostaglandin E2 synthase 1 (mPGES-1) and 5-lipoxygenase (5-LOX) (Feisst et al., 2005; Koeberle et al., 2009) to affect arachidonic acid metabolism. To further probe the Hsp60 biology with MC and assess its therapeutic potential, it will be critical to develop MC analogs that are devoid of these other biological activities. Its high hydrophobicity (cLogP = 5.5) and presence of multiple redox-active groups pose nontrivial challenges to develop improved analogs.

In addition to the above-mentioned natural products, several other natural products were also reported to interact with Hsp60 although stringent validation data are lacking. Stephacidin B (**5**, **Figure 5**) is a natural product isolated from *Aspergillus ochraceus* WC76466 (Qian-Cutrone et al., 2002) while avrainvillamide (**6**) was isolated from *Aspergillus* sp. CNC358 (Fenical et al., 2000). Both of them showed potent *in vitro* anticancer activities. It was found that dimeric stephacidin B (**5**) was converted into monomeric **6** in tissue culture media and suggested that **6** was the actual active species during cellular experiments (Wulff et al., 2007). Indeed, after correcting molar equivalent, **5** and **6** had almost identical activity in the cellular assays. Furthermore, a simplified undimerizable analog **7** also presented anticancer activity albeit with reduced potency (Wulff et al., 2007). To identify the potential binding targets of **7**, a biotinylated derivative of **7** was prepared to pulldown its targets. This identified Hsp60 as one of the putative targets for **7** and perhaps for **5** and **6** (Wulff et al., 2007). However, further validation studies have yet to be performed and whether these complex natural products are *bona fide* Hsp60 modulators remains to be established.

Hsp60 Inhibitors Originated From Synthetic Sources

Besides the natural products identified above as potential Hsp60 modulators, quite a few synthetic molecules have also been discovered to be able to modulate Hsp60. In 2010, *o*-carboranylphenoxyacetanilide **8** (**Figure 6**) was identified as a hypoxia-inducible factor 1 alpha (HIF-1α) inhibitor using a transcription reporter assay (Shimizu et al., 2010). HIF-1α is often stabilized and activated in cancer tissues and inhibiting HIF-1α's transcription activity has great potential to develop novel cancer therapeutics (Semenza, 2003). To identify the direct molecular targets of *o*-carboranylphenoxyacetanilide, a clickable photoaffinity probe **9** was designed and synthesized based on *o*-carboranylphenoxyacetanilide (**Figure 6**; Ban et al., 2010). The benzophenone moiety in probe **9** could covalently crosslink with the direct target proteins upon ultraviolet (UV) irradiation. Then the propargyl group in probe **9** can be clicked with Alexa Fluor 488 azide to visualize the proteins bound to the probe. Using this strategy, it was found that *o*-carboranylphenoxyacetanilide bound to Hsp60 (Ban et al., 2010). Under the same conditions, the probe **9** did not label other heat shock proteins including Hsp90 and Hsp70 (Ban et al., 2010), suggesting specific binding to Hsp60. Further validation studies showed that compound **8** inhibited Hsp60-Hsp10's refolding activity and Hsp60's ATPase activity. Importantly, Hsp60 was found to interact with HIF-1α (Ban et al., 2010), suggesting that binding of **8** to Hsp60 can be implicated in inhibition of HIF-1α-mediated gene transcription. Since HIF-1α is a nuclear located protein, it is possible that the interaction between Hsp60 and HIF-1α occurs inside the nucleus, but other possibilities cannot be excluded.

The other class of synthetic compounds identified to inhibit Hsp60 is gold (III) porphyrin complexes. Many gold (III) complexes were shown to possess anticancer activity against different cancer cell lines (Nobili et al., 2010). However, their therapeutic potential was limited due to their instability under physiological conditions. This limitation has been overcome by synthesizing gold (III) complexes with strong donor ligands, which are much more stable under physiological conditions and also presented significant anticancer activities (Lease et al., 2013; Teo et al., 2014). A prototype gold (III) complex [Au(TPP)Cl] (**10**) is shown in **Figure 7**. One of the major challenges to move these gold (III) complexes forward is our limited understanding of their mechanism of action. As a first step toward this challenge, the binding protein targets of the gold (III) complexes need to be identified. A chemoproteomics strategy was designed to identify the binding targets of **10** using a clickable photoaffinity probe **11** (**Figure 7**;

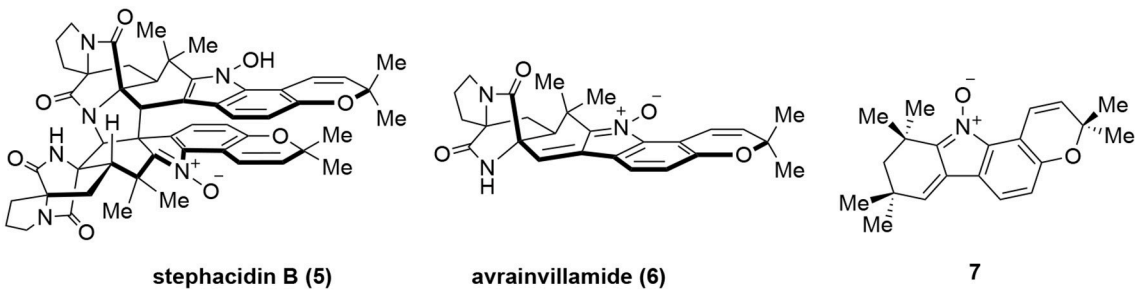

FIGURE 5 | Chemical structures Stephacidin B (**5**), avrainvillamide (**6**), and a simplified analog **7**.

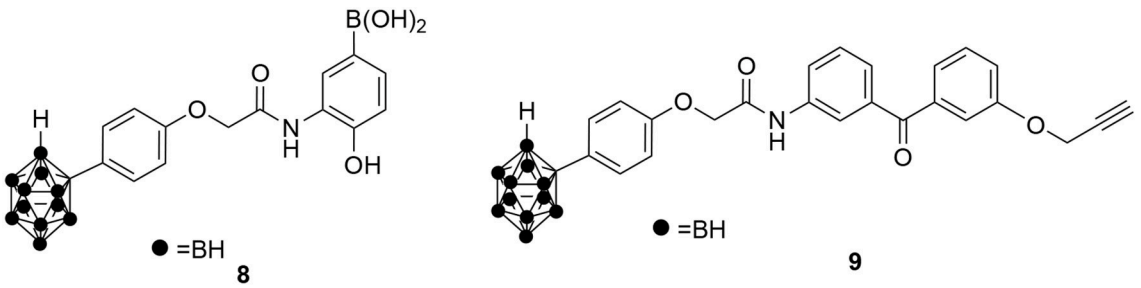

FIGURE 6 | Chemical structures of *o*-carboranylphenoxyacetanilide **8** and its clickable photoaffinity probe **9**.

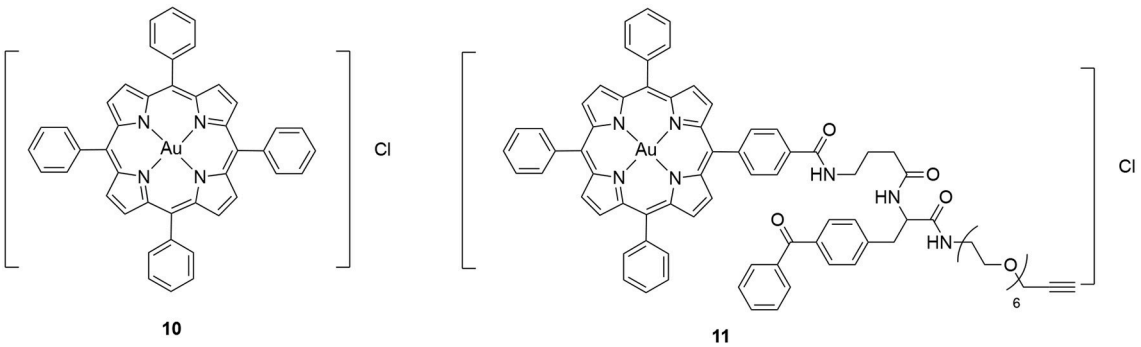

FIGURE 7 | Chemical structure of gold (III) porphyrin [Au(TPP)]Cl (**10**) and its clickable photoaffinity probe **11**.

Hu et al., 2016). This target identification strategy is similar to that used for *o*-carboranylphenoxyacetanilide. Through this strategy, Hsp60 was identified as a direct molecular target of **10**. Further biochemical and cellular studies using saturation-transfer difference-nuclear magnetic resonance (STD-NMR) and cellular thermal shift assays demonstrated that **10** engaged interaction with Hsp60 both *in vitro* and in cells (Hu et al., 2016). It was further found that **10** inhibited the refolding activity of the Hsp60-Hsp10 complex. Additional SAR studies demonstrated that both the gold (III) ion and porphyrin ligand are necessary for the inhibitory activity (Hu et al., 2016). It is unclear if the ATPase activity of Hsp60 or other chaperone proteins was inhibited by **10** and its derivatives. It is speculated that the gold (III) ion may interact with Hsp60 electrophilically and the porphyrin ligand may bind to Hsp60 through hydrophobic interactions (Hu et al., 2016). However, the detailed mechanism of action of these gold (III) complexes remain to be elucidated.

CONCLUSIONS AND OUTSTANDING QUESTIONS

Since the initial discovery of Hsp60 as the mitochondrial molecular chaperone, many studies have shown that it is also localized outside mitochondria with perhaps both chaperoning and non-chaperoning activities. Therefore, it is not surprising that many different disease states especially autoimmune diseases and cancers have presented altered expression level of

Hsp60. This presents a great opportunity to develop potential therapeutics by targeting Hsp60. Quite a few different small molecule modulators of Hsp60 have been identified. These include both natural products and synthetic molecules. It is striking that these different small molecules have no common structural motifs or pharmacophores, yet they all modulate Hsp60's activity. It will be critical to understand how these different inhibitors can all interact with the Hsp60-Hsp10 complex. Some differences have already been noticed among different inhibitors. While all of the identified inhibitors can inhibit the refolding activity, not all of them inhibit the ATPase activity. It is possible that some of these reported inhibitors, especially the hydrophobic ones, may also inhibit the spontaneous folding of the substrate proteins independent of Hsp60. Future characterization of the inhibitors should include this type of critical controls to determine the extent of Hsp60 involvement. The recent breakthrough in determining the X-ray crystal structure of the human Hsp60-Hsp10 complex (Nisemblat et al., 2015) shall facilitate our understanding of how the inhibitors interact with Hsp60. Given the structural diversity of the reported Hsp60 modulators, both orthosteric and allosteric modulation mechanisms are possible. As a consequence, different inhibitors may distinctly affect the Hsp60-Hsp10 dynamics and the individual steps in the folding cycle (Weiss et al., 2016). Mechanistically, it will also be critical to elucidate how the inhibitors binding to Hsp60 can result in the distinct phenotype of the inhibitors (e.g., anticancer activity) because most of these Hsp60 modulations were discovered after the initial findings of the bioactivities of the inhibitors through chemoproteomics approaches. These studies will in turn inform their future development into potential therapeutics.

While mizoribine was shown to be selective in targeting human Hsp60-Hsp10 vs. bacterial GroEL-GroES (Tanabe et al., 2012), a large number of small molecules were identified as GroEL-GroES inhibitors from a high-throughput screening of ∼700,000 compounds (Johnson et al., 2014; Abdeen et al., 2016a). Interestingly, most of these inhibitors are more selective against GroEL-GroES vs. Hsp60-Hsp10 (Abdeen et al., 2016a,b). Some of these may even potentially inhibit the Hsp60-Hsp10 complex from *Trypanosoma brucei* (Abdeen et al., 2016b) to treat African sleeping sickness. These results suggest that selectively targeting one protein complex is feasible. Ongoing extensive studies are attempting to resolve if the Hsp60 protein complexes in different subcellular compartments have unique activities or oligomeric equilibria (Vilasi et al., 2017), which may offer additional opportunities to develop small molecules to target one complex over the others. For example, can we selectively target one Hsp60 complex that is more disease relevant than the mitochondrial Hsp60-Hsp10 complex that is essential for normal mitochondrial homeostasis?

As we expect that more inhibitors are being developed and more mechanistic details are being elucidated, targeting Hsp60 can be a powerful strategy to develop therapeutics in multiple indications. When assessing these inhibitors, it is critical that appropriate controls are included to ensure that the inhibitors are indeed targeting Hsp60 instead of other components in the assay system (e.g., spontaneous folding or other enzymes included for coupled biochemical assays). In this regard, both substrates that can refold spontaneously (e.g., green fluorescent protein and dihydrofolate reductase) and substrates whose refolding depends on Hsp60 (e.g., rhodanese and malate dehydrogenase) should be used. Refolding reactions in the absence of the chaperonin complex should also be included to evaluate potential inhibitors. With these proper controls, one can ascertain that the inhibitors indeed directly target Hsp60-dependent activity and even possibly tease out the exact step that the inhibitors actually act on in this multi-step folding process. The potencies of the current inhibitor are in general low (μM to mM) and more potent inhibitors (preferably low to high nM range) need to be developed for further studies. It is tempting to speculate that small molecules that can enhance the Hsp60's chaperone activity may provide a novel opportunity to treat neurodegenerative disorders where Hsp60 mutations cause defective chaperones. Molecules possessing this activity have not been reported yet, but allosteric modulators to enhance Hsp60's refolding efficiency are likely to be discovered. On the other hand, the small molecules that can inhibit Hsp60's activities including refolding activity, ATPase activity and perhaps other moonlighting activities would be great starting points for new therapeutics in inflammatory diseases, autoimmune diseases and various cancers. As we better characterize the moonlighting functions of Hsp60 in the future, it will also be critical to assess the correlation between different compounds' inhibitory potency in Hsp60 refolding and the moonlighting function in question. Such studies will further shed insights into the biochemical properties of Hsp60 in different subcellular compartments. Most of the inhibitors developed so far possess different degrees of anticancer activities. When deciding the future preclinical and clinical applications of these small molecule modulators, it will be critical to determine the selectivity profiles of the inhibitors and to what degree the mitochondrial homeostasis will be altered by the small molecules and how this effect will confer potential deleterious side effects.

AUTHOR CONTRIBUTIONS

All authors listed have made a substantial, direct and intellectual contribution to the work, and approved it for publication.

ACKNOWLEDGMENTS

XX is grateful to the financial supports from the National Institutes of Health (RO1GM122820 and R21CA220061). All the authors would like to acknowledge the reviewers for providing critical comments.

REFERENCES

Abdeen, S., Salim, N., Mammadova, N., Summers, C. M., Frankson, R., Ambrose, A. J., et al. (2016a). GroEL/ES inhibitors as potential antibiotics. *Bioorg. Med. Chem. Lett.* 26, 3127–3134. doi: 10.1016/j.bmcl.2016.04.089

Abdeen, S., Salim, N., Mammadova, N., Summers, C. M., Goldsmith-Pestana, K., McMahon-Pratt, D., et al. (2016b). Targeting the HSP60/10 chaperonin systems of *Trypanosoma brucei* as a strategy for treating African sleeping sickness. *Bioorg. Med. Chem. Lett.* 26, 5247–5253. doi: 10.1016/j.bmcl.2016.09.051

Anfinsen, C. B. (1973). Principles that govern the folding of protein chains. *Science* 181, 223–230. doi: 10.1126/science.181.4096.223

Appendino, G., Bianchi, F., Minassi, A., Sterner, O., Ballero, M., and Gibbons, S. (2002). Oligomeric acylphloroglucinols from myrtle (*Myrtus communis*). *J. Nat. Prod.* 65, 334–338. doi: 10.1021/np010441b

Astarloa, R., and Castrillo, J. C. M. (1996). Humoral response to the human heat shock 60 kDa protein in myasthenia gravis. *J. Neurol. Sci.* 135, 182–183. doi: 10.1016/0022-510X(95)00191-4

Ban, H. S., Shimizu, K., Minegishi, H., and Nakamura, H. (2010). Identification of HSP60 as a primary target of o-carboranylphenoxyacetanilide, an HIF-1alpha inhibitor. *J. Am. Chem. Soc.* 132, 11870–11871. doi: 10.1021/ja104739t

Bini, L., Magi, B., Marzocchi, B., Arcuri, F., Tripodi, S., Cintorino, M., et al. (1997). Protein expression profiles in human breast ductal carcinoma and histologically normal tissue. *Electrophoresis* 18, 2832–2841. doi: 10.1002/elps.1150181519

Birk, O. S., Gur, S. L., Elias, D., Margalit, R., Mor, F., Carmi, P., et al. (1999). The 60-kDa heat shock protein modulates allograft rejection. *Proc. Natl. Acad. Sci. U.S.A.* 96, 5159–5163. doi: 10.1073/pnas.96.9.5159

Bross, P., and Fernandez-Guerra, P. (2016). Disease-associated mutations in the HSPD1 gene encoding the large subunit of the mitochondrial Hsp60/Hsp10 chaperonin complex. *Front. Mol. Biosc.* 3:49. doi: 10.3389/fmolb.2016.00049

Bross, P., Naundrup, S., Hansen, J., Nielsen, M. N., Christensen, J. H., Kruhøffer, M., et al. (2008). The Hsp60-(p.V98I) mutation associated with hereditary spastic paraplegia SPG13 compromises chaperonin function both *in vitro* and *in vivo*. *J. Biol. Chem.* 283, 15694–15700. doi: 10.1074/jbc.M800548200

Bukau, B., and Horwich, A. L. (1998). The Hsp70 and Hsp60 chaperone machines. *Cell* 92, 351–366. doi: 10.1016/S0092-8674(00)80928-9

Campanella, C., Bucchieri, F., Merendino, A. M., Fucarino, A., Burgio, G., Corona, D. F., et al. (2012). The odyssey of Hsp60 from tumor cells to other destinations includes plasma membrane-associated stages and Golgi and exosomal protein-trafficking modalities. *PLoS ONE* 7:e42008. doi: 10.1371/journal.pone.0042008

Campanella, C., D'Anneo, A., Marino Gammazza, A., Caruso Bavisotto, C., Barone, R., Emanuele, S., et al. (2016). The histone deacetylase inhibitor SAHA induces Hsp60 nitration and its extracellular release by exosomal vesicles in human lung-derived carcinoma cells. *Oncotarget* 7, 28849–28867. doi: 10.18632/oncotarget.6680

Cappello, F., and Zummo, G. (2005). HSP60 expression during carcinogenesis: a molecular "proteus" of carcinogenesis? *Cell Stress Chaperones* 10, 263–264. doi: 10.1379/1466-1268(2005)10[263:HEDCAM]2.0.CO;2

Cappello, F., Bellafiore, M., Palma, A., David, S., Marcianò, V., Bartolotta, T., et al. (2003a). 60KDa chaperonin (Hsp60) is over-expressed during colorectal carcinogenesis. *Eur. J. Histochem.* 47, 105–110. doi: 10.4081/814

Cappello, F., Bellafiore, M., Palma, A., Marciano, V., Martorana, G., Belfiore, P., et al. (2002). Expression of 60-kD heat shock protein increases during carcinogenesis in the uterine exocervix. *Pathobiology* 70, 83–88. doi: 10.1159/000067304

Cappello, F., Caramori, G., Campanella, C., Vicari, C., Gnemmi, I., Zanini, A., et al. (2011). Convergent sets of data from *in vivo* and *in vitro* methods point to an active role of Hsp60 in chronic obstructive pulmonary disease pathogenesis. *PLoS ONE* 6:e28200. doi: 10.1371/journal.pone.0028200

Cappello, F., Marino Gammazza, A., Palumbo Piccionello, A., Campanella, C., Pace, A., Conway de Macario, E., et al. (2014). Hsp60 chaperonopathies and chaperonotherapy: targets and agents. *Expert Opin. Ther. Targets* 18, 185–208. doi: 10.1517/14728222.2014.856417

Cappello, F., Marino Gammazza, A., Zummo, L., Conway de Macario, E., and Macario, A. J. (2010). Hsp60 and AChR cross-reactivity in myasthenia gravis: an update. *J. Neurol. Sci.* 292, 117–118. doi: 10.1016/j.jns.2010.02.021

Cappello, F., Rappa, F., David, S., Anzalone, R., and Zummo, G. (2003b). Immunohistochemical evaluation of PCNA, p53, HSP60, HSP10 and MUC-2 presence and expression in prostate carcinogenesis. *Anticancer Res.* 23, 1325–1331.

Caruso Bavisotto, C., Cappello, F., Macario, A. J. L., Conway de Macario, E., Logozzi, M., Fais, S., et al. (2017). Exosomal HSP60: a potentially useful biomarker for diagnosis, assessing prognosis, and monitoring response to treatment. *Expert Rev. Mol. Diagn.* 17, 815–822. doi: 10.1080/14737159.2017.1356230

Castilla, C., Congregado, B., Conde, J. M., Medina, R., Torrubia, F. J., Japón, M. A., et al. (2010). Immunohistochemical expression of Hsp60 correlates with tumor progression and hormone resistance in prostate cancer. *Urology* 76, 1017.e1–1017.e6. doi: 10.1016/j.urology.2010.05.045

Cheng, M. Y., Hartl, F. U., Martin, J., Pollock, R. A., Kalousek, F., Neupert, W., et al. (1989). Mitochondrial heat-shock protein hsp60 is essential for assembly of proteins imported into yeast mitochondria. *Nature* 337, 620–625. doi: 10.1038/337620a0

Christensen, J. H., Nielsen, M. N., Hansen, J., Füchtbauer, A., Füchtbauer, E. M., West, M., et al. (2010). Inactivation of the hereditary spastic paraplegia-associated Hspd1 gene encoding the Hsp60 chaperone results in early embryonic lethality in mice. *Cell Stress Chaperones* 15, 851–863. doi: 10.1007/s12192-010-0194-x

Chun, J. N., Choi, B., Lee, K. W., Lee, D. J., Kang, D. H., Lee, J. Y., et al. (2010). Cytosolic Hsp60 is involved in the NF-κB-dependent survival of cancer cells via IKK regulation. *PLoS ONE* 5:e9422. doi: 10.1371/journal.pone.0009422

Czarnecka, A. M., Campanella, C., Zummo, G., and Cappello, F. (2006). Mitochondrial chaperones in cancer: from molecular biology to clinical diagnostics. *Cancer Biol. Ther.* 5, 714–720. doi: 10.4161/cbt.5.7.2975

Desmetz, C., Bibeau, F., Boissière, F., Bellet, V., Rouanet, P., Maudelonde, T., et al. (2008). Proteomics-based identification of HSP60 as a tumor-associated antigen in early stage breast cancer and ductal carcinoma in situ. *J. Proteome Res.* 7, 3830–3837. doi: 10.1021/pr800130d

Elias, D., Markovits, D., Reshef, T., van der Zee, R., and Cohen, I. R. (1990). Induction and therapy of autoimmune diabetes in the non-obese diabetic (NOD/Lt) mouse by a 65-kDa heat shock protein. *Proc. Natl. Acad. Sci. U.S.A.* 87, 1576–1580. doi: 10.1073/pnas.87.4.1576

Elias, D., Meilin, A., Ablamunits, V., Birk, O. S., Carmi, P., Könen-Waisman, S., et al. (1997). Hsp60 peptide therapy of NOD mouse diabetes induces a Th2 cytokine burst and downregulates autoimmunity to various beta-cell antigens. *Diabetes* 46, 758–764. doi: 10.2337/diab.46.5.758

Feisst, C., Franke, L., Appendino, G., and Werz, O. (2005). Identification of molecular targets of the oligomeric nonprenylated acylphloroglucinols from *Myrtus communis* and their implication as anti-inflammatory compounds. *J. Pharmacol. Exp. Ther.* 315, 389–396. doi: 10.1124/jpet.105.090720

Feng, H., Zeng, Y., Graner, M. W., and Katsanis, E. (2002). Stressed apoptotic tumor cells stimulate dendritic cells and induce specific cytotoxic T cells. *Blood* 100, 4108–4115. doi: 10.1182/blood-2002-05-1389

Fenical, W., Jensen, P. R., and Cheng, X. C. (2000). Avrainvillamide, a cytotoxic marine natural product, and derivatives there of US patent. US6066635A.

Finka, A., Mattoo, R. U., and Goloubinoff, P. (2016). Experimental milestones in the discovery of molecular chaperones as polypeptide unfolding enzymes. *Annu. Rev. Biochem.* 85, 715–742. doi: 10.1146/annurev-biochem-060815-014124

Füst, G., Uray, K., Bene, L., Hudecz, F., Karadi, I., and Prohaszka, Z. (2012). Comparison of epitope specificity of anti-heat shock protein 60/65 IgG type antibodies in the sera of healthy subjects, patients with coronary heart disease and inflammatory bowel disease. *Cell Stress Chaperones* 17, 215–227. doi: 10.1007/s12192-011-0301-7

Gammazza A. M., Bucchieri, F., Grimaldi, L. M., Benigno, A., de Macario, E. C., Macario, A. J., et al. (2012). The molecular anatomy of human Hsp60 and its similarity with that of bacterial orthologs and acetylcholine receptor reveal a potential pathogenetic role of anti-chaperonin immunity in myasthenia gravis. *Cell. Mol. Neurobiol.* 32, 943–947. doi: 10.1007/s10571-011-9789-8

Grandjenette, C., Schnekenburger, M., Morceau, F., Mack, F., Wiechmann, K., Werz, O., et al. (2015). Dual induction of mitochondrial apoptosis and senescence in chronic myelogenous leukemia by myrtucommulone A. *Anticancer Agents Med. Chem.* 15, 363–373. doi: 10.2174/1871520614666141202143757

Gupta, S., and Knowlton, A. A. (2007). HSP60 trafficking in adult cardiac myocytes: role of the exosomal pathway. *Am. J. Physiol. Heart Circ. Physiol.* 292, H3052–H3056. doi: 10.1152/ajpheart.01355.2006

Hamelin, C., Cornut, E., Poirier, F., Pons, S., Beaulieu, C., Charrier, J. P., et al. (2011). Identification and verification of heat shock protein 60 as a potential serum marker for colorectal cancer. *FEBS J.* 278, 4845–4859. doi: 10.1111/j.1742-4658.2011.08385.x

Hanahan, D., and Weinberg, R. A. (2011). Hallmarks of cancer: the next generation. *Cell* 144, 646–674. doi: 10.1016/j.cell.2011.02.013

Hansen, J. J., Dürr, A., Cournu-Rebeix, I., Georgopoulos, C., Ang, D., Nielsen, M. N., et al. (2002). Hereditary spastic paraplegia SPG13 is associated with a mutation in the gene encoding the mitochondrial chaperonin Hsp60. *Am. J. Hum. Genet.* 70, 1328–1332. doi: 10.1086/339935

Hansen, J., Svenstrup, K., Ang, D., Nielsen, M. N., Christensen, J. H., Gregersen, N., et al. (2007). A novel mutation in the HSPD1 gene in a patient with hereditary spastic paraplegia. *J. Neurol.* 254, 897–900. doi: 10.1007/s00415-006-0470-y

Hayoun, D., Kapp, T., Edri-Brami, M., Ventura, T., Cohen, M., Avidan, A., et al. (2012). HSP60 is transported through the secretory pathway of 3-MCA-induced fibrosarcoma tumour cells and undergoes N-glycosylation. *FEBS J.* 279, 2083–2095. doi: 10.1111/j.1742-4658.2012.08594.x

He, Y., Wu, Y., Mou, Z., Li, W., Zou, L., Fu, T., et al. (2007). Proteomics-based identification of HSP60 as a tumor-associated antigen in colorectal cancer. *Proteomics Clin. Appl.* 1, 336–342. doi: 10.1002/prca.200600718

Hemmingsen, S. M., Woolford, C., van der Vies, S. M., Tilly, K., Dennis, D. T., Georgopoulos, C. P., et al. (1988). Homologous plant and bacterial proteins chaperone oligomeric protein assembly. *Nature* 333, 330–334. doi: 10.1038/333330a0

Henderson, B., Fares, M. A., and Lund, P. A. (2013). Chaperonin 60: a paradoxical, evolutionarily conserved protein family with multiple moonlighting functions. *Biol. Rev. Camb. Philos. Soc.* 88, 955–987. doi: 10.1111/brv.12037

Hjelholt, A., Carlsen, T., Deleuran, B., Jurik, A. G., Schiøttz-Christensen, B., Christiansen, G., et al. (2013). Increased levels of IgG antibodies against human HSP60 in patients with spondyloarthritis. *PLoS ONE* 8:e56210. doi: 10.1371/journal.pone.0056210

Hjerpe, E., Egyhazi, S., Carlson, J., Stolt, M. F., Schedvins, K., Johansson, H., et al. (2013). HSP60 predicts survival in advanced serous ovarian cancer. *Int. J. Gynecol. Cancer* 23, 448–455. doi: 10.1097/IGC.0b013e318284308b

Honda, M., Itoh, H., Suzuki, T., and Hashimoto, Y. (2006). Population pharmacokinetics of higher-dose mizoribine in healthy male volunteers. *Biol. Pharm. Bull.* 29, 2460–2464. doi: 10.1248/bpb.29.2460

Horwich, A. L., and Fenton, W. A. (2009). Chaperonin-mediated protein folding: using a central cavity to kinetically assist polypeptide chain folding. *Q. Rev. Biophys.* 42, 83–116. doi: 10.1017/S0033583509004764

Hu, D., Liu, Y., Lai, Y. T., Tong, K. C., Fung, Y. M., Lok, C. N., et al. (2016). Anticancer gold(III) porphyrins target mitochondrial chaperone Hsp60. *Angew. Chem. Int. Ed. Engl.* 55, 1387–1391. doi: 10.1002/anie.201509612

Hwang, Y. J., Lee, S. P., Kim, S. Y., Choi, Y. H., Kim, M. J., Lee, C. H., et al. (2009). Expression of heat shock protein 60 kDa is upregulated in cervical cancer. *Yonsei Med. J.* 50, 399–406. doi: 10.3349/ymj.2009.50.3.399

Itoh, H., Kobayashi, R., Wakui, H., Komatsuda, A., Ohtani, H., Miura, A. B., et al. (1995). Mammalian 60-kDa stress protein (chaperonin homolog). Identification, biochemical properties, and localization. *J. Biol. Chem.* 270, 13429–13435. doi: 10.1074/jbc.270.22.13429

Itoh, H., Komatsuda, A., Wakui, H., Miura, A. B., and Tashima, Y. (1999). Mammalian HSP60 is a major target for an immunosuppressant mizoribine. *J. Biol. Chem.* 274, 35147–35151. doi: 10.1074/jbc.274.49.35147

Izgi, K., Iskender, B., Jauch, J., Sezen, S., Cakir, M., Charpentier, M., et al. (2015). Myrtucommulone-A induces both extrinsic and intrinsic apoptotic pathways in cancer cells. *J. Biochem. Mol. Toxicol.* 29, 432–439. doi: 10.1002/jbt.21716

Jindal, S., Dudani, A. K., Singh, B., Harley, C. B., and Gupta, R. S. (1989). Primary structure of a human mitochondrial protein homologous to the bacterial and plant chaperonins and to the 65-kilodalton mycobacterial antigen. *Mol. Cell. Biol.* 9, 2279–2283. doi: 10.1128/MCB.9.5.2279

Johnson, S. M., Sharif, O., Mak, P. A., Wang, H. T., Engels, I. H., Brinker, A., et al. (2014). A biochemical screen for GroEL/GroES inhibitors. *Bioorg. Med. Chem. Lett.* 24, 786–789. doi: 10.1016/j.bmcl.2013.12.100

Kakeya, H., Takahashi, I., Okada, G., Isono, K., and Osada, H. (1995). Epolactaene, a novel neuritogenic compound in human neuroblastoma cells, produced by a marine fungus. *J. Antibiot.* 48, 733–735. doi: 10.7164/antibiotics.48.733

Kalderon, B., Kogan, G., Bubis, E., and Pines, O. (2015). Cytosolic hsp60 can modulate proteasome activity in yeast. *J. Biol. Chem.* 290, 3542–3551. doi: 10.1074/jbc.M114.626622

Kirchhoff, S. R., Gupta, S., and Knowlton, A. A. (2002). Cytosolic heat shock protein 60, apoptosis, and myocardial injury. *Circulation* 105, 2899–2904. doi: 10.1161/01.CIR.0000019403.35847.23

Koeberle, A., Pollastro, F., Northoff, H., and Werz, O. (2009). Myrtucommulone, a natural acylphloroglucinol, inhibits microsomal prostaglandin E(2) synthase-1. *Br. J. Pharmacol.* 156, 952–961. doi: 10.1111/j.1476-5381.2009.00070.x

Koll, H., Guiard, B., Rassow, J., Ostermann, J., Horwich, A. L., Neupert, W., et al. (1992). Antifolding activity of hsp60 couples protein import into the mitochondrial matrix with export to the intermembrane space. *Cell* 68, 1163–1175. doi: 10.1016/0092-8674(92)90086-R

Lease, N., Vasilevski, V., Carreira, M., de Almeida, A., Sanaú, M., Hirva, P., et al. (2013). Potential anticancer heterometallic Fe-Au and Fe-Pd agents: initial mechanistic insights. *J. Med. Chem.* 56, 5806–5818. doi: 10.1021/jm4007615

Lewthwaite, J., Owen, N., Coates, A., Henderson, B., and Steptoe, A. (2002). Circulating human heat shock protein 60 in the plasma of British civil servants: relationship to physiological and psychosocial stress. *Circulation* 106, 196–201. doi: 10.1161/01.CIR.0000021121.26290.2C

Lin, Z., Madan, D., and Rye, H. S. (2008). GroEL stimulates protein folding through forced unfolding. *Nat. Struct. Mol. Biol.* 15, 303–311. doi: 10.1038/nsmb.1394

Magen, D., Georgopoulos, C., Bross, P., Ang, D., Segev, Y., Goldsher, D., et al. (2008). Mitochondrial hsp60 chaperonopathy causes an autosomal-recessive neurodegenerative disorder linked to brain hypomyelination and leukodystrophy. *Am. J. Hum. Genet.* 83, 30–42. doi: 10.1016/j.ajhg.2008.05.016

Marino Gammazza, A., Rizzo, M., Citarrella, R., Rappa, F., Campanella, C., Bucchieri, F., et al. (2014). Elevated blood Hsp60, its structural similarities and cross-reactivity with thyroid molecules, and its presence on the plasma membrane of oncocytes point to the chaperonin as an immunopathogenic factor in Hashimoto's thyroiditis. *Cell Stress Chaperones* 19, 343–353. doi: 10.1007/s12192-013-0460-9

Martin, J. (1998). Role of the GroEL chaperonin intermediate domain in coupling ATP hydrolysis to polypeptide release. *J. Biol. Chem.* 273, 7351–7357. doi: 10.1074/jbc.273.13.7351

Merendino, A. M., Bucchieri, F., Campanella, C., Marcianò, V., Ribbene, A., David, S., et al. (2010). Hsp60 is actively secreted by human tumor cells. *PLoS ONE* 5:e9247. doi: 10.1371/journal.pone.0009247

Mizuno, K., Tsujino, M., Takada, M., Hayashi, M., and Atsumi, K. (1974). Studies on bredinin. I. Isolation, characterization and biological properties. *J. Antibiot.* 27, 775–782. doi: 10.7164/antibiotics.27.775

Nagumo, Y., Kakeya, H., Shoji, M., Hayashi, Y., Dohmae, N., and Osada, H. (2005). Epolactaene binds human Hsp60 Cys442 resulting in the inhibition of chaperone activity. *Biochem. J.* 387, 835–840. doi: 10.1042/BJ20041355

Nagumo, Y., Kakeya, H., Yamaguchi, J., Uno, T., Shoji, M., Hayashi, Y., et al. (2004). Structure-activity relationships of epolactaene derivatives: structural requirements for inhibition of Hsp60 chaperone activity. *Bioorg. Med. Chem. Lett.* 14, 4425–4429. doi: 10.1016/j.bmcl.2004.06.054

Nakamura, H., and Minegishi, H. (2013). HSP60 as a drug target. *Curr. Pharm. Des.* 19, 441–451. doi: 10.2174/138161213804143626

Nisemblat, S., Yaniv, O., Parnas, A., Frolow, F., and Azem, A. (2015). Crystal structure of the human mitochondrial chaperonin symmetrical football complex. *Proc. Natl. Acad. Sci. U.S.A.* 112, 6044–6049. doi: 10.1073/pnas.1411718112

Nobili, S., Mini, E., Landini, I., Gabbiani, C., Casini, A., and Messori, L. (2010). Gold compounds as anticancer agents: chemistry, cellular pharmacology, and preclinical studies. *Med. Res. Rev.* 30, 550–580. doi: 10.1002/med.20168

Ostermann, J., Horwich, A. L., Neupert, W., and Hartl, F. U. (1989). Protein folding in mitochondria requires complex formation with hsp60 and ATP hydrolysis. *Nature* 341, 125–130. doi: 10.1038/341125a0

Pace, A., Barone, G., Lauria, A., Martorana, A., Piccionello, A. P., Pierro, P., et al. (2013). Hsp60, a novel target for antitumor therapy: structure-function features and prospective drugs design. *Curr. Pharm. Des.* 19, 2757–2764. doi: 10.2174/1381612811319150011

Parnas, A., Nadler, M., Nisemblat, S., Horovitz, A., Mandel, H., and Azem, A. (2009). The MitCHAP-60 disease is due to entropic destabilization of the human mitochondrial Hsp60 oligomer. *J. Biol. Chem.* 284, 28198–28203. doi: 10.1074/jbc.M109.031997

Parnas, A., Nisemblat, S., Weiss, C., Levy-Rimler, G., Pri-Or, A., Zor, T., et al. (2012). Identification of elements that dictate the specificity of mitochondrial Hsp60 for its co-chaperonin. *PLoS ONE* 7:e50318. doi: 10.1371/journal.pone.0050318

Piselli, P., Vendetti, S., Vismara, D., Cicconi, R., Poccia, F., Colizzi, V., et al. (2000). Different expression of CD44, ICAM-1, and HSP60 on primary tumor and metastases of a human pancreatic carcinoma growing in scid mice. *Anticancer Res.* 20, 825–831.

Pockley, A. G. (2003). Heat shock proteins as regulators of the immune response. *Lancet* 362, 469–476. doi: 10.1016/S0140-6736(03)14075-5

Pockley, A. G., Bulmer, J., Hanks, B. M., and Wright, B. H. (1999). Identification of human heat shock protein 60 (Hsp60) and anti-Hsp60 antibodies in the peripheral circulation of normal individuals. *Cell Stress Chaperones* 4, 29–35. doi: 10.1379/1466-1268(1999)004<0029:IOHHSP>2.3.CO;2

Qian-Cutrone, J., Huang, S., Shu, Y. Z., Vyas, D., Fairchild, C., Menendez, A., et al. (2002). Stephacidin A and B: two structurally novel, selective inhibitors of the testosterone-dependent prostate LNCaP cells. *J. Am. Chem. Soc.* 124, 14556–14557. doi: 10.1021/ja028538n

Radons, J. (2017). The ATP-driven Hsp60 machinery: biological and clinical implications. *Curr. Immunol. Rev.* 13, 19–43. doi: 10.2174/1573395513666170327165811

Reading, D. S., Hallberg, R. L., and Myers, A. M. (1989). Characterization of the yeast HSP60 gene coding for a mitochondrial assembly factor. *Nature* 337, 655–659. doi: 10.1038/337655a0

Rosa, A., Deiana, M., Casu, V., Corona, G., Appendino, G., Bianchi, F., et al. (2003). Antioxidant activity of oligomeric acylphloroglucinols from *Myrtus communis* L. *Free Radic. Res.* 37, 1013–1019. doi: 10.1080/10715760310001595739

Rossi, A., Di Paola, R., Mazzon, E., Genovese, T., Caminiti, R., Bramanti, P., et al. (2009). Myrtucommulone from *Myrtus communis* exhibits potent anti-inflammatory effectiveness *in vivo*. *J. Pharmacol. Exp. Ther.* 329, 76–86. doi: 10.1124/jpet.108.143214

Rotstein, A., Lifshitz, A., and Kashman, Y. (1974). Isolation and antibacterial activity of acylphloroglucinols from *Myrtus communis*. *Antimicrob. Agents Chemother.* 6, 539–542. doi: 10.1128/AAC.6.5.539

Schneider, J., Jimenez, E., Marenbach, K., Romero, H., Marx, D., and Meden, H. (1999). Immunohistochemical detection of HSP60-expression in human ovarian cancer. Correlation with survival in a series of 247 patients. *Anticancer Res.* 19, 2141–2146.

Semenza, G. L. (2003). Targeting HIF-1 for cancer therapy. *Nat. Rev. Cancer* 3, 721–732. doi: 10.1038/nrc1187

Shamaei-Tousi, A., Steptoe, A., O'Donnell, K., Palmen, J., Stephens, J. W., Hurel, S. J., et al. (2007). Plasma heat shock protein 60 and cardiovascular disease risk: the role of psychosocial, genetic, and biological factors. *Cell Stress Chaperones* 12, 384–392. doi: 10.1379/CSC-300.1

Shimizu, K., Maruyama, M., Yasui, Y., Minegishi, H., Ban, H. S., and Nakamura, H. (2010). Boron-containing phenoxyacetanilide derivatives as hypoxia-inducible factor (HIF)-1alpha inhibitors. *Bioorg. Med. Chem. Lett.* 20, 1453–1456. doi: 10.1016/j.bmcl.2009.12.037

Shtilerman, M., Lorimer, G. H., and Englander, S. W. (1999). Chaperonin function: folding by forced unfolding. *Science* 284, 822–825. doi: 10.1126/science.284.5415.822

Soltys, B. J., and Gupta, R. S. (1996). Immunoelectron microscopic localization of the 60-kDa heat shock chaperonin protein (Hsp60) in mammalian cells. *Exp. Cell Res.* 222, 16–27. doi: 10.1006/excr.1996.0003

Soltys, B. J., and Gupta, R. S. (1997). Cell surface localization of the 60 kDa heat shock chaperonin protein (hsp60) in mammalian cells. *Cell Biol. Int.* 21, 315–320. doi: 10.1006/cbir.1997.0144

Tabeta, K., Yamazaki, K., Hotokezaka, H., Yoshie, H., and Hara, K. (2000). Elevated humoral immune response to heat shock protein 60 (hsp60) family in periodontitis patients. *Clin. Exp. Immunol.* 120, 285–293. doi: 10.1046/j.1365-2249.2000.01216.x

Tajima, A., Hata, M., Ohta, N., Ohtawara, Y., Suzuki, K., and Aso, Y. (1984). Bredinin treatment in clinical kidney allografting. *Transplantation* 38, 116–118. doi: 10.1097/00007890-198408000-00005

Tanabe, M., Ishida, R., Izuhara, F., Komatsuda, K., Wakui, H., Sawada, K., et al. (2012). The ATPase activity of molecular chaperone HSP60 is inhibited by immunosuppressant mizoribine *Am. J. Mol. Biol.* 2, 93–102. doi: 10.4236/ajmb.2012.22010

Teo, R. D., Gray, H. B., Lim, P., Termini, J., Domeshek, E., and Gross, Z. (2014). A cytotoxic and cytostatic gold(III) corrole. *Chem. Commun.* 50, 13789–13792. doi: 10.1039/C4CC06577H

Thomas, X., Campos, L., Mounier, C., Cornillon, J., Flandrin, P., Le, Q. H., et al. (2005). Expression of heat-shock proteins is associated with major adverse prognostic factors in acute myeloid leukemia. *Leuk. Res.* 29, 1049–1058. doi: 10.1016/j.leukres.2005.02.010

Tomasello, G., Rodolico, V., Zerilli, M., Martorana, A., Bucchieri, F., Pitruzzella, A., et al. (2011). Changes in immunohistochemical levels and subcellular localization after therapy and correlation and colocalization with CD68 suggest a pathogenetic role of Hsp60 in ulcerative colitis. *Appl. Immunohistochem. Mol. Morphol.* 19, 552–561. doi: 10.1097/PAI.0b013e3182118e5f

Tonello, L., Conway de Macario, E., Marino Gammazza, A., Cocchi, M., Gabrielli, F., Zummo, G., et al. (2015). Data mining-based statistical analysis of biological data uncovers hidden significance: clustering Hashimoto's thyroiditis patients based on the response of their PBMC with IL-2 and IFN-gamma secretion to stimulation with Hsp60. *Cell Stress Chaperones* 20, 391–395. doi: 10.1007/s12192-014-0555-y

Tretiakova, I., Blaesius, D., Maxia, L., Wesselborg, S., Schulze-Osthoff, K., Cinatl, J. Jr., et al. (2008). Myrtucommulone from *Myrtus communis* induces apoptosis in cancer cells via the mitochondrial pathway involving caspase-9. *Apoptosis* 13, 119–131. doi: 10.1007/s10495-007-0150-0

Trieb, K., Gerth, R., Berger, P., and Margreiter, R. (2000). Serum antibodies to heat shock proteins are of no diagnostic value for human kidney allograft rejection. *Transpl. Int.* 13, 46–48. doi: 10.1111/j.1432-2277.2000.tb01035.x

Tsai, Y. P., Yang, M. H., Huang, C. H., Chang, S. Y., Chen, P. M., Liu, C. J., et al. (2009). Interaction between HSP60 and beta-catenin promotes metastasis. *Carcinogenesis* 30, 1049–1057. doi: 10.1093/carcin/bgp087

Turka, L. A., Dayton, J., Sinclair, G., Thompson, C. B., and Mitchell, B. S. (1991). Guanine ribonucleotide depletion inhibits T cell activation. Mechanism of action of the immunosuppressive drug mizoribine. *J. Clin. Invest.* 87, 940–948. doi: 10.1172/JCI115101

van Niel, G., D'Angelo, G., and Raposo, G. (2018). Shedding light on the cell biology of extracellular vesicles. *Nat. Rev. Mol. Cell Biol.* 19, 213–228. doi: 10.1038/nrm.2017.125

Vilasi, S., Bulone, D., Caruso Bavisotto, C., Campanella, C., Marino Gammazza, A., San Biagio, P. L., et al. (2017). Chaperonin of group I: oligomeric spectrum and biochemical and biological implications. *Front. Mol. Biosci.* 4:99. doi: 10.3389/fmolb.2017.00099

Weaver, J., Jiang, M., Roth, A., Puchalla, J., Zhang, J., and Rye, H. S. (2017). GroEL actively stimulates folding of the endogenous substrate protein PepQ. *Nat. Commun.* 8:15934. doi: 10.1038/ncomms15934

Weiss, C., Jebara, F., Nisemblat, S., and Azem, A. (2016). Dynamic complexes in the chaperonin-mediated protein folding cycle. *Front. Mol. Biosci.* 3:80. doi: 10.3389/fmolb.2016.00080

Wick, C. (2016). Tolerization against atherosclerosis using heat shock protein 60. *Cell Stress Chaperones* 21, 201–211. doi: 10.1007/s12192-015-0659-z

Wiechmann, K., Müller, H., Huch, V., Hartmann, D., Werz, O., and Jauch, J. (2015). Synthesis and biological evaluation of novel myrtucommulones and structural analogues that target mPGES-1 and 5-lipoxygenase. *Eur. J. Med. Chem.* 101, 133–149. doi: 10.1016/j.ejmech.2015.06.001

Wiechmann, K., Müller, H., König, S., Wielsch, N., Svatoš, A., Jauch, J., et al. (2017). Mitochondrial chaperonin Hsp60 is the apoptosis-related target for Myrtucommulone. *Cell Chem. Biol.* 24, 614.e6–623.e6. doi: 10.1016/j.chembiol.2017.04.008

Wulff, J. E., Herzon, S. B., Siegrist, R., and Myers, A. G. (2007). Evidence for the rapid conversion of stephacidin B into the electrophilic monomer

avrainvillamide in cell culture. *J. Am. Chem. Soc.* 129, 4898–4899. doi: 10.1021/ja0690971

Xu, X., Wang, W., Shao, W., Yin, W., Chen, H., Qiu, Y., et al. (2011). Heat shock protein-60 expression was significantly correlated with the prognosis of lung adenocarcinoma. *J. Surg. Oncol.* 104, 598–603. doi: 10.1002/jso.21992

Zhong, Y., Tang, H., Wang, X., Zeng, Q., Liu, Y., Zhao, X. I., et al. (2016). Intranasal immunization with heat shock protein 60 induces CD4(+) CD25(+) GARP(+) and type 1 regulatory T cells and inhibits early atherosclerosis. *Clin. Exp. Immunol.* 183, 452–468. doi: 10.1111/cei.12726

Conflict of Interest Statement: The authors declare that the research was conducted in the absence of any commercial or financial relationships that could be construed as a potential conflict of interest.

frontiers in Molecular Biosciences

ORIGINAL RESEARCH
published: 15 May 2018
doi: 10.3389/fmolb.2018.00046

The Chaperonin GroEL: A Versatile Tool for Applied Biotechnology Platforms

Pierce T. O'Neil[1†], Alexandra J. Machen[1†], Benjamin C. Deatherage[1], Caleb Trecazzi[1], Alexander Tischer[2], Venkata R. Machha[2], Matthew T. Auton[2], Michael R. Baldwin[3], Tommi A. White[4,5] and Mark T. Fisher[1]*

[1] Department of Biochemistry and Molecular Biology, University of Kansas Medical Center, Kansas City, KS, United States, [2] Division of Hematology, Department of Internal Medicine, Mayo Clinic, Rochester, MN, United States, [3] Department of Molecular Microbiology and Immunology, University of Missouri, Columbia, MO, United States, [4] Department of Biochemistry, University of Missouri, Columbia, MO, United States, [5] Electron Microscopy Core Facility, University of Missouri, Columbia, MO, United States

OPEN ACCESS

Edited by:
Abdussalam Azem,
Tel Aviv University, Israel

Reviewed by:
Janine Kirstein,
Leibniz Institute for Molecular Pharmacology (FMP), Germany
Antonio Trovato,
Università degli Studi di Padova, Italy

***Correspondence:**
Mark T. Fisher
mfisher1@kumc.edu

[†]*These authors have contributed equally to this work.*

Specialty section:
This article was submitted to Protein Folding, Misfolding and Degradation, a section of the journal Frontiers in Molecular Biosciences

Received: *15 February 2018*
Accepted: *23 April 2018*
Published: *15 May 2018*

Citation:
O'Neil PT, Machen AJ, Deatherage BC, Trecazzi C, Tischer A, Machha VR, Auton MT, Baldwin MR, White TA and Fisher MT (2018) The Chaperonin GroEL: A Versatile Tool for Applied Biotechnology Platforms. Front. Mol. Biosci. 5:46. doi: 10.3389/fmolb.2018.00046

The nucleotide-free chaperonin GroEL is capable of capturing transient unfolded or partially unfolded states that flicker in and out of existence due to large-scale protein dynamic vibrational modes. In this work, three short vignettes are presented to highlight our continuing advances in the application of GroEL biosensor biolayer interferometry (BLI) technologies and includes expanded uses of GroEL as a molecular scaffold for electron microscopy determination. The first example presents an extension of the ability to detect dynamic pre-aggregate transients in therapeutic protein solutions where the assessment of the kinetic stability of any folded protein or, as shown herein, quantitative detection of mutant-type protein when mixed with wild-type native counterparts. Secondly, using a BLI denaturation pulse assay with GroEL, the comparison of kinetically controlled denaturation isotherms of various von Willebrand factor (vWF) triple A domain mutant-types is shown. These mutant-types are single point mutations that locally disorder the A1 platelet binding domain resulting in one gain of function and one loss of function phenotype. Clear, separate, and reproducible kinetic deviations in the mutant-type isotherms exist when compared with the wild-type curve. Finally, expanding on previous electron microscopy (EM) advances using GroEL as both a protein scaffold surface and a release platform, examples are presented where GroEL-protein complexes can be imaged using electron microscopy tilt series and the low-resolution structures of aggregation-prone proteins that have interacted with GroEL. The ability of GroEL to bind hydrophobic regions and transient partially folded states allows one to employ this unique molecular chaperone both as a versatile structural scaffold and as a sensor of a protein's folded states.

Keywords: chaperonin GroEL, electron microscopy, tilt series, tetanus neurotoxin, anthrax toxin, von Willebrand Factor, biolayer interferometry, cryoSPARC

INTRODUCTION

The complete functional GroE chaperonin system (GroEL, GroES) is an exquisite allosteric machine that can initially capture transient hydrophobic pockets on folded proteins or partially unfolding protein intermediates. If the size of the captured protein is sufficiently small (<50 kDa), the folding intermediates are released into the highly-structured GroEL-GroES (GroE) nanochamber where folding can continue (Gruber and Horovitz, 2016). Although initial structural work clearly indicates that the interior of the GroEL nanochamber becomes more hydrophilic to aid the folding reaction (Saibil et al., 2013), there is new evidence suggesting that this simple explanation needs to be amended. Specifically, there is increasing mechanistic and structural evidence indicating the unstructured hydrophobic Gly-Gly-Met tetra-repeat C-terminal tails play an important kinetic/structural role in both binding and unfolding the captured protein (Weaver et al., 2017). ATP nucleotide hydrolysis results in timed allosteric disruption of the GroE nanochamber to release the protein substrate back into solution. In the absence of any nucleotide (ATP or ADP), GroEL is capable of both capturing and arresting the folding of any protein that is either completely unfolded or, more interestingly, fluctuating in a dynamic equilibrium between folded and partially folded states (Viitanen et al., 1991; Smith and Fisher, 1995; Smith et al., 1998). As shown initially by Martin and Hartl and later by the Valpuesta group, the physiological relevant capture of transient dynamic states could be particularly relevant for organismal survival to prevent mass aggregation during heat stress (Martin et al., 1992; Llorca et al., 1998).

The nucleotide-free form of GroEL is one of the most promiscuous binders of partially folded proteins that has been encountered to date. Indeed, early purification schemes for GroEL were plagued by co-purification of large and diverse amounts of contaminating proteins and peptides. These contaminants were bound tightly to the now nucleotide-free GroEL as endogenous ATP was diluted and depleted during cell disruption. Early visual analysis by the Lorimer group of the GroEL-captured proteins revealed the contaminating proteins were nascent, unfolded *E. coli* proteins (Viitanen et al., 1992). Clark and Frieden further analyzed these contaminants using mass spectroscopy and found a substantial amount of short, cleaved polypeptides were also present prior to removal during final purification steps (Clark et al., 1998). Using a very clever *in vivo* experimental design, the Horwich group generated a temperature sensitive GroEL mutant which immediately loses its ability to adopt its nucleotide-bound low affinity state upon upshift to non-permissive temperatures (Sewell et al., 2004). Using this mutant, it was found that a significantly large number of nascent *E. coli* proteins (estimated >330 proteins by MudPIT analysis) aggregated or co-precipitated with GroEL *in vivo* (Chapman et al., 2006). Curiously, EM analysis of *E. coli* containing this temperature-sensitive mutant showed highly structured, regular arrays within the cytoplasm. These arrays look quite similar to the inclusions found in some mitochondrial diseases, such as ragged red fiber syndrome, where protein homeostasis and production of the electron transport chain proteins are disrupted. Independently, our laboratory confirmed that large protein substrates with multiple opposing hydrophobic surfaces can induce chaining into extended linear arrays when captured by GroEL and these chains are easily visualized by negative-stain EM (Akkaladevi et al., 2015). The key finding from all these experimental observations demonstrates that the nucleotide-free GroEL can capture a wide variety of partially folded proteins with high affinity.

The promiscuous nature of the nucleotide-free chaperonin has been used as a tool to capture and isolate transient protein folding intermediates with the intent to prevent aggregation during concentration. This capture and pause in folding permits folding of target proteins at high concentrations (Fisher, 1993). Notably, capture and successful folding using the chaperonin was accomplished in the mg/mL range as compared to the limited success of only observing folding at the μg/mL range in the absence of the chaperonin (Fisher, 1993; Smith and Fisher, 1995). The chaperonin can be rapidly separated from the substrate protein following ATP release either by attaching GroEL to beads and spinning down (Voziyan et al., 2005) or by immunoprecipitating GroEL (Fisher and Yuan, 1994; Fisher, 1998).

The presence of the nucleotide-free chaperonin can be used to prevent protein aggregation resulting from the presence of dynamic transient states. This aggregation is dependent on both the lifetime of the transient state and the interaction between one of these transient open hydrophobic states with other transient open states. The population of open states results from naturally occurring native structural fluctuations that persist longer in missense mutation disease states. These open, aggregation prone states can collide with one another to form initial small aggregates (dimers or greater) that can either be reversible or irreversible depending on the strength of the protein-protein interaction (Roberts, 2014). This aggregation process is particularly problematic for biotherapeutic proteins where the requirement of a long shelf life provides ample opportunities for aggregation to occur. In relation to human health, if similar deleterious long-lived transient misfolding processes occurs within cells, this can lead to detrimental protein aggregation or abnormal protein clearance *in vivo*, ultimately resulting in a protein folding disease phenotype.

In this work, additional experiments are presented that extend our use of GroEL biosensor technologies to (1) detect partially folded populations of mutant-type when mixed with wild-type counterparts, (2) detect differences between wild-type, gain of function, and loss of function folding disease mutations and, (3) utilize GroEL molecular scaffolds to capture or maintain solubility of aggregation prone proteins for EM structural analysis. Specifically, in the first example, GroEL biosensors detect and can potentially quantitate the amount of partially folded mutant-type maltose-binding protein (MBP) when mixed with wild-type. Furthermore, the data demonstrate that this detection response is linear with respect to the amount of mutant-type protein within a low concentration range. The second application expands on our previous work comparing wild- and mutant-type proteins. Using the automated denaturant pulse protocol, one can rapidly assess differences through the acquisition of distinct and separate kinetically

controlled denaturation isotherms. In the case presented herein, this comparison is made between wild-type and two missense folding disease mutants for von Willebrand factor (vWF). In the final application, GroEL is used as a scaffold to aid negative-stain EM and tilt series image acquisition to construct low-resolution structures of the aggregation-prone tetanus neurotoxin (TeNT) from a mixed population while also visualizing the GroEL-TeNT complexes.

MATERIALS AND METHODS

Materials

Bovine Serum Albumin Fraction V (BSA FV) (Sigma Aldrich A9647) was diluted to 1 mg/mL with GroEL Buffer (GB) from a 300 mg/mL BSA FV stock in ultrapure (18.2 MΩ) water. All other materials (buffer agents and salts) were obtained from Fisher Scientific. The cryoSPARC system (Structura Biotechnology) is run on a single Supermicro 4U workstation equipped with 2x NVIDIA Titan Xp GPUs, Intel® Xeon® E5-1630 v4 processor, 4x 16 GB DDR4-2400 RAM, 1.2 TB Intel® SSD DC S3610 for runtime caching, and 4x 4 TB Seagate HDD for data storage (Silicon Mechanics assembled), which is housed in lab.

GroEL Purification

GroEL was purified following protocols outlined previously (Voziyan and Fisher, 2000; Lea et al., 2016). GroEL stock solutions were stored in GroEL buffer (50 mM Tris, 50 mM KCl, 10 mM $MgCl_2$, 0.5 mM EDTA, pH 7.5) at 50 μM tetradecamer with 50% glycerol at 4°C.

MBP Purification

Wild-type and W169G MBP were expressed in *E. coli* and purified using methods described previously for His_6 tagged proteins (Xia et al., 2013). Purified protein was stored in 20 mM phosphate buffer at pH 7.0 with 100 mM NaCl.

vWF A1-A2-A3 Purification

Wild- and mutant-type vWF A1-A2-A3 tridomains with von Willebrand Disease point mutations (V1314D and F1369) engineered into the A1 domain (Tischer et al., 2014) were expressed with a C-terminal His_6 tag on the A3 domain and purified as previously described (Auton et al., 2007a). Purified protein was stored in vWF buffer (25 mM TRIS, 150 mM NaCl, pH 7.5) at 4°C and used within 2 weeks.

TeNT Purification

Tetanus neurotoxin was purified in the Baldwin laboratory as previously described (Burns and Baldwin, 2014). In brief, site directed mutagenesis was performed to remove the catalytic residues (R372A/Y375F). TeNT(RY) was expressed in *E. coli* and cell lysate was passed over both Ni-NTA and Strep-Tactin resins to twin affinity purify the neurotoxin. Purified protein was concentrated to 1.5 mg/mL in TeNT buffer (30 mM HEPES, 500 mM NaCl, pH 7.6) and frozen at −80°C until use.

GroEL-BLI Biosensor Construction

Preparation of the GroEL-BLI biosensor followed similarly to methods previously described (Naik et al., 2014; Pace et al., 2018). GroEL stock solution was buffer exchanged with GroEL buffer (GB) using an Amicon Ultra-4 30 MWCO to remove glycerol and monomers. The exchanged GroEL was then biotinylated using NHS-PEG12-Biotin (Thermo Scientific 21312) at a 20:1 biotin:GroEL ratio for 30 min at room temperature. Biotinylated GroEL (bGroEL) was then buffer exchanged into fresh GB in order to remove excess biotinylation reagent from solution. The GroEL-BLI biosensor was prepared in the beginning of each BLI run by hydrating a streptavidin tip (*forté*Bio 18-5019) in GB for 10 min, followed by a 1 min binding step in 0.5 μM bGroEL with a wash step in GB for 30 s to remove non-bound bGroEL. Loading amplitudes were 5–6 nm indicating saturation of the biosensor surface. As a precaution, GroEL tips were incubated in a BSA solution to block non-specific binding sites (Naik et al., 2014; Pace et al., 2018). Natively folded BSA does not bind to GroEL or inhibit its ability to bind hydrophobic patches. The GroEL-BLI biosensor was then used for subsequent experiments.

Standard Curve Construction for MBP Experiments

The following seven steps were performed using the BLItz to generate a standard curve using varying MBP concentrations (0.5, 1.0, 1.5, 2.0 μM) for both wild-type and W169G:

Step	Time (s)	Event	Composition
1	30	Initial Baseline	GroEL Buffer (GB)
2	300	Loading	0.5 μM bGroEL in (GB)
3	30	Baseline	GB
4	300	Custom	1 mg/mL BSA FV in GB
5	30	Baseline	GB
6	300	Association	MBP WT/W169G/Mix in GB
7	300	Dissociation	GB

For wild-type/W169G mixture, concentrations of 0.5, 1.0, 1.5, and 2.0 μM W169G MBP were tested in the presence of 0.5 μM wild-type MBP in order to determine whether the mixture would more closely resemble either the wild-type or W169G MBP response. Each sample concentration for the above experiments was tested three times for reproducibility. Experiments were all conducted at room temperature. Binding responses were extracted at 988.50 s into each run, or 298.50 s into the association step in the above table so as to diminish small contributions from buffer induced refractive index changes during the dip and read procedure.

Z′ Factor Calculation

Z′ factor (read Z prime factor) is calculated for high throughput screening using the formula:

$$Z'Factor = 1 - \frac{3\left(\hat{\sigma}_1 + \hat{\sigma}_2\right)}{\left|\hat{\mu}_1 - \hat{\mu}_2\right|}$$

In the formula above, $\hat{\sigma}_1$, $\hat{\sigma}_2$, $\hat{\mu}_1$, and $\hat{\mu}_2$ are the sample standard deviations and sample means, respectively, for condition 1 and condition 2. In this study, binding response is the input with condition 1 being pure wild-type and condition 2 being pure mutant-type population. $Z^{'}$ factors can range from 0 to 1 with any score of 0.5 or better indicating those conditions are appropriate for assay development. If the sample standard deviations are equal, a score of 0.5 indicates there are 12 standard deviations separating the sample means. This data was collected on the single-channel BLItz unit and the assay sensitivity and reproducibility can be improved if the eight-channel Octet is utilized (Lea et al., 2016).

Denaturant Pulse Assay for vWFA1-A2-A3

A sample complete run for von Willebrand Factor is represented in **Figure 1A**. This triple A domain protein (A1-A2-A3-His_6 tag) was attached to a Ni-NTA BLI biosensor in an orientation where the A3 domain is closest to the biosensor surface. The vWF denaturant pulse assays were performed on an automated eight-channel Octet RED96 instrument (*forté*BIO) shaking at 1,000 rpm, 25°C. For detailed programming of the denaturant pulse system, see our previous publication (Lea et al., 2016). The programmed steps were as follows with the urea range from 0 to 7 M by 1 M step:

Step	Time (s)	Event	Composition
1	30	Initial Baseline	vWF Buffer (vWFB)
2	300	Loading	0.6 μM vWF Protein in vWFB
3	30	Baseline	vWFB
4	600	Custom	Urea Range
5	10	Baseline	GroEL Buffer (GB)
6	300	Association	0.5 μM GroEL in GB
7	300	Dissociation	GB
8	5	Regeneration	10 mM glycine, pH 1.7
9	5	Regeneration	GB
10	5	Regeneration	10 mM glycine, pH 1.7
11	5	Regeneration	GB
12	5	Regeneration	10 mM glycine, pH 1.7
13	5	Regeneration	GB
14	60	Regeneration	10 mM $NiCl_2$

Runs were performed in triplicate with tip regeneration performed after runs 1 and 2 only. The GroEL binding signal was plotted as a function of denaturant concentration to create kinetically controlled denaturation isotherms for wild-type, gain of function (V1314D), and loss of function (F1369I) mutant vWF (**Figures 1B,C**). For **Figure 1**, Step 4 above was run for 300 s resulting in less GroEL association as compared with the GroEL binding amplitudes presented in **Figure 4**. The denaturant pulse isotherms for both experiments followed the same trend (data available upon request).

Transmission Electron Microscope Sample Preparation

Two hundred mesh carbon-coated copper grids (Electron Microscopy Sciences CF200-Cu) were glow discharged for 20 s at −15 mA in 39 mBar atmosphere. After glow discharge, grids were rested for approximately 20 min before sample application. 4 μL of sample was applied to the rested grid for 1 min and then wicked off using Fisherbrand™ P8 Grade filter paper. Grids were washed once with ultrapure water and wicked off as fast as possible. The grids were then stained for 5 s with 0.022 μm filtered 0.75% uranyl formate (Electron Microscopy Sciences 22451) in ultrapure water and then wicked dry. Grids were completely dried overnight on filter paper inside a 100 mm Petri plate. All EM images were acquired using 100 keV JEOL-JEM 1400 transmission electron microscope aside from the tilt series.

Tilt Series Acquisition and Alignment

A pre-made grid was loaded into a single tilt axis holder and inserted into a FEI Tecnai F30 G2 Twin transmission electron microscope. After beam alignment, the grids were manually scanned for well-isolated complexes. Once found, a tilt series was taken from 0° to +60° and then 0° to −60° every 2°. The series was combined in order by the microscope's capture software. The single .mrc stack file was separated into single micrograph .mrc files using *excludeviews* command from IMOD (Kremer et al., 1996). The single frames were manually realigned using midas from IMOD. Frames −60° to −56° and +58° to +60° were excluded from final processing as the grid bar blocked the electron beam.

GroEL-TeNT ATP Release Sample Preparation

The following steps were run on the single channel BLItz unit:

Step	Time (s)	Event	Composition
1	30	Initial Baseline	GroEL Buffer (GB)
2	60	Loading	0.5 μM bGroEL in GB
3	30	Baseline	GB
4	600	Association	0.5 μM TeNT in GB
5	30	Baseline	GB

After the run was completed, the biosensor tip was transferred into a PCR tube containing GB + 450 mM NaCl + 10 mM ATP (stock solution at pH 7.5) for 10 min to release the captured TeNT. After release, the sample was stained for EM without resting the grid first and with 2 additional wash steps between sample and stain to remove phosphate ions, which precipitates uranyl ions.

GroEL-mAb Complex Sample Preparation

Modified biotin GroEL biosensors were prepared exactly as it would be for normal GroEL biosensors with the sole difference the replacement of NHS-PEG12-Biotin with NHS-SS-Biotin. Once adequate binding of the IgG was observed via BLI, the tip

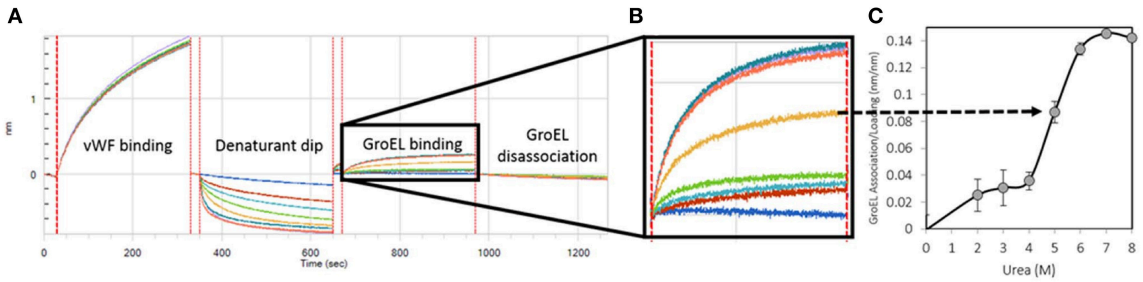

FIGURE 1 | Generation of a Kinetically Controlled Denaturant Pulse Isotherm for the Wild-type von Willebrand Factor A1-A2-A3 Triple Domain Fragment. **(A)** Protein is partially denatured during automated urea pulse steps, and **(B)** the GroEL binding amplitude was **(C)** plotted as a function of urea concentration to generate a kinetically controlled denaturation isotherm (Lea et al., 2016).

was manually held in a 3 μL drop of 50 mM DTT for 20 s. The sample was then processed as normal for EM analysis.

GroEL-TeNT Thermal Sample Preparation

Equimolar concentration (500 nM) of TeNT and GroEL were mixed in GroEL Buffer and incubated at 25°C 200 rpm for 24 h. Samples were diluted to 7 nM and stained as described.

TeNT Reconstruction Using Cryosparc System

Single particle reconstructions were performed on images taken on a 100 keV JEOL-JEM 1400 transmission electron microscope of thermal GroEL-TeNT complex grids. EMAN2 was used to pick particles, perform CTF correction, generate structure factor, and generate .star files for future processing (Tang et al., 2007). The data from 537 particles was then imported into the cryoSPARC system using the .mrc and .star files (Punjani et al., 2017). *Ab initio* modeling and one round of refinement were performed in cryoSPARC using default settings aside from double the pre- and post-annealing default iterations. Twenty-two angstrom (22 Å) resolution was generated using a 0.143 FCS score. cryoSPARC was used for the tilt series reconstruction using the same steps, but the input images were of only 28 TeNT particles, with each particle having 57 views, corresponding to each angle in the tilt series. These views from the tilt series were input as individual 3D particles. The total number of 2D tilted views that went in the reconstruction of the tilt series generated dataset was 1,500. The I-TASSER structure (Zhang, 2008) was fit into both the single particle reconstruction and tilt series electron density maps using molecular dynamics flexible fitting (Trabuco et al., 2008).

DEVELOPING GROEL INTO A DIRECT BIOSENSOR TO DETECT PARTIALLY FOLDED PROTEIN POPULATIONS WITHIN PROTEIN MIXTURES

GroEL Biosensors

Noting the promiscuous capture efficiency of the chaperonin GroEL, biosensors were developed with the goal of detecting protein populations that possess exposed hydrophobic regions. Many proteins exist as dynamic equilibrium mixtures of folded and hydrophobic, partially folded species. These hydrophobic entities (and regions) can either exist as long-lived, stable species or flickering, transient species that appear and disappear as a function of time. It is possible to detect the presence of transiently unfolded species that exist for a long enough window of time to collide with GroEL in their open state. The existence of this fluctuating equilibrium is particularly important when evaluating the integrity of protein populations that may be susceptible to slow aggregation reactions. Protein populations that expose transient hydrophobic patches are often the primary event that eventually leads to deleterious aggregation. This makes this approach relevant when determining if pre-aggregation hydrophobic species are present in concentrated biotherapeutic formulations. The binding site of GroEL can accommodate domains of large protein to detect partially folded hydrophobic regions which cannot fully enter the nanochamber. The visualization of the GroEL-protein complexes may be useful in identifying regions that lead to aggregation during long-term storage.

The pharmaceutical industry is intensely interested in stabilizing biotherapeutic proteins to increase shelf-life, enhance or engineer product stability, increase drug delivery efficacy, and to avoid patient immune response against the biotherapeutic protein arising from aggregation products. The development of the biolayer interferometry (BLI) GroEL biosensor permits direct assessment of protein stability in concentrated protein solutions of biotherapeutics or related examples (Naik et al., 2014; Pace et al., 2018). BLI label-free methods are preferable over surface plasmon resonance (SPR) methods because the former technique does not rely on microfluidic flow through microchannels. The latter method (SPR) can be easily compromised by aggregation events, resulting in microchannel blockage and fouling. In addition to the aggregation phenomenon, high protein concentrations will result in immense refractive index changes during an SPR run that must be subtracted from the sensogram. The scheme illustrated in **Figure 2** demonstrates a typical BLI GroEL biosensor output sensogram. A unique feature of this GroEL biosensor system is the release of the partially folded protein or hydrophobic transients from the biosensor surface during ATP incubation. This ATP dependent reversal

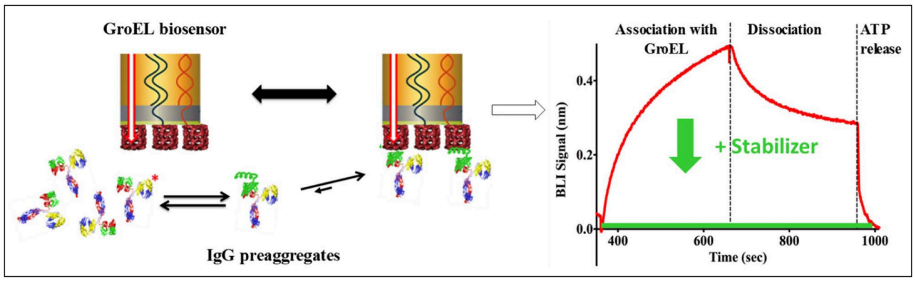

FIGURE 2 | General Scheme on the Use of Biolayer Interferometry and GroEL Biosensor**.** The biosensor can be used to detect the appearance of pre-aggregates (here shown on the left as IgG localized unfolding (green helix). The GroEL biosensor can capture the unfolded region even though the majority of the IgG is properly folded. On the right-hand side, a representative sensogram is shown where association and dissociation phases can easily be seen. The dissociation is non-specific interactions. This is confirmed by specific interaction reversal by ATP addition. The green curve demonstrates how a specific stabilizer could limit IgG association with GroEL.

of protein binding to GroEL results in a return to the baseline before capture indicating that the GroEL-protein interaction specific for the GroEL binding site (Naik et al., 2014; Pace et al., 2018). If stabilization of the protein is achieved either through the alteration of the formulation solution, the addition of stabilizing ligand, or genetic engineering, the capture by the GroEL biosensor is diminished, sometimes quite dramatically (Naik et al., 2014; Lea et al., 2016; Pace et al., 2018).

In an expansion of the use of the GroEL biosensor, it is of interest to determine if one can detect increases in mutant-type population within a mixture of wild- and mutant-type protein. Proof of concept experiments are presented in this section for the model protein maltose-binding protein (MBP). MBP with the W169G missense mutation is a less thermally stable protein, resulting in a dynamic equilibrium between folded and partially folded conformers. First, demonstration of a linear binding response with respect to the protein concentration after a certain time (**Figure 3A** – dotted line) is generated for pure populations of either wild- or mutant-type protein and the amplitudes are plotted as a function of concentration. Next, it is of interest to determine how this linear response of the mutant-type protein behaves when MBP species are mixed in solution. Experimental setups such as these may help determine if the mutant protein misfolding is independent or dependent of the presence of the wild type protein. In the latter situation, this type of an assay may be helpful in assessing the ability of mutant-type proteins to induce misfolding of stable wild-type species. The potential interactions between wild- and mutant-type folds leading to an induction of misfolding can be applicable toward understanding the impact of protein misfolding in some disease states. This situation is particularly relevant for instances where one mutant allele results in dominant negative phenotypes as seen with many tumor suppressor p53 mutations.

Detection of Mutant Population Within a Mixed Solution of Wild- and Mutant-Type MBP

The GroEL biosensor detected the greatest increase in binding amplitude for the mutant population alone as compared with the synonymous concentration of wild-type MBP (**Figures 3A,B**). The mixed population biosensor binding amplitudes showed a slight decline in sensitivity as compared to the pure populations. However, the mixture of wild type and mutant protein still show an increased binding response as compared to the wild-type protein alone (**Figure 3B**). Additionally, this increased response is linear with respect to the concentration of mutant-type subpopulation with the shallower slope indicating the lessened sensitivity. Light scattering measurements at 320 nm showed no increase suggesting that the presence of large aggregate species is not prevalent in any of the mixture samples, supporting the notion that the binding amplitude from the GroEL biosensor was due to the presence of pre-aggregate subpopulations. This lessened sensitivity is most likely due to reduced collisional frequency effects simply from the presence of native folded MBP. The calculated Z' factor between the pure wild- and mutant-type populations at 2 μM concentration is 0.649. Any Z' factor above 0.5 indicates that this concentration and conditions is useful for assay development (Zhang et al., 1999; Lea et al., 2016).

Thus, it is possible to detect a change in binding signal due to the increased presence of less stable hydrophobic species. Disparities in linear response between mutant-type alone and wild-/mutant-type mixture populations are predicted to be substantially altered (diminished) if the wild- and mutant-type proteins interact to bury the exposed hydrophobic faces.

COMPARISON OF KINETICALLY CONTROLLED DENATURATION ISOTHERMS OF WILD- AND MUTANT-TYPE VON WILLEBRAND FACTOR USING GROEL-BLI DENATURANT PULSE ASSAY

Denaturant Pulse Assay

The kinetic stability of aggregation-prone proteins can be determined using a unique chaperonin dependent denaturant pulse assay. This technique assesses the stability of proteins immobilized on BLI biosensor surfaces after a time-controlled

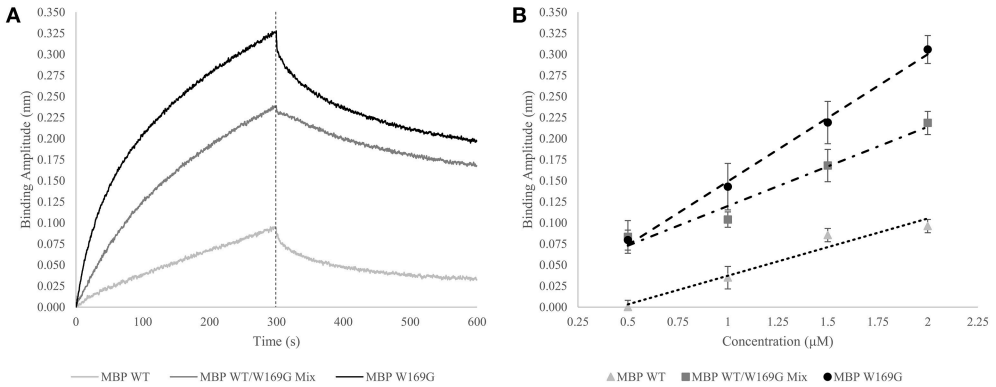

FIGURE 3 | Wild- vs. Mutant-Type MBP Capture by GroEL Biosensor. **(A)** Raw biosensor traces at 2 μM for wild-type (light gray), W169G (black), and the mixed population (dark gray). The dotted line indicates the end of association, which is the amplitudes used for the linear response. **(B)** Linear response of wild-type and destabilized mutant-type MBP capture versus concentration (triangles and circles, respectively). For pure protein population, the x-axis is absolute concentration. Dose-dependent response of doping mutant-type MBP into wild-type is shown in squares. For the protein mixtures, the x-axis value is the concentration of mutant-type added to a solution containing 0.5 μM wild-type. R-squared values for the wild-type, W169G, and mixture are 0.964, 0.996, and 0.961, respectively. The Z' factor for wild-type versus mutant-type response at 2 μM is 0.649, which indicates the response of this system is reliable to develop an assay that can distinguish between mixtures and homogenous proteins.

pulse in various denaturant solutions. GroEL binding to hydrophobic patches on the unfolded protein amplifies the unfolded protein signal. The development of this method is discussed in a previous publication from this laboratory (Lea et al., 2016). Kinetically controlled denaturation isotherms were rapidly and reproducibly generated for several protein systems. In this current work, the denaturant pulse approach is expanded to encompass new and more complex systems. To illustrate the expanding utility of this method, denaturation isotherms of wild- and mutant-type von Willebrand Factor (vWF) triple A domain were collected and compared. Many missense mutants have a tendency to aggregate in solution during conventional stability analysis. Therefore, the immobilization of missense mutants prior to performing the denaturant pulse assay avoids this common difficulty.

von Willebrand Factor

vWF is a multimeric plasma glycoprotein which initiates platelet adhesion at sites of vascular injury. Under high shear stress, vWF unravels and binds to platelets and collagen to create a plug to stop bleeding. von Willebrand Disease (vWD) is a bleeding disorder affecting approximately 1% of the world population. This hereditary disease is caused by mutations that cause quantitative deficiencies of vWF or qualitatively alter vWF function. Mutations in A1 of the triple A domain of vWF alter its specificity for the platelet receptor GP1bα. Mutations in A3 can affect its collagen binding affinity. Finally, mutations in A2 cause defective intracellular transport or enhance proteolysis of a scissile bond recognized by the soluble blood metalloprotease (ADAMTS13), which helps regulate the multimeric size of vWF (Keeney and Cumming, 2001). Some vWD mutations that change A1-GP1bα binding specificity result in local misfolding of the A1 domain (Tischer et al., 2014, 2017; Zimmermann et al., 2015; Machha et al., 2017) causing both gain and loss of function phenotypes. Two such mutations are V1314D, a gain of function mutation that causes increased platelet adhesion, and F1369I, a loss of function mutation that does not adhere to platelets at all. The GroEL-based BLI denaturant pulse assay was used to assess the kinetic stability of vWF A1-A2-A3 for both wild-type and partially disordered vWD point mutants.

vWF Wild- & Mutant-Type Denaturant Isotherms

The kinetically controlled denaturant isotherms for wild-type, F1369I, and V1314D vWF triple A domains are shown in **Figure 4**. GroEL binding to these misfolded triple A domain variants was assessed as a function of urea concentration using a BLI denaturation pulse assay. vWF-GroEL association was confirmed with direct observation using EM (see section Release and EM Analysis of Proteins Released From Biosensor Surfaces). Although, the gain of function mutant V1314D had exposed hydrophobic patches under little or no denaturant as evidenced by GroEL association at these urea concentrations, the denaturant pulse profiles for wild-type and V1314D were similar at high urea concentrations. By contrast, F1369I and wild-type had similar GroEL binding at low urea concentrations, but at high denaturant conditions the F1369I exhibited significantly higher binding by GroEL.

In equilibrium denaturation profiles using urea, the thermodynamics of vWF triple A domain unfolding has been described as three domains linked in a linear fashion in which unfolding of each domain proceeds orderly with the simultaneous unfolding of A1 and A2 at low urea followed by A3 at high urea (Auton et al., 2007b). Evidence suggests that in the absence of urea, the A1, A2, and A3 domains interact with each other and mutations can disrupt these interactions as a result of their intrinsic effects on the single domain (Auton et al., 2010). It is possible that the interactions between domains observed in

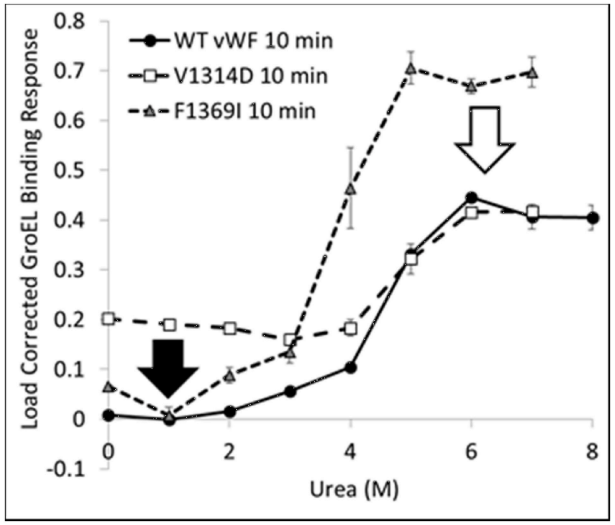

FIGURE 4 | vWF Kinetically Controlled Denaturant Pulse Isotherms for Wild- and Mutant-Types. Kinetic denaturation isotherms for the wild-type (circles), gain of function mutant (squares), and loss of function mutant (triangle) overlaid for comparison. The closed and open arrows denote the potential corrective ligand induced responses that may restore wild-type denaturant pulse profile and protein function.

the wild-type protein are differentially altered depending on the structural location of a mutation (Zimmermann et al., 2015), whether the mutation occurs at a domain interface, its intrinsic effect on thermodynamic stability of a domain (Auton et al., 2009), and/or its propensity for local disorder (Zimmermann et al., 2015). These intrinsic properties of the vWF triple A domain would therefore lead to different GroEL binding efficacies thus altering the urea denaturant pulse dependence of GroEL binding.

For V1369D, the disordered structure of the A1 domain (Tischer et al., 2014) is such that GroEL is able to bind to the vWF triple A domains even with low urea concentrations. By contrast, F1369I requires a much higher urea concentration to yield extensive GroEL binding. These observations imply that structural disorder induced in the A1 domain by these mutations result in altered quaternary A1-A2-A3 domain interactions that are differentially recognized by GroEL. The structural disruption of A1 by V1314D is so severe that GroEL readily recognizes exposed hydrophobic regions without urea denaturation. Conversely, F1369I, which also misfolds the A1 domain, may cause A1-A2-A3 domain to reorganize its quaternary structure forming unnatural domain interfaces which are stabilized against urea denaturation, thereby requiring higher urea to achieve similar levels of GroEL binding. This differential binding by GroEL depending on the mutation may be reduced by post-translational glycosylation, which normally decorates the vWF surface but are lacking when bacterially expressed.

The BLI denaturation pulse assay for the wild- and mutant-type proteins may have potential to be used as a rapid drug discovery platform. Performed with candidate small molecule stabilizers generated using *in silico* selection algorithms, this assay could be used to determine if the test compounds rectify the structural origins of misfolding. Any compound which returns proper folding to the mutant-type protein would return the mutant denaturation isotherm to match that for wild-type (**Figure 4** arrows). Although these mutations presented herein are both in the A1 domain, a different stabilizing compound may be required to correct each specific mutation as the two mutants do not have the same effect on the denaturation isotherm and likely represent two different misfolding events which need to be stabilized.

The ability to generate kinetically controlled denaturation isotherms for entire sets of phenotypically distinct single site mutations may offer researchers a unique tool with the advantage of distinguishing properties of different mutant-types. A recent comparison of the wild type and mutant maltose binding protein constructs used in section Introduction also shows clearly different denaturation isotherms (Trecazzi and Fisher, 2018). For specific missense disease proteins, the observation of these kinetic differences in mutant stabilities indicate that one may have to design very specific correctors for specific mutations, strengthening the case for implementing personalized/precision medicine approaches to rectify both common and rare protein folding diseases.

TRANSMISSION ELECTRON MICROSCOPY ANALYSIS OF GROEL CAPTURED PROTEINS

Protein 3D Reconstruction Using cryoEM

Advances in obtaining atomic resolution structures using cryo-electron microscopy (cryoEM) still depend on sample integrity and purity (Earl et al., 2017). Before starting cryoEM imaging, it is imperative to assess sample integrity, which is usually accomplished by visualizing the sample using negative-stain EM. Optimal samples are those that are highly pure and homogenous with respect to conformation. Additionally, these negative-stained images can sometimes be used to generate preliminary 3D envelopes that can be useful to train automated particle picking programs. As with all negative-stain protein samples, there are caveats that must be considered, such as flattening and grid adherence effects, which in turn may lead to diminished conformational and orientation diversity. Despite these caveats, negative staining is still the much preferred first step in sample evaluation due to ease of preparation and relatively low cost. In solution, GroEL stabilizes aggregation prone proteins by temporarily removing misfolding species and preventing them from interacting with other proteins (Horwich et al., 2009; Tyagi et al., 2011). By pairing GroEL with the biosensors we can extend the use of this tool to study both the stability of target proteins and the location of the unfolding. The use of the chaperonin as both a capture-release and a capture scaffold platform that can facilitate visualization of the structures of aggregation-prone proteins using a very small quantity of sample will be discussed. The ability to immobilize and assemble complexes on the biosensor surface followed by

release into microvolume drops permits determination of their structural integrity. Importantly, by demonstrating that it is possible to visualize proteins released from the GroEL biosensor surfaces, this capture-release technique enables one to potentially view conformations of aggregation prone proteins, a common problem that confronts many researchers who want to obtain credible 3D protein structures for their protein system of choice.

GroEL Stabilization of Aggregation-Prone Proteins

GroEL-anthrax Protective Antigen Stabilization

The observation that the large 440 kDa protective antigen (PA) prepore structure can form stable complexes with the GroEL chaperonin in solution (see Figure 1 from Katayama et al., 2008) led to surmise GroEL-folded protein substrate complexes could also be visualized using EM. Thus, initial work from this laboratory confirmed that one can capture large folded protein complexes on the GroEL chaperonin and easily visualize these stable captured complexes using negative-stain EM. From these micrographs, low-resolution negative-stain reconstructions of the bound anthrax pore structure were obtained while simultaneously avoiding misfolding of this aggregation-prone toxin pore (see Figure 2 from Katayama et al., 2008). The compiled results from this analysis are summarized in **Figure 5**. These early results using GroEL as a molecular scaffold to capture the transitioned pore indicated that these low-resolution structures are quite similar in shape to the atomic resolution anthrax pore structures solved by Hong Zhou's group in 2015 (see Figure 1 from Jiang et al., 2015). In further agreement, domain 4 lacked electron density in both the atomic and the GroEL captured PA pore electron density maps, which is attributed to increased flexibility of this domain and not the limitation of the capture system. The formation of the complex between GroEL and the anthrax pore were driven primarily by electrostatic interactions and were easily reversed when ATP was added. In contrast to the physiological transition condition of low pH, the GroEL-PA prepore transition was accomplished by incubation in 1 M urea at 37°C. This condition is tolerated by both GroEL and GroEL-PA complex and is sufficient to permit the PA unfolding/refolding transition to occur while remaining bound to GroEL as a scaffold. This GroEL capture of the PA prepore allows successful transition from PA prepore to PA pore without allowing off-pathway aggregation, which predominates when PA transitions in solution. This is likely due to the fact that the GroEL-PA pore complex has a larger size (1.24 MDa) and, therefore, has a much slower diffusion rate as compared with the PA pore alone. Most importantly, this approach shows large macromolecular structures can be easily resolved while bound to GroEL. In the following sections, numerous examples are presented where this methodology is useful in aiding in the visualization of other folded proteins that are captured by the GroEL chaperonin.

Solution Stabilization of Tetanus Neurotoxin

Tetanus neurotoxin

From the past 200 years of research into tetanus neurotoxin (TeNT), much about its functionality is known. However, the mechanistic details and the physical changes which accompany membrane insertion and protein transport across membranes under low pH conditions are unknown. To better understand this process, it is important to obtain the atomic structures of the neurotoxin upon neuron binding, membrane interface association, and membrane insertion via cryoEM. At the time that this manuscript was being assembled, a crystal structure and a cryoEM structure of tetanus neurotoxin was published (Masuyer et al., 2017). Even so, the negative-stain images of GroEL-TeNT and TeNT presented herein possess great similarity to the cryoEM TeNT structure with the 3D reconstructed electron density maps being in agreement. The following section highlights the ease by which this was accomplished and indicates that even a single resulting electron microscopy tilt series of the GroEL-TeNT complex exhibited discernable electron density surface topology that is highly similar to the cryoEM surface representation. In addition, it is demonstrated that a 3D reconstruction of TeNT can be generated using as few as 28 individual particles imaged as a tilt series.

GroEL prevents aggregation under low salt conditions

The previous three examples (MBP, IgG, & vWF) have demonstrated the use of GroEL in conjunction with BLI, but, as previously mentioned, GroEL can also be used in solution to prevent protein misfolding and aggregation. Once purified, TeNT is stored in a high salt solution (0.5 M NaCl) as it will aggregate under low salt conditions (0.05 M). However, aggregation of TeNT under low salt conditions can be prevented by addition of GroEL, presumably through the capture and release cycles of aggregation-prone, misfolded TeNT molecules. This permits visualization of TeNT using negative-stain EM, where the staining protocol becomes problematic due to high salinity.

Tilt series on the GroEL-stabilized TeNT

With the ability to visualize TeNT without aggregation, the gridded and stained TeNT can be imaged using a tilt enabled electron microscope and specimen holder. A tilt series was collected for this sample using a 200 keV field emission gun (**Figure 6**). A representative aligned tilt series is provided as a movie in Supplemental Video 1. One can clearly discern the cross like structure of the bound TeNT protein and the domain that interacts with GroEL appears to be the extended receptor binding domain. Comparison with the cryoEM single particle reconstruction envelope (EMD 3588) supports this conclusion. Supplied with only one single tilt series, 3D reconstruction of tetanus is not possible due to the limitation of the tilt angle preventing total conformation coverage. Additionally, as there is no preferred binding orientation between TeNT and GroEL, the pooling of images from multiple complexes does not result in a 3D envelope of the toxin likely due to differential GroEL capture of TeNT. This difficulty did not hamper the reconstruction of the GroEL-PA pore complex as the entire toxin was exclusively bound on top of the GroEL nanochamber as well as the complementary 7-fold symmetry match which aided to orient all PA pore in the same orientation relative to GroEL (Katayama et al., 2008). The reconstruction of the current complex is

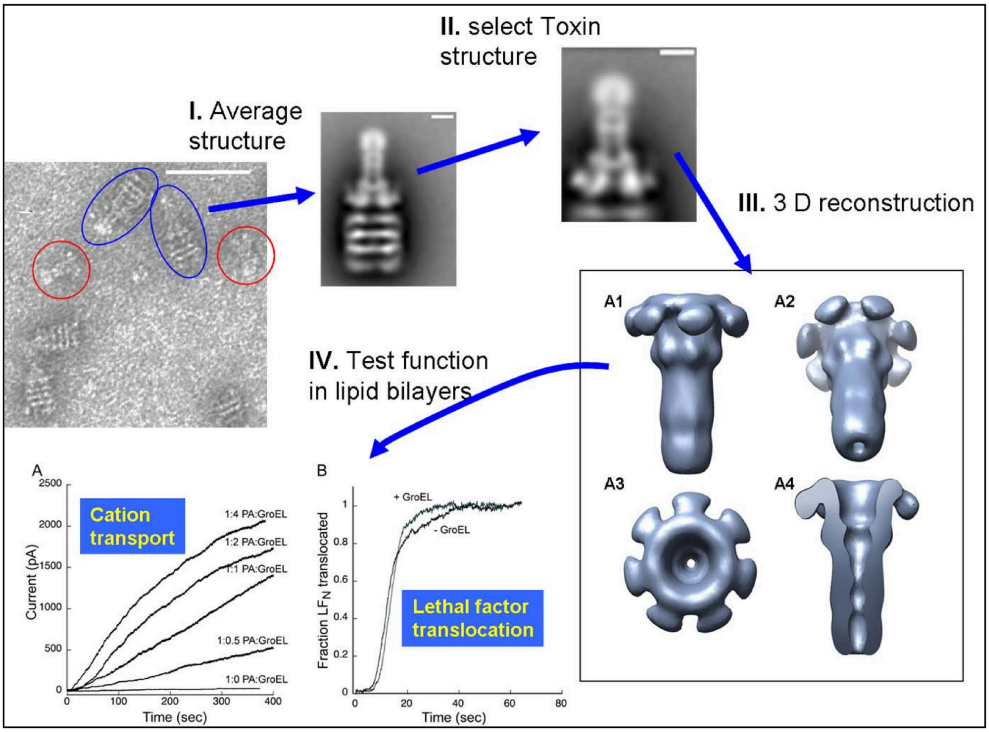

FIGURE 5 | Schematic of the Protective Antigen Anthrax Pore Capture and Conversion. **(I)** 2D class computational averaging of GroEL-PA pore from the micrographs. **(II)** Masking of 2D class averages to reconstruct PA pore alone. **(III)** 3D envelope of isolated PA pore reconstructed using SPIDER, revealing the long β-barrel pore. **(IV)** PA pore functionality was as tested by both **(A)** cation transport and **(B)** lethal factor translocation assays. Micrographs obtained at UMKC. Adapted from Katayama et al. (2008).

hindered by flattening effects due to dehydration and staining inherent in the negative-staining protocol. This flattening is evident by the GroEL appearing flat in the tilt series, lacking its characteristic barrel shape (Supplemental Video 1). This solution based reconstruction does not rule out the possibility of generating molecular structure for the GroEL-TeNT complex. Immobilization of TeNT in the same orientation may force GroEL binding at one site generating identical complexes. Orientation specific attachments have been engineered for TeNT previously (see discussion in Figure 10 in Lea et al., 2016).

TeNT reconstruction from negative-stain tilt series

Unlike the GroEL-TeNT complexes, the non-aggregated monomeric TeNT within the same field can be reconstructed using both single particle reconstruction and particle tilt series. Single particle reconstruction uses only the 0° tilts and hundreds of picked particles. In contrast, fewer particles can be used for reconstruction if the protein is repeatedly imaged while adjusting the tilt angle. The tilt angle is controlled by the acquisition software to ensure equal spacing of 2° between images. Using the cryoSPARC system, an electron density map can be constructed from only 28 unique particles (**Figure 7**; purple mesh, right). The movie for one aligned TeNT tilt series can be seen in Supplemental Video 2. This limited dataset reconstruction matches the traditional single particle reconstruction, which required >500 particles, (**Figure 7**; blue mesh, left) but did not require hundreds of particles to be picked. With further constraints on the input views as shown in Bartesaghi et al. (2012), higher resolution information could be obtained. The number of images generated from the tilt series of 28 particles yielded 1,500 views. Additionally, these two negative-stain reconstructions correlate, despite lower resolution, with the recently published work which solved the high resolution structure of TeNT by both cryoEM, created using 200,000 particles, and the SAXS ensemble (Masuyer et al., 2017). The resolution of these two negative-stain electron density maps can most certainly be improved by using higher tilt angles, increasing the number of particles picked, and ensuring the particles represent greater orientation coverage. However, the purpose of these initial reconstructions was not for high resolution but to demonstrate that low particle numbers can render reasonable low-resolution reconstructions using the cryoSPARC system. This approach may be very useful in situations where small amounts of purified complexes are assembled on BLI biosensors that are then released into microvolumes and visualized using negative-stain EM (see section Release and EM Analysis of Proteins Released From Biosensor Surfaces; Naik et al., 2013, 2014; Pace et al., 2018); thus, the reconstructions only achieved low-resolution. Although this molecular envelope is low-resolution (approximately 22 Å), the model can be used as a valid training dataset for automated neural network particle

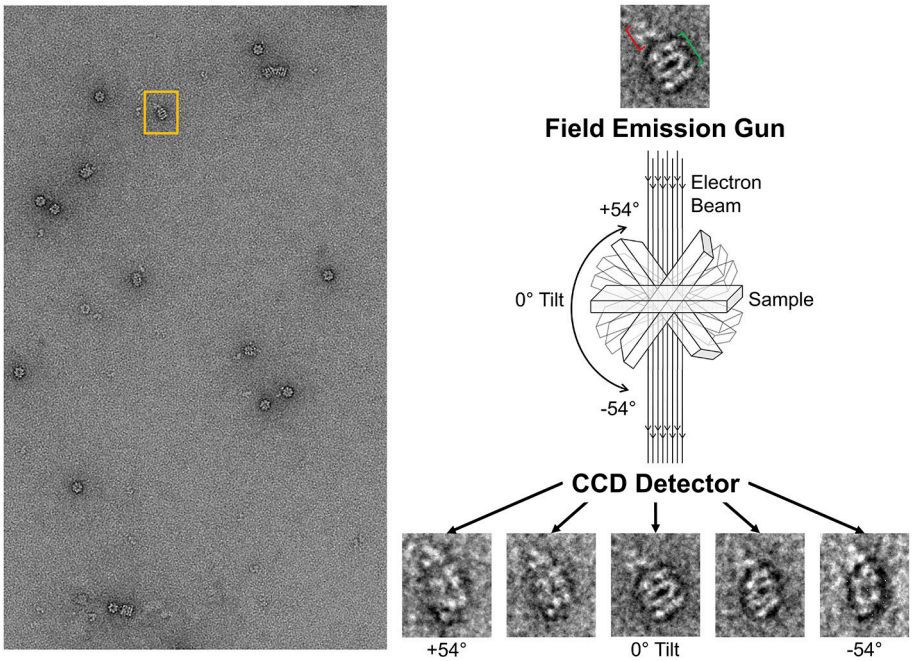

FIGURE 6 | Schematic of Tilt Series Image Capture. **(Left)** Representative micrograph of negative-stained GroEL bound to TeNT. The grid is scanned for isolated complexes to avoid protein overlap at high tilt angles. An appropriate complex is boxed in orange. **(Right)** Enlargement of boxed complex for detail. GroEL can be seen as four parallel bands (green bracket). Captured TeNT (red bracket) can be seen as white density above GroEL. This complex is then repeatedly imaged at 2° increments. Representative tilted image captures are shown at the bottom. Micrographs obtained at MU EMC.

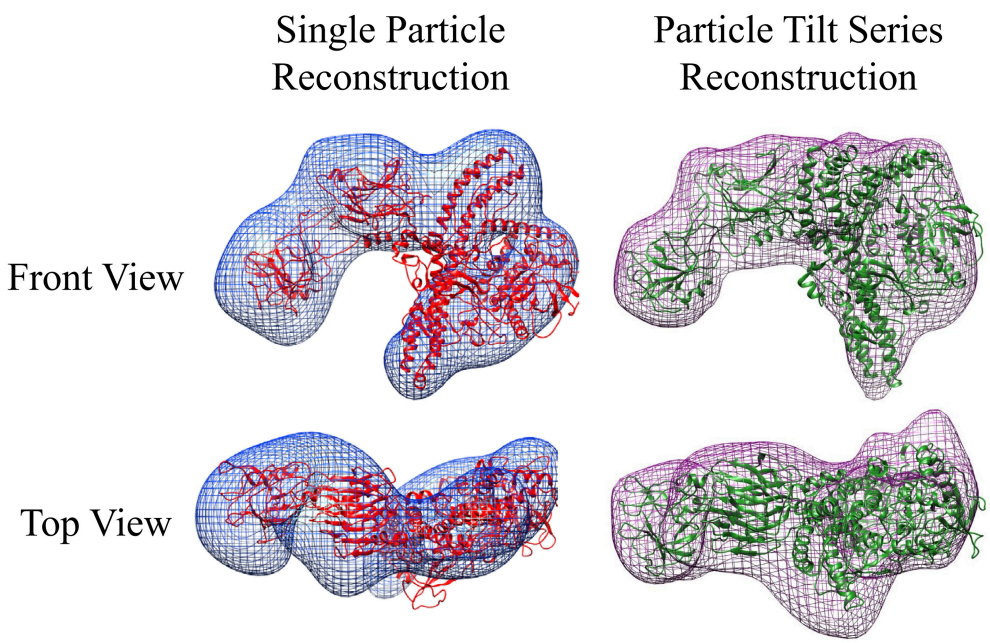

FIGURE 7 | Negative-stain EM Comparative Reconstructions: Single Particle Reconstruction & Particle Tilt Series Reconstruction. **(Left)** Blue envelope of traditional single particle reconstruction using micrographs from **Figure 6**. Red ribbon structure of I-TASSER modeled protein fit using molecular dynamics into the envelope. **(Right)** Purple surface representation of reconstruction of 28 particles from tilt series acquisition. The green ribbon structure is the same I-TASSER fit into the map using MDFF. In this orientation, the receptor binding domain is placed on the left in each reconstruction.

picking programs for both negative-stain EM and cryoEM micrographs.

Release and EM Analysis of Proteins Released From Biosensor Surfaces

As has been shown in sections Developing GroEL into a direct biosensor to detect partially folded protein populations within protein mixtures and Comparison of kinetically controlled denaturation isotherms of wild- and mutant-type von Willebrand Factor using GroEL-BLI denaturant pulse assay, the combination of BLI and GroEL is a powerful tool to assess protein stability. However, as BLI output is in nanometer shift in the interference spectrum and does not carry structural data, it requires the assumption that the expected protein complexes are being constructed on the biosensor surface. To validate complex assembly, the purported GroEL-protein complexes can be orthogonally confirmed using negative-stain EM. Using the proper conditions, the complexes formed in the previous sections can be released from the biosensors after complex assembly, and then gridded and stained with heavy metals (see section Materials and Methods for Experimental Details). Using this technique, the GroEL-protein complexes can be directly visualized. For other techniques that reveal high and low resolution election density envelops of protein complexes such as crystallography or small angle X-ray scattering respectively, it is ideal that the sample consists of homogeneous complexes. If the target protein is inherently varied with respect to conformational heterogeneity (multiple conformations), analyzing the structural outputs by these methods becomes problematic. With EM analysis, each complex can be examined individually and therefore the binding heterogeneity can potentially be revealed in each case, particularly if random tilt series methods are applied. While mass spectroscopy can also identify target protein composition upon ATP induced release from the GroEL chaperonin, the maintenance of solubility during EM analysis is critical. Including the natural anti-aggregation chaperonin protein allows one to obtain low resolution structures of both free and bound substrate protein chaperonin complexes. With GroEL-Protein substrate complexes, previous and new examples shown below indicate that direct EM visualization allows one to broadly identify which folded yet hydrophobic region(s) of the target protein interact with the GroEL chaperonin at its promiscuous protein substrate binding site.

Release of GroEL-vWF Complexes From Ni-NTA Biosensors

For experiments where the GroEL-protein complexes were formed in the reverse orientation where the protein of interest is immobilized, like the vWF denaturation pulse assay presented section Comparison of kinetically controlled denaturation isotherms of wild- and mutant-type von Willebrand Factor using GroEL-BLI denaturant pulse assay of this paper, it is possible to visually confirm of the denaturant induced GroEL association. For experiments where the protein of interest has a His_6 tag, the protein can be immobilized using Ni-NTA biosensors. The coordination between the His_6 tag and the Ni^{++} ion can be gently reversed using either imidazole competition or EDTA chelation. It is imperative to optimize the eluent concentration and elution time using the BLI. By releasing captured proteins into a microvolume drop (3–4 μL), the concentration of any released protein will be relatively high and appropriate for EM. As an example of this release and visualization, the Ni-NTA tip used for the 2 M urea pulse on V1314D was released and stained for negative-stain EM. In this micrograph, it is possible to discern the distinct A1-A2-A3 domain extension, especially in the top view (**Figure 8**; red box). As the His_6 tag is on the C-terminus of vWF, this orients the A3 domain closest to the biosensor surface and, therefore, sterically hindered against GroEL binding. Additionally, the previous solution equilibrium data indicates the A1 domain unfolds first (Auton et al., 2007a). With these two facts, it is most likely the A1 domain captured by GroEL. Although it is not possible to definitively identify the interacting domain with this sample, additional experiments could identify the interacting domains. For example, the addition of an anti-A1 antibody and its distinct density on the GroEL-vWF complex would help identify the GroEL interacting domain via negative-stain EM. In this particular field, the free GroEL observed is a consequence of not washing the biosensor before release. Extensive dissociation of the GroEL from vWF is not observed (see **Figure 1** GroEL dissociation trace).

GroEL-IgG Complexes Released From GroEL Biosensor Surface

As shown in section Developing GroEL into a direct biosensor to detect partially folded protein populations within protein mixtures, GroEL biosensors are capable of detecting pre-aggregate transients that exist in solution before it is possible to observe larger scale aggregates using size exclusion chromatography or microflow imaging (Naik et al., 2014; Pace et al., 2018). In order to discern what region of IgG preferentially interact with GroEL, a cleavable biotinylation reagent needs to be employed so the GroEL-protein complex can be released. Replacing the standard biotinylation reagent with one containing a disulfide bond between the biotin moiety and the amine reactive group accomplishes this feat. Incubating the modified GroEL biosensor in 50 mM DTT will reduce the disulfide linkage to release GroEL-IgG complexes into solution. Similar to the imidazole release, optimization of the DTT incubation and release should be performed using BLI. Additionally, the same methodology for microvolume release and EM processing can be used as described above and previously (Naik et al., 2013, 2014; Pace et al., 2018). An example of this release is shown in **Figure 9**. The four, parallel dark bands are GroEL and the extra density to the top right of GroEL is the captured IgG (Naik et al., 2014). Although there was clear protein densities bound to GroEL in the 2014 Naik paper, upon further inspection of the micrographs there were individual EM images of the entire IgG molecule bound to GroEL. In views of the clearer, well-defined complexes, the IgG is bound to GroEL through its Fc portion of the antibody. This region is commonly found to be where aggregation prone antibodies display enhanced fluctuations (Pace et al., 2018).

Although the GroEL binding platform only indicates general regions where hydrophobic region exposure occurs on the Fc

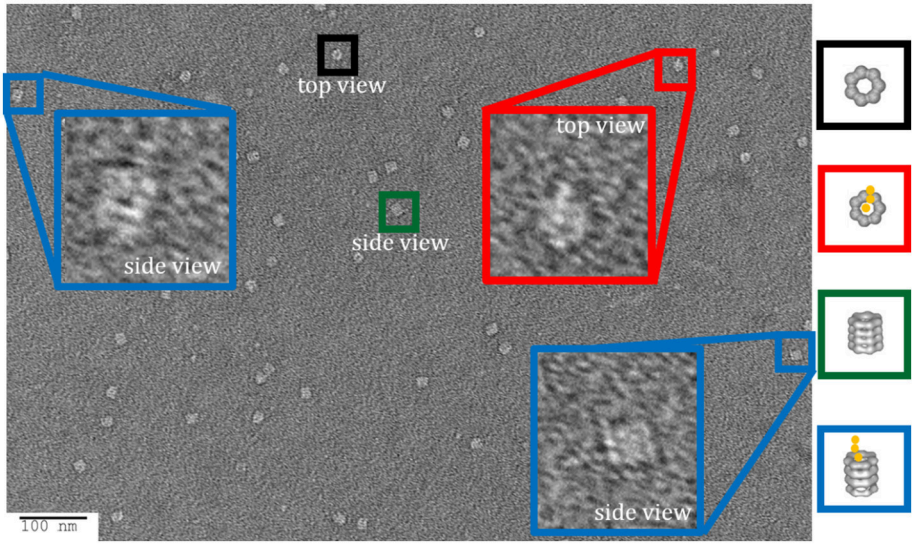

FIGURE 8 | Imidazole Release of GroEL-vWF Complexes from Ni-NTA Biosensor. Representative field of gridded and stained V1314D vWF-GroEL complexes formed after a 2 M urea denaturant pulse. Multiple complexes can be seen as white on dark background. Top view of the complex is boxed in red, in which it is possible to observe the three domains of vWF. Side view of the complex is boxed in blue. Non-complexed GroEL top and side views are boxed in black and green, respectively. Micrographs obtained at KUMC.

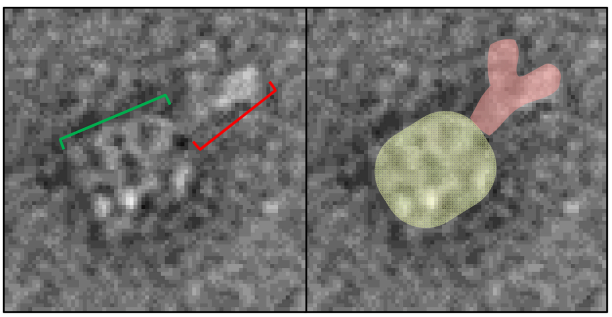

FIGURE 9 | GroEL-IgG complex EM image. **(Left)** Representative particle of the DTT released complex from the modified bGroEL biosensor. The four parallel dark bars are GroEL (green bracket). The dark, extra density to the top right of GroEL is the captured IgG (red bracket). **(Right)** Same image where the proteins are false colored to aid in visualizing the protein boundaries. Images obtained at KUMC.

regions, the EM visualization of these GroEL-Ab complexes may also indicate aggregation prone regions (Pace et al., 2018). In some cases, these hydrophobic regions are pinpointed more precisely through the use of the more sensitive and elegant HDX assay. HDX examines which protein regions have changes in the dynamics and electrostatic interactions governing transient protein-protein interactions and finds them to be located within Fc regions (Majumdar et al., 2015; Arora et al., 2016, 2017). Of note, some these reversible interactions have been documented to be governed by electrostatic interactions. It is also possible that the ring of negative charge which surrounds the GroEL substrate binding site could also contribute to GroEL-Ab interactions. This notion, that some of these interactions may be electrostatic in nature, has not been specifically tested. This could be easily determined by adjusting the ionic strength of the solution or by adding in positively charged species such as arginine.

Release of GroEL Captured Aggregation Prone Proteins From Biosensor Surfaces

For the GroEL biosensors, one can exploit the native functions of the chaperonin to release the captured proteins for visualization. As previously stated, GroEL can hydrolyze ATP to initiate folding and subsequent release of substrate proteins from GroEL. If the GroEL biosensor is introduced to an ATP solution, the captured proteins will be released into solution. As previously, the microvolume method and optimization by BLI should be utilized. An example using TeNT as the protein substrate is given in **Figure 10**. As can be seen in the sensogram, 10 mM ATP achieves nearly full release within 5 min. The experiment can be repeated in the microvolume drop and prepared for EM imaging (**Figure 11**). The enlarged fields show the distinct three domain structure of TeNT.

CONCLUSION

The GroE chaperonin system has a distinct advantage that the nucleotide-free state of the large chaperonin oligomer maintains a constant hydrophobic surface that can capture transient or existing solvent exposed hydrophobic patches. This fact offers a superior level of detection capabilities for partially folded states that are unique to this particular chaperone. While other protein chaperone classes such as the Hsp90, 70 and small Hsp proteins exhibit similar global recognition properties of hydrophobicity, the GroEL chaperonin class (Hsp60) has a high affinity substrate

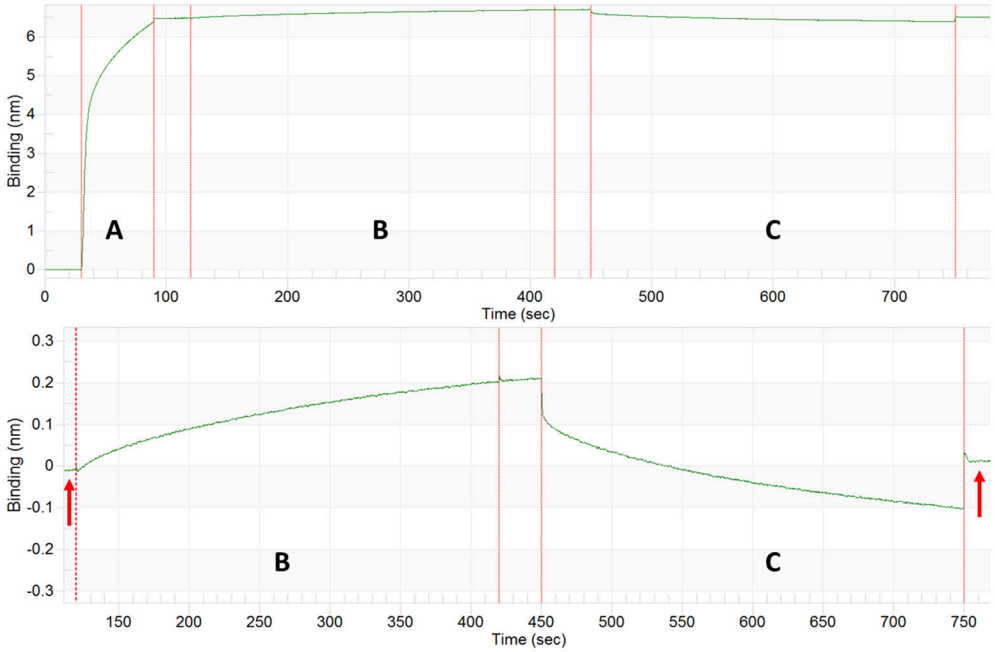

FIGURE 10 | Tetanus Neurotoxin Capture and ATP Release by GroEL Biosensor. Top: BLI sensogram indicating biotinylated GroEL association **(A)**, TeNT capture by the GroEL biosensor **(B)**, and ATP release of TeNT from GroEL biosensor **(C)**. Bottom: Enlargement of TeNT capture and release steps to highlight amplitude change for capture and release. The baselines before association and after ATP dissociation match indicating that the signal increase and decrease are solely from GroEL capturing and releasing TeNT (red arrows). The large initial shifts in the trace for the ATP phase **(C)** are due to a refractive index changes and not a change in protein binding.

capture state that is more promiscuous than other systems. Most importantly, specific binding is easily reversed. Although there are many reviews indicating the absolute requirement of the Hsp10 co-chaperonin class for release of more stringent substrates, our laboratory has found that this requirement is not necessary if folding osmolytes or osmolyte mixtures are included along with ATP to reverse binding to the chaperonin (Voziyan et al., 2000; Voziyan and Fisher, 2002; Fisher and Katayama, 2015). With regard to the other chaperone classes, the Hsp90 and Hsp70 proteins exhibit various binding states for hydrophobic proteins, but their nucleotide-free forms are often not the highest affinity capture state. In the Hsp90 class, there are a number of co-chaperone accessory proteins that are required for substrate specificity and binding. The small heat shock protein class certainly binds to hydrophobic regions to sequester aggregation-prone proteins, and so they have been termed holdases. However, these small heat shock proteins require other chaperone protein systems such as the Hsp70 system to facilitate release and folding (Zwirowski et al., 2017). For other Hsp families, such as the Hsp100 class, the oligomeric forms, which bind to protein aggregates, are not stable as these chaperone proteins assemble and disassemble in a nucleotide dependent manner (Zolkiewski et al., 1999). From the standpoint of constructing immobilized chaperone biosensor platforms, the above-mentioned chaperone classes for the most part have to be specifically oriented on the biosensor surface to properly position the one prominent substrate binding site on these Hsp classes. In contrast, the GroEL chaperonin system is much easier to immobilize as it possesses two opposing binding sites. Even random immobilization schemes always result in the exposure of at least one binding site.

Based on the properties of the chaperonin, there are a few limitations that may impair the utility of the GroEL based detection platforms. The simplest limitation for chaperonin based detection of partially folded substrates depends on the surface electrostatic field that surrounds the chaperonin binding site (Coyle et al., 1997). For example although the chaperonin readily binds to neural folding disease proteins such as Aβ amyloid and α synuclein (Ojha et al., 2016; O'Neil et al., 2018) the chaperonin was unable to bind to aggregation prone tau perhaps due to electrostatic repulsion effects (preliminary data). Indeed, electrostatic effects on binding were also demonstrated with the anthrax toxin (discussed above in section GroEL-anthrax protective antigen stabilization) In this work, we present the use of GroEL and biosensors together to distinguish differential kinetic binding and stability differences that can be observed with between wild type and mutant variants of two proteins, MBP and vWF. Although we have previously demonstrated that the chaperonin capture platform can distinguish between native and mutant forms of various other mutant proteins (Naik et al., 2010 – wild type and mutant transthyretin mutants; Correia et al., 2014 – wild type and mutants of frataxin), the previous chaperonin bead-based methods were tedious and cumbersome. The biosensor denaturant pulse approach applied

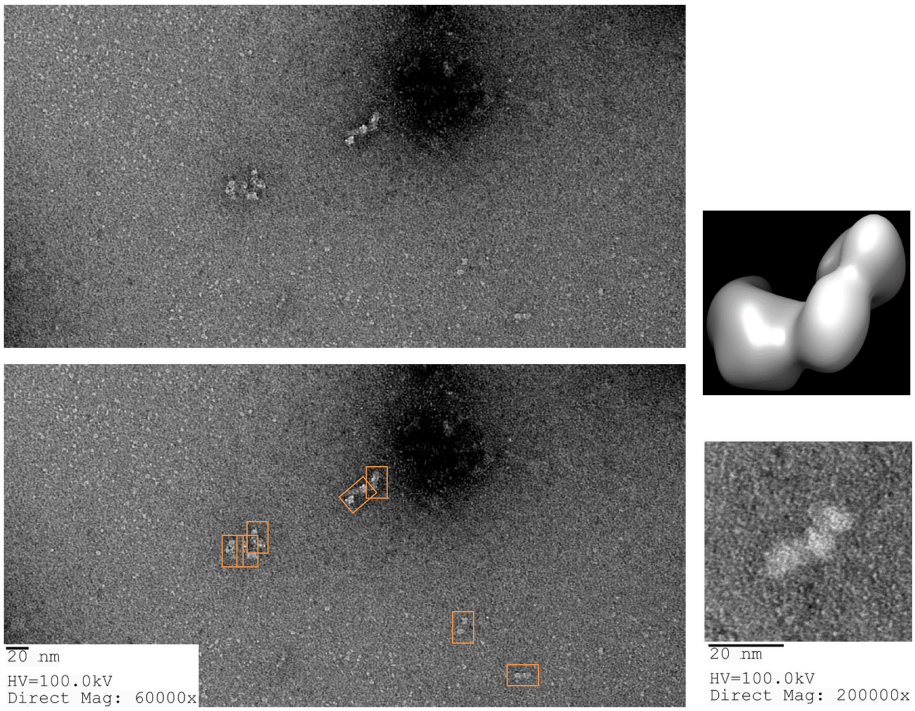

FIGURE 11 | ATP Release of Tetanus Neurotoxin from GroEL Biosensor. **(Left)** Representative field of gridded and stained TeNT after release from GroEL biosensor using ATP. Multiple copies of the protein can be seen as white on dark background (orange boxes on the duplicate image below). **(Right)** Higher magnification of isolated TeNT molecules. In the magnified field, the three domains of tetanus can be observed. For comparison, the envelope and ribbon structure from **Figure 7** have been oriented in the same view as the particle and recolored to match the white on black of the EM image. Images obtained at KUMC.

with the vWF variants shows that this type of comparative analysis easily highlight kinetic stabilities differences between wild type and various mutant forms and most importantly, dramatically accelerates mutant comparison analysis. The GroEL biosensor is based upon the GroEL chaperonin and its properties, namely its promiscuous nature to bind and capture any exposed hydrophobic patches. Therefore, the GroEL biosensor should bind to any target protein with exposed regions. Since mutant hydrophobic surfaces can be variable (e.g., different m values from chemical denaturation profiles), the kinetic partitioning binding reactions of the chaperonin onto the target protein biosensor results in distinct kinetic profiles. We can certainly envision instances where mutant vs. wild type comparisons may fail, seen previous for protein fragment comparisons (e.g., CFTR NDB1 in Lea et al., 2016). For detecting mutant populations in solution using the chaperonin biosensor approach, rapid aggregation of mutants will also interfere with one's ability to clearly differentiate between mutant classes. In addition, there could also be instances where mutant and wild type proteins may naturally exist in kinetically destabilized states (i.e., intrinsically disordered regions). In this latter case, the chaperonin biosensor systems may not be able to distinguish between these two dynamic states.

In the first set of experiments, the prospect of analyzing protein mixtures with the chaperonin system was explored. This approach is particularly intriguing given the wide range of alterations in protein integrity that can lead to enhanced downstream aggregation. The GroEL biosensor systems are useful in discriminating between stable and dynamically unstable species that can exist within one protein solution. To expand on this approach, it may be useful to assess the degree of possible chemical modification of protein populations that result in destabilization, resulting in more aggregation prone species. These altered protein populations can then be released from the GroEL biosensor and analyzed by highly sensitive mass spectroscopy methods. To further enhance the chaperonin detection methodologies, it will be useful to develop bulk approaches where larger concentrations of chaperonins are used to interact with the bulk system rather than a smaller biosensor. Indeed, bulk type experiments have been used to capture entire dynamic transient protein systems that rely on insuring that the chaperonin protein is present in excess of the target protein (Smith et al., 1998; Correia et al., 2014).

However, it is important to reemphasize how the chaperonin biosensor approaches can dramatically accelerate the detection of these transient dynamic states that exist in solution over the above mentioned bulk methods. This development is particularly relevant in that it provides rapid solution-based kinetic analysis that can even complement other more structurally intensive evaluations of protein dynamics such as hydrogen/deuterium exchange mass spectroscopy methods. For example, our previous evaluations of examining the protein stability of particular IgG

molecules (Pace et al., 2018) both with biosensor partitioning kinetics and examining GroEL-IgG complexes by electron microscopy are orthogonally supported by comprehensive HD exchange mapping of dynamic regions within same antibody samples (Toth et al., 2018). It will be particularly interesting to compare the association kinetics of protein solutions that contain dynamically fluctuating populations of native and partially unfolded populations with global HD exchange kinetic profiles. For example, the association kinetics of proteins partitioning onto chaperonin biosensors contain multiple kinetic phases where in some instances, a burst in association kinetics is followed by a slower steady rise in signal (**Figure 3**). This burst kinetics profile followed by a slow steady rise in signal is also observed in global HD exchange kinetic outputs (Yan and Maier, 2009).

While the mesophilic GroEL chaperonin system isolated from *Escherichia coli* is broadly applicable in monitoring the stability of target proteins using the denaturant pulse experimental platform used in the second experimental section, it may be very interesting to expand the denaturation conditions to include those that are sometimes encountered in cellular environments. For example, the *E. coli* chaperonin exhibits a broad stability range across temperature and pH as assessed by various structural monitors (Naik et al., 2014). It will be intriguing to determine if this stability range can be expanded or dramatically shifted by using chaperonin systems isolated from extremophiles. It may be possible to assess the cold stability of a target protein using a chaperonin isolated from psychrophilic organisms in a similar denaturation platform. Psychrophilic chaperonins are often used in bacterial expression system to help fold proteins that have a tendency to aggregate at higher temperatures. Likewise, chaperonins from thermophilic, acidophilic, barophilic, and halophilic organisms may be useful to expand the denaturation conditions of target protein to include higher temperatures, acidic conditions, high hydrostatic pressures, and high ionic strength solutions. Similar to the *E. coli* chaperonin, these extremophile systems will likely be able to detect the pre-aggregate states of target proteins. The detection of pre-aggregate states are much more rapid and most importantly, detection occurs before large scale aggregation takes places. Popular evaluation aggregation propensity depends on techniques such as microflow imaging and size exclusion chromatography where these methods rely on separation or direct visualization of time dependent increases in molecular weight (Pace et al., 2018). GroEL biosensors, on the other hand, appear to detect the formation of transient or long-lived hydrophobic patches on monomeric states.

Finally, others have begun to use chaperonins as both capture platforms and enhanced structural probes for electron microscopy to probe the nature of protein aggregation reactions. Recently, G. M. Clore's group used the *E. coli* chaperonin protein to decorate prion polymers to enhance visualization of hydrophobic patches using EM analysis. What was particular striking from the image analysis in this work was the observation that GroEL bound to the extended fibular arrays in a surprisingly discernable repeating pattern. Given that the chaperonin is primarily binding hydrophobic patches, it is logical to conclude that regular hydrophobic patterns exist within these aggregated arrays (Wälti et al., 2017). In a related approach, the demonstration that large proteins can bind to the chaperonin binding site may be useful in pinpointing specific aggregation prone regions if enough complexes can be formed for reconstruction analysis, particularly if one simply focuses on the interaction regions exclusively without including more flexible regions (Naik et al., 2014; Pace et al., 2018; **Figure 9** this work).

The data presented herein illustrates the broad utility of using the promiscuous chaperonin to (1) capture kinetic transients, (2) distinguish various mutant-type folds, and (3) enhance structure assessment of large proteins using electron microscopy. All of these applications arose from the simple observation that the binding affinity of some folding proteins leads to folding arrest and long-term sequestration of protein substrates. As noted above, it will be interesting to expand the role of chaperonin capture and release strategies to examine initial structural stages of protein aggregation, a truly elusive reaction time regime that may provide enormous benefits in understanding the molecular basis of some human protein folding diseases.

AUTHOR CONTRIBUTIONS

MF, PO, and AM conceived and designed the experiments. PO, AM, BD, and TW performed the experiments. PO, AM, BD, and CT analyzed the data. PO and CT performed computation. CT acquired and installed computational tools and necessary libraries. MF, PO, AM, and BD wrote the manuscript. PO, MF, AM, CT, AT, MA, VM, MB, and TW edited the manuscript. PO, BD, CT, AT, VM, MA, and MB, purified protein.

ACKNOWLEDGMENTS

This work was supported by NIH R01AI090085 (MF), NIH R21AI121492 (MB and MF), Biomolecule Interaction Technologies Center (BITC) Grant (MF), NIH 5T32GM008359 (PO), KUMC Biomedical Research Training Program (PO), NIH HL109109 (MA), Madison and Lila Self Graduate Fellowship (AM), and KUMC Bridging Funds (CT). In addition, we thank Barb Fegley at KUMC Electron Microscopy Core for assistance with EM image acquisition. We thank Dr. David D. Weis and Tyler S. Hageman for the MBP plasmids for protein expression.

SUPPLEMENTARY MATERIAL

The Supplementary Material for this article can be found online at: https://www.frontiersin.org/articles/10.3389/fmolb.2018.00046/full#supplementary-material

REFERENCES

Akkaladevi, N., Mukherjee, S., Katayama, H., Janowiak, B., Patel, D., Gogol, E. P., et al. (2015). Following natures lead: on the construction of membrane-inserted toxins in lipid bilayer nanodiscs. *J. Membr. Biol.* 248, 595–607. doi: 10.1007/s00232-014-9768-3

Arora, J., Hu, Y., Esfandiary, R., Sathish, H. A., Bishop, S. M., Joshi, S. B., et al. (2016). Charge-mediated Fab-Fc interactions in an IgG1 antibody induce reversible self-association, cluster formation, and elevated viscosity. *MAbs* 8, 1561–1574. doi: 10.1080/19420862.2016.1222342

Arora, J., Joshi, S. B., Middaugh, C. R., Weis, D. D., and Volkin, D. B. (2017). Correlating the effects of antimicrobial preservatives on conformational stability, aggregation propensity, and backbone flexibility of an IgG1 mAb. *J. Pharm. Sci.* 106, 1508–1518. doi: 10.1016/j.xphs.2017.02.007

Auton, M., Cruz, M. A., and Moake, J. (2007a). Conformational stability and domain unfolding of the von willebrand factor a domains. *J. Mol. Biol.* 366, 986–1000. doi: 10.1016/j.jmb.2006.10.067

Auton, M., Holthauzen, L. M., and Bolen, D. W. (2007b). Anatomy of energetic changes accompanying urea-induced protein denaturation. *Proc. Natl. Acad. Sci. U.S.A.* 104, 15317–15322. doi: 10.1073/pnas.0706251104

Auton, M., Sedlák, E., Marek, J., Wu, T., Zhu, C., and Cruz, M. A. (2009). Changes in thermodynamic stability of von Willebrand factor differentially affect the force-dependent binding to platelet GPIbalpha. *Biophys. J.* 97, 618–627. doi: 10.1016/j.bpj.2009.05.009

Auton, M., Sowa, K. E., Smith, S. M., Sedlák, E., Vijayan, K. V., and Cruz, M. A. (2010). Destabilization of the A1 domain in von Willebrand factor dissociates the A1A2A3 tri-domain and provokes spontaneous binding to glycoprotein Ibalpha and platelet activation under shear stress. *J. Biol. Chem.* 285, 22831–22839. doi: 10.1074/jbc.M110.103358

Bartesaghi, A., Lecumberry, F., Sapiro, G., and Subramaniam, S. (2012). Protein secondary structure determination by constrained single-particle cryo-electron tomography. *Structure* 20, 2003–2013. doi: 10.1016/j.str.2012.10.016

Burns, J. R., and Baldwin, M. R. (2014). Tetanus neurotoxin utilizes two sequential membrane interactions for channel formation. *J. Biol. Chem.* 289, 22450–22458. doi: 10.1074/jbc.M114.559302

Chapman, E., Farr, G. W., Usaite, R., Furtak, K., Fenton, W. A., Chaudhuri, T. K., et al. (2006). Global aggregation of newly translated proteins in an *Escherichia coli* strain deficient of the chaperonin GroEL. *Proc. Natl. Acad. Sci. U.S.A.* 103, 15800–15805. doi: 10.1073/pnas.0607534103

Clark, A. C., Ramanathan, R., and Frieden, C. (1998). Purification of GroEL with low fluorescence background. *Meth. Enzymol.* 290, 100–118. doi: 10.1016/S0076-6879(98)90010-6

Correia, A. R., Naik, S., Fisher, M. T., and Gomes, C. M. (2014). Probing the kinetic stabilities of Friedreich's ataxia clinical variants using a solid phase GroEL chaperonin capture platform. *Biomolecules* 4, 956–979. doi: 10.3390/biom4040956

Coyle, J. E., Jaeger, J., Gross, M., Robinson, C. V., and Radford, S. E. (1997). Structural and mechanistic consequences of polypeptide binding by GroEL. *Fold. Des.* 2, R93–R104. doi: 10.1016/S1359-0278(97)00046-1

Earl, L. A., Falconieri, V., Milne, J. L., and Subramaniam, S. (2017). Cryo-EM: beyond the microscope. *Curr. Opin. Struct. Biol.* 46, 71–78. doi: 10.1016/j.sbi.2017.06.002

Fisher, M. T. (1993). On the assembly of dodecameric glutamine synthetase from stable chaperonin complexes. *J. Biol. Chem.* 268, 13777–13779.

Fisher, M. T. (1998). GroE chaperonin-assisted folding and assembly of dodecameric glutamine synthetase. *Biochemistry Mosc.* 63, 382–398.

Fisher, M. T., and Katayama, H. (2015). *Osmolyte Mixture for Protein Stabilization*. Patent # 61/237,451 United States Patent and Trademark Office.

Fisher, M. T., and Yuan, X. (1994). The rates of commitment to renaturation of rhodanese and glutamine synthetase in the presence of the groE chaperonins. *J. Biol. Chem.* 269, 29598–29601.

Gruber, R., and Horovitz, A. (2016). Allosteric mechanisms in chaperonin machines. *Chem. Rev.* 116, 6588–6606. doi: 10.1021/acs.chemrev.5b00556

Horwich, A. L., Apetri, A. C., and Fenton, W. A. (2009). The GroEL/GroES cis cavity as a passive anti-aggregation device. *FEBS Lett.* 583, 2654–2662. doi: 10.1016/j.febslet.2009.06.049

Jiang, J., Pentelute, B. L., Collier, R. J., and Zhou, Z. H. (2015). Atomic structure of anthrax protective antigen pore elucidates toxin translocation. *Nature* 521, 545–549. doi:10.1038/nature14247

Katayama, H., Janowiak, B. E., Brzozowski, M., Juryck, J., Falke, S., Gogol, E. P., et al. (2008). GroEL as a molecular scaffold for structural analysis of the anthrax toxin pore. *Nat. Struct. Mol. Biol.* 15, 754–760. doi: 10.1038/nsmb.1442

Keeney, S., and Cumming, A. M. (2001). The molecular biology of von Willebrand disease. *Clin. Lab. Haematol.* 23, 209–230. doi: 10.1046/j.1365-2257.2001.00400.x

Kremer, J. R., Mastronarde, D. N., and McIntosh, J. R. (1996). Computer visualization of three-dimensional image data using IMOD. *J. Struct. Biol.* 116, 71–76. doi: 10.1006/jsbi.1996.0013

Lea, W. A., O'Neil, P. T., Machen, A. J., Naik, S., Chaudhri, T., McGinn-Straub, W., et al. (2016). Chaperonin-based biolayer interferometry to assess the kinetic stability of metastable, aggregation-prone proteins. *Biochemistry* 55, 4885–4908. doi: 10.1021/acs.biochem.6b00293

Llorca, O., Galán, A., Carrascosa, J. L., Muga, A., and Valpuesta, J. M. (1998). GroEL under heat-shock. Switching from a folding to a storing function. *J. Biol. Chem.* 273, 32587–32594. doi: 10.1074/jbc.273.49.32587

Machha, V. R., Tischer, A., Moon-Tasson, L., and Auton, M. (2017). The von willebrand factor A1-collagen III interaction is independent of conformation and type 2 von willebrand disease phenotype. *J. Mol. Biol.* 429, 32–47. doi: 10.1016/j.jmb.2016.11.014

Majumdar, R., Middaugh, C. R., Weis, D. D., and Volkin, D. B. (2015). Hydrogen-deuterium exchange mass spectrometry as an emerging analytical tool for stabilization and formulation development of therapeutic monoclonal antibodies. *J. Pharm. Sci.* 104, 327–345. doi: 10.1002/jps.24224

Martin, J., Horwich, A. L., and Hartl, F. U. (1992). Prevention of protein denaturation under heat stress by the chaperonin Hsp60. *Science* 258, 995–998.

Masuyer, G., Conrad, J., and Stenmark, P. (2017). The structure of the tetanus toxin reveals pH-mediated domain dynamics. *EMBO Rep.* 18, 1306–1317. doi: 10.15252/embr.201744198

Naik, S., Brock, S., Akkaladevi, N., Tally, J., McGinn-Straub, W., Zhang, N., et al. (2013). Monitoring the kinetics of the pH-driven transition of the anthrax toxin prepore to the pore by biolayer interferometry and surface plasmon resonance. *Biochemistry* 52, 6335–6347. doi: 10.1021/bi400705n

Naik, S., Haque, I., Degner, N., Kornilayev, B., Bomhoff, G., Hodges, J., et al. (2010). Identifying protein stabilizing ligands using GroEL. *Biopolymers* 93, 237–251. doi: 10.1002/bip.21319

Naik, S., Kumru, O. S., Cullom, M., Telikepalli, S. N., Lindboe, E., Roop, T. L., et al. (2014). Probing structurally altered and aggregated states of therapeutically relevant proteins using GroEL coupled to bio-layer interferometry. *Protein Sci.* 23, 1461–1478. doi: 10.1002/pro.2515

Ojha, B., Fukui, N., Hongo, K., Mizobata, T., and Kawata, Y. (2016). Suppression of amyloid fibrils using the GroEL apical domain. *Sci. Rep.* 6:31041. doi: 10.1038/srep31041

O'Neil, P. T., Machen, A. J., Thompson, J. A., Wang, W., Hoang, Q. Q., Baldwin, M. R., et al. (2018). Constructing kinetically controlled denaturation isotherms of folded proteins using denaturant-pulse chaperonin binding. *Methods Mol. Biol.* 55, 4885–4908.

Pace, S. E., Joshi, S. B., Esfandiary, R., Stadelman, R., Bishop, S. M., Middaugh, C. R., et al. (2018). The use of a GroEL-BLI biosensor to rapidly assess preaggregate populations for antibody solutions exhibiting different stability profiles. *J. Pharm. Sci.* 107, 559–570. doi: 10.1016/j.xphs.2017.10.010

Punjani, A., Rubinstein, J. L., Fleet, D. J., and Brubaker, M. A. (2017). cryoSPARC: algorithms for rapid unsupervised cryo-EM structure determination. *Nat. Methods* 14, 290–296. doi: 10.1038/nmeth.4169

Roberts, C. J. (2014). Protein aggregation and its impact on product quality. *Curr. Opin. Biotechnol.* 30, 211–217. doi: 10.1016/j.copbio.2014.08.001

Saibil, H. R., Fenton, W. A., Clare, D. K., and Horwich, A. L. (2013). Structure and allostery of the chaperonin GroEL. *J. Mol. Biol.* 425, 1476–1487. doi: 10.1016/j.jmb.2012.11.028

Sewell, B. T., Best, R. B., Chen, S., Roseman, A. M., Farr, G. W., Horwich, A. L., et al. (2004). A mutant chaperonin with rearranged inter-ring electrostatic contacts and temperature-sensitive dissociation. *Nat. Struct. Mol. Biol.* 11, 1128–1133. doi: 10.1038/nsmb844

Smith, K. E., and Fisher, M. T. (1995). Interactions between the GroE chaperonins and rhodanese. Multiple intermediates and release and rebinding. *J. Biol. Chem.* 270, 21517–21523. doi: 10.1074/jbc.270.37.21517

Smith, K. E., Voziyan, P. A., and Fisher, M. T. (1998). Partitioning of rhodanese onto GroEL. Chaperonin binds a reversibly oxidized form derived from the native protein. *J. Biol. Chem.* 273, 28677–28681. doi: 10.1074/jbc.273.44.28677

Tang, G., Peng, L., Baldwin, P. R., Mann, D. S., Jiang, W., Rees, I., et al. (2007). EMAN2: an extensible image processing suite for electron microscopy. *J. Struct. Biol.* 157, 38–46. doi: 10.1016/j.jsb.2006.05.009

Tischer, A., Machha, V. R., Frontroth, J. P., Brehm, M. A., Obser, T., Schneppenheim, R., et al. (2017). Enhanced local disorder in a clinically elusive von willebrand factor provokes high-affinity platelet clumping. *J. Mol. Biol.* 429, 2161–2177. doi: 10.1016/j.jmb.2017.05.013

Tischer, A., Madde, P., Moon-Tasson, L., and Auton, M. (2014). Misfolding of vWF to pathologically disordered conformations impacts the severity of von Willebrand disease. *Biophys. J.* 107, 1185–1195. doi: 10.1016/j.bpj.2014.07.026

Toth, R. T. IV, Pace, S. E., Mills, B. J., Joshi, S. B., Esfandiary, R., Middaugh, C. R., et al. (2018). Evaluation of hydrogen exchange mass spectrometry as a stability-indicating method for formulation excipient screening for an IgG4 monoclonal antibody. *J. Pharm. Sci.* 107, 1009–1019. doi: 10.1016/j.xphs.2017.12.009

Trabuco, L. G., Villa, E., Mitra, K., Frank, J., and Schulten, K. (2008). Flexible fitting of atomic structures into electron microscopy maps using molecular dynamics. *Structure* 16, 673–683. doi: 10.1016/j.str.2008.03.005

Trecazzi, C., and Fisher, M. T. (2018). Detecting protein pre-aggregation states using chaperonin biosensor bio-layer interferometry. *Am. Pharm. Rev.* 21, 52–55.

Tyagi, N. K., Fenton, W. A., Deniz, A. A., and Horwich, A. L. (2011). Double mutant MBP refolds at same rate in free solution as inside the GroEL/GroES chaperonin chamber when aggregation in free solution is prevented. *FEBS Lett.* 585, 1969–1972. doi: 10.1016/j.febslet.2011.05.031

Viitanen, P. V., Donaldson, G. K., Lorimer, G. H., Lubben, T. H., and Gatenby, A. A. (1991). Complex interactions between the chaperonin 60 molecular chaperone and dihydrofolate reductase. *Biochemistry* 30, 9716–9723. doi: 10.1021/bi00104a021

Viitanen, P. V., Gatenby, A. A., and Lorimer, G. H. (1992). Purified chaperonin 60 (groEL) interacts with the nonnative states of a multitude of *Escherichia coli* proteins. *Protein Sci.* 1, 363–369. doi: 10.1002/pro.5560010308

Voziyan, P. A., and Fisher, M. T. (2000). Chaperonin-assisted folding of glutamine synthetase under nonpermissive conditions: off-pathway aggregation propensity does not determine the co-chaperonin requirement. *Protein Sci.* 9, 2405–2412. doi: 10.1110/ps.9.12.2405

Voziyan, P. A., and Fisher, M. T. (2002). Polyols induce ATP-independent folding of GroEL-bound bacterial glutamine synthetase. *Arch. Biochem. Biophys.* 397, 293–297. doi: 10.1006/abbi.2001.2620

Voziyan, P. A., Jadhav, L., and Fisher, M. T. (2000). Refolding a glutamine synthetase truncation mutant in vitro: identifying superior conditions using a combination of chaperonins and osmolytes. *J. Pharm. Sci.* 89, 1036-1045. doi: 10.1002/1520-6017(200008)89:8<1036::AID-JPS8>3.0.CO;2-5

Voziyan, P. A., Johnston, M., Chao, A., Bomhoff, G., and Fisher, M. T. (2005). Designing a high throughput refolding array using a combination of the GroEL chaperonin and osmolytes. *J. Struct. Funct. Genomics* 6, 183–188. doi: 10.1007/s10969-005-2646-6

Wälti, M. A., Schmidt, T., Murray, D. T., Wang, H., Hinshaw, J. E., and Clore, G. M. (2017). Chaperonin GroEL accelerates protofibril formation and decorates fibrils of the Het-s prion protein. *Proc. Natl. Acad. Sci. U.S.A.* 114, 9104–9109. doi: 10.1073/pnas.1711645114

Weaver, J., Jiang, M., Roth, A., Puchalla, J., Zhang, J., and Rye, H. S. (2017). GroEL actively stimulates folding of the endogenous substrate protein PepQ. *Nat. Commun.* 8:15934. doi: 10.1038/ncomms15934

Xia, Y., DiPrimio, N., Keppel, T. R., Vo, B., Fraser, K., Battaile, K. P., et al. (2013). The designability of protein switches by chemical rescue of structure: mechanisms of inactivation and reactivation. *J. Am. Chem. Soc.* 135, 18840–18849. doi: 10.1021/ja407644b

Yan, X., and Maier, C. S. (2009). Hydrogen/deuterium exchange mass spectrometry. *Methods Mol. Biol.* 492, 255–271. doi: 10.1007/978-1-59745-493-3_15

Zhang, J. H., Chung, T. D., and Oldenburg, K. R. (1999). A simple statistical parameter for use in evaluation and validation of high throughput screening assays. *J. Biomol. Screen.* 4, 67–73. doi: 10.1177/108705719900400206

Zhang, Y. (2008). I-TASSER server for protein 3D structure prediction. *BMC Bioinformatics* 9:40. doi: 10.1186/1471-2105-9-40

Zimmermann, M. T., Tischer, A., Whitten, S. T., and Auton, M. (2015). Structural origins of misfolding propensity in the platelet adhesive von Willebrand factor A1 domain. *Biophys. J.* 109, 398–406. doi: 10.1016/j.bpj.2015.06.008

Zolkiewski, M., Kessel, M., Ginsburg, A., and Maurizi, M. R. (1999). Nucleotide-dependent oligomerization of ClpB from *Escherichia coli*. *Protein Sci.* 8, 1899–1903. doi: 10.1110/ps.8.9.1899

Zwirowski, S., Kłosowska, A., Obuchowski, I., Nillegoda, N. B., Piróg, A., Zietkiewicz, S., et al. (2017). Hsp70 displaces small heat shock proteins from aggregates to initiate protein refolding. *EMBO J.* 36, 783–796. doi: 10.15252/embj.201593378

Conflict of Interest Statement: The authors declare that the research was conducted in the absence of any commercial or financial relationships that could be construed as a potential conflict of interest.

Advantages of publishing in Frontiers

OPEN ACCESS
Articles are free to read for greatest visibility and readership

FAST PUBLICATION
Around 90 days from submission to decision

HIGH QUALITY PEER-REVIEW
Rigorous, collaborative, and constructive peer-review

TRANSPARENT PEER-REVIEW
Editors and reviewers acknowledged by name on published articles

Frontiers
Avenue du Tribunal-Fédéral 34
1005 Lausanne | Switzerland

Visit us: www.frontiersin.org
Contact us: info@frontiersin.org | +41 21 510 17 00

REPRODUCIBILITY OF RESEARCH
Support open data and methods to enhance research reproducibility

DIGITAL PUBLISHING
Articles designed for optimal readership across devices

FOLLOW US
@frontiersin

IMPACT METRICS
Advanced article metrics track visibility across digital media

EXTENSIVE PROMOTION
Marketing and promotion of impactful research

LOOP RESEARCH NETWORK
Our network increases your article's readership